Second Series *August 1, 1930* *Vol. 36, No. 3*

THE

PHYSICAL REVIEW

THE FINE STRUCTURE OF He AS A TEST OF THE SPIN INTERACTIONS OF TWO ELECTRONS

By G. Breit

Department of Physics, New York University

(Received June 16, 1930)

Abstract

A tentative expression for the quantum Hamiltonian of two electrons has been set up in a previous paper. The equation is discussed again. It is shown that the last term in it is subject to doubt. The Hamiltonian is tested by applying it to the calculation of the fine structure of the He 2^3P level. It is found that the above mentioned term in e^4 is in contradiction with experiment. Removing the term from the equation one is left essentially with Heisenberg's old Hamiltonian. The spin interaction in it is shown to agree well with experiment. The calculation has been applied also to Li^+.

The essential improvements on previous work are: (1) an increase in the precision of the unperturbed eigenfunctions; (2) a determination from experimental data of a constant D which depends directly on spin—spin interactions (see Eq. (1) below) and which can be calculated with fair accuracy. Comparing the theoretical and empirical values of D a clearer test of the magnitude of spin—spin interactions can be obtained than by calculating the relative positions of the three components of the triplet. The reason for this is that the relative positions of the lines depend also on another constant C which is a difference of two approximately equal numbers and is more difficult to calculate accurately.

§1 Purpose of Work and Results

THE motion of one electron in an external field is treated very satisfactorily by the Dirac equation. It is desirable to have a similar treatment of the two or many electron problem. A partial attempt in this direction has been made by the writer.[1] Considerations in configuration space and also the application of the Heisenberg-Pauli[2] wave field theory led to the Eq. (6) of the above paper. This equation appeared at the time as a likely one, but it was impossible to give a rigorous derivation. The writer has used the first form of the Heisenberg-Pauli theory. Because of the indefiniteness due to the infinite self interactions of point charges with themselves a certain amount of

[1] Breit, Phys. Rev. **34**, 553 (1929).

[2] W. Heisenberg and W. Pauli Jr., Zeits. f. Physik **56**, 1, 1929, Zeits. f. Physik **59**, 168 (1930).

arbitrariness was necessary in removing the infinite terms of the total energy. Also the interaction was derived only to the first approximation in e^2. The same problem has been treated in more detail by Oppenheimer[3] who showed that even to higher powers of e^2 the writer's Eq. (6) could be derived if certain infinite terms of the interaction energy are systematically neglected. However, Oppenheimer also shows that a strict application of the wave field theory leads to infinite relative displacements of the atomic energy levels. The failure of quantum mechanics to give a satisfactory account of the electromagnetic interaction of two particles appears to be connected with two difficult questions: (1) the size of the electron i.e. whether the electron can be located at a point and (2) the Dirac jumps to states of negative energy which make it impossible to have normal states for a finite number of particles. Neither of these questions can be answered at present and it seems that no satisfactory purely theoretical solution of the two electron problem can be obtained before this is done.

The derivation of (6) in configuration space was obtained by using Darwin's classical Hamiltonian function. The choice of quantum symbols has been made in such a way as to obtain equations of motion in agreement with the classical ones. This however was not sufficient to establish the validity of the equation. In fact a discussion in configuration space enables one to see a fault in the equation. In order to explain this unsatisfactory feature we explain first in somewhat more detail the satisfactory side of it. With (6) as it stands we have, omitting the external field, the following equations of motion:

$$(A)\quad \dot{x}_k^{\mathrm{I}} = -c\alpha_k^{\mathrm{I}};\ \dot{p}_k^{\mathrm{I}} = -e_{\mathrm{I}}e_{\mathrm{II}}\frac{\partial}{\partial x_k^{\mathrm{I}}}\left\{r^{-1} - \frac{1}{2}[(\mathbf{a}^{\mathrm{I}}\mathbf{a}^{\mathrm{II}})r^{-1} + r^{-3}(\mathbf{a}^{\mathrm{I}}\mathbf{r})(\mathbf{a}^{\mathrm{II}}\mathbf{r})]\right\}$$

The classical expressions obtained from Darwin's Hamiltonian are:

$$(B)\ \dot{x}_k^{\mathrm{I}} = v_k = \frac{p_k^{\mathrm{I}}}{m_{\mathrm{I}}} - \frac{p_k^{\mathrm{I}}p_{\mathrm{I}}^2}{2c^2m_{\mathrm{I}}^3} - \frac{e_{\mathrm{I}}e_{\mathrm{II}}}{2m_{\mathrm{I}}m_{\mathrm{II}}c^2}[p_k^{\mathrm{II}}r^{-1} + r^{-3}(x_k^{\mathrm{II}} - x_k^{\mathrm{I}})(\mathbf{p}_{\mathrm{II}}\mathbf{r})]$$

$$(C)\ \dot{p}_k^{\mathrm{I}} = -e_{\mathrm{I}}e_{\mathrm{II}}\frac{\partial}{\partial x_k^{\mathrm{I}}}\{r^{-1} - (1/2m_{\mathrm{I}}m_{\mathrm{II}}c^2)[r^{-1}(\mathbf{p}^{\mathrm{I}}\mathbf{p}^{\mathrm{II}}) + r^{-3}(\mathbf{p}^{\mathrm{I}}\mathbf{r})(\mathbf{p}^{\mathrm{II}}\mathbf{r})]\}.$$

The first equation (A) is an exact relation between the velocity and α_k. Equation (B) connects the velocities with the momenta. It was supposed that, in the sense of the correspondence principle, (B) is also true in the quantum theory. It then followed that (C) agrees with the second equation (A) to within terms in $(v/c)^2$. The p_k^I of Eq. (6) therefore replaces Darwin's p_k^I because they have the same rate of change. The employment of equation (B) in the quantum theory is, of course, questionable. All that can be said is that the correct quantum equation should give (B) as an effective equation holding for wave packages. This has to be proved for whatever equation is finally devised.

[3] J. R. Oppenheimer, Phys. Rev. **35**, 461 (1930).

For the discussion of positive energy levels we can use the writer's Eq. (48) which is equivalent to (6). Here if terms in h are dropped the Hamiltonian becomes exactly the classical one with the exception that the last term does not disappear. This shows that (B) and (C) are not satisfied consistently in Eq. (6) the error being of the order of e^4/mc^2r^2. The writer is very grateful to Professors Pauli and Heisenberg for emphasizing the fact that this last term does not contain h.

There is another unsatisfactory property of Eq. (6). Equation (B) gives p_k^I, p_k^{II} in terms of v_k^I, v_k^{II}. Thus

$$\boldsymbol{p}_I = m_I\boldsymbol{v}_I + m_I\boldsymbol{v}_I(v_I^2/2c^2) + (e_Ie_{II}/2c^2)[r^{-1}\boldsymbol{v}_{II} + r^{-3}\boldsymbol{r}(\boldsymbol{v}_{II}\boldsymbol{r})]$$

This is a purely classical relation. In (6) $\boldsymbol{p}_I$ is replaced by $(h/2\pi i)\nabla_I$. For a single particle of charge e_I in an external field of vector potential $\boldsymbol{A}_I$ we replace $m_I\boldsymbol{v}_I(1-\beta_I^2)^{-1/2}$ by $(h/2\pi i)\nabla_I - (e_I/c)\boldsymbol{A}_I$. In this case, to a sufficient approximation $\boldsymbol{A}_I = e_{II}\boldsymbol{v}_{II}/cr$. We should expect that a correct theory will replace $m_I\boldsymbol{v}_I(1-\beta_I^2)^{-1/2} \cong m_I\boldsymbol{v}_I + m_I\boldsymbol{v}_I(v_I^2/2c^2)$ by $\boldsymbol{p}_I - (e_Ie_{II}\boldsymbol{v}_{II}/c^2r)$. We have identified however the quantum operator $(h/2\pi i)\nabla_I$ with Darwin's $\boldsymbol{p}_I$. We see therefore that $\boldsymbol{p}_I$ in (6) replaces the classical

$$\left[\frac{m_I\boldsymbol{v}_I}{(1-\beta_I^2)^{1/2}} + \frac{e_Ie_{II}\boldsymbol{v}_{II}}{c^2r}\right] + \frac{e_Ie_{II}}{2c^2}\left[-\frac{\boldsymbol{v}_{II}}{r} + \frac{\boldsymbol{r}(\boldsymbol{v}_{II}\boldsymbol{r})}{r^3}\right]$$

while it would be more satisfactory if it replaced only the first part of that expression. This means that if m_{II} becomes very large and the reaction on particle II negligible there is no exact agreement between (6) and Dirac's equation. It is thus seen that (6) is likely to be right only to the first order in e^2. Also from the point of view of the wave field theory there is much less arbitrariness in the derivation of first order effects in e^2.

With Eq. (6) it is possible to derive an equation involving two row, two column spin matrices and showing therefore the interaction of electrons as a function of their spins. This is Eq. (48). The interaction energy contains, in addition to the ordinary spin interactions, the extra term in e^4. It is seen from the above considerations that the presence of this term is subject to doubt. In the writer's previous paper it has been supposed that the term might have a physical significance. Some rough estimates of the order of magnitude of its effect indicated that it might be reconcilable with experimental facts. It was felt however that a more accurate test is needed.

A possibility of testing the spin interaction in e^4 is offered by the fine structure of the He triplet spectrum and to some extent by that of Li^+. It has been shown by Heisenberg[4] that the inverted positions of the triplet components in these spectra can be explained by taking into account the interaction of electron spins with each other. The magnitude of the separations was also shown by him to be approximately in agreement with experiment. An attempt to refine Heisenberg's calculation has been made by Sugiura.[5]

[4] Heisenburg, Zeits. f. Physik **39**, 499 (1926).

[5] Suguira, Zeits. f. Physik **44**, 190 (1927).

He considered in an approximate way the effect of polarization of the charge distribution formed by the inner electron due to the electric field of the outer one. A somewhat better agreement with the total separation in the yellow He has been obtained by using this correction. Gaunt[6] has also attempted to improve on Heisenberg's calculation but has not reached a definite conclusion. The difficulty in the application of Gaunt's calculation lies in the insufficiently accurate unperturbed eigenfunctions used by him.

In the present paper the effect of all the spin interactions is calculated using unperturbed eigenfunctions determined by the variational equation derived in the writer's recent paper.[7] These functions are also not exact but they are more accurate than those previously used. The result of the calculation is that satisfactory agreement with the experimentally observed fine structure is obtained if the extra terms in e^4 are neglected. The agreement with experiment is spoiled if the supposed additional effect of these terms is taken into account. This conclusion follows from the fine structure of He and to some extent also from the fine structure of Li^+ if the recent interpretation of the hyperfine structure of that spectrum is adopted.[8] The conclusion is therefore that the terms in e^4 have no physical significance and that Eq. (6) is not correct to higher orders than e^2. With terms of the first order in e^2 satisfactory agreement with experiment is obtained.

The present test is not able to distinguish between Gaunt's equation or Eq. (6) with the terms in e^4 omitted. Both of these agree with the observed fine structure. It is hard to believe however that the terms in $(1/2r)[(\boldsymbol{p}^I\boldsymbol{p}^{II}) + (\boldsymbol{p}^I r)\,(\boldsymbol{p}^{II}r)/r^2]$ do not exist and are replaced by $(\boldsymbol{p}^I\boldsymbol{p}^{II})/r$. For this reason Gaunt's equation is also very likely to be incorrect. Further, Eq. (36) of the writer's previous paper is equivalent to Gaunt's and is seen also to contain terms in e^4. These terms do not have any influence on the fine structure being of the form $(e^4/4mc^2r^2)\,(3-2(\sigma^I\sigma^{II}))$. They cannot have a physical significance since they do not vanish if $h\to 0$.

The calculations which follow are rather laborious and it is advisable to explain at this point the comparison of the results with the experimental fine structure. The effect of spin interactions is taken into account by the ordinary method of perturbation calculations. Both in He and Li^+ this method should give, in the first order, results much more accurate than the experimental precision. This is seen directly from the fact that the separations in the fine structure are of the order of a few cm^{-1} while the total term value is of the order of 2×10^4 cm^{-1}. In the perturbation calculation the effect of the spins is first of all neglected and the eigenfunctions used are determined. Their form is that of (21) in the writer's previous paper.[7] Quite independently of the form of the function F it may be shown that the relative position of the three components of a triplet P term is given to the first order of the spin perturbations (and therefore very accurately in our case) by the following expression for the energy

[6] Gaunt, Phil. Transactions of the Roy. Soc. **A228,** 151 (1929).
[7] Breit, Phys. Rev. **35,** 569 (1930).
[8] Schüler and Brück, Zeits. f. Physik **58,** 735 (1929).

$$E = E_0 + [-3(C+D), 2(D-C), 0] \tag{1}$$

for $j = 0, \quad 1, \quad 2$

where j is the inner quantum number, and C, D are certain integrals in terms of F. The term C is due to the interaction of the electric field with the electron spins. It is this term that gives rise to the ordinary multiplet structure and commonly goes under the name of the interaction of the spin with orbital angular momentum. By itself (i.e. neglecting D) it would give rise to the Landé interval rule. Although there are at present no accurate quantitative confirmations of the correctness of C, there appears to be no reason for doubting it particularly on account of the large number of cases which are in qualitative agreement and it is therefore supposed that the physical nature of C is correct. The integral D however involves the interactions of the two electronic spins with each other in the form of $f(r)\ (\sigma_1 \mathbf{r})\ (\sigma_2 \mathbf{r})$.[9] The questionable terms in e^4 give rise to a part of D which will be called D_1, while the terms in e^2 give rise to another part D_0.

$$D = D_0 + D_1 \text{ with terms in } e^4 \tag{2}$$

$$\text{or } D = D_0 \text{ without terms in } e^4$$

The experimentally known fine structure determines from (1) both $C+D$ and $C-D$, and therefore also C and D. These values will be called *empirical* values of C and D. The comparison with experiment is made by computing D according to the first and the second Eq. (2). It is found that the first equation is in disagreement with the empirical value of D while the second agrees well with it. This agreement does not appear to be accidental because D_0 consists mainly of terms of the same sign and also because the agreement holds in He and Li^+.[10]

Since the physical nature of C appears to be sound this constant has been used as a check on the accuracy of the approximate form of F. It has proved difficult to obtain absolute agreement of the empirical and theoretical values of C. The difficulty lies in the laboriousness of the determination of eigenfunctions by the variational method and particularly in the fact that C is a difference of two numbers which are of approximately the same magnitude. These two approximately equal but opposite contributions to C are due to (1) the electric field of the nucleus acting on the spin of each electron and (2) the electric field of one electron acting on the spin of the other. The latter of these two effects turns out to be the larger one numerically. It depends essentially on the average value of $1/r^3$. From the agreement of the empirical and theoretical values of C it is possible to estimate the accuracy of the second part of C. The constant D_0 also depends essentially on $1/r^3$. The estimated accuracy of the second part of C gives one therefore a guide as to the accuracy of the computation for D_0.

[9] r is written here and later for the distance between the two electrons. The two electrons are referred to from now on as 1 and 2 rather than I and II.

[10] The numerical calculations on Li^+ were made jointly with Mr. L. P. Granath of this

For He the result of the calculation is

$$(C, D_0, D_1) = (R_H\alpha^2/24)(-0.91, -0.62, +0.27) \qquad (3)$$

where R_H is the Rydberg constant for hydrogen and α is the fine structure constant. In comparing this with empirical material we find somewhat different data. The results of Houston[11] and of Hansen[12] agree in giving $\Delta\nu_{02}/\Delta\nu_{12}=14$ with $\Delta\nu_{02}=-3(C+D)=1.068$ cm^{-1}; $\Delta\nu_{12}=-2(C-D)=0.077$ cm^{-1}. The results of Wei[13] are somewhat different giving $\Delta\nu_{02}/\Delta\nu_{12}=10$ or 11. With the results of Hansen and Houston the empirical value of D is $(R_H\alpha^2/24)$ (-0.65) cm^{-1} while using the results of Wei it is $(R_H\alpha^2/24)$ (-0.60) cm^{-1}. Either of these values is in good agreement with D_0 and is definitely in disagreement with D_0+D_1. From the Hansen, Houston data we obtain as the empirical value of $C=-(R_H\alpha^2/24)$ 0.81. This is not in very good agreement with the computed value listed in (3). However the agreement is as good as can be expected. This may be seen by considering the numerical part of the calculation for C. In the final step of the calculation we have $C=1.302$ $R_H(\alpha^2/24)$ $(1.020-1.719)$. The first of these numbers 1.020 is due to the action of the electric field of the nucleus and the second -1.719 is due to the field of the electrons. An error of 5% in the second number is likely to be accompanied by an approximately equal error in the opposite direction for the first number because the eigenfunction is normalized. An error of 10% in 1.719 is 0.17 and this constitutes an error of 24% in the result $-0.70=1.02-1.72$. It is therefore likely that the disagreement of 12% between the computed and the empirical value of C is an indication of an accuracy of about 2.5% in the computation of either the first or the second part of it. In other words the apparently low accuracy is due to the fact that C is the difference of two parts which are approximately equal in numerical magnitude. Using Wei's value for the separation ratio $C=-(R_H\alpha^2/24)$ (0.84). If this value is right the computation for C is correct to 8.3% and a likely accuracy of the calculation of each part is 1.7%. For Wei's value of the separation ratio the empirical values of both C and D come out lower than the calculated by consistent amounts. Using Houston and Hansen's observations the empirical D is higher than the calculated and the empirical C is lower. This is somewhat inconsistent because the error in the calculation is likely to be such as to overestimate the square of the eigenfunction for low r. It is likely however that neither the experiment nor the calculation is accurate enough to decide this point. It is only clear that the computed D_0 agrees well with either set of data and that the computed C, although different from the empirical, does not differ from it by more than can be explained by reasonable errors in the calculation. The presence of D_1 is definitely excluded since it would imply an inaccuracy of 43% in the calculation of D_0. The value of the nuclear spin is immaterial for the present application.

laboratory and the writer is very grateful to him for his permission to quote here the results.

[11] Houston, Proc. Nat. Acad. **13**, 91 (1927).

[12] Hansen, Nature **119**, 237 (1927). Also see Grotrian Graphische Darstellung etc. vol. I, pp. 111–115, Springer, 1928.

[13] Wei, Astrophys. J. **68**, 194 (1928).

§II Determination of Approximate Unperturbed Functions

It has been shown by the writer[7] that ^3P states of a two electron configuration involving two electronic states with unequal azimuthal quantum numbers have the following complete set of normal orthogonal eigenfunctions

$$\begin{aligned} u_1 &= (3^{1/2}/4\pi)(F \sin\theta_1 e^{i\phi_1} - \tilde{F} \sin\theta_2 e^{i\phi_2}) \\ u_0 &= (6^{1/2}/4\pi)(F \cos\theta_1 - \tilde{F} \cos\theta_2) \\ u_{-1} &= (3^{1/2}/4\pi)(F \sin\theta_1 e^{-i\phi_1} - \tilde{F} \sin\theta_2 e^{-i\phi_2}) \\ F &= F(r_1, r_2; \theta), \tilde{F} = F(r_2, r_1; \theta) \end{aligned} \tag{4}$$

where (r_1, θ_1, ϕ_1), (r_2, θ_2, ϕ_2) are polar coordinates for each electron and $\cos\theta = \cos\theta_1 \cos\theta_2 + \sin\theta_1 \sin\theta_2 \cos(\phi_2 - \phi_1)$ so that θ is the angle between r_1, r_2. This form is exact as long as the spin interactions are not brought in. If we had the exact form of F the whole problem could be solved quite accurately because as has been explained in §1 the first order of the perturbation calculation for the effect of spins should give a result of much higher accuracy than that of the experimental determinations. Unfortunately it is very difficult to determine F precisely and it is more practical to use good approximations for its form. Again, without approximations F is determined by the following conditions

$$\begin{aligned} \delta \int \Big\{ & \sum_{i=1,2} \left[\left(\frac{\partial F}{\partial r_i}\right)^2 - 2\cos\theta \frac{\partial F}{\partial r_i}\frac{\partial \tilde{F}}{\partial r_i} + \left(\frac{\partial \tilde{F}}{\partial r_i}\right)^2 \right] + 2F^2/r_1^2 + 2\tilde{F}^2/r_2^2 \\ & + 2\sin\theta F \frac{\partial \tilde{F}}{r_1^2 \partial\theta} + 2\sin\theta \tilde{F}\frac{\partial F}{r_2^2\partial\theta} + \left(\frac{1}{r_1^2} + \frac{1}{r_2^2}\right)\left[\left(\frac{\partial F}{\partial\theta}\right)^2 - 2\cos\theta \frac{\partial F}{\partial\theta}\frac{\partial \tilde{F}}{\partial\theta} + \left(\frac{\partial \tilde{F}}{\partial\theta}\right)^2\right] \\ & + (8\pi^2 m/h^2)(V - E)(F^2 - 2F\tilde{F}\cos\theta + \tilde{F}^2) \Big\} dV = 0 \end{aligned}$$

$$dV = r_1^2 r_2^2 \sin\theta dr_1 dr_2 d\theta \tag{4}$$

with the normalization condition

$$\int (F^2 - 2F\tilde{F}\cos\theta + \tilde{F}^2) dV = 1. \tag{5}$$

The ranges of integration are here $0 < r_1 < \infty$, $0 < r_2 < \infty$, $0 < \theta < \pi$. In order to determine F precisely it would be sufficient to expand it in the form of a sum of a complete set of orthogonal functions with arbitrary coefficients and then to determine the coefficients by means of (4) and (5). Since the labor involved in this is very great and since the resultant series must subsequently be used in the perturbation calculation an approximate solution of the problem has been obtained by the current variety of the Ritz method. It has been supposed that to a sufficient approximation

$$F = r_1(1 + c\cos\theta)\exp[-ar_1/2 - br_2/2]. \tag{6}$$

This form is suggested by the usual screening considerations. The first electron (1) can be thought of approximately as moving in a screened field force subject to a potential $(Z-1)/e^2r$ while the second electron (2) is moving mainly in an unscreened field Ze^2/r. If this is supposed to be true then it is found that (1) is actually likely to be found outside of the region where there is a large probability of finding (2). Approximately therefore the radial part of (6) should give the solution. It is this kind of approximation that has been used by Gaunt with values of a, b derived directly by the screening considerations. This consideration is not exact and it can be improved by introducing the dependence on c and adjusting a, b, c so that (4), (5) are satisfied. The improvement to be expected from using (6) with adjustable constants amounts essentially to correcting the field of force acting on (1) for the incomplete screening of the nucleus by (2) and also to taking into account the fact that the two electrons cannot be considered as distributed on spherical shells and that the probability of a configuration r_1, r_2, θ depends on θ. We let

$$A_{r_i} = \left(\frac{\partial F}{\partial r_i}\right)^2 - 2\mu\frac{\partial F}{\partial r_i}\frac{\partial \tilde{F}}{\partial r_i} + \left(\frac{\partial \tilde{F}}{\partial r_i}\right)^2; \mu = \cos\theta$$

$$A_\theta = \left[\left(\frac{\partial F}{\partial \theta}\right)^2 - 2\mu\frac{\partial F}{\partial \theta}\frac{\partial \tilde{F}}{\partial \theta} + \left(\frac{\partial \tilde{F}}{\partial \theta}\right)^2\right](r_1^{-2} + r_2^{-2}). \tag{7}$$

$$B_\theta = 2r_1^{-2}F^2 + 2r_2^{-2}\tilde{F}^2 + 2r_1^{-2}\sin\theta F\frac{\partial F}{\partial \theta} + 2r_2^{-2}\sin\theta\tilde{F}\frac{\partial \tilde{F}}{\partial \theta}.$$

Substituting (6) and performing integrations involving only simple exponentials we find:

$$\int A_{r_i}dV = (1 + c^2/3)(8a^{-3}b^{-3} + 24a^{-5}b^{-1}) + bc(16\beta^{-7} - 24a\beta^{-8});\ 2\beta = a + b$$

$$\int B_\theta dV = 32a^{-3}b^{-3}(1 + c^2/3) - 32c\beta^{-6};\quad \int A_\theta dV = (c^2/3)(192a^{-5}b^{-1} + 32a^{-3}b^{-3})$$

$$\int (r_1^{-1} + r_2^{-1})(F^2 - 2\mu F\tilde{F} + \tilde{F}^2)dV = (1 + c^2/3)(48a^{-4}b^{-3} + 96a^{-5}b^{-2}) - 64c\beta^{-7} \tag{8}$$

$$\int (F^2 - 2\mu F\tilde{F} + \tilde{F}^2)dV = 192[(1 + c^2/3)a^{-5}b^{-3} - (c/2)\beta^{-8}]. \tag{9}$$

The integrations involving r^{-1} are somewhat more complicated. Expanding r^{-1} in zonal harmonics and powers of r_1, r_2, and then using[14]

$$\int_{-1}^{+1} \mu^n P_m(\mu)d\mu = \frac{2^{m+1}n!}{(n+m+1)!}\frac{\left(\frac{n}{2} + \frac{m}{2}\right)!}{\left(\frac{n}{2} - \frac{m}{2}\right)!} \quad (n \geq m) \tag{10}$$

[14] Whittaker and Watson, Modern Analysis, p. 311.

we have

$$\int_{-1}^{+1}(1+c\mu)^2 r^{-1}d\mu = 2(1+c^2/3)\rho_1^{-1} + (4c/3)\rho_2\rho_1^{-2} + (4c^2/15)\rho_2^2\rho_1^{-3}$$
$$\int_{-1}^{+1}\mu(1+c\mu)^2 r^{-1}d\mu = (4c/3)\rho_1^{-1} + (2/3+2c^2/5)\rho_2\rho_1^{-2} \tag{11}$$
$$+ (8c/15)\rho_2^2\rho_1^{-3} + (4c^2/35)\rho_2^3\rho_1^{-4}$$

with the convention

$$r_1, r_2 = \rho_1, \rho_2 \text{ if } r_1 < r_2; r_1, r_2 = \rho_2, \rho_1 \text{ if } r_1 < r_2$$

Using

$$\int\int_{r_1>r_2} \exp(-ar_1 - br_2)dr_1dr_2 = a^{-1}(a+b)^{-1},$$
$$\int\int_{r_1<r_2} \exp(-ar_1 - br_2)dr_1dr_2 = b^{-1}(a+b)^{-1} \tag{12}$$

we derive by successive differentiations with respect to a, b

$$\int_0^\infty\int_0^\infty r_1^2r_2^2\rho_1^{-1}\exp(-ar_1-br_2)dr_1dr_2 = 2[a^{-2}b^{-2}(a+b)^{-1}+a^{-1}b^{-1}(a+b)^{-3}] \tag{13}$$

Again using (12)

$$\int_0^\infty\int_0^\infty r_1^2r_2^2\rho_2\rho_1^{-2}\exp(-ar_1-br_2)dr_1dr_2 = 6/[ab(a+b)^3].$$

Integrating (12) with respect to a and using

$$\int_0^\infty r^{-1}[\exp(-ar) - \exp((-a-b)r)]dr = \log(1+b/a)$$

we get

$$\int_0^\infty\int_0^\infty r_1^2r_2^2\rho_2^2\rho_1^{-3}\exp(-ar_1-br_2)dr_1dr_2 = 24a^{-5}\log(1+a/b)$$
$$+ 24b^{-5}\log(1+b/a) - 24(a^{-4}+b^{-4})(a+b)^{-1} - 12(a+b)^{-2}(a^{-3}+b^{-3}) \tag{15}$$
$$- 8(a+b)^{-3}(a^{-2}+b^{-2}) - 6(a+b)^{-4}(a^{-1}+b^{-1}).$$

Using (11), (13), (14), (15) one part of the integral involving r^{-1} is evaluated as

$$\int F^2r^{-1}dV = \frac{\partial^2}{\partial a^2}\int(1+c\mu)^2r^{-1}\exp(-ar_1-br_2)dV = \frac{24}{ab(a+b)^2}\left[\frac{2a+b}{a^2b} + \right.$$
$$\left.\frac{3a+b}{a(a+b)^2}\right] + c\left[\frac{16}{a^3b(a+b)^2} + \frac{48}{a^2b(a+b)^4} + \frac{96}{ab(a+b)^5}\right] + c^2\left[192a^{-7}\log\right. \tag{16}$$
$$\left.\frac{a+b}{b} - \frac{192}{a^6(a+b)} - \frac{96}{a^5(a+b)^2} + \frac{32}{5b^4a^2(a+b)} + \frac{32}{5b^4a(a+b)^2}\right.$$

$$-\frac{56a^{-4}+(64/5)b^{-4}}{(a+b)^3}-\frac{24a^{-3}+(96/5)b^{-3}}{(a+b)^4}+\frac{48(a^{-2}-b^{-2})}{5(a+b)^5}$$
$$+\frac{48(a^{-1}+b^{-1})}{(a+b)^5}\Big]$$

Another part of the integral in r^{-1} is given by the second line of (11). Using (12) we find

$$\begin{aligned}
&\tfrac{1}{2}\int_0^\infty\int_0^\infty r_1^3r_2^3\rho_2^3\rho_1^{-4}\exp\left[-\beta(r_1+r_2)\right]dr_1dr_2=(720\log 2-497.625)\beta^{-7}\\
&\tfrac{1}{2}\int_0^\infty\int_0^\infty r_1^3r_2^3\rho_2^2\rho_1^{-3}\exp\left[-\beta(r_1+r_2)\right]dr_1dr_2=(15/8)\beta^{-7}\\
&\tfrac{1}{2}\int_0^\infty\int_0^\infty r_1^3r_2^3\rho_2\rho_1^{-2}\exp\left[-\beta(r_1+r_2)\right]dr_1dr_2=(21/8)\beta^{-7}\\
&\tfrac{1}{2}\int_0^\infty\int_0^\infty r_1^3r_2^3\rho_1^{-1}\exp\left[-\beta(r_1+r_2)\right]dr_1dr_2=(33/8)\beta^{-7}.
\end{aligned}\tag{17}$$

Substituting these expressions (17) into the second line of (11) it is found that

$$\int\mu F\tilde{F}r^{-1}dV=\{3.5+13c+[2.1+(8/35)(720\log 2-497.625)]c^2\}\beta^{-7}\tag{18}$$

Combining (16) and (18) we also have $\int r^{-1}(F^2-2\mu F\tilde{F}+\tilde{F}^2)dV$. The variational Eq. (4) with the restricting condition (5) is now obtained by using (8), (9), (16), (18). On performing the substitutions it is convenient to use dimensionless variables x, y defined by

$$a=xG,\quad b=yG,\quad G=8\pi^2mZe^2/h^2.\tag{19}$$

The constant G is related to the Rydberg constant by

$$4R_Z=GZe^2.\tag{20}$$

The variational Eq. (4) becomes equivalent to the requirement that the fraction

$$\frac{E}{R_Z}=\frac{\alpha_0+2\alpha_1c+\alpha_2c^2}{\beta_0+2\beta_1c+\beta_2c^2}\tag{21}$$

should become a minimum. Here

$$\begin{aligned}
\alpha_0&=x^2+y^2-x-2y+\frac{x}{Z}\left[\frac{x^2y^2}{(x+y)^2}\left\{\frac{2x+y}{x^2y}+\frac{3x+y}{(x+y)^3}\right\}-\frac{56x^4y^3}{3(x+y)^7}\right]\\
2\alpha_1&=x^5y^3\left\{\frac{256y}{3(x+y)^7}-\frac{256xy}{(x+y)^8}-\frac{128}{3(x+y)^6}+\frac{512}{3(x+y)^7}\right.\\
&\quad\left.+\frac{2}{Z}\left[\frac{1}{3x^3y(x+y)^3}+\frac{1}{x^2y(x+y)^4}+\frac{2}{xy(x+y)^5}-\frac{104}{3(x+y)^7}\right]\right\}\\
\alpha_2&=(5/3)y^2+(5/9)x^2-x/3-2y/3+\frac{2}{Z}[x^5y^3(\zeta/180)-6.48x^5y^3(x+y)^{-7}]
\end{aligned}\tag{22}$$

$$\beta_0 = 1,\ 2\beta_1 = -128x^5y^3(x+y)^{-8},\ \beta_2 = 1/3 \tag{23}$$

$$\begin{aligned}\zeta = {} & 720x^{-7}\log(1+x/y) - 720x^{-6}(x+y)^{-1} - 360x^{-5}(x+y)^{-2} \\ & + 24x^{-2}y^{-4}(x+y)^{-1} + 24x^{-1}y^{-4}(x+y)^{-2} - (210x^{-4}+48y^{-4})(x+y)^{-3} \\ & - (90x^{-3}+72y^{-3})(x+y)^{-4} + 36(x^{-2}-y^{-2})(x+y)^{-5} + 180x^{-1}(x+y)^{-6} \\ & + 180y^{-1}(x+y)^{-6}.\end{aligned}$$

The number 6.48 in the last term α_2 is the approximate value of $(32/15)$ $[(21/8)+(2/7)\ (720\log 2-497.625)]$. The result of minimizing (21) is[15]

$$x = 0.273,\ y = 1.00\quad c = -0.0089 \tag{25}$$

and the value of E/R_z corresponding to this is

$$E/R_Z = -1.0654$$

while the experimental value is

$$(E/R_Z)_{exp} = -1.0666.$$

Of the three constants entering the eigenfunction the constant x is the most important one for the following computations because it determines the mean radius of the outer electron and enters as a factor x^3 in most of the important terms of the formulas for fine structure separations. It should be observed here that the eigenfunction is sufficiently exact to determine the energy value to 0.1% which is a higher order of accuracy than that aimed at in the calculation of the fine structure.

§III Secular Equation for Fine Structure

Denoting, as is customary, the electronic spin functions by S_α, S_β with $S_\alpha = \binom{1}{0}$, $S_\beta = \binom{0}{1}$ we have a system of three normal orthogonal linearly independent functions

$$S_1 = S_\alpha^1 S_\alpha^2,\ S_0 = 2^{-1/2}(S_\alpha^1 S_\beta^2 + S_\alpha^2 S_\beta^1),\ S_{-1} = S_\beta^1 S_\beta^2 \tag{26}$$

the upper indices referring to the two electrons. These three functions when combined with the three coordinate functions (4) form a complete set of normal orthogonal functions of an unperturbed ^3P state. The system may be arranged in a table as follows

m			
2	u_1S_1		
1	u_1S_0	u_0S_1	
0	u_1S_{-1}	u_0S_0	$u_{-1}S_1$
−1		u_0S_{-1}	$u_{-1}S_0$
−2			$u_{-1}S_{-1}$

(27)

[15] Dr. R. W. G. Wyckoff of the Rockefeller Institute has performed most of the numerical calculations on a calculating machine. The writer is very grateful to him for this assistance.

each row corresponding to a fixed magnetic quantum number m. The perturbation energy[16] is

$$\Delta H = \boldsymbol{A}\boldsymbol{\sigma}_1 + \boldsymbol{B}\boldsymbol{\sigma}_2 + \mathcal{D}_0 + \mathcal{D}_1 \tag{28}$$

with

$$\boldsymbol{A} = \frac{he^2}{8\pi m^2c^2}\{Zr_1^{-3}\boldsymbol{M}_1 + r^{-3}[(\boldsymbol{r}_1 - \boldsymbol{r}_2) \times (2\boldsymbol{p}_2 - \boldsymbol{p}_1)]\}$$
$$\boldsymbol{B} = \frac{he^2}{8\pi m^2c^2}\{Zr_2^{-3}\boldsymbol{M}_2 + r^{-3}[(\boldsymbol{r}_2 - \boldsymbol{r}_1) \times (2\boldsymbol{p}_1 - \boldsymbol{p}_2)]\} \tag{28'}$$

$$\mathcal{D}_0 = R_0(r)(\boldsymbol{\sigma}_1\boldsymbol{r})(\boldsymbol{\sigma}_2\boldsymbol{r}), \quad R_0(r) = -(eh/4\pi mc)^2 3r^{-5} \tag{28''}$$

$$\mathcal{D}_1 = R_1(r)(\boldsymbol{\sigma}_1\boldsymbol{r})(\boldsymbol{\sigma}_2\boldsymbol{r}), \quad R_1(r) = (e^4/8mc^2)r^{-4} \tag{28'''}$$

The $\boldsymbol{M}$ are the orbital angular momentum operators $[\boldsymbol{r}\times\boldsymbol{p}]$. We have included here only those terms of the perturbation energy which have an influence on the fine structure and we have omitted therefore terms in $(\boldsymbol{\sigma}_1\boldsymbol{\sigma}_2)$. The first three terms of (28) i.e. (28′), (28″) are of the second degree in the electronic charge e and the last is of the fourth degree. We have written this last term separately so as to be able to see the result with it and without it. Letting

$$\boldsymbol{C} = \boldsymbol{A} + \boldsymbol{B} \tag{29}$$

we have

$$\begin{aligned}
(\boldsymbol{A}\boldsymbol{\sigma}_1 + \boldsymbol{B}\boldsymbol{\sigma}_2)uS_1 &= C_z uS_1 + 2^{-1/2}(C_x + iC_y)uS_0 \\
(\boldsymbol{A}\boldsymbol{\sigma}_1 + \boldsymbol{B}\boldsymbol{\sigma}_2)uS_0 &= 2^{-1/2}(C_x - iC_y)uS_1 + 2^{-1/2}(C_x + iC_y)uS_{-1} \\
(\boldsymbol{A}\boldsymbol{\sigma}_1 + \boldsymbol{B}\boldsymbol{\sigma}_2)uS_{-1} &= 2^{-1/2}(C_x - iC_y)uS_0 - C_z uS_{-1}
\end{aligned} \tag{30}$$

On the right side of these formulas all terms in the antisymmetric combinations $2^{-1/2}\,(S_\alpha{}^1S_\beta{}^2 - S_\alpha{}^2S_\beta{}^1)$ have been omitted since they do not belong to the triplet state. We are justified in doing this in the present calculation because the formulas (30) are to be used in the calculation of matrix elements for the secular equation and only matrix elements between eigenfunctions belonging to the unperturbed ^3P state are of interest to us. Similarly we find[17]

$$\begin{aligned}
(\boldsymbol{\sigma}_1\boldsymbol{r})(\boldsymbol{\sigma}_2\boldsymbol{r})S_1 &= z^2S_1 + (2)^{1/2}z(x + iy)S_0 + (x + iy)^2S_{-1} \\
(\boldsymbol{\sigma}_1\boldsymbol{r})(\boldsymbol{\sigma}_2\boldsymbol{r})S_0 &= (2)^{1/2}z(x - iy)S_1 + (x^2 + y^2 - z^2)S_0 - (2)^{1/2}z(x + iy)S_{-1} \\
(\boldsymbol{\sigma}_1\boldsymbol{r})(\boldsymbol{\sigma}_2\boldsymbol{r})S_1 &= (x - iy)^2S_1 - (2)^{1/2}z(x - iy)S_0 + z^2S_{-1}
\end{aligned} \tag{31}$$

Formulas (30), (31) give the effect of all the operations due to the spins. Other angular momentum operations are involved in the operator C itself.

[16] See (1). The σ's are here Pauli's matrices with unchanged signs i.e. with signs opposite to those used in the above reference.

[17] A systematic way of obtaining the matrices involved in (30) and (31) is to observe that $\boldsymbol{A}\boldsymbol{\sigma}_1 + \boldsymbol{B}\boldsymbol{\sigma}_2$ with symmetrical $\boldsymbol{A}, \boldsymbol{B}$ is equivalent to an angular momentum matrix so far as operations on symmetric spin functions are concerned. From this point of view (30) is obvious and is easily generalized to any number of electrons. For (31) we can use (30) if it is remembered that $(\boldsymbol{\sigma}_1\boldsymbol{r} + \boldsymbol{\sigma}_2\boldsymbol{r})^2 = 2r^2 + 2(\boldsymbol{\sigma}_1\boldsymbol{r})(\boldsymbol{\sigma}_2\boldsymbol{r})$.

We see that

$$\mathbf{C} = \frac{he^2}{8\pi m^2 c^2}\{Z(r_1^{-3}\boldsymbol{M}_1 + r_2^{-3}\boldsymbol{M}_2) - 3^{-3}[(\boldsymbol{r}_1 - \boldsymbol{r}_2) \times (\boldsymbol{p}_1 - \boldsymbol{p}_2)]\}. \quad (30')$$

Applying C to the eigenfunctions u_1, u_0, u_{-1} it is found that

$$\begin{aligned} C_z(u_1, u_0, u_{-1}) &= C(u_1, u_0, u_{-1}) \\ (C_x + iC_y)(u_1, u_0, u_{-1}) &= C(0, -(2)^{1/2}u_1, (2)^{1/2}u_0) \\ (C_x - iC_y)(u_1, u_0, u_{-1}) &= C(-(2)^{1/2}u_0, (2)^{1/2}u_{-1}, 0) \end{aligned} \quad (32)$$

where

$$\begin{aligned} \mathbf{C} = \left(\frac{eh}{4\pi mc}\right)^2 \Big\{ & Z \int \Big[\frac{F^2}{r_1^3} + \frac{\bar{F}^2}{r_2^3} - \left(\frac{1}{r_1^3} + \frac{1}{r_2^3}\right)F\bar{F}\cos\theta + \frac{1}{2}\left(\frac{1}{r_2^3} \right. \\ & \left. - \frac{1}{r_1^3}\right)\left(\bar{F}\frac{\partial F}{\partial\theta} - F\frac{\partial\bar{F}}{\partial\theta}\right)\sin\theta\Big]dV - 3\int\frac{1}{r^3}\Big[F^2 + \bar{F}^2 - 2F\bar{F}\cos\theta \\ & + \frac{r_1}{r_2}\bar{F}(F - \bar{F}\cos\theta) + \frac{r_2}{r_1}F(\bar{F} - F\cos\theta) + \frac{1}{2}\sin^2\theta\Big\{r_2\Big(\bar{F}\frac{\partial F}{\partial r_1} \\ & - F\frac{\partial\bar{F}}{\partial r_1}\Big) - r_1\Big(\bar{F}\frac{\partial F}{\partial r_2} - F\frac{\partial\bar{F}}{\partial r_2}\Big) + \left(\frac{r_2}{r_1} - \frac{r_1}{r_2}\right)\Big(\bar{F}\frac{\partial F}{\partial\theta} - F\frac{\partial\bar{F}}{\partial\theta}\Big)\cot\theta \\ & - \left(\frac{r_2}{r_1} + \frac{r_1}{r_2}\right)F\bar{F}\Big\}\Big]dV\Big\}. \end{aligned} \quad (33)$$

It is also found that:

$$\begin{aligned} (2)^{1/2}z(x + iy)R(r)(u_1, u_0, u_{-1}) &= (0, Du_1, Du_0) \\ (2)^{1/2}z(x - iy)R(r)(u_1, u_0, u_{-1}) &= (Du_0, Du_{-1}, 0) \\ (x + iy)^2R(r)(u_1, u_0, u_{-1}) &= (2Du_{-1}, 0, 0) \\ (x - iy)^2R(r)(u_1, u_0, u_{-1}) &= (0, 0, 2Du_1) \\ (r^2 - 3z^2)R(r)(u_1, u_0, u_{-1}) &= (Du_1, -2Du_0, Du_{-1}) \\ z^2R(r)(u_1, u_0, u_{-1}) &= (D'u_1, (D + D')u_0, D'u_{-1}) \end{aligned} \quad (34)$$

with

$$\begin{aligned} D &= \int \tfrac{1}{5}\{2(a\alpha + b\beta)^2 - (a\beta - \alpha b)^2\}R(r)dV \\ D' &= \int \tfrac{1}{5}\{(a\alpha + b\beta)^2 + 2(a\beta - \alpha b)^2\}R(r)dV \end{aligned} \quad (35)$$

where

$$a = F - \bar{F}\cos\theta,\ b = \bar{F}\sin\theta,\ \alpha = r_1 - r_2\cos\theta,\ \beta = r_2\sin\theta. \quad (35')$$

In formulas (32), (34) we omit everywhere terms involving other functions than u_1, u_0, u_{-1}. The reason for this is the same as that for the omission of terms in $2^{-1/2}(S_\alpha{}^1S_\beta{}^2-S_\alpha{}^2S_\beta{}^1)$ in (30), (31). These formulas (30), (31), (32), (34) can be used to form the secular determinant for the whole problem.

It is known that the matrix elements of ΔH between any two eigenfunctions belonging to different rows in (27) must vanish and that, therefore, the secular determinant can be broken up into five independent subdeterminants. With the aid of the results just described it is found that the subdeterminant $m=0$ is

$$\begin{vmatrix} -C-\lambda', & C+D, & 2D \\ C+D & -D-\lambda' & -C-D \\ 2D, & -C-D, & -C-\lambda' \end{vmatrix} = 0, \quad \lambda' = \lambda - D' \tag{36}$$

having roots $\lambda'=(-2C-3D,\ 2D-C,\ C)$. The other subdeterminants are similarly found and give some of the same roots the first occurring on the whole 1, the second 3, and the third 5 times. The result is that the energy is to within a common additive constant

$$E = E_0 + [-3(C+D),\ 2(D-C),\ 0] \tag{1}^{18}$$

for $j=0,\ 1,\ 2$.

§IV Computation of C and D[19]

Formula (6) is substituted into (33) and the integrations are performed. It is found that

$$\int (F^2r_1^{-3} + \tilde{F}^2r_2^{-3} - F\tilde{F}r_1^{-3}\cos\theta - F\tilde{F}r_2^{-3}\cos\theta)dV = 8a^{-2}b^{-3}(1+c^2/3) + 16c(a/2+b/2)^{-5}. \tag{37}$$

In the remainder of the calculation terms in c^2 are dropped, this being justified by the small numerical value of c.

$$\int r^{-3}\left\{2F^2 - 2F\tilde{F}\cos\theta + 2(r_1/r_2)(F\tilde{F} - \tilde{F}^2\cos\theta) + (1/2)\sin^2\theta\left[2r_2\left(\tilde{F}\frac{\partial F}{\partial r_1} - F\frac{\partial\tilde{F}}{\partial r_1}\right) - 2(r_2/r_1)F\tilde{F}\right]\right\}dV = 8\left[\frac{1}{a^2b(a+b)^2} + \frac{2b-a}{ab(a+b)^4} + \frac{20b}{(a+b)^6}\right] + 16c\left[\frac{2b-a}{ab(a+b)^4} + \frac{2}{(a+b)^5} + 4.168\frac{b-a}{(a+b)^6}\right]. \tag{38}$$

Here $4.168=(16/5)\ (120\log 2-81.875)$. Substituting these expressions into (33), remembering the normalization condition (5) and (9), then substituting

[18] The same result can be checked by using the theorem emphasized by Slater: the sum of the roots of a secular determinant is equal to the sum of the diagonal elements. The first row in (27) gives the last root ($j=2$), the second gives the sum of the last two, the third the sum of the three roots.

[19] The writer is very grateful to Dr. F. W. Doermann for checking some of these formulas.

the dimensionless constants x, y by means of (19) and noting that $G^3\mu^2 = 4Z^3R_H\alpha^2$ we have

$$\left(1 - 128\frac{x^5y^3}{(x+y)^8}c\right)C = R_HZ^3\alpha^2x^3\left\{\frac{Z}{6}\left[1 - \frac{64x^2y^3}{(x+y)^5}c\right] - \frac{1}{2}\left[\frac{y^2}{(x+y)^2} + \frac{xy^2(2y-x)}{(x+y)^4} + 20\frac{x^2y^4}{(x+y)^6}\right] - c\left[\frac{xy^2(2y-x)}{(x+y)^4} + \frac{2x^2y^3}{(x+y)^5} + 4.168\frac{y-x}{(x+y)^6}\right]\right\}.$$

The first term involving Z is due to the action of the electric field of the nucleus and the remaining part of C is due to the interaction of the two electrons. It is seen that the two parts of C have opposite signs. For large Z the first part predominates and gives the usual effect for high atomic numbers. For small Z the second part may be numerically the larger one and C may be negative.

The part of D arising from $\mathfrak{D}_0$, given by (28″), is similarly found to be D_0 given by

$$\left(1-128\frac{x^5y^3}{(x+y)^8}c\right)D_0 = -(R_HZ^3\alpha^2x^3/5)\left\{\frac{y^2}{(x+y)^2} + \frac{xy^2(2y-x)}{(x+y)^4} + 2c\left[\frac{xy^2(2y-x)}{(x+y)^4} + \frac{xy^2}{(x+y)^3} - \frac{4x^2y^3}{(x+y)^5}\right]\right\}. \tag{40}$$

The part of D arising from $\mathfrak{D}_1$, given by (28‴), is, neglecting c altogether

$$D_1 = (R_HZ^3\alpha^2x^2/120)\left[3 + \frac{256x^3y^3}{(x+y)^6} + 48\frac{x^4y^4(x^2+3y^2)}{(x^2-y^2)^5}\log\frac{x}{y} + 2x^2y^2\frac{x^4-11y^4-38x^2y^2}{(x^2-y^2)^4} + \frac{2x^2y^2}{(x^2-y^2)^2} + \frac{y^2+3x^2}{y^2-x^2}\right] \tag{41}$$

Substituting the numerical values of x, y, c of §2 the values of C, D_0, D_1 listed in § 1 are obtained.

THE SINGLET SYSTEM OF THE OXYGEN ARC SPECTRUM AND THE ORIGIN OF THE GREEN AURORAL LINE

By Rudolf Frerichs*
California Institute of Technology, Pasadena

(Received June 2, 1930)

Abstract

The oxygen arc spectrum has been investigated under varied conditions in the extreme ultraviolet. A number of observed lines have been arranged in the singlet system of terms. The values of the low terms $^1D_2$ and $^1S_0$ have been fixed

As J. C. McLennan has shown,[1] the green auroral line $\lambda = 5577.35$A gives the Zeeman pattern of a singlet line and is therefore probably the forbidden combination between the low metastable terms $^1D_2$ and $^1S_0$ of the oxygen atom. Although many attempts have been made to locate these terms, either by extrapolating the values of the corresponding terms of similar spectra or by connecting the structure of the oxygen band spectra with the dissociation energy, the exact position of these terms could not be fixed. The direct method of locating the terms by spectroscopic analysis was not used in former investigations.

The following paper gives an attempt to classify all the stronger ultraviolet singlet lines of the oxygen atom. The classification of singlet lines is usually more difficult than the classification of lines of higher multiplicity. Therefore, we have investigated the oxygen arc spectrum under different controlled conditions in order to obtain information regarding the excitation potential of the different lines. The results so obtained are given in part 2 after a short description of the experimental arrangement in part 1. Part 3 discusses the series analysis of the new lines.

Apparatus and Procedure

Two different gratings were used. The first one, ruled by Anderson, (Focus = 1 m, area 5 × 8 cm, dispersion: first order 17A per mm) gives very good definition (see Table I) but unfortunately scatters the light so much that it could not be used for weak lines. The other one, ruled at the National Physical Laboratory, (Focus = 1 m, area 3.5 × 5 cm, dispersion 18A per mm) shows very bright and sharp lines down to 520A, the smallest wave-length here investigated, although it was not made with light rulings for the ultraviolet.

The spectrograph built for this investigation was very simply constructed. It consists of a brass tube which carries at one end the grating, at the other

* International Education Board Fellow.

[1] J. C. McLennan, J. H. McLeod, and McQuarrie, Proc. Roy. Soc. **A114, 1** (1927). J. C. McLennan, J. H. McLeod and R. Ruedy, Phil. Mag. **6,** 558 (1928); also L. A. Sommer, Zeits. f. Physik **51,** 451 (1928).

end, the slit and holder for uncurved plates 1″×4″ in size. The cover plates on the two ends of the spectrograph are sealed with rubber gaskets inserted in small circular grooves and are held in place with screws. These gaskets proved to be very satisfactory. Over one hundred exposures were made without the slightest trouble from leaks in the spectrograph.

Much care was taken in the arrangement of the pumping system and the light source. Small traces of oxygen in the spectrograph cause absorption of the light as well as serious fogging of the plates. In order to obtain as great a pressure difference as possible between the discharge tube and spectrograph we used two slits in series. The outer slit, narrow (0.01 mm) and short (2 mm) was sealed to the spectrograph so that the only communication between the discharge tube and the spectrograph was through this narrow aperture. A small distance behind this slit, there was a second slightly larger slit arranged at the end of a conical tube. One two-stage pump evacuated the space between these two slits, a second one the spectrograph directly, all connections were made with short and large tubes.

In order to make experiments on the excitation energy of the singlet lines the spectrograph was equipped with arrangements to work either with pure oxygen or with circulating mixtures of oxygen and rare gases. The oxygen was generated electrolytically. Small traces of hydrogen could be oxidized by a glowing platinum wire. The gas was dried with phosphorus pentoxide and then stored under low pressure in a bulb with a side tube immersed in liquid air. The flow of the oxygen in the discharge tube was regulated by a narrow capillary. A variable valve was not used but the amount of gas flowing in the tube was kept exactly constant by regulating the pressure in the storage bulb. The discharge tube was evacuated through two single stage pumps in series. For the experiments with pure oxygen, these four pumps were backed by an oil-pump. For the experiments with helium-oxygen and with neon-oxygen, the four pumps exhausted the gas from the spectrograph and discharge tube into a large bulb with a back pressure of about five millimeters. From this bulb the gas flowed back to the discharge tube through a heated quartz tube with copper oxide and a large charcoal trap in liquid air. The charcoal kept all impurities back and after a short time of circulation, the spectrum of the discharge tube was free from impurities. The charcoal also adsorbed the oxygen of the mixture and we had therefore to add continuously a small amount of oxygen to the rare gas after it had passed the charcoal. Argon is strongly adsorbed by charcoal. Therefore, the argon-oxygen mixture was circulated over calcium heated to about 300 degrees C in an iron tube and through a trap in liquid air, and new oxygen was added to replace that absorbed in the calcium tube.

The experiments were made with the positive column as well as with the hollow cathode in pure oxygen and in different mixtures. The discharge tube that was finally adopted had a diameter of about 15 mm and a length of 250 mm. Large electrodes of heavy aluminum allowed the use of currents of between 350 and 750 milliamperes. Direct current at 1300 volts was supplied by two small generators of 650 volts each, connected in series. Suit-

able ballast-resistance was used. The hollow cathode consisted either of a small aluminum tube 10 mm in diameter and 40 mm in length or of a hole of similar size in a solid piece of aluminum, which was cooled by water flowing through a copper-tubing surrounding the aluminum. The hollow cathodes carried currents of between 150 and 500 milliamperes.

TABLE I. *Ultraviolet OI lines.*

Intensity	Wave-length	Frequency obs.	Frequency calc.	Classification	
	1217.60	82128	82128	$2p^1S_0-(^2P)3s^1P_1$	
	1152.06	86801	86801	$2p^1D_2-(^2D)3s^1D_2$	
	999.47	100053	100053	$2p^1D_2-(^2P)3s^1P_1$	
1	990.86	100922	100922	$2p^3P_0-(^2D)3s^3D_1$	
3	990.27	100983	100983	$2p^3P_1-(^2D)3s^3D_2$	
3	990.21	100989	100989	$2p^3P_1-(^2D)3s^3D_1$	
4	988.84	101128	101128	$2p^3P_2-(^2D)3s^3D_3$	
3	988.72	101141	101141	$3p^3P_2-(^2D)3s^3D_2$	
1	988.66	101147	101147	$2p^3P_2-(^2D)3s^3D_1$	II. Order
	935.15	106935	106934	$2p^1D_2-(^2D)4s^1D_2$	
	922.02	108457	108457	$2p^1D_2-(^2D)3d^1F_3$	
	882.88	113266	113265	$2p^1D_2-(^2D)5s^1D_2$	
1	879.65	113681	113687	$2p^3P_0-(^2P)3s^3P_1$	
			113744	$2p^3P_1-(^2P)3s^3P_2$	
5	879.14	113747	113755	$2p^3P_1-(^2P)3s^3P_1$	
			113761	$2p^3P_1-(^2P)3s^3P_0$	
			113903	$2p^3P_2-(^2P)3s^3P_2$	
4	877.97	113899	113914	$2p^3P_2-(^2P)3s^3P_1$	
	861.63	116059	116058	$2p^1D_2-(^2D)6s^1D_2$	I.Order
	850.74	117545	117544	$2p^1D_2-(^2D)7s^1D_2$	
3	812.09	123139	123122	$2s^22p^4\,^3P_0-2s2p^5\,^3P_1$	
			123130	$2s^22p^4\,^3P_1-2s2p^5\,^3P_2$	
1	811.69	123200	123189	$2s^22p^4\,^3P_1-2s2p^5\,^3P_1$	
1	811.43	123239	123221	$2s^22p^4\,^3P_1-2s2p^5\,^3P_0$	
4	811.02	123301	123289	$2s^22p^4\,^3P_2-2s2p^5\,^3P_2$	II. Order
1	810.62	123362	123348	$2s^22p^4\,^3P_2-2s2p^5\,^3P_1$	
3	792.92	126346			
1	792.50	126274			
1	792.20	126231			
3	791.93	126183			
1	791.48	126116			
0	770.70	129752		71	II. Order
1	770.28	129823			
2	769.39	129973		150	
0	—	—			
1	756.7	132152		158	
2	755.8	132310			
0	—	—			I. Order
1	749.3	133457	∽133000	$2p^3P_{0,1,2}-(^2P)4s^3P_{0,1,2}$?	
1	748.4	133618			

In front of the slit, there was a small shutter which was closed before an exposure, while the discharge tubes were run at the heaviest possible currents until the last traces of visible bands and of the hydrogen lines disappeared. Table I gives the observed lines which we can attribute with safety to the spectrum of the oxygen atom. The exposures were made with times between 15 minutes and three hours. Most of the lines were measured in the second order against some lines of impurities: O II, NI, N II, CI, CII which have

been determined by Bowen and Ingram[2] with great accuracy, and which occurred weakly in our discharge. A few weaker lines have been measured only in the first order against O II, O I, Ne, He. As the intensities vary considerably with the source, intensity values are only relative and only given for lines which belong to one group.

The Excitation Potential of the Ultraviolet Oxygen Lines

In order to obtain a classification of the oxygen lines, we investigated the spectrum under varied conditions. A few pictures were taken with the above mentioned positive column in the mixtures: $He-O_2$, $Ne-O_2$ and $A-O_2$. The pressure of the rare gas was not measured but was always adjusted to give the minimum potential drop across the tube. The amount of oxygen added continuously was so small that the stronger lines were just visible in a spectroscope of considerable dispersion. The excitation phenomena of mixtures of rare gases with other gases and vapors have been studied much and discussed in the last years. Although there are some discrepancies between the results of different observers, we can state with safety that the maximum amount of energy available in such a discharge is given by the ionization potential of the rare gas, when the amount of the other component of the mixture is small. These investigations differ only as to whether this amount is transferred to neutral atoms, to metastable atoms or to ions of the second component. In the case of discharges through mixtures of rare gases and molecular gases, the process is complicated by dissociation. By looking over various experiments carried on in this field, one gains the impression that the assumptions of different kinds of collisions are made *ad hoc* in order to obtain agreement with the observed facts.[3] Therefore, because the prediction of the excitation limit of unclassified lines seemed to be rather uncertain, we have made no special assumptions as to the processes involved, but we have empirically calibrated our results by the well-known excitation energy of the already classified oxygen lines. Table II gives the results so obtained. The fifth column contains the excitation energy of the upper level of each line in frequency units, the second, third and fourth column the intensities in $A-O_2$, $Ne-O_2$ and $He-O_2$. Fig. 1 illustrates these results. The exposures are so chosen, that the resonance lines appear on all spectrograms with nearly the same intensity. In argon, only those lines whose upper level is not higher than about 100,000 frequency units above the $^3P_2$ level are excited with considerable intensity (>1). This photograph shows clearly that 1152 is the lowest excited line of the singlet system because the other lines are either very weak or absent in argon-oxygen. Neon has a very remarkable effect on the intensities. Table II shows that in neon, the line 935.15, whose upper level is about 122800 above the ^3P term, is strongly

[2] I. S. Bowen and S. B. Ingram, Phys. Rev. **28,** 444 (1926).

[3] For a discussion of the various kinds of collision which are necessary to explain the observed facts in mixtures of rare gases and molecular gases, see O. S. Duffendack and H. L. Smith, Phys. Rev. **34,** 68 (1929) and O. S. Duffendack and R. A. Wolfe, Phys. Rev. **34,** 409 (1929).

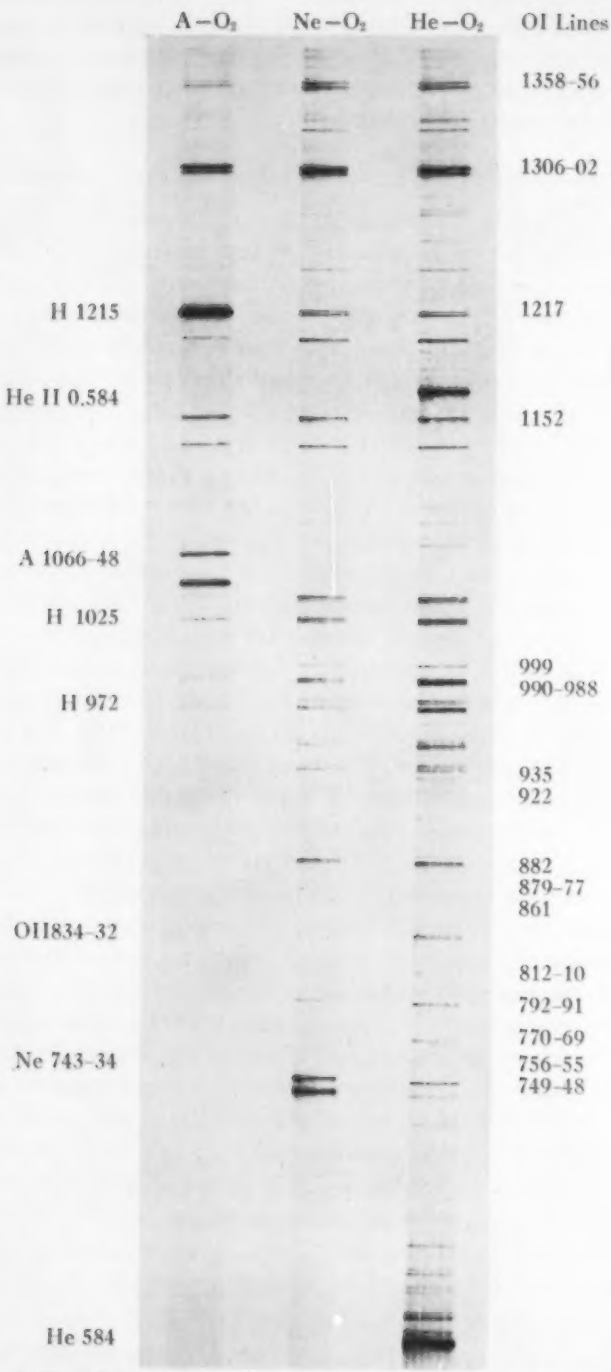

Fig. 1. The ultraviolet OI spectrum in $A-O_2$, $Ne-O_2$ and $He-O_2$.

excited. This phenomenon of increased intensities of certain lines in such discharges often has been mentioned.[4] It occurs always when either the ionization energy or the energy of the metastable state of the rare gas is approximately equal to the excitation energy of the line of the other component.

TABLE II. *Intensities of the ultraviolet O I. Lines under different conditions.*

Wave-length	Intensity			Excitation energy frequency units
	$A-O_2$	$Ne-O_2$	$He-O_2$	
1358–56	4	6	6	73760
1306–02	10	10	10	76788
1217	—	3	3	115922
1152	3	4	5	102670
1041–39	1	4	5	95222
1028–25	1	4	5	97481
999	—	4	5	115922
990–988	1	5	8	101147
978–76	—	2	3	102406
973–71	—	2	3	102906
935	—	4	3	122803
922	—	—	1	124326
882	—	—	2	129134
879–77	—	4	4	113914
861	—	—	1	131927
850	—	—	0	133413
812–810	—	1	2	123348
792–791	—	2	3	126231
770–769	—	1	2	
756–55	—	0	1	
749–48	—	—	0	133618

These lines are strongly excited in helium-oxygen but on the other hand, some more lines can be observed in helium which are either weak or absent in neon.

A few words may be said about the excitation of the oxygen arc spectrum in other sources. The positive column in pure oxygen also shows these lines but the intensity at the same amount of current passing through the tube is much smaller than in the mixtures of rare gases and oxygen. In pure oxygen the lines show the usual decrease in intensity with increasing excitation.

The highest amount of excitation with direct current is obtained in the hollow cathode in pure oxygen. In the hollow cathode, all the lines of of O II which have been classified by Bowen[5] are strongly developed. We also observed the hollow cathode discharge in mixtures of He-O and Ne-O. The spectra so obtained show generally the same lines as the spectra taken with the positive column. The intensity is much smaller and the spectra cannot be so brilliantly excited as in the positive column with great current density.

[4] H. Beutler and B. Josephy, Naturwiss. **15,** 540 (1927); F_c Paschen, Berl. Ber. p. 536. (1928); Y. Takahashi, Ann. d. Physik **3,** 25 (1929); R. A. Sawyer and R. J. Lang, Phys. Rev, **34,** 712 (1929).

[5] I. S. Bowen, Phys. Rev. **29,** 38 (1927).

The Classification of the New Oxygen Lines

A discussion of the structure of the oxygen arc spectrum has been given in the above mentioned paper.[6] It was also shown in this paper that the approximate position of the new terms can be obtained by displacing the Runge-Paschen terms by the distance from the limit ^4S to the limit ^2D and ^2P respectively. These approximate positions are marked by the horizontal dotted lines in the energy diagram Fig. 2. Almost all of the terms of these two other sets are located quite high above the ordinary ionization limit and the corresponding lines will therefore be weak. The lowest term of the oxygen arc spectrum is built by the addition of a $2p$-electron to the core $2s^22p^3$. It combines therefore with the terms of the configurations $2s^22p^3ns$ and $2s^22p^3nd$. The lowest terms of these groups, besides the Runge-Paschen terms, are the terms $(^2D)3s^3D$, $(^2D)3s^1D$, $(^2P)3s^3P$ and $(^2P)3s^1P$. The position of the triplet terms is already given in the previous paper. Table I shows that the strong diffuse triplet 990–988A is resolved in the second order into its six components. The other triplet term $(^2P)3s^3P$ was located in the

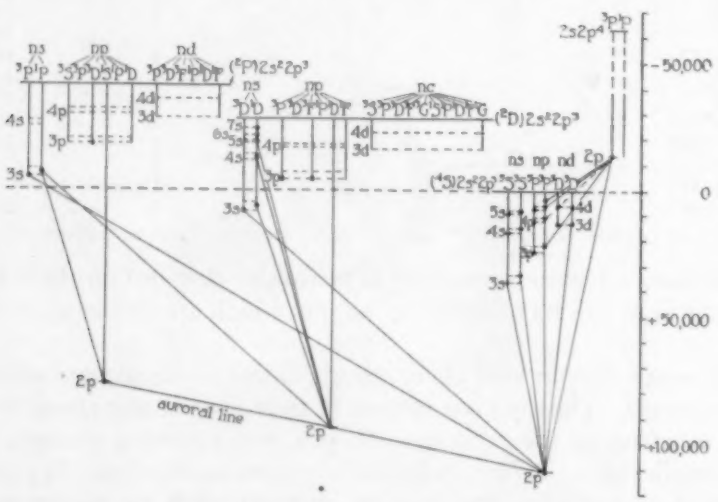

Fig. 2. The term diagram of the OI spectrum.

former paper by a strong combination with the term $(^4S)3p^3P$. Table I gives the combination with the lowest term, $2p^3P$ a strong diffuse triplet at 879–877A. In the second order of the grating, it was impossible to resolve this $^3P^3P'$ group in its six components. This triplet is very strong in the discharge through neon and oxygen.

As Hopfield[7] has shown the frequency difference of the two strong singlet lines 1217.60 and 999.47 is exactly equal to the frequency of the green auroral line = 17925 frequency units. We showed in the former paper that these lines are probably the combinations $2p^1S_0-(^2P)3s^1P_1$ and $2p^1D_2-(^2P)3s^1P_1$ and that a third strong line at 1152A is the combination $2p^1D_2-(^2D)$

[6] R. Frerichs, Phys. Rev. **34**, 1239 (1929).
[7] J. J. Hopfield, Phys. Rev. **29**, 923 (1927).

$3s^1D_2$. Our experiments on the excitation of the different lines (Table II) show that this last line has a lower excitation potential than the other two, in accordance with this classification.

We have now succeeded in finding five members of the series: $2p^1D_2-(^2D)ns^1D_2$. According to Table III, their frequency differences are always between the corresponding frequency differences of the $(^4S)ns^5S_2$ and $(^4S)ns^3S$ terms. This demonstrates again how accurately the new terms can be obtained by the above mentioned displacement of the Runge-Paschen terms. We have used these five members to calculate the limit of this series in order to locate the important $2p^1D_2$ term.

These $(^2D)ns^1D_2$ terms have for their limit the low metastable term ^2D of the O II spectrum. This term has been located by Bowen[8] not only by ultraviolet combinations with higher terms but also more accurately by the forbidden combinations with the lowest term: ^4S, i.e. the nebulium lines 3729.91 and 3727.12, according to his well-known theory. As Hund has shown in Table 34 of his book, the series of the $^1D_2$ terms have in this case the $^2D_{2\frac{1}{2}}$ component of the doublet term for a limit. This term is inverted and according to Shenstone,[9] there are some deviations known from Hund's rule in the case of inverted terms. But Shenstone states in his second paper that, in the case of the addition of an *s*-electron, this rule holds even for inverted terms. The possible error caused by a failure of Hund's rule would be in this case, $^2D_{2\frac{1}{2}}-{}^2D_{1\frac{1}{2}}=20$ frequency units.

TABLE III. *The OI series* $2p^1D_2-(^3D)ms^1D_2$.

$(^4S)ns^3S_1$:		33043.3	13612.5	7425.6	4672.8	3210.2	2340.9
$\Delta(^4S)ns^3S_1$:		19430.8	6186.9	2752.8	1462.6	869.3	
$2p^1D_2-(^3D)ns^1D_2$	λ	1152.06	935.15	882.88	861.63	850.74	
	ν	86801	106935	113266	116059	117545	
	$\Delta\nu$	20134	6331	2793	1486		
$\Delta(^4S)ns^5S_2$:		21710.5	6637.7	2902.9	1526.0	900.3	
$(^4S)ns^5S_2$:		36069.0	14358.5	7720.8	4817.9	3291.9	2391.6

We have tried to get higher series members under conditions where the first four members are strong, but the fifth is always weak and it was not possible to obtain higher members. This is not astonishing when one considers how highly unstable such an atom is in a state 24,000 frequency units above the ordinary ionization limit. However, we can estimate the accuracy of this calculation in the following way. The value for the terms $(^4S)ns^3S_1$ and $(^4S)3s^5S_2$ which is obtained by applying the Rydberg formula to four series members departs only about 6 frequency units from the value which can be obtained by using eight or nine series members. Adding the fifth member reduces this error to 3 frequency units. We believe, therefore, that the error in the limit of our singlet series caused by this method of calculation is not greater than about 3 frequency units, because these terms are located

[8] I. S. Bowen, reference 5.

[9] A. G. Shenstone, Nature **121**, 619 (1928); Nature **122**, 727 (1928).

exactly between the corresponding $(^4S)ns^3S_1$ and $(^4S)ns^5S_2$ terms. The only important source of error will therefore be the comparatively small accuracy in the frequencies at these short wave-lengths.

By this determination the energy values of the terms involved in the emission of the green auroral line are fixed. As we have mentioned above, the classification of this line has been suggested some time ago by McLennan. In the meantime, many attempts have been made to locate these terms. Some predictions of their position have been made by assuming that the relative position of the metastable low terms $^1S_0$ and $^1D_2$ is the same for similar spectra. Sommer as well as Kaplan[10] calculate from the known position of the $^1S_0$, $^1D_2$ and ^3P term in O III the distance $^1D_2-{}^3P$ to be about 15500 frequency units. This is apparently in very good agreement with the observed position although Sommer as well as Kaplan could not give any theoretical reason for their assumption. In a letter to Nature,[11] J. C. McLennan and M. F. Crawford find that the ratio $^1D_2-{}^3P:{}^1S_0-{}^1D_2$ is constant and equal to 0.585 for selenium and tellurium and they assume that this ratio is the same for sulphur and oxygen. Thus, by using the value $^1S_0-{}^1D_2=17925$, they find $^1D_2-{}^3P=10490$. But by comparing the relative positions of such terms in other columns of the periodic table: i.e., C I, Si I, Ge I, Sn I, Pb I or O II, S II, one finds that the ratio between the low terms in all the cases where they are known, is never constant and, therefore, it seems to be without any justification to predict unknown terms in this way.

Another method of prediction of the approximate position of this $^1D_2$ term is based on the calculation of the dissociation energy by means of the convergence point of the oxygen bands. Herzberg[12] has shown that the convergence limit of the Birge-Sponer bands does not correspond to a dissociation into two oxygen atoms in the normal $^3P_2$ state, but to a dissociation into one atom in the $^3P_2$ state and another atom in the $^1D_2$ state. By comparison of the so calculated dissociation energy $O_2\rightarrow O_{1D_2}+O_{3P_2}$ with the chemically measured value $O_2\rightarrow O_{3P_2}+O_{3P_2}$, one obtains the value $O_{1D_2}-O_{3P_2}$. In this way Mecke[13] obtains $^1D_2-{}^3P_2=1.4$ volts, Henri:[14] $^1D_2-{}^1P_2=1.7$ volts the latter value being in better agreement with the observed value: 1.95 volts.

A few words may be said about some other combinations which can be calculated from the known position of the singlet terms. We have not found any intercombination between singlet and triplet terms. The theory of the intensity of intercombinations between singlet and triplet terms has been developed by Houston[15] for atoms with two outer electrons. This theory predicts, in good agreement with the observations, that intercombinations are strong only when the interval between singlet and triplet terms is small compared with the intervals between the different components of the triplet

[10] L. A. Sommer, Zeits. f. Physik **51,** 451 (1928); J. Kaplan, Phys. Rev. **33,** 638 (1929).
[11] J. C. McLennan and M. F. Crawford, Nature **124,** 874 (1929).
[12] G. Herzberg, Zeits. f. Physik Chem. **4,** 13, 233 (1929).
[13] R. Mecke, Naturwiss. **17,** 996 (1929).
[14] V. Henri, Nature **125,** 201 (1930).
[15] W. V. Houston, Phys. Rev. **33,** 297 (1929).

TABLE IV. *Term table of the OI spectrum.*

	$2p$	$^3P_2$: 109831 $^3P_1$: 109672 $^3P_0$: 109605	$^1D_2$: 93962	$^1S_0$: 76037	
		$2s^22p^3$: ^4S	$2s^22p^3$: ^2D	$2s^22p^3$: ^2P	$2s2p^4$
	$3s$	$^5S_2$: 36069.0 $^3S_1$: 33043.3	$^3D_3$: 8702.9 $^3D_2$: 8690.9 $^3D_1$: 8683.0 $^1D_2$: 7161.0	$^3P_2$: −4072.1 $^3P_1$: −4082.5 $^3P_0$: −4088.8 $^1P_1$: −6091	
	$3p$	$^5P_1$: 23211.9 $^5P_2$ 23209.2 $^5P_3$: 23205.8 $^3P_0$: 21207.7 $^3P_1$: 21207.7 $^3P_2$: 21207.2	$^3F_4$: −3876.1 $^3F_3$: −3883.0 $^3F_2$: −3888.7 $^3D_{1,2,3}$ $^3P_2$: −3456.4 $^3P_1$: −3459.8 $^1F_3$ $^1D_2$ $^1P_1$	$^3D_3$: −17443.8 $^3D_2$: −17449.5 $^3D_1$: −17452.9 $^3P_{0,1,2}$ $^3S_1$ $^1D_2$ $^1P_1$ $^1S_0$	
2^2s2p^3	$3d$	$^5D_{0,1,2,3,4}$: 12417.3 $^3D_{1,2,3}$: 12350.0	$^3G_{1,4,5}$ $^3F_{2,3,4}$ $^3D_{1,2,3}$ $^3P_{0,1,2}$ $^3S_1$ $^1G_4$ $^1F_3$: −14495 $^1D_2$ $^1P_1$ $^1S_0$	$^3F_{2,3,4}$ $^3D_{1,2,3}$ $^3P_{0,1,2}$ ^1F $^1D_2$ $^1P_1$	
	$4s$	$^5S_2$: 14358.5 $^3S_1$: 13612.5	$^3D_{1,2,3}$ $^1D_2$: −12972	$^3P_{0,1,2}$ $^1P_1$	
	$4p$	$^5P_1$: 10742.5 $^5P_2$: 10743.7 $^5P_3$: 10734.3 $^3P_{0,1,2}$: 10157.5	$^3F_{2,3,4}$ $^3D_3$: −15936.6 $^3D_2$: −15944.0 $^3D_1$: −15949.0 $^3P_{0,1,2}$ ^1F $^1D_2$ $^1P_1$	$^3D_{1,2,3}$ $^3P_{0,1,2}$ $^3S_1$ $^1D_2$ $^1P_1$ $^1S_0$	
	$5s$	$^5S_2$: 7720.8 $^3S_1$: 7425.6	$^3D_{1,2,3}$ $^1D_2$: −19303	$^3P_{0,1,2}$ $^1P_1$	
	$6s$	$^5S_2$: 4817.9 $^3S_1$: 4672.8	$^3D_{1,2,3}$ $^1D_2$: −22096	$^3P_{0,1,2}$ $^1P_1$	
	$7s$	$^5S_2$: 3291.9 $^3S_1$: 3210.2	$^3D_{1,2,3}$ $^1D_2$: −23582	$^3P_{0,1,2}$ $^1P_1$	
$2s2p^4$	$2p$				$^3P_2$: −13458.0 $^3P_1$: −13516.9 $^3P_0$: −13548.9

TABLE V. *Transitions $2s2p^5 \rightarrow 2s^22p^3np$ in the OI spectrum.*

		$2s^22p^4$			$(^4S)2s^22p^33p$			$(^4S)2s^22p^34p$	$(^4S)2s^22p^35p$	$(^4S)2s^22p^36p$
		$^3P_2$	$^3P_1$	$^3P_0$	$^3P_2$	$^3P_1$	$^3P_0$	$^3P_{0,1,2}$	$^3P_{0,1,2}$	$^3P_{0,1,2}$
		109831	109672	109605	21207.2	21207.7	21207.7	10157.5	5968.6	3926.9
$^3P_2$:	−13458.0	123289	123130		34665.2	34665.7		23615.5	19426.6	17384.9
calc. $2s2p^6\,^3P_1$:	−13516.9	123348	123189	123122	34724.1	34724.6	34724.6	23674.4	19485.5	17443.8
$^3P_0$:	−13548.9		123221			34756.6		23706.4	19517.5	17475.8
	ν	123301	123139		34666.6	34666.6		23615.5	19426.6	17384.9
	λ	811.02	812.09		2883.78*	2883.78*		4233.32	5146.1**	5750.42
obs.	ν	123362	123200	123139	34724.8	34724.8	34724.8	23674.4	19485.5	17443.8
	λ	810.62	811.69	812.09	2878.95*	2878.95*	2878.95*	4222.78	5130.6**	5731.0
	ν		123239			34756.7		23706.4	19517.5	17475.81
	λ		811.43			2876.30*		4217.09	5122.1**	5720.61

** Not observed.

* See: A. Fowler Proc. Roy. Soc. **(A) 110,** 476, (1926) unclassified OII lines.

term. Although this theory cannot be applied to the more complicated case of the oxygen atom, the very small intervals of the oxygen terms may be responsible for the missing intercombination lines. It is in agreement with Houston's theory that, in the case of selenium and tellurium, where the intervals are much larger, such intercombinations have been found by McLennan.

The green auroral line is according to its classification, the exact analogue of the nebular line 4363.21A. We should therefore expect to find also the other combinations $^3P_2-{}^1D_2$ and $^3P_1-{}^1D_2$ which correspond to the nebular lines 5006.84 and 4958.91A. According to Table IV, these lines are located at 6299 and 6363A with an error of approximately ± 5A. These lines are neither found in the laboratory nor in the spectrum of the aurora or of the night sky.

Among the new triplet terms (Table IV), the term: $2s2p^5\,{}^3P$ is especially interesting. By application of the irregular doublet law to the oxygen-like isoelectronic spectra, Mack and Sawyer[16] have predicted its position as about 15000 frequency units above the ordinary ionization limit, the ^4S term of the ion, in good agreement with the observed value. Under the unclassified lines in the near ultraviolet and in the visible, there are some triplets which give the intervals 58.9 and 32 frequency units. Table V shows that these triplets are combinations of this $2s2p^{53}P$ term with the terms: $(^4S)2s^22p^3\,np\,{}^3P$. The combination $(^4S)2s^22p^35p\,{}^3P-2s2p^5\,{}^3P$ is not known, perhaps due to the small sensitivity of the photographic plates in this region. The term: $2s2p^5\,{}^3P$ combines with a ^3P term at 3926 and the application of the Rydberg formula shows that this term is the hitherto unknown term $(^4S)2s^2\,2p^3\,6p\,{}^3P$.

We are indebted to the Rockefeller Foundation for the grant of a fellowship, to Professor R. A. Millikan for extending the facilities of the Norman Bridge Laboratory and to Professor I. S. Bowen for helpful discussions and suggestions.

Note added with proof: Prof. Paschen writes me that he has recently observed the two lines $^3P_2-{}^1D_2$ and $^3P_1-{}^1D_2$ at 6300.06 and 6363.86A respectively in a discharge through pure oxygen. This proves that the above given calculation of the singlet terms is accurate within 0.5 frequency units. S. Goudsmit, Phys. Rev. **35,** 1325, (1930) finds by theoretical calculations the above mentioned value of McLennan in disagreement with our measurements. V. Kondratjew, Zeits. f. Phys. Chem. **B. 7,** 70, (1930) obtains from the oxygen bandspectra the value 1.91 volts for the difference $^3P_2-{}^1D_2$ in very good agreement with the observed value 1.95 volts.

[16] J. E. Mack and R. A. Sawyer, Phys. Rev. **35,** 299 (1930).

BAND SPECTRA INTENSITIES FOR SYMMETRICAL DIATOMIC MOLECULES

By Elmer Hutchisson
Berlin, Germany

(Received June 20, 1930)

Abstract

The intensity of a spectral line may be calculated in the new quantum mechanics by evaluating the integral of the product of the electric moment and the wave functions of the initial and of the final states. The complete wave function may be written approximately as a product of a nuclear wave function and an electronic wave function. Furthermore, the electric moment can be approximately written as the sum of a function of the nuclear coordinates only and a function of the electronic coordinates only. For symmetrical diatomic molecules the term in the electric moment which is a function of the nuclear coordinates only is zero so that the intensity integral reduces to a double integral which may be written as a product of an electronic integral and a nuclear integral. The electronic integral is constant for all the lines corresponding to the same electronic transition and the integrand of the nuclear integral consists only of the product of the radial wave functions for the initial and the final states. The integration of the nuclear integral is carried out using harmonic oscillator wave functions whose origins are shifted due to the change of the nuclear separation during the electronic transition.

A comparison is made between the intensities calculated in the above manner and those obtained by experiment. In the case of Na_2 good quantitiative agreement is obtained between the experimental and the calculated results. Accurate values of the moments of inertia in the initial and final states are not known for K_2 but it is possible to show that if a value of the change in the nuclear separations during the transition is assumed, agreement is possible for all of the lines corresponding to low quantum numbers. Good qualitative agreement is obtained for I_2. Calculations are made for the absorption spectra and the $3'B-2'S$ emission band system of H_2 but the agreement in these cases is not as good as for Na_2 and K_2.

I. Introduction

ON THE basis of the old quantum theory Condon[1] was able to show that in connection with a given electronic transition in a diatomic molecule certain transitions were more probable than others. His calculations were based upon Franck's[2] assumption that during an electronic transition nuclei which are originally in a non-vibrating state remain momentarily fixed because of their large masses compared with those of the electrons. Since the equilibrium distance between the nuclei is altered due to the motion of the electrons, the nuclei acquire a potential energy with respect to the new equilibrium points and begin to vibrate. The amplitude of the vibration acquired after the transition is approximately equal to the change in the equilibrium

[1] E. Condon, Phys. Rev. **28**, 1182 (1926).
[2] J. Franck, Trans. Faraday Society (1925).

separations, therefore it is possible for the most probable nuclear transition to be calculated.

If the nuclei are vibrating in the initial state then almost any amplitude in the end state is possible. A calculation similar to that mentioned above can be employed except that instead of focusing our attention on the equilibrium position in the initial state, we focus our attention on the positions in which the nuclei spend most of the time. These positions will naturally be the turning points of the vibratory motion. With potential energy diagrams to determine the turning points of the vibration Condon was able to show that the positions of maximum intensities in the well-known double entry tables lie along a parabolic path and agree fairly well with experiment. As Condon's theory is essentially only one of transition probabilities the distribution in the initial state is not included.[3]

In a second paper Condon[4] showed that the ideas expressed above on the basis of the old quantum theory could be carried over into the new quantum mechanics. In the new quantum mechanics the intensity of a spectral line may be calculated by evaluating the integral of the product of the electric moment and the wave functions of the initial and final states where the integration is carried out over all of the coordinates of the electrons and the nuclei. Thus a measure of the intensity is given by the expression (following Condon):

$$I = \int\int M(x, r)\psi_{e'n'}(x, r)\psi_{e''n''}(x, r)dxdr,$$

where M is the instantaneous electric moment, $\psi_{e'n'}$ and $\psi_{e''n''}$ are the wave functions of the initial and final states, x and r are total coordinates of the electron and of the nuclei respectively and e and n are electronic and vibrational quantum numbers. According to the work of Born and Oppenheimer[5] the complete wave function ψ_{en} can be approximately expressed as a product of an electronic wave function $\Phi_e(x)$ and an oscillatory wave function $\Psi_{en}(r)$. The latter function corresponds to the motion of the nuclei moving under an effective force arising from the moving electrons and the repulsion of the nuclei. We may write our integral:

$$I = \int\int M(x, r)\Phi_{e'}(x)\Psi_{e'n'}(r)\Phi_{e''}(x)\Psi_{e''n''}(r)dxdr.$$

The electric moment is defined as the vector sum of the coordinates of the electrons times their charge and the coordinates of the nuclei times their charge. This may be approximately expressed in the following way:

$$M(x, r) = A(x) + B(r)$$

because during the transition of the electrons the nuclei remain practically fixed and the first term (representing the vector sum of the electronic charges

[3] Cf. G. Herzberg, Zeits. f. Physik **49**, 761 (1928).
[4] E. Condon, Phys. Rev. **32**, 858 (1928).
[5] M. Born and Oppenheimer, Ann. d. Physik **84**, 457 (1927).

times x) will be a constant over the integration of the electron coordinates. The second term (representing the vector sum of the nuclear charge times r) will be a function of only the nuclear coordinates because the heavy nuclei cannot respond immediately to the changes in the electronic arrangement. We have therefore:

$$I = \int A(x)\Phi_{e'}(x)\Phi_{e''}(x)dx \int \Psi_{e'n'}(r)\Psi_{e''n''}(r)dr + \int \Phi_{e'}(x)\Phi_{e''}(x)dx \int B(r)\Psi_{e'n'}(r)\Psi_{e''n''}(r)dr.$$

The integrals involving the electron coordinates will be constant for a given electronic transition so that

$$I = C_1 \int \Psi_{e'n'}(r)\Psi_{e''n''}(r)dr + C_2 \int B(r)\Psi_{e'n'}(r)\Psi_{e''n''}(r)dr.$$

This integral cannot be evaluated in general because we do not know the ratio of the constants ($B(r)$ is probably a linear function). However if we restrict ourselves to symmetrical diatomic molecules the nuclear electric moment will always be zero so that the last term drops out and we have only

$$I = C_1 \int \Psi_{e'n'}(r)\Psi_{e''n''}(r)dr. \tag{1}$$

It is the purpose of this paper to evaluate this integral and to compare the results with experiment in several cases.

II. Intensities for Harmonic Oscillations

The approximate wave equation for the nuclear motions of the diatomic molecule may be written

$$\nabla^2\Psi + \frac{8\pi^2\mu}{h^2}\left[W - \frac{Z^2e^2}{r} + V_e(r)\right]\Psi = 0 \tag{2}$$

where Ze is the charge on one of the nuclei, μ is the equivalent mass ($=M_1M_2/M_1+M_2$), r is the separation of the nuclei and $V_e(r)$ is the mean potential energy due the electrons. The wave function may be separated into three functions in the usual manner by setting $\Psi = N\Phi(\phi)\cdot\Theta(\theta)\cdot R(r)/r$ where N is a normalizing factor. The equations in ϕ and θ will not have any effect[6] on the calculated intensities of the spectral lines and we may therefore pass immediately to the equation in r

$$\frac{d^2R}{dr^2} - \frac{m(m+1)}{r^2}R + \frac{8\pi^2\mu}{h^2}\left[W - \frac{Z^2e^2}{r} + V_e(r)\right]R = 0 \tag{3}$$

[6] A. Sommerfeld, Ergänzungsband, p. 69.

where m is the rotational quantum number. Making the substitution $\rho = r/r_0$ (r_0 = equilibrium separation of the nuclei) we obtain

$$R'' + \left[\frac{8\pi^2 J_0}{h^2}(W - f(\rho)) - \frac{m(m+1)}{\rho^2}\right]R = 0 \tag{4}$$

in which $J_0 = \mu r_0^2$ and $f(\rho)$ represents the effective potential energy.

In this paper we will restrict ourselves to linear oscillations and we may therefore put $f(\rho) = -D + [(2\pi\nu_0)^2 J_0/2]\,\xi^2$ where $\xi = \rho - 1$ and D is the dissociation energy and ν_0 is the frequency of vibration for very small amplitudes. Making use of this expression in Eq. (4) and expanding ρ in terms of ξ (or, one could set $m = 0$) and finally making the substitution $\eta = 2\pi(\nu_0 J_0)^{1/2}/(h)^{1/2}\,\xi$, we obtain

$$R'' + \left[\frac{2}{h\nu_0}\left\{W + D - m(m+1)\frac{h^2}{8\pi^2 J_0}\right\} - \eta^2\right]R = 0 \tag{5}$$

which is the wave equation for the linear oscillator.[7]

The solution of this equation is well known and may be written

$$R_n = \frac{1}{N_n}e^{-\eta^2/2}H_n(\eta) \quad \text{and} \quad W + D - m(m+1)\frac{h^2}{8\pi^2 J_0} = \left[n + \frac{1}{2}\right]h\nu_0 \tag{6}$$

where n is the vibrational quantum number and $H_n(\eta)$ is a Hermitian polynominal.

We wish to evaluate the integral (1) which may now be written in terms of (ρ) and the radial wave function, in the following manner:

$$I = \text{const.}\int_0^\infty R_{e'n'}(\rho)R_{e''n''}(\rho)d\rho. \tag{7}$$

As far as the nuclei are concerned the effect of an electron transition is, that besides the change in the equilibrium positions of the nuclei there is also a change in the binding or potential energy such that the nuclei acquire a new vibration frequency after the transition. Therefore if we take $R_{e'n'} = (1/N_{n'})e^{-\eta^2/2}H_{n'}(\eta)$ as the nuclear part of the wave function for the upper state, we will have for the lower state $R_{e''n''} = (1/N_{n''})\exp -[(\alpha\eta+\delta)^2/2]\,H_{n''}(\alpha\eta+\delta)$ where α and δ represent respectively measures of the change in frequency and the change in equilibrium position. From the definition of η we see that

$$\eta = [2\pi(\nu_0' J_0')^{1/2}/(h)^{1/2}r_0]r - 2\pi(\nu_0' J_0')^{1/2}/(h)^{1/2}$$

so that

$$\alpha\eta + \delta = [(\alpha 2\pi(\nu_0' J_0')^{1/2}/(h)^{1/2}r_0'][r + \delta r_0'(h)^{1/2}/2\pi\alpha(\nu_0' J_0')^{1/2}]$$
$$- \alpha 2\pi(\nu_0' J_0')^{1/2}/(h)^{1/2} = [2\pi(\nu_0''\mu)^{1/2}/(h)^{1/2}]r - 2\pi(\nu_0''\mu)^{1/2}r_0''/(h)^{1/2}.$$

Thus $\alpha = (\nu_0''/\nu_0')^{1/2}$ and

[7] E. Fues, Ann. d. Physik **80**, 367 (1926).

$$\delta = (r_0' - r_0'')2\pi(\nu_0''\mu)^{1/2}/(h)^{1/2} = 0.1221(r_0' - r_0'')(\nu_0''M)^{1/2}$$

where ν_0'' is expressed in cm^{-1}, M is the atomic weight (O = 16) of one of the atoms and $(r_0' - r_0'')$ is in Angstroms.

The integral (7) then becomes

$$I = \text{const} \int_{-\infty}^{+\infty} (N_{n'}N_{n''})^{-1} e^{-\eta^2/2} e^{-(\alpha\eta+\delta)^2/2} H_{n'}(\eta) H_{n''}(\alpha\eta + \delta) d\eta \qquad (8)$$

where the limits are taken from $-\infty$ to $+\infty$ instead of from -1 to $+\infty$ since the addition of the region from -1 to $-\infty$ will not appreciably affect the value of the integral for small quantum numbers. The values of the normalizing factors are well known for the linear oscillator, being

$$N_{n'} = [2^{n'}n'!\pi^{1/2}h^{1/2}/2\pi(\nu_0'\mu)^{1/2}]^{1/2}$$

$$N_{n''} = [2^{n''}n''!\pi^{1/2}h^{1/2}/2\pi(\nu_0''\mu)^{1/2}]^{1/2} \qquad (9)$$

In order to carry through the integration of Eq. (8) the method used by Schrödinger[8] in the Stark effect may be applied. The "erzeugende" function[9] for the Hermitian polynomial is

$$\sum_{n'=0}^{n'=\infty} \frac{H_{n'}(\eta)}{n'!} s^{n'} = e^{-s^2+2s\eta}$$

and for the function of the lower state

$$\sum_{n''=0}^{n''=\infty} \frac{H_{n''}(\alpha\eta + \delta)}{n''!} t^{n''} = e^{-t^2+2t(\alpha\eta+\delta)}.$$

If these expressions are multiplied together and also multiplied by the exponentials in Eq. (8) we have after integration

$$\sum_{n'=0}^{n'=\infty} \sum_{n''=0}^{n''=\infty} \frac{s^{n'}t^{n''}}{n'!n''!} \int_{-\infty}^{+\infty} H_{n'}(\eta) H_{n''}(\alpha\eta + \delta) e^{-\eta^2/2} e^{-(\alpha\eta+\delta)^2/2} d\eta$$

$$= \int_{-\infty}^{+\infty} e^{-s^2+2s\eta-\eta^2/2} e^{-t^2+2t(\alpha\eta+\delta)-(\alpha\eta+\delta)^2/2} d\eta \qquad (10)$$

$$= \left(\frac{2\pi}{\alpha^2+1}\right)^{1/2} e^{-\delta^2/2(\alpha^2+1)} e^{[(s^2-t^2)(1-\alpha^2)-2\alpha\delta s+2\delta t+4\alpha st]/(1+\alpha^2)}.$$

By expanding the last exponential factor in powers of s and t and then equating the like powers of s and t on both sides of the equation we obtain for the expression for the integral for each value of n' and n''. Making use of Eqs. (9), Eq. (8) becomes

$$\int_{-\infty}^{+\infty} (N_{n'}N_{n''})^{-1} e^{-\eta^2/2} e^{-(\alpha\eta+\delta)^2/2} H_{n'}(\eta)\ H_{n''}(\alpha\eta + \delta) d\eta \qquad (11)$$

$$= C_3 \frac{(n'!n''!)^{1/2}}{2^{(n'+n'')/2}} \sum_{l=0}^{n' \text{ or } n''} \sum_{i=0}^{(n'-l)/2} \sum_{j=0}^{(n''-l)/2} a_{2i}b_{2i}c_{2j}d_{n'-2i-l}e_{n''-2j-l}$$

[8] E. Schrödinger, Ann. d. Physik **80**, 486 (1926).

[9] Courant and Hilbert, Methoden der mathematischen Physik I (Berlin 1924) p. 76.

where

$$C_3 = \left(\frac{h}{2\pi^2\mu\nu_0'\alpha(\alpha^2+1)}\right)^{1/2} e^{-\delta^2/2(\alpha^2+1)} \qquad a_{2l} = \frac{1}{l!}\left(\frac{4\alpha}{1+\alpha^2}\right)^l$$

$$b_{2i} = \frac{1}{i!}\left(\frac{1-\alpha^2}{1+\alpha^2}\right)^i \qquad c_{2j} = \frac{1}{j!}\left(\frac{-(1-\alpha^2)}{1+\alpha^2}\right)^j$$

$$d_{n'-2i-l} = \frac{1}{(n'-2i-l)!}\left(\frac{-2\alpha\delta}{1+\alpha^2}\right)^{(n'-2i-l)}$$

$$e_{n''-2j-l} = \frac{1}{(n''-2j-l)!}\left(\frac{2\delta}{1+\alpha^2}\right)^{(n''-2j-l)}$$

and where the upper limit of the first sum is the smaller of n' or n'' and the upper limits of the second and third sums are either the upper or lower figures depending upon whether $n-k$ is even or odd. In order to visualize these terms and to use them in the numerical calculations the smallest ones are given in Table I. The value of the integral for (n'', n') can be obtained from

TABLE I.

n'	n''	Value of the integral (11)
0	0	1
0	1	$(1/2^{1/2})e_1$
0	2	$(1/2^{1/2})[e_2+c_2]$
1	1	$(1/2)[d_1e_1+a_2]$
0	3	$(3^{1/2}/2)[e_3+c_2e_1]$
1	2	$(1/2)[d_1e_2+c_2d_1+a_2e_1]$
0	4	$(3/2)^{1/2}[e_4+c_2e_2+c_4]$
1	3	$(3/8)^{1/2}[d_1e_3+c_2d_{1+1}+a_2e_2+a_2c_2]$
2	2	$(1/2)[d_2e_2+c_2d_2+b_2e_2+b_2c_2+a_2d_1e_1+a_4]$
0	5	$(15^{1/2}/2)[e_5+c_2c_3+c_4e_1]$
1	4	$(3^{1/2}/2)[d_1e_4+c_2d_1e_2+c_4d_1+a_2e_3+a_2c_2e_1]$
2	3	$(3/8)^{1/2}[d_2e_3+c_2d_2e_1+b_2e_3+b_2c_2e_1+a_2d_1e_2+a_2c_2d_1+a_4e_1]$
1	5	$(15/8)^{1/2}[d_1e_5+c_2d_1e_3+c_4d_1e_1+a_2e_4+a_2c_2e_2+a_2c_4]$
2	4	$(3^{1/2}/2)[d_2e_4+c_2d_2e_2+c_4d_2+b_2e_4+b_2c_2e_2+b_2c_4+a_2d_1e_3+a_2c_2d_1e_1+a_4e_2+a_4c_2]$
3	3	$(3/4)[d_2e_3+c_2d_2e_1+b_2d_1e_3+b_2c_2d_1e_1+a_2d_2e_2+a_2c_2d_2+a_2b_2e_2+a_2b_2c_2+a_4d_1e_1+a_6]$
2	5	$(15/8)^{1/2}[d_2e_5+c_2d_2e_3+c_4d_2e_1+b_2e_5+b_2c_2e_3+b_2c_4e_1+a_2d_1e_4+a_2c_2d_1e_2+a_2c_4d_1+a_4e_3+a_4c_2e_1]$
3	4	$(3/8^{1/2})[d_2e_4+c_2d_2e_2+c_4d_2+b_2d_1e_4+b_2c_2d_1e_2+b_2c_4d_1+a_2d_2e_3+a_2c_2d_2e_1+a_2b_2e_3+a_2b_2c_2e_1+a_4d_1e_2+a_4c_2d_1+a_6e_1]$
4	4	$(3/2)[d_4e_4+c_2d_4e_2+b_2d_2e_4+b_2c_2d_2e_2+b_4e_4+c_4d_4+b_4c_4+a_2d_2e_3+a_2b_2d_1e_3+a_2c_2d_2e_1+a_2c_2b_2d_1e_1+a_4d_2e_2+a_4c_2d_2+a_4b_2e_2+a_4b_2c_2+a_6d_1e_1+a_8]$

$(n'n'')$ by interchanging subscripts on "b" and "c" and on "d" and "e", i.e $a_2b_2c_0d_1e_2$ becomes $a_2b_0c_2d_2e_1$. All coefficients with the subscript zero are equal to unity and are therefore omitted.

III. COMPARISON WITH EXPERIMENT

In the preceding section a formula is developed which allows the matrix elements of the electric moment to be calculated for vibration transitions in symmetrical diatomic molecules. The relative intensities of the bands in the electronic-vibration spectra of these molecules are calculated by squaring the integral (11) and multiplying by the fourth power of the frequency and by the

distribution factor of molecules in the initial state.[9] It is somewhat difficult to know exactly what frequency to multiply by because the intensity obtained should apply to the sum of all the rotational transitions which have the same vibrational and electronic quantum numbers. If the rotational quantum number in Eq. (4) is set equal to zero then we should expect our calculated intensities to agree with those in the $Q(0)$ branch corresponding to the given electronic and vibrational transition. However, in any case, the changes in the frequencies associated with different vibrational transitions are very small since the change in vibrational energy is very small compared to the change in the electronic energy. Since the frequency factors do not appreciably affect the comparison of the calculated results with experiment, they have been omitted in the tables given below.

It is practically impossible at present to calculate accurately the expected intensity in emission spectra because the distribution factor for the initial state depends not only upon the temperature but also upon the method of excitation and upon whether or not the molecules have reached their initial excited levels by means of a transition from a higher level. It should be possible however, to calculate the relative intensities of those bands which originate from the same initial vibrational level and the emission diagrams should show agreement in the horizontal rows. In absorption spectra it is easily possible to calculate the expected absorption intensity for a given temperature because in this case the distribution factor is merely the appropriate Boltzmann factor. However, when we try to compare the calculated results with experiment we find that the exact temperature or pressure is seldom recorded in absorption spectrum intensity measurements. In the following calculated results no attempt has been made to include the temperature factor because of the uncertainty in the exact temperatures used in obtaining the experimental results. We have calculated the intensities for the first few vibrational levels only (because of the restriction to harmonic oscillations) so that in some cases the temperature distribution will not vary greatly from a uniform distribution and merely the squares of the integral (11) should be in approximate agreement with the experimental results, in other cases, only the agreement in the columns (for absorption) should be considered.

In making the theoretical intensity calculations the values of α and δ are first calculated. The value of α which is given by $(\nu_0''/\nu_0')^{1/2}$ is usually very well known since it comes from an analysis of the vibrational energy levels themselves. The value of α may therefore be determined to within three significant figures. The value of δ depends upon the values of the separations of the nuclei which in turn depend upon the values of the moments of inertia given by the analysis of the rotational spectrum. The values of the nuclear separations thus calculated are usually accurate only to within about 1 percent so that δ which depends upon the difference in the separations in the initial and final states ($\delta = 0.1221\ (r_0' - r_0'')\ (\nu_0'' M)^{1/2}$) is, in general, susceptible to quite large errors. The next step in the calculations

[9] Cf. A. Sommerfeld, Ergänzungband, p. 96.

is to evaluate the coefficients a, b, c, d, and e given after Eq. (11). The triple sum in Eq. (11) is then evaluated which in the highest state ($n'=4$, $n''=3$) considered, consists of 13 terms. In the diagrams given below the observed and calculated intensities are given in the usual double-entry form. In every case the observed intensities are placed on top and the corresponding calculated ones are given directly underneath them. Each element will be treated in a separate section.

a. Sodium.

The experimental and calculated data for the green absorption band of sodium (Na_2) are shown completely in Fig. 1. It may be seen that here the agreement is rather remarkable, perhaps much better than one would expect

n' \ n''	0	1	2	3	4
0	2 2.00	5 4.52	5 4.78	5 5.32	4 3.98
1	9 5.82	6 5.00	— 1.22	— 0.04	4 1.32
2	8 7.78	— 0.68	— 1.22	3 3.26	— 1.70
3	6 6.28	— 1.02	3 3.26	2 0.40	— 2.38
4	5 3.42	2 4.82	3 0.60	— 1.53	

Fig. 1. Observed and calculated intensities in the green Na_2 absorption band. The observed values are placed on top.

with the available intensity measurements which are only estimates.[10] The experimental intensities are taken from Fredrickson and Watson.[11] The values of the frequencies and of the nuclear separations are taken from Loomis and Wood[12] and give for α and δ the values 1.130 and 2.43 respectively. Fredrickson and Watson give the nonappearance of the bands (1–2), (2–1), (3–1), (2–2) and (1–3) as an especial characteristic of this system and the calculated intensities indicate very definitely the fact that these particular bands should be very faint. The calculated intensities in the positions (1–2) and (2–1) are quite sensitive to changes in the nuclear separations and indeed, when the writer first calculated these intensities, he used the value $r_0'-r_0''=0.40\cdot 10^{-8}$ cm given by Fredrickson and Watson and found complete disagreement with experiment since the values in the positions (1–2) and (2–1) were approximately 12 on the same scale as used in Fig. 1. Later he found that Loomis

[10] The Physical Review Referee has kindly pointed out that since at 1000°K the relative distribution in the initial states $n''=0,1,2,3,4$ is 1.00, 0.80, 0.64, 0.51, 0.41 respectively, the agreement in the top row of Fig. 1 can only be accidental and that the agreement in the columns only should be noticed.

[11] W. R. Fredrickson and W. W. Watson, Phys. Rev. **30**, 429 (1927).

[12] F. W. Loomis and R. W. Wood, Phys. Rev. **32**, 223 (1928).

and Wood had pointed our errors in Fredrickson and Watson's analysis and that they gave instead the value $r_0' - r_0'' = 0.33 \cdot 10^{-8}$ cm from which the values given were calculated.

b. Potassium.

Fredrickson and Watson[11] give an intensity diagram for the near red potassium absorption band which is very similar to the green band of sodium. However, as was the case with sodium, the nuclear separations which they give ($r_0' - r_0'' = 0.43 \cdot 10^{-8}$ cm) do not give calculated intensities which agree at all with experiment. It is interesting however, that because of the absence of the (1–2) and (2–1) bands and because of the likeness to Na_2 it is possible to estimate the change in the nuclear separation for K_2. The value of δ which is obtained is almost the same as that for Na_2 and since $(\nu_0'' M)^{1/2}$ is practically identical in both cases the value of $r_0' - r_0''$ can be estimated to be close to the same value as for sodium ($0.33 \cdot 10^{-8}$ cm) although it may possibly be as low as $0.29 \cdot 10^{-8}$ cm. The agreement for only the first few terms when $0.33 \cdot 10^{-8}$ cm is used is shown in Fig. 2. The principle point in favor of the

n' \ n''	0	1	2
0	3 3.00	8 7.02	9 8.97
1	10 8.64	5 7.68	— 1.80
2	8 11.55	— 1.13	2 1.86

Fig. 2. Observed and calculated intensities in the near red K_2 absorption band. The observed values are placed on top.

argument for the change in separations chosen is that the *only* value, which gives a general agreement throughout all terms, is just the value which reduces the (2–1) and (1–2) terms to a very small value.

c. Iodine.

The iodine spectrum is characterized by the fact that intense bands correspond to changes of very large quantum numbers. Because of this fact it is obvious that we cannot expect to calculate the exact intensities by the integral (11) which is derived on the assumption of harmonic oscillations. We can however, draw important qualitative conclusions from this formula. If we restrict ourselves to the first column, that is, to all bands which result from a transition from the lowest initial vibrational state, we find that the most important term in the theoretical calculation is the d term which has the same index as the vibrational quantum number of the end state n'. The constants given by Mecke[13] for iodine give $\alpha = 1.300$ and $\delta = 14.9$. Because of the large value of δ we find it is just the d coefficients which are extremely

[13] Mecke, Handbuch der Physik XXI, p. 547.

large, in fact d_{14} is about 20,000 times d_0. The values of the coefficients go up rather rapidly to a maximum at d_{14} and then slowly decrease. To calculate the intensities we must square these values of d and multiply by the square of the normalizing coefficient which tends to shift the maximum intensity in the direction of large quantum numbers. It requires therefore no stretch of the imagination to conclude that the first terms will be insignificant with respect to later ones and that observable terms will begin to appear at about $n'=14$ and extend out into the neighborhood of $n'=60$ or more. The appearance of lines in these positions is in agreement with the experimentally observed intensities.

Because of the effect of the Boltzmann distribution factor, there are very few molecules in the higher n'' states so that the absence of transitions starting from the higher n'' levels is explained even though their calculated transition probabilities are large.

d. Hydrogen.

In the absorption spectrum of hydrogen all the transitions have the same initial quantum level ($n''=0$) and we should therefore expect Eq. (11) to give a fairly accurate representation of their intensities. The intensiy constants for the hydrogen absorption spectra are obtained from the molecular constants given by Richardson and Davidson[14] and are $\alpha=1.786$ and $\delta=4.45$ The agreement of the calculated intensities with the absorption data given by Dieke and Hopfield[15] is shown in Fig. 3. The agreement in this case is not

n'	0	1	2	3	4	5	6	7	8	9
I_0	2	6	8	5	4	8	3	6	4	6
I_c	1.0	7.2	22.5	38.5	39.0	20.7	4.2	0.02	1.2	0.19

Fig. 3. Observed (I_o) and calculated (I_c) intensities for the ultra-violet absorption spectrum of the hydrogen molecule. The initial vibrational state of all of these transitions is the same.

good although it will be seen that the theoretical calculations give about the right number of bands at least. No explanation of these discrepancies can be given but it must be realized that the intensities are in the extreme ultraviolet where it is very difficult to make accurate absorption estimates. Because of the similarity of the higher wave functions one would expect the intensities of the higher observed bands to become gradually smaller rather than to break off suddenly as is shown in the figure. It may be possible too that the fact that a harmonic oscillator was assumed will explain the discrepancies in the bands at the right of the figure.

Although as was stated earlier, we cannot expect very close agreement between emission spectra and the calculated intensities the emission spectra of the $3^1B \rightarrow 2^1S$ band system of hydrogen shows some interesting points. The notation and constants are taken from Richardson and Davidson[14] and we find $\alpha=0.784$ and $\delta=-1.008$. The experimental values are taken from

[14] A. W. Richardson and P. M. Davidson, Proc. Roy. Soc. **A125**, 35 (1929).
[15] G. H. Dieke and J. J. Hopfield, Phys. Rev. **30**, 400 (1927).

Kapucinsky and Eymers'[16] intensity measurements. These measurements are in the visible region and were carefully made by means of a registering microphotometer so that great faith may be had in the results. The experimental and calculated intensities are shown together in Fig. 4. It will be seen in this

n \ n''	0	1	2	3
0	286 286	95 223	29 41.8	9.1 1.4
1 2	375 137	35.4 42.6	159 257	56 26.9
2	75.2 73.5	395 72.4	5.4 6.6	61 194
3	(8) 32.6	102 88.4	142 10.9	29.3 24.6

Fig. 4. Observed and calculated intensities in the $3'B \rightarrow 2'S$ emission band system of hydrogen. The observed intensities are placed on top.

figure that good agreement is obtained except at the positions in which n changes by ± 1 units. At these positions the intensities are apparently reversed, that is, the one corresponding to a change in n of $+1$ agrees better in every case with the experimental intensity corresponding to a change of -1 in n and vice versa. No explanation of this fact can be given at the present time.

IV. Conclusion

On the basis of wave mechanics the intensity of a spectral line is measured by the integral of the product of the electric moment and the wave functions of the initial and of the final states. It is possible to carry this integration through approximately for vibration electronic transitions in symmetrical diatomic molecules. In this way a formula is developed for the intensity of any band in the electronic vibration spectra of these molecules. The intensities of certain spectral bands of Na_2, K_2, I_2, and H_2 are calculated and in some cases rather good agreement with experiment is obtained. It should be noticed that although there are discrepancies in many of the results the general intensity values and the number of lines to be expected agree well with experiment in all cases in spite of the fact that the important constant (depending upon nuclear separations) varies from -1.01 in the $3'B-2'S$ band of hydrogen to $+14.9$ in the absorption spectrum of iodine.

The writer wishes to express his sincere appreciation to Professor E Schrödinger for many helpful suggestions and for the privilege of using the facilities of the Institut für theoretische Physik at Berlin. The writer wishes also to thank the University of Pittsburgh for a grant which helped to make his stay in Europe possible.

[16] W. Kapucinsky and J. G. Eymers, Proc. Roy. Soc. **A122**, 58 (1929).

VIBRATIONAL QUANTUM ANALYSIS OF THE POTASSIUM INFRARED ABSORPTION BANDS

By W. O. Crane and Andrew Christy

Ryerson Physical Laboratory, University of Chicago

(Received June 19, 1930)

Abstract

The heads of the red system of the K_2 molecule have been remeasured, and twenty six new bands have been found. The vibrational constants derived from our measurements are: $\omega_e''=92.64$ cm^{-1}, $\omega_e''x''=0.354$ cm^{-1}, $\omega_e'=74.73$ cm^{-1}, and $\omega_e'x'=0.327$ cm^{-1}.

The bands of the infrared system of K_2 (λ7735 to λ8850) have been measured and a new vibrational analysis for this system is given, which removes the objections inherent in the analysis of Ritschl and Villars. The constants for this system, as found by us, are: $\omega_e''=92.64$ cm^{-1}, $\omega_e''x''=0.354$ cm^{-1}, $\omega_e'=69.09$ cm^{-1}, and $\omega_e'x'=0.153$ cm^{-1}. It is shown that the upper state of each of the two systems dissociates into a normal and a ^2P excited atom. The energies of dissociation obtained for the upper levels of the two systems agree to within 0.02 volts, the average value being 2.41 volts. From this average value we obtain for the heat of dissociation of the lower level 0.81 volts, while from the formula $(\omega_e'')^2/4\omega_e''x''$, we obtain 0.75 volts.

THE absorption spectrum of the K_2 molecule thus far investigated contains three band systems: in the blue, $D\leftarrow A^1\Sigma$, (λ4243 to λ4613), in the red, $C^1\Pi\leftarrow A^1\Sigma$ (λ6280 to λ6925), and in the infrared, $B^1\Sigma\leftarrow A^1\Sigma$($\lambda$7735 to λ8850).

The vibrational analysis of the blue system has been given by Yamamoto[1,2] The equation of the band heads in terms of half quantum numbers is:

$$\nu = 22970.0 + 61.28(v' + \tfrac{1}{2}) - 0.24(v' + \tfrac{1}{2})^2 - 92.54(v'' + \tfrac{1}{2}) + 0.353(v'' + \tfrac{1}{2})^2 \quad (1)$$

The red system, $C^1\Pi\leftarrow A^1\Sigma$, was analyzed by Fredrickson and Watson.[3] The equation connecting the heads in terms of half quantum numbers is:

[1] H. Yamamoto, Nat. Research Council Japan **5**, 146 (1929).

The equation actually given is:

$$\nu=22954.6+(61.13n'-0.24n'^2)-(91.96n''-0.32n''^2)$$

The constants for the equation, according to Yamamoto, were obtained by the least square method. However, there must have been some error in the calculation of ω_0'' and $\omega_0''x''$. When the least square method is applied to all the intervals as actually obtained from the heads given in the paper the authors find: $\omega_0''=92.19$ cm^{-1} and $\omega_0''x''=0.353$ cm^{-1}. These values are used in Eq. (1). These corrected values of the constants ω_0'' and $\omega_0''x''$ agree exactly with the constants as derived by the authors from the two other systems.

[2] See also W. Weizel and U. Kulp, Ann. d. Physik **4**, 971 (1930). The analysis of the same system as given by these authors is based on seventeen heads measured by Walter and Barrat, Proc. Roy. Soc. **A119**, 257 (1928).

[3] W. R. Fredrickson and W. W. Watson, Phys. Rev. **30**, 429 (1927).

$$\nu = 15377.35 + 74.88(v' + \tfrac{1}{2}) - 0.30(v' + \tfrac{1}{2})^2 - 92.35(v'' + \tfrac{1}{2}) + 0.34(v'' + \tfrac{1}{2})^2 \quad (2)$$

The infrared system was first photographed by McLennan and Ainslee.[4] They gave the measurements of nine heads extending from λ8212 to λ8602. It is mainly with the latter system that this paper deals.

The region of the spectrum from λ6200 to λ8850 was photographed in the first order of a Rowland concave grating giving a dispersion of 2.632A per mm. The vapor was contained in a glass tube 80 cm long heated electrically. The source of light was a 150 watt lamp. In the process of this investigation the heads of the bands of the red system were measured in an attempt to obtain a more accurate equation.

Shortly after this work had begun Ritschl and Villars[5] published a short note on the vibrational analysis of the infrared system, $B^1\Sigma \leftarrow A^1\Sigma$, giving the following equation, as expressed in half quantum numbers:

$$\nu = 11584.9 + 71.43(v' + \tfrac{1}{2}) - 0.40(v' + \tfrac{1}{2})^2 - 91.40(v'' + \tfrac{1}{2}) + 0.30(v'' + \tfrac{1}{2})^2. \quad (3)$$

No data or measurements were given in that note and insofar as we know none were given subsequently. This equation has been tested by the authors and, as will be shown later, is probably incorrect.

Results

Red system: In this system twenty six new heads were obtained bringing the total to seventy. These additional bands correspond to transitions involving higher quantum numbers than the bands measured by Frederickson and Watson.[3] With the new measurements the following equation was obtained:

$$\nu = 15377.73 + 74.73(v' + \tfrac{1}{2}) - 0.327(v' + \tfrac{1}{2})^2 - 92.64(v'' + \tfrac{1}{2}) + 0.354(v'' + \tfrac{1}{2})^2 \quad (4)$$

The new equation is believed to be more accurate since it includes heads of higher quantum numbers than Eq. (2). Table I gives the wave-length and wave-number values for this system. The average observed minus calculated difference is 0.39 cm^{-1}.

Far red system: The far red system contains many more observable heads than the one discussed above. Also, the bands are less clearly differentiated due to the great amount of overlapping throughout the entire system. This overlapping is also responsible for the presence of many faint markings on the plates whose appearance does not show whether they are heads or accidental condensations of lines. In all, two hundred apparent heads have been measured. It is doubtful, however, whether or not all of these are actually heads.

[4] J. C. McLennan and D. S. Ainslee, Proc. Roy. Soc. **A103,** 304 (1923).
[5] R. Ritschl and D. Villars, Naturwiss. **16,** 219 (1928).

TABLE I. *Near red system.*

$v'-v''$	$\lambda_{(air)}$ (I.A.)	$\nu_{(vac)}$ (cm^{-1})	O−C (cm^{-1})	$v'-v''$	$\lambda_{(air)}$ (I.A.)	$\nu_{(vac)}$ (cm^{-1})	O−C (cm^{-1})
11–20	6922.19	14442.31	−0.96	3– 2	6489.03	15406.37	+0.64
10–19	6916.82	14453.53	−0.69	1– 0	6473.91	15442.35	−0.36
9–18	6911.37	14464.93	−0.30	2– 0	6443.15	15516.08	−0.05
8–17	6906.18	14475.80	−0.48	4– 1	6421.26	15568.96	−0.11
7–16	6900.86	14486.96	−0.44	3– 0	6413.03	15588.14	−0.75
6–15	6895.51	14498.21	−0.36	5– 1	6391.61	15641.01	+0.48
5–14	6890.49	14508.74	−1.05	4– 0	6383.67	15660.65	−0.36
4–13	6884.76	14520.82	−0.24	8– 3	6379.80	15670.15	+0.93
9–17	6873.70	14544.18	−0.95	7– 2	6371.53	15690.00	−0.25
8–16	6867.93	14556.40	−0.49	6– 1	6363.22	15710.98	−0.35
7–15	6862.24	14568.47	−0.24	10– 4	6360.99	15716.48	+0.04
6–14	6856.87	14579.89	−0.70	5– 0	6354.55	15732.41	−0.05
5–13	6850.94	14592.55	+0.03	13– 6	6351.42	15740.17	+0.59
4–12	6845.41	14604.40	−0.10	8– 2	6343.33	15760.23	+0.49
9–16	6835.88	14624.67	−1.06	16– 8	6343.33	15760.23	+0.57
8–15	6829.49	14638.33	+0.12	12– 5	6342.19	15763.08	+0.33
7–14	6823.96	14650.00	−0.74	7– 1	6334.63	15781.89	+0.41
6–13	6817.79	14663.47	+0.15	15– 7	6334.63	15781.89	−0.49
5–12	6812.00	14675.93	−0.03	11– 4	6333.90	15783.71	−0.26
4–11	6805.91	14689.06	+0.41	6– 0	6325.99	15803.44	+0.17
3–10	6800.33	14701.13	−0.26	10– 3	6325.03	15805.84	−0.41
5–11	6773.47	14759.42	−0.69	14– 6	6325.03	15805.84	+0.69
4–10	6767.00	14773.52	+0.01	9– 2	6315.90	15828.68	+0.09
3– 9	6760.79	14787.28	+0.32	13– 5	6315.90	15828.68	+0.71
2– 8	6754.68	14800.46	−0.01	8– 1	6307.05	15850.88	−0.09
1– 7	6748.22	14814.64	+0.61	12– 4	6307.05	15850.88	+0.03
4– 9	6728.08	14859.00	−0.07	7– 0	6298.11	15873.40	−0.01
3– 8	6721.19	14874.24	+1.01	11– 3	6298.11	15873.40	−0.39
2– 7	6715.08	14887.75	+0.30	10– 2	6288.51	15897.63	+0.86
1– 6	6708.78	14801.73	+0.02	13– 4	6280.79	15917.16	+0.08
0– 5	6702.38	14815.97	−0.07				
3– 7	6682.39	14860.59	+0.36				
2– 6	6675.79	14875.37	+0.24				
1– 5	6669.22	14890.11	+0.02				
0– 4	6662.51	15005.23	+0.09				
1– 4	6629.84	15079.15	−0.06				
0– 3	6622.81	15095.16	+0.21				
4– 6	6611.62	15120.74	+0.73				
3– 5	6605.11	15135.61	−0.68				
0– 2	6583.37	15185.60	+0.13				
4– 5	6573.06	15209.42	+1.01				
2– 3	6558.45	15243.31	+0.86				
0– 1	6544.13	15276.67	−0.03				
2– 2	6520.02	15333.19	+0.23				
1– 1	6512.58	15350.66	−0.11				
0– 0	6505.08	15368.35	−0.29				

The first step in the investigation was to test the formula of Ritschl and Villars. It was found that a large number of heads could be fitted into this formula if it were modified slightly. It was noticed further that on the basis of the above equation the distribution of the bands within the system was somewhat erratic. The main objections to this formula however were two: (1) the value of ω_e'', (2) the heat of dissociation derived from their equation for the upper state.

It will be seen that ω_e'' of Eq. (3) differs somewhat from that of Eqs. (1) or (4). Ritschl and Villars did not state the number of heads from which Eq. (3) was derived, but it was thought that when a large number of heads

were included into this system the discrepancy would disappear. Indeed, we have found that the ω_e'' obtained by us, in testing Eq. (3), was 91.92, a difference of 0.72 cm^{-1} from the ω_e'' of Eq. (4), as compared with 1.24 cm^{-1} resulting from the equation as given by Ritschl and Villars. When, however, the value of 92.64 was inserted into Eq. (3) it was found that the deviations were far greater than the experimental accuracy warranted. The heads of the infrared system actually did not fit this modified equation. An attempt was then made to account for the discrepancy by the fact that the theoretical equations are derived for band origins, while in both systems band heads had been used. However with any reasonable assumption as to distance of heads to origins the correction introduced is about 1/100 of the above discrepancy.[6]

The second objection to Eq. (3) is the calculated heat of dissociation of the upper state. It has been assumed that the lowest state of K_2, $A^1\Sigma$, dissociates into two normal potassium atoms, while the excited state, $C^1\Pi$, dissociates into a normal atom and an excited ^2P atom as illustrated in Fig. 1. Birge[7] using Eq. (2) calculated the heat of dissociation of the upper state as 0.57 volts. From this he derived the heat of dissociation for the lower state as 0.89 volts, by making use of the assumption noted above. Using the more accurate Eq. (4) we obtain for the upper state:

$$A^1\Pi: \quad D' = \frac{(74.73)^2}{4 \times 0.327 \times 8106} = 0.527 \text{ volts} \tag{5}$$

and for the lower state:

$$A^1\Sigma: \quad D'' = \frac{(92.64)^2}{4 \times 0.354 \times 8106} = 0.748 \text{ volts} \tag{6}$$

From Eq. (5) we obtain:

$$H_{red} = \frac{15377.73}{8106} + 0.527 = 2.424 \text{ volts} \tag{7}$$

where $H = \nu_e + D'$; ν_e being the electronic energy of the system involved and D' the heat of dissociation of the upper level of that system. D'' is not expected to be as accurate as D' since fewer levels are known for the lower state.

Reverting to Eq. (3) of Ritschl and Villars; the lower state of the infrared system is the same as that of the red system i.e., $A^1\Sigma$. Therefore we would expect the upper state to dissociate into one normal and one ^2P excited atom, or into a normal atom and an atom with higher excitatoin potential than the atomic ^2P state. Calculating D' from Eq. (3) we get:

$$D' = \frac{(71.40)^2}{4 \times 0.40 \times 8106} = 0.393 \text{ volts} \tag{8}$$

[6] The values of ω_e'' as obtained independently from two different systems by Yamamoto and us agree to within 0.1 percent.

[7] International Critical Tables, **V**, 410–418 (1929).

The total energy is:

$$H_{\text{infrared}} = \frac{11584.9}{8106} + 0.393 = 1.822 \text{ volts} \qquad (9)$$

as compared with 2.424 volts.

H, as derived from Eq. (9) is too small, and since the first excited state of K is the ^2P state, and there is no intermediate atomic state into which the molecule can dissociate the equation necessarily must be wrong. The difference, 0.608 volts, is almost twice as much as D' of Eq. (8) and although

TABLE II. *Far red system.*

$v'-v''$	$\lambda_{(air)}$ (I.A.)	$\nu_{(vac)}$ (cm^{-1})	O−C (cm^{-1})	$v'-v''$	$\lambda_{(air)}$ (I.A.)	$\nu_{(vac)}$ (cm^{-1})	O−C (cm^{-1})
0– 4	8840.82	11308.06	+0.7	10– 4	8342.49	11983.54	+1.9
4– 7	8834.14	11316.60	−1.0	6– 1	8339.84	11988.34	+1.2
3– 6	8819.42	11335.54	+0.1	13– 6	8331.28	12000.50	+0.2
2– 5	8803.14	11355.84	+0.0	5– 0	8321.93	12013.29	+1.5
0– 3	8773.15	11395.28	−2.0	11– 4	8298.35	12047.28	−0.0
4– 6	8765.70	11404.97	+1.7	7– 1	8294.79	12053.31	−0.8
3– 5	8752.92	11421.62	−2.2	14– 6	8286.48	12064.52	−0.6
2– 4	8735.33	11444.61	−0.1	10– 3	8280.21	12073.67	+1.3
6– 7	8729.85	11451.81	+1.4	6– 0	8275.42	12080.67	+1.6
1– 3	8719.74	11465.13	−1.0	13– 5	8270.51	12087.83	+0.1
0– 2	8702.00	11488.46	+0.7	9– 2	8206.70	12093.34	−2.4
4– 5	8700.95	11489.85	−1.9	16– 7	8259.44	12104.04	−2.1
1– 2	8651.79	11555.20	+1.9	12– 4	8255.02	12110.51	−2.7
5– 5	8650.00	11557.52	−1.7	11– 3	8237.91	12135.67	−1.4
0– 1	8634.43	11578.41	−0.6	14– 5	8226.85	12151.99	−1.5
4– 4	8632.00	11581.60	+0.8	10– 2	8220.09	12161.99	+0.1
8– 7	8629.59	11584.82	+0.8	17– 7	8214.24	12170.64	+0.6
3– 3	8616.29	11602.74	−0.0	12– 3	8192.50	12202.28	−0.2
2– 2	8599.15	11625.66	−0.7	8– 0	8186.45	12211.94	−0.8
6– 5	8599.15	11625.66	−0.8	15– 5	8181.49	12219.33	+1.3
1– 1	8582.40	11647.80	0.0	11– 2	8175.83	12227.80	+0.2
5– 4	8582.40	11647.80	−0.5	18– 7	8173.15	12231.83	−1.8
9– 7	8580.66	11650.90	+0.6	21– 9	8160.56	12250.70	+0.6
0– 0	8566.30	11670.46	−0.1	20– 8	8145.80	12272.90	−0.0
3– 2	8549.89	11692.83	−0.4	19– 7	8130.74	12295.64	−1.3
6– 4	8533.51	11715.30	−0.3	15– 4	8122.31	12308.39	+1.3
2– 1	8532.50	11716.68	+0.4	11– 1	8117.13	12316.26	−2.5
10– 7	8532.50	11716.68	+0.3	17– 6	8114.36	12320.45	−0.9
1– 0	8515.75	11739.72	−0.0	14– 3	8107.71	12331.55	−0.9
4– 2	8499.51	11762.17	+1.1	16– 4	8081.93	12369.90	−1.4
3– 1	8483.08	11784.97	+0.5	23– 9	8078.32	12375.41	+1.7
10– 6	8468.23	11805.60	+1.5	12– 1	8071.10	12384.00	−0.0
6– 3	8468.23	11805.60	+0.2	19– 6	8071.10	12384.00	−0.6
2– 0	8468.23	11805.60	−2.6	22– 8	8062.89	12399.09	+1.2
9– 5	8453.60	11826.03	−0.4	11– 0	8054.71	12412.69	+1.9
5– 2	8450.75	11830.07	+1.4	20– 6	8030.75	12448.77	+1.2
12– 7	8438.04	11847.84	+0.3	13– 1	8030.75	12448.77	−0.6
8– 4	8438.04	11847.84	−1.4	19– 5	8014.74	12473.59	+0.6
4– 1	8434.47	11852.86	+0.6	21– 6	7990.34	12512.48	+2.5
7– 3	8419.99	11873.30	+1.0	14– 1	7988.33	12514.77	+0.4
3– 0	8418.25	11875.69	−0.7	24– 8	7985.31	12519.57	−2.1
10– 5	8405.84	11893.24	−0.7	17– 3	7980.68	12526.84	+1.8
6– 2	8403.55	11896.47	+0.6	27–10	7977.78	12531.36	−1.9
5– 1	8387.83	11918.80	−1.1	13– 0	7972.02	12540.43	+1.3
4– 0	8370.62	11943.27	−0.9	23– 7	7968.52	12545.97	−1.1
11– 5	8359.85	11958.65	+0.4	16– 2	7964.36	12552.50	+0.8
7– 2	8358.61	11961.10	−1.8	26– 9	7961.22	12557.44	−0.6

TABLE II. (*Continued*)

$v'-v''$	$\lambda_{(air)}$ (I.A.)	$\nu_{(vac)}$ (cm^{-1})	O−C (cm^{-1})
19– 4	7956.88	12564.29	+2.1
22– 6	7952.69	12570.88	−1.8
15– 1	7946.90	12579.80	+1.1
25– 8	7943.48	12585.33	+2.2
18– 3	7942.32	12587.32	−1.3
21– 5	7934.69	12599.57	+1.0
14– 0	7931.11	12605.13	−1.0
24– 7	7929.25	12608.08	−0.6
27– 9	7922.18	12619.21	+0.3
20– 4	7918.90	12625.00	−0.1
23– 6	7911.95	12635.65	+1.0
16– 1	7907.23	12643.18	+0.3
29–10	7900.78	12653.50	−0.5
22– 5	7895.46	12662.00	+1.0
25– 7	7890.22	12670.40	+0.3
24– 6	7873.70	12697.00	+0.6
27– 8	7868.48	12705.45	+0.3
17– 1	7866.53	12708.60	+1.8
29– 9	7848.54	12737.70	−1.9
28– 8	7831.28	12765.80	+0.2
18– 1	7829.07	12769.40	0.0
31–10	7827.66	12771.70	−1.8
20– 2	7807.20	12805.30	−0.1
23– 4	7803.10	12812.20	+0.1
26– 6	7798.83	12818.90	−0.1
29– 8	7793.90	12827.02	+1.1
31– 9	7774.18	12859.60	+0.5
18– 0	7772.80	12816.60	−0.7
21– 2	7768.96	12868.96	−0.0
29– 7	7732.60	12911.60	−1.2
32– 9	7728.30	12918.80	+0.4

the equation from which the heats of dissociation are obtained may be first approximations, we would not expect that the deviations would be so large.

The equation of Ritschl and Villars was therefore abandoned and combinations between the heads were sought so that the ω_e'' derived from this system would be the same, within experimental error, as those obtained from the blue and the red systems. Such combinations were found, resulting in a new analysis in which 119 heads were included. The equation connecting these heads is:

$$\nu = 11683.58 + 69.09(v' + \tfrac{1}{2}) - 0.153(v' + \tfrac{1}{2})^2 - 92.64(v'' + \tfrac{1}{2}) + 0.354(v'' + \tfrac{1}{2})^2 \quad (10)$$

In this equation the origin and all the constants are different from those given by Ritschl and Villars. The average observed minus calculated value based on this equation is 0.93 $cm.^{-1}$. Table II gives the heads of the system and their assigned quantum numbers. The remaining 80 heads have been examined carefully and most of them are apparently accidental condensations of lines.

It is seen from Eq. (10) that the constants of the lower state are exactly the same as those of the red and blue systems.

Heats of Dissociation

From the upper level of the red system we obtained $H_{red} = 2.424$ volts. Calculating D' from Eq. (10) we obtain:

$$B^1\Sigma: D' = \frac{(69.09)^2}{4 \times 0.153 \times 8106} = 0.962 \text{ volts} \tag{11}$$

and

$$H_{\text{infrared}} = \frac{11683.58}{8106} + 0.964 = 2.402 \text{ volts}. \tag{12}$$

The values of H as obtained from two different states agree within 1 percent.

From the blue system, we obtain:[8]

$$D' = \frac{(61.28)^2}{4 \times 0.24 \times 8106} = 0.483 \text{ volts} \tag{13}$$

and

$$H_{\text{blue}} = \frac{22970.0}{8106} + 0.483 = 3.311 \text{ volts}. \tag{14}$$

From the equation $H = \nu_{0(\text{mol})} + D' = D'' + \nu_{(\text{atom})}$
we obtain for the excitation potential of the atom $\nu_{(\text{atom})}$:

$$\nu_{(\text{atom})} = 3.31 - 0.81 = 2.50 \text{ volts} \tag{15}$$

as compared with

$$5^2S - 4^2S = 2.596 \text{ volts}$$

$$4^2D - 4^2S = 2.658 \text{ volts}.$$

The last two values are within the experimental error involved in Eq. (15). It is probable, however, that the upper state of the blue system is also $^1\Sigma$, which upon dissociating gives a normal atom and a 5^2S atom.[9]

Taking H'' as the mean of the two values in Eqs. (7) and (12) i.e. 2.41 volts we find that[10]

$$D'' = 0.81 \text{ volts}$$

On the other hand, from the constants of the lower state we obtain:

$$D'' = 0.75 \text{ volts}$$

a difference of only 0.06 volts between the two values.

[8] These are essentially the same values as given by Yamamoto.

[9] Professor Mulliken has pointed out that the lowest state of K_2, (cf. the corresponding state of Na_2), since it is a singlet state, must be $A^1\Sigma_g^+$. The first excited state is $B^1\Sigma_u$, the second $C^1\pi_u$ while the third is in all probability a $D^1\Sigma_u^+$. g (gerade) = even, u (ungerade) = odd, in the sense of these terms used by Hund.

[10] We have taken $4^2S - 4^2P$ of the K atom to be 1.608 volts.

In Figure 1 the four $U(r)$ curves for the states A, B, C, and D, are drawn using the formula given by Morse.[11] r_0 values were obtained by means of the equation given in the same paper, i.e. $\omega_0 r_0^3 = 3000 \times 10.^{-24}$

The heat of dissociation for the normal state of K_2 was obtained by Carelli and Pringsheim[12] from two somewhat similar methods, the values given by them being 0.63 volts and 0.53 volts. Somewhat later Ditchburn[13] calculated the heat of dissociation as 0.51 volts.

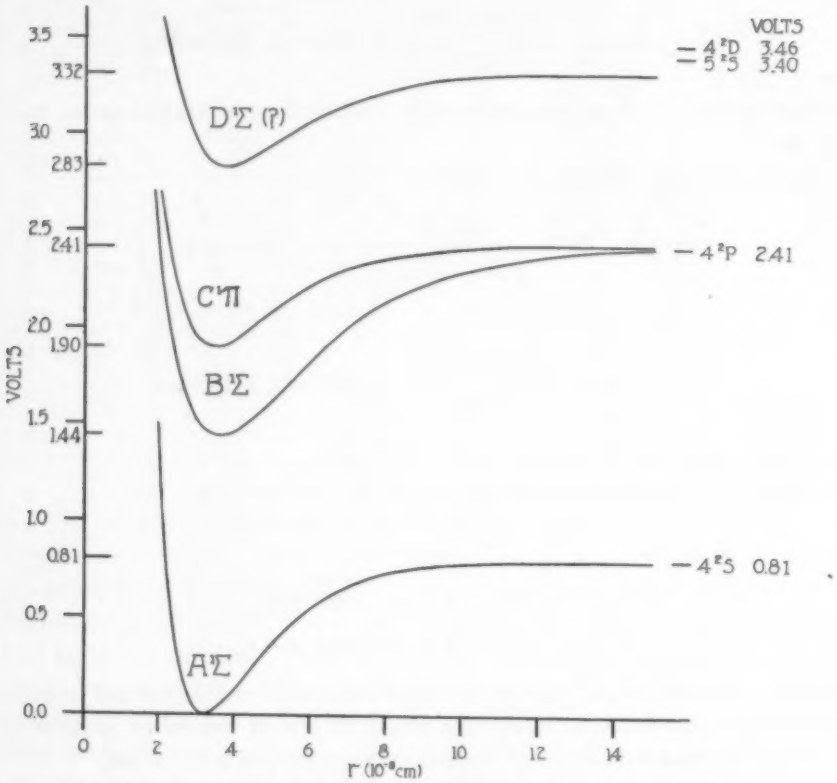

Fig. 1. $U(r)$ curves for the electronic states A, B, C and D.

In the experiment of Carelli and Pringsheim the vapor pressure of the molecules in thermodynamic equilibrium with the atoms was measured at several different temperatures. However the vapor pressure was not directly measured but was assumed to be proportional to the intensity of the band fluorescence produced when white light was passed through the vapor. The experimental errors involved in measuring the blackening of the plate etc. are rather large. Furthermore the heat of dissociation is obtained from the slope of the equation (first method, the second method is exactly analogous) $\log (IT) = f(1/T)$, where I is the intensity of the band fluorescence and T

[11] P. R. Morse, Phys. Rev. **34,** 61 (1929).
[12] A. Carelli and P. Pringsheim, Zeits. f. Physik **55,** 643 (1927).
[13] R. W. Ditchburn, Proc. Roy. Soc. **A117,** 486 (1928).

the absolute temperature. It can be shown easily that this method would not give an accurate value of the heat of dissociation. A very slight change in the slope of the line drawn through their points would give a totally different value for the heat of dissociation. The value 0.75 volts is within their experimental error, and it is actually obtained from one of the four curves given in their paper.[14]

In Ditchburn's experiment white light was passed through a tube containing potassium vapor and the wave-length of the maximum in the region of continuous absorption was found. Ditchburn finds a maximum absorption at about 5820A corresponding to 2.12 volts, and interprets this value as being the sum of the dissociation energy of the molecule in the lower state plus the energy required to excite the atom from the 4^2S to the 4^2P state. Since the latter energy is known accurately, he derives the dissociation energy of the molecule as $D''=0.5$ volts. The value obtained by him 2.12 volts, is to be compared with the mean value of H obtained from Eqs. (7) and (12), i.e. 2.41 volts. It should be noted that our value corresponds to a transition from the lowest vibrational state of A (refer to Fig. 1) to the threshold value of dissociation in the two upper states B and C, i.e. 2.41 volts corresponds to dissociation at $T=0°\text{K}$.

The position of the maximum in the continuum depends upon two factors, first, upon the number of molecules in the lower states from which by absorption of light a molecule dissociates, and second, upon the probability of such transitions. The first factor depends upon the temperature of the absorbing gas, while the second depends upon the shape of the $U(r)$ curves of the states involved, here A and C. It is seen from Fig. 1 that the maximum probability of transitions from A to the threshold value of C is from the vibrational level of A corresponding to an energy of 0.45 volts. However we would expect the number of molecules in this particular level to be less than that of lower vibrational states. Hence the maximum will occur for transitions arising from vibrational levels lower than 0.45 volts.[15] Ditchburn's value indicates that the maximum corresponds to transitions from the vibrational level of 0.3 volts. He does not give the temperature at which this experiment was performed, however we can see from Fig. 1 that in general heats of dissociation obtained by measuring the wave-lengths of the region of maximum absorption from states A to C will be too low.

It is with pleasure that the authors acknowledge their indebtedness to Professor W. W. Watson for suggesting this problem and to Professor R. S. Mulliken for his valuable criticism and advice.

[14] Carelli and Pringsheim, Zeits. f. Physik **44**, 645, dotted line of Fig. 2.

[15] See discussion on transition probabilities by R. S. Mulliken, Rev. Modern Physics **2**, 78–83 (1930).

THE ROTATIONAL MOTION OF MOLECULES IN CRYSTALS

By Linus Pauling
Gates Chemical Laboratory, California Institute of Technology

(Received May 7, 1930)

Abstract

It is shown by the discussion of the wave equation for a diatomic molecule in a crystal that the motion of the molecule in its dependence on the polar angles θ and ϕ may approach either one of two limiting cases, oscillation and rotation. If the intermolecular forces are large and the moment of inertia of the molecule is large (as in I_2, for example), the eigenfunctions and energy levels approach those corresponding to oscillation about certain equilibrium orientations; if they are small (as in H_2), the eigenfunctions and energy levels may approximate those for the free molecule, even in the lowest quantum state.

It is found in this way that crystalline hydrogen at temperatures somewhat below the melting point is a nearly perfect solid solution of symmetric and antisymmetric molecules, the latter retaining the quantum weight 3 for the state with $j=1$ as well as the spin quantum weight 3. This leads to the expression

$$S = -n_A R \log n_A - (1-n_A) R \log (1-n_A) + n_A R \log 9 + S_{tr},$$

in which S_{tr} is the translational entropy, for the entropy of the solid at these temperatures. At lower temperatures (around 5°K) the solid solution becomes unstable relative to phases of definite composition, and the entropy falls to

$$S = n_A R \log 3 + S_{tr},$$

the entropy of mixing and of the quantum weight 3 for $j=1$ being lost at the same time. Only at temperatures of about 0.001°K will the spin quantum weight entropy be lost.

Gradual transitions covering a range of temperatures and often unaccompanied by a change in crystal structure, reported for CH_4, HCl, the ammonium halides, and other substances, are interpreted as changes from the state in which most of the molecules are oscillating to that in which most of them are rotating. The significance of molecular rotation in the interpretation of other phenomena is also discussed.

I. Introduction

THE calculation of the difference in entropy of gaseous molecular hydrogen and crystalline hydrogen has recently been made by Giauque and Johnston.[1] At temperatures between the melting point (14°K) and about 10°K the heat capacity of the solid is well represented by a Debye function with $\beta\nu = 91°$. Assuming the validity of extrapolation to 0°K by means of this function, it is found that the difference in entropy of the solid at 0°K and the gas at standard conditions is 29.7 ± 0.1 E. U. The molal entropy of the gas at standard conditions is given by the Sackur-Tetrode equation as 34.00 E. U., using the band spectrum value of the moment of inertia, and taking into account the symmetry number term ($-R \log 2$), the entropy of mixing of sym-

[1] W. F. Giauque and H. L. Johnston, J. A. C. S. **50**, 3221 (1928).

metric and antisymmetric molecules, present in the ratio of $1:3(-1/4\ R \log 1/4 - 3/4\ R \log 3/4)$, and the nuclear spin quantum weight of the antisymmetric molecules ($3/4\ R \log 3$). Thus the molal entropy of ordinary crystalline hydrogen (the metastable mixture of symmetric and antisymmetric molecules in the ratio of 1:3) at temperatures somewhat below the melting point is found to be 4.3 ± 0.1 E. U. in addition to the translational entropy. In the attempt to account for this deviation from the value zero to be expected from the third law of thermodynamics, it was found necessary to carry through the quantum mechanical discussion of the motion of molecules in crystals.

Before proceeding with this task, it may be illuminating to mention the concept of the motion of a molecule in a crystal which we would form on the basis of classical mechanics. All but six of the degrees of freedom for the molecule can be assigned to represent relative motions of the atoms within the molecule, corresponding to internal oscillations. The six remaining degrees of freedom can be represented by the three coordinates x, y, z of the center of mass of the molecule referred to an arbitrarily chosen set of axes, and the Eulerian angles φ, θ, χ determining the orientation of the molecule with respect to the same axes. In case the forces between atoms in a molecule are much stronger than those between atoms in different molecules, a crystal of the substance may be considered as a first approximation to be a collection of rigid molecules held in a regular arrangement by the rather weak intermolecular forces. Each molecule will remain in the neighborhood of its equilibrium position, the coordinates x, y, z varying through only a small region of values about x_0, y_0, z_0. Similarly, there will be one or more sets of values of φ, θ, χ for which the potential energy is a minimum, corresponding to equilibrium orientations of the molecule. There are two types of motion then possible for the molecule. If the potential energy for values of φ, θ, χ in the neighborhood of φ_0, θ_0, χ_0 is very small compared with that for other values, the difference being much larger than kT, the average molecule at the temperature T will carry out only small vibrations about its equilibrium orientation. This may be spoken of as oscillation about the equilibrium orientation. But if the potential energy undergoes a total variation smaller than kT, the kinetic energy of the average molecule will suffice to carry it into any orientation, so that the molecule will undergo non-uniform rotation, speeding up as it passes through the equilibrium orientations and slowing down as it goes over the potential maxima. A molecule with a given amount of energy and acted upon by a given potential would according to the classical theory assume a succession of orientations corresponding either to one or to the other of these possibilities, oscillation or rotation.

The introduction of the quantum mechanics does not require this picture to be changed essentially. The allowed states of the system can approximate either of two extremes, oscillation and rotation, or can lie between these extremes, approximating neither more closely than the other. For with the quantum mechanics, in contradistinction to the classical theory, the transition from one extreme to the other is unbroken.

II. The Diatomic Molecule in a Crystal

In Fig. 1 there is shown the structure of the orthorhombic crystal iodine as determined with the use of x-rays.[2] The atoms are joined in pairs to form molecules by strong shared-electron-pair bonds, and the molecules are

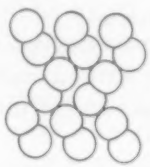

Fig. 1. The arrangement of atoms in one layer in a crystal of iodine. It is seen that the atoms are in groups of two(the molecules I_2) which are oriented by the intermolecular forces.

grouped together in such a way that the figure axis for each assumes a definite orientation. This is the equilibrium orientation, with the polar angle $\theta = 0$, say. The symmetry of the molecule requires that there also be another equilibrium orientation at $\theta = \pi$.

Let us consider a diatomic molecule in such a crystal. As a first approximation we may neglect the translational oscillations of the molecule under consideration and both the translational and rotational motion of the other molecules in the crystal. The wave equation then may be written

$$\nabla^2\psi + \frac{8\pi^2 I}{h^2}(W - V)\psi = 0, \tag{1}$$

in which I is the moment of inertia of the molecule and $V = V(\theta, \varphi)$ is a potential function representing the averaged interaction of the molecule with surrounding molecules. The simplest form that can be given this function and have it represent a diatomic molecule with two equilibrium orientations is

$$V = V_0(1 - \cos 2\theta), \tag{2}$$

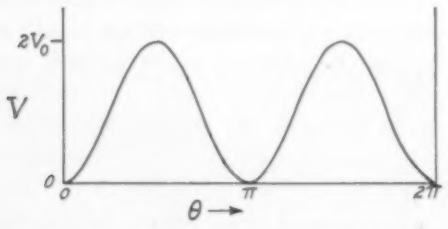

Fig. 2. The potential function $V = V_0\ (1 - \cos 2\theta)$.

in which V_0 is a constant. This potential function is shown in Fig. 2. The wave equation then becomes

$$\frac{1}{\sin^2\theta}\frac{\partial^2\psi}{\partial\phi^2} + \frac{1}{\sin\theta}\frac{\partial}{\partial\theta}\sin\theta\frac{\partial\psi}{\partial\theta} + \frac{8\pi^2 I}{h^2}(W - V_0 + V_0\cos 2\theta)\psi = 0. \tag{3}$$

[2] P. M. Harris, E. Mack and F. C. Blake, J. A. C. S. **30**, 1583 (1928).

The characteristic value equation in θ obtained from this has not been solved except for limiting cases. The corresponding problem in a plane has, however, been fully treated. If the molecule were restricted to motion in a plane the wave equation would be

$$\frac{d^2\psi}{d\theta^2} + \frac{8\pi^2 I}{h^2}(W - V_0 + V_0 \cos 2\theta)\psi = 0 \tag{4}$$

or, writing

$$\alpha = \frac{2\pi^2 I}{h^2}(W - V_0)$$

$$q = \frac{\pi^2 I V_0}{2h^2},$$

$$\frac{d^2\psi}{d\theta^2} + (4\alpha + 16q \cos 2\theta)\psi = 0. \tag{5}$$

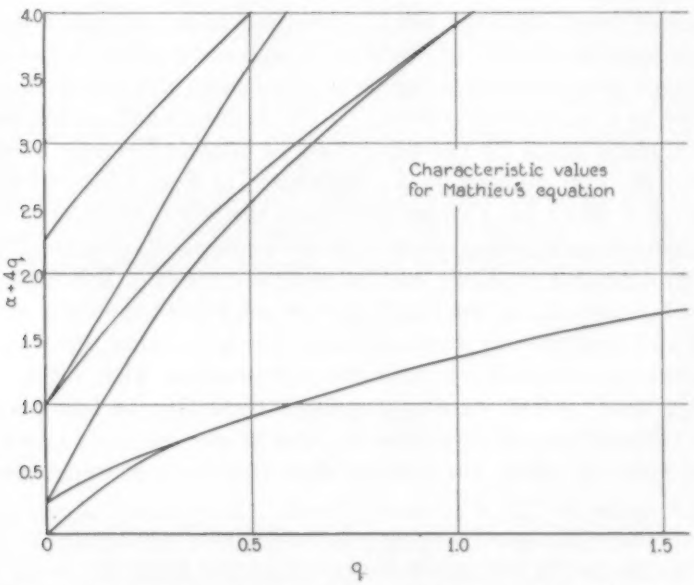

Fig. 3. The characteristic values for the six lowest Mathieu functions.

This equation is Mathieu's equation in the usual form.

The requirement that ψ be periodic in θ with the period 2π leads to the functions known as Mathieu functions.[3] These are usually designated by the symbols ce_0, se_1, ce_1, se_2, ce_2, etc. The functions and the corresponding characteristic values of α as functions of q have been evaluated by Goldstein.[4] The energy values for the five lowest states are shown in Fig. 3. It is seen

[3] E. Mathieu, Liouville's Jour. **13**, 137 (1868); Whittaker and Watson, "Modern Analysis," pp. 404–428. E. U. Condon, Phys. Rev. **31**, 891 (1928), pointed out that the Mathieu functions of even order are the eigenfunctions for the plane pendulum.

[4] S. Goldstein, Trans. Cambridge Phil. Soc. **23**, 303 (1927).

that for $q=0$ Eq. (5) reduces to the equation for the plane rotator, with energy levels $W_m=(m^2h^2/8\pi^2I)$. For q large the eigenfunction ψ is appreciably different from zero only for values of θ close to 0 and π, and approximates a combination of Hermite orthogonal functions, the eigenfunctions for the harmonic oscillator. The energy levels for this case are $(n+1/2)\ h\nu_0$, in which $\nu_0=h(2q)^{1/2}/\pi I$. Each energy level shows two-fold degeneracy, the corresponding eigenfunctions being approximately

$$\frac{1}{2^{1/2}}\{\psi_n\theta/\theta_0+\psi_n(\theta-\pi)/\theta_0\}\quad\text{and}\quad\frac{1}{2^{1/2}}\{\psi_n\theta/\theta_0-\psi_n(\theta-\pi)/\theta^0\},$$

in which $\psi_n(\theta/\theta_0)$ and $\psi_n((\theta-\pi)/\theta_0)$ represent Hermite orthogonal functions of the indicated arguments, and θ_0 is given by the equation $h\nu_0/2=V_0\theta_0^2$.

This can be used as the basis of a perturbation treatment of the problem, using the method of variation of constants,[5] as in the treatment of aperiodic phenomena.[6] It is found that in case it were possible to carry out an experiment to determine whether the molecule were undergoing vibrations about $\theta=0$ or about $\theta=\pi$, with the use of a method of investigation involving an interaction unsymmetrical in the two atoms composing the molecule, the probability of observing the molecule in one orientation rather than the other would vary in a way corresponding to the molecule's changing end for end with a frequency given by the separation of adjacent energy levels (ce_0 and se_1, ce_1 and se_2, etc) divided by h. Reference to Fig. 3 shows that this frequency is very small for q large, justifying the interpretation of the corresponding states as oscillational states, the molecule oscillating about an equilibrium orientation and changing end for end only rarely. But for q small this frequency becomes large, approaching the principal frequency of motion of the molecule; then we say that the molecule is rotating, its rotation being made somewhat non-uniform through interactions with other molecules. The energy levels in this case approximate those for the free plane rotator, and their behavior for small values of q can be conveniently followed by perturbation methods using the rotator eigenfunctions as zeroth order eigenfunctions.

These considerations, involving a hypothetical investigation of the orientation of the molecule, are, while illuminating, not essential to the discussion of the type of motion of the molecule. We can define the motion of the molecule in a given state as oscillational in case the eigenfunction for that state can be closely approximated by a combination of Hermite functions and the energy of the state is given approximately by $(n+1/2)\ h\nu_0$. For rotational motion the eigenfunction and energy level should approximate those for a free rotator. This definition is equivalent to that given above: the study of Goldstein's Fourier series representation of the Mathieu functions shows that the transition of the eigenfunctions from approximation to Hermite

[5] P. A. M. Dirac, Proc. Roy. Soc. **A112**, 661 (1926); J. C. Slater, Proc. Nat. Acad. **13**, 7 104 (1927); M. Born, Zeits f. Physik **40**, 172 (1926).

[6] See the clear exposition given the process of radioactive decomposition by M. Born, Zeits. f. Physik **58**, 306 (1929).

functions to approximation to sines and cosines takes place rather sharply at the value of q where the separation of adjacent energy levels becomes appreciable. A similar treatment can be applied to the spatial rotator with two potential minima. The discussion of the qualitative course of the energy levels and the nature of the eigenfunctions is similar to that given above, and a detailed treatment is not needed for our purposes.

III. Rough Criteria for Oscillation and Rotational Motion

Let us tentatively assume that the motion is oscillationa. Then we can approximate the lower part of $V(\theta)=V_0(1-\cos 2\theta)$ by a parabola by expanding in powers of θ and $\theta-\pi$ obtaining $-2V_0\vartheta^2$ and $-2V_0(\theta-\pi)^2$ as the expansions in the neighborhood of $\theta=0$ and $\theta=\pi$. These correspond to energy levels

$$W_n = (n+1)h\nu_0, \quad n = 0, 1, 2, 3, \cdots \tag{6}$$

for the two-dimensional harmonic oscillator, with

$$\nu_0 = \frac{1}{\pi}\left(\frac{V_0}{I}\right)^{1/2}. \tag{7}$$

In case that $W_n=(n+1)\ h\nu_0$ is less than $2V_0$, the top of the potential hill separating the two-valleys, the molecule will change orientation only rarely. (The exceptional case with V_0 and n small for which there is a large probablility of the molecule turning end for end even when its energy is not sufficient to carry it over the hill, is discussed later). But for W_n larger than $2V_0$ the motion will be rotational. Thus we obtain the following criteria:

$$\begin{aligned} n+1 &< \frac{2\pi(IV_0)^{1/2}}{h}, \quad \text{oscillational motion,} \\ n+1 &> \frac{2\pi(IV_0)^{1/2}}{h}, \quad \text{rotational motion.} \end{aligned} \tag{8}$$

The uncertain quantity of these expressions is V_0. A rough value for it can be obtained from the observed heat capacity of the solid. If the molecules oscillate about equilibrium orientations the molal heat capacity would be given as a first approximation by the sum of a Debye function of parameter $\beta\nu$, corresponding to the translational oscillations, and twice an Einstein function of parameter $\beta\nu_0=h\nu_0/k$, with ν_0 the characteristic frequency of Eq. (7). It is found that such a curve does not give a very close fit with observed heat capacities since the model is too greatly simplified; but the heat capac, ity curve does show that $\beta\nu$ and $\beta\nu_0$ are nearly the same for many substances and a rough value for them can be obtained by taking three times the temperature at which the heat capacity reaches 5 cal/mole degree; that is, half the high-temperature value for five degrees of freedom.[7] Values of

[7] This procedure is based on the fact that an Einstein function reaches half its maximum value at the temperature $0.33\beta\nu_0$.

TABLE I.

Molecule	$\beta\nu_0$	Θ	n_0+1	V_0	Heat of fusion and transition
				cal/mole	cal/mole
I_2	75°	0.053°	350	25000	4000
N_2	65°	2.33°	7.0	450	222
O_2	70°	2.06°	8.5	600	306
CO	75°	2.65°	7.1	500	354
CH_4	55°	8.5°	1.6	90	242
HCl	160°	14.9°	10.7	1700	760
HBr	125°	11.9°	10.5	1300	803
HI	105°	9.2°	11.4	1200	897
H_2	<135°	82°	<0.4	<56	28

$\beta\nu_0$ for several substances[8] are given in Table I, together with the characteristic temperature for rotational degeneracy, Θ, which is related to the moment of inertia I (obtained from band spectral data) by the equation

$$\Theta = \frac{h^2}{8\pi^2 I k}. \tag{9}$$

The heat capacity of solid hydrogen provides no information regarding $\beta\nu_0$ for H_2. An upper limit for $\beta\nu_0$ can, however, be found in the following way. It is seen that for many substances the total heat change accompanying transitions and fusion is about equal to $V_0/2$ (compare columns 6 and 7 of Table I). Assuming this to hold for H_2, we find $V_0 = 56$ cal/mole, which, from the trend of the ratio $V_0/\Delta H$ with molecular weight, can be accepted as a maximum value. This corresponds to $\beta\nu_0 < 135°$. The approximate constancy of $\beta\nu_0$ in the series I_2, O_2, N_2 suggests a value of this order of magnitude for H_2 also; it and derived quantities are included in Table I.

In terms of $\beta\nu_0$ and Θ the criteria 8 become

$$\begin{aligned} n + 1 &< \beta\nu_0/4\Theta, \quad \text{oscillational motion,} \\ n + 1 &> \beta\nu_0/4\Theta, \quad \text{rotational motion.} \end{aligned} \tag{10}$$

The transition from oscillational to rotational motion should occur for $n = n_0$, with

$$n_0 + 1 = \frac{\beta\nu_0}{4\Theta}. \tag{11}$$

Values of n_0+1 are given in Table I. There are also included data for unsymmetric molecules such as HCl. For these a reasonable potential function

[8] Since these calculations were made some direct verification of them has been provided by the work of L. Vegard (Nature **125**, 14 (1930)) who has obtained spectra from solid nitrogen at very low temperatures involving an electronic transition, a change in oscillation within the molecule, and an additional energy change corresponding to frequencies of 40 cm^{-1} and 69 cm^{-1} which he interprets as oscillational jumps for the molecule in the lattice. One of these frequencies probably is the frequency of rotational vibration of the molecule. 40 cm^{-1} and 69 cm^{-1} correspond to $\beta\nu_0 = 57°$ and 99° respectively, the first of which is in good agreement with the rough value 65° of Table I.

is $V = V_0(1-\cos\theta)$, corresponding to an electric dipole in a uniform field. This leads to a transitional value n_0 given by

$$n_0 + 1 = \frac{\beta\nu_0}{\Theta}. \tag{12}$$

For CO it is doubtful as to whether 11 or 12 is more nearly applicable; the former has been used.

The value $n_0+1<0.4$ found for H_2 shows that *even in the lowest state* the molecules are rotating freely, the intermolecular forces producing only small perturbations from uniform rotation. Indeed, the estimated $\beta\nu_0<135°$ corresponds to $V_0<28\,k$, which is small compared with the energy difference $164\,k$ of the rotational states $j=0$ and $j=1$, giving the frequency with which the molecule in either state reverses its orientation. The perturbation treatment shows that with this value of V_0 the eigenfunctions and energy levels in all states closely approximate those for the free spatial rotator.[9]

The other extreme is provided by I_2, for which the transition from oscillation to rotation takes place at about $n=300$. At the melting point the molecules are in states with $n=10$ or 15, so that there are no rotating molecules in this crystal. This agrees with the fact that equilibrium positions for the atoms have been found by x-ray methods.

The remaining substances form intermediate cases, the molecules in lower states oscillating and in higher states rotating. Whether the transition to rotational states takes place in the main before the crystal melts will be considered in Section V.

IV. Crystalline Hydrogen and its Entropy

In ordinary crystalline hydrogen there are three molecules with $j=1$ for every one with $j=0$. The eigenfunctions for these molecules approximate those for free molecules, namely

$$j = 0,\ \psi_0 = 1/(4\pi)^{1/2},$$
$$j = 1,\ \psi_1 = (3/4\pi)^{1/2}\cos\theta,\ (3/4\pi)^{1/2}\sin\theta\cos\phi,\ (3/4\pi)^{1/2}\sin\theta\sin\phi, \tag{13}$$

in terms of angles θ and ϕ relative to an arbitrary coordinate system. These rotating molecules interact with each other as though they were nearly spherically symmetrical.[10] Hence we expect the crystal to have a close-packed structure—cubic close-packed, say, with molecules at 000, $0\frac{1}{2}\frac{1}{2}$, $\frac{1}{2}0\frac{1}{2}$, $\frac{1}{2}\frac{1}{2}0$. This agrees with the known cubic symmetry of crystalline hydrogen.[11] The

[9] It is worthy of especial mention that in the state with $j=0$ the molecules are to be considered as rotating when V_0 is sufficiently small (less than the separation of the levels $j=0$ and $j=1$) even though the energy of the state ($\sim V_0$) is not sufficient to carry the molecule over the potential maximum ($2V_0$). This is shown by the close approximation of the corresponding eigenfunction to the lowest tesseral harmonic and by the high frequency of end-for-end interchange given by the perturbation treatment, starting with oscillational eigenfunctions.

[10] The forces holding the rotating molecules result from interpenetration of the molecules, as for the noble gases.

[11] The observed density 0.0808 at 11°K corresponds to a unit with $a=5.46$A, the distance between adjacent molecules being 3.86A.

x-ray investigation of the crystals should not lead to the determination of atomic positions, but only of molecular positions.

In cubic close-packing each molecule is surrounded by twelve others, whose interaction with the central molecule can be represented by a potential function of cubic point-group symmetry in case that the twelve molecules are spherically symmetrical or oriented at random. The energy change produced by this potential function, f say, is

$$W^1 = \int\int \psi f \bar{\psi} \sin\theta d\theta d\phi,$$

which is easily shown by the consideration of the symmetry of f to be the same for all four eigenfunctions. Thus a molecule of symmetrical hydrogen, with $j=0$, has in a crystal the same energy as a molecule of antisymmetrical hydrogen, with $j=1$. As a result the two forms of hydrogen should form a complete series of nearly perfect solid solutions, and, moreover, the energy content of the crystal, aside from rotational energy, should be independent of the composition. This has been verified by the measurements of Clusius and Hiller,[12] who found symmetrical hydrogen to have the same heat capacity and heat of fusion as the 1:3 mixture.

Additional experimental verification that molecules of hydrogen in condensed phases are in states approximating those for free molecules is provided by the Raman effect measurements of McLennan and McLeod.[13] A comparison of the Raman frequencies found by them and the frequencies corresponding to the rotational transitions $j=0\rightarrow j=2$ and $j=1\rightarrow j=3$ (Table II) shows that the intermolecular interaction in liquid hydrogen produces only a very small change in these rotational energy levels.

TABLE II.

Transition	Raman effect	Band spectra
$j=0\rightarrow j=2$	354 cm^{-1}	347 cm^{-1}
$j=1\rightarrow j=3$	588	578
$0\rightarrow 1$ in intramolecular oscillation	4149	4159

These considerations permit a calculation of the entropy of crystalline hydrogen at temperatures somewhat below the melting point. Ordinary crystalline hydrogen, consisting of the symmetrical and antisymmetrical forms in the ratio of 1:3, has an entropy of mixing of $-(1/4)R\log(1/4) - (3/4)R\log(3/4)$, for the solid solution can be considered ideal. The symmetrical molecules have a quantum weight 1 in the normal state, with $j=0$, and the antisymmetrical molecules a quantum weight 9, corresponding to the three rotational eigenfunctions for $j=1$, each of which is associated with any one of the three spin eigenfunctions. This gives a predicted total entropy of the solid at temperatures just below the melting point of

$$S_{H_2} = -(\tfrac{1}{4})R\log(\tfrac{1}{4}) - (\tfrac{3}{4})R\log(\tfrac{3}{4}) + (\tfrac{3}{4})R\log 9 + S_{tr} = 4.39\text{E. U.} + S_{tr}, \quad (14a)$$

[12] K. Clusius and K. Hiller, Zeit. f. phys. Chem. **B4**, 158 (1929).

[13] J. C. McLennan and J. H. McLeod, Nature **123**, 160 (1929).

in which S_{tr} is the translational entropy. This value is in excellent agreement with the experimental value $4.3 \pm 0.1 + S_{tr}$ of Giauque and Johnston.[14] In general a mixture containing n_A mole-fraction of antisymmetric molecules would have

$$S = -n_A R \log n_A - (1 - n_A) R \log (1 - n_A) + n_A R \log 9 + S_{tr}. \quad (14b)$$

At very low temperatures a separation of the three rotational levels with $j=1$ will take place. This is a second-order effect, depending on the mutual orientation of two or more molecules. As an illustration, let us assume that we could obtain a crystal of pure antisymmetric hydrogen. At temperatures not too near 0°K the molecules would be in cubic close-packing, and an arbitrary molecule could be represented by any one of the three eigenfunctions with $j=1$. But there are possible states of the crystal somewhat more stable than those in which the three rotational eigenfunctions with $j=1$ are represented by random molecules. Thus if each molecule were in the state with $j=1$, $m=0$, corresponding to the eigenfunction $(3/4\pi)^{1/2} \cos\theta$, with θ referred to trigonal axes which for the various molecules are oriented as are the figure axes of CO_2 in crystals of this substance, then the energy of the crystal would be less than that of a crystal in which the three eigenfunctions with $j=1$ were represented at random. In crystalline CO_2 each molecule is surrounded by twelve others, of which the six in the equatorial plane point towards the central molecule, bringing six oxygen atoms to within 3.25A, while the other six molecules place oxygen atoms 4.12A away. As a result the stable orientation for the central molecule is along the trigonal axis. The distribution function $\psi^2 = 3/4\pi \cos^2\theta$ for a hydrogen molecule with $j=1$ and $m=0$ shows a tendency for the molecule to line up parallel to the axis $\theta=0$, leading to the decreased energy of the CO_2-similar structure described above. Since this is a second-order effect the energy decrease will be considerably smaller than V_0, of the order of magnitude of $V_0/5$. With V_0 equal to about 28 k at the most, the temperature at which this structure would become stable relative to the random one would be of the order of magnitude of 5°K.

With other simple ratios of symmetric to antisymmetric molecules other structures might become stable at very low temperatures. Since the energy change depends on the interaction of two antisymmetric molecules, which would drop off very rapidly as the molecules were separated, crystals containing only a small fraction of antisymmetric molecules would be unstable, breaking down into two phases, pure crystalline symmetric hydrogen and crystals with n_A (the mole-fraction of antisymmetric molecules) equal to 1, 1/2, or some other simple fraction. This process, involving diffusion of the molecules, might take some time, so that care would be necessary to insure equilibrium in the study of mixtures with n_A small.

The entropy change accompanying this transition is predicted to be

[14] The possibility of the expression of the entropy of hydrogen as the sum of these terms was first noted by Giauque, who observed that it indicated the formation of nearly ideal solid solutions between symmetrical and antisymmetrical hydrogen and the retention of the quantum weight 9 for the latter.

$$S = -n_A R \log n_A - (1 - n_A) R \log (1 - n_A) + n_A R \log 3 \qquad (15)$$

corresponding to the restriction of each antisymmetric molecule to one of the three rotational states with $j = 1$, and to the removal of the entropy of mixing of the solid solution existing above the transition temperature.[15] The entropy of the crystals then becomes

$$S = n_A R \log 3 + S_{tr}. \qquad (16)$$

The discovery of a transition which we identify with this has been reported by Simon, Mendelssohn, and Ruhemann,[16] who measured the heat capacity of hydrogen with $n_A = 1/2$ down to 3°K. They found that the heat capacity, after following the Debye curve down to about 11°K, rose at lower temperatures, having the value 0.4 cal/deg., 25 times that of the Debye function, at 3°K. The observed entropy of transition down to 3°K, at which the transition is not completed, was found to be about 0.5 E.U. That predicted by Eq. (15) for the transition is 2.47 E.U.

In crystals for which n_0 is large, such as iodine, the lowest symmetric and the lowest antisymmetric state have practically the same energy and properties, and each corresponds to one eigenfunction only. As a result a mixture of symmetric and antisymmetric molecules at low temperatures will behave as a perfect solid solution, each molecule having just its spin quantum weight, and the entropy of the solid will be the translational entropy plus the same entropy of mixing and spin entropy as that of the gas. This has been verified for I_2 by Giauque.[17] Only at extremely low temperatures will these entropy quantities be lost.

V. The Transition from Oscillational to Rotational Motion

A consideration of the values of n_0 for CH_4, N_2, O_2, and the hydrogen halides indicates that these molecules oscillate at low temperatures but go over mainly to rotational states before the melting point is reached. This process should be accompanied by thermal phenomena, as is shown by the following argument. With $n < n_0$ the eigenfunctions in θ and ϕ change only slightly as n is increased; the probability function $\psi\bar{\psi}$, with maxima in the neighborhood of the equilibrium values of θ and ϕ, falls off rapidly from these maxima, and increase in n causes only some spread, corresponding to larger amplitudes of oscillation. But a radical change takes place as n goes through the transition value. The eigenfunctions change completely in nature, becoming much more nearly constant, as may be verified by a study of the Fourier series coefficients given by Goldstein for the Mathieu functions. This change increases the repulsive forces between molecules, and tends to spread the crystal lattice

[15] The entropy $n_A R$ log 3 arising from the three spin eigenfunctions for antisymmetrical molecules will be lost only at temperatures of the order of magnitude of 0.001°K, at which the very small nuclear interaction energy would become appreciable. It may be pointed out that the magnitude of the interaction energy with other molecules for the three states with $j = 1$ as compared with the spin-rotation interaction energy is such as not to permit coupling of i and the spin moment to form a resultant.

[16] F. Simon, K. Mendelssohn, and M. Ruhemann, Naturwiss. **18**, 34 (1930).

[17] Personal communication.

as soon as an appreciable number of molecules have begun to rotate. But spreading the lattice decreases the forces between molecules and decreases $\beta\nu_0$ and V_0, so that more molecules can rotate. The effect builds up to give a transition, which often is not accompanied by an essential change in the structure of the crystal. The transition is usually not sharp, but covers a range of temperature of several degrees, and is foreshadowed on the low temperature side by an abnormal increase in heat capacity.

Such a transition is shown by methane.[18] The heat capacity rises rapidly from 18°K to a very sharp maximum (over 48 cal/mole deg.) at 20.4°, and then drops sharply to 4.6 cal/mole deg. at 22.8°. The temperature of transition agrees with the low value (about 1) predicted for n_C. A methane crystal between 20° and 90.6°K (the melting point) would be described as consisting of rotating molecules in cubic close-packing;[19] below 20° the tetrahedral molecules oscillate about equilibrium orientations. It would be very interesting to have Raman effect or infrared spectral data for solid methane; above 20° the lines should very closely approximate the rotation lines for the gaseous molecules, and below that temperature should show pronounced changes, the frequencies of the lines increasing and tending to become constant as the motion approaches harmonic oscillation.

The course of the heat capacity curves also indicates that the transitions shown by N_2 and O_2 at 35.4° and 43.76° respectively are accompanied by the setting in of rotation of the molecules. This is supported by the known crystallographic symmetry of the high temperature forms; nitrogen cubic (indicating cubic close-packing of N_2 molecules) and oxygen hexagonal (indicating hexagonal close-packing).

The gradual transitions shown[20] by HCl (at 98°K), HBr (at 89°, 113°, and 117°K), and HI (at 70° and 126°K) are to be given a similar interpretation.[21] Each of the successive transitions in HBr and HI may be connected with incipient rotation about one crystal axis and the expansion of the crystal along that axis alone. In every case freely rotating molecules would assume a close-packed arrangement (cubic close-packing of molecules has been found with x-rays by Simon and Simson[22] for the high temperature form of HCl); on cooling below the temperature at which oscillation sets in the molecules may merely orient themselves, giving a structure similar to that of CO_2, for example, or the orientation may be accompanied by a change of position of molecular centers. That this takes place for HCl is indicated by the low symmetry of the low-temperature form shown by Simon and Simson's powder photographs.

[18] K. Clusius, Zeits. f. phys. Chem. **B3**, 41 (1929).

[19] J. C. McLennan and W. G. Plummer, Phil. Mag. **7**, 761 (1929), have found that powder photographic data indicate cubic close-packing of the molecules.

[20] W. F. Giauque and R. Wiebe, J. Am. Chem. Soc. **50**, 101 (1928); **50**, 2193 (1928); **51**, 1441 (1929).

[21] Giauque and Wiebe suggested essentially this explanation, writing "The results suggest the following possibility: the transition starts as a changing thermal equilibrium between energy states of the hydrogen iodide molecule, both in the same crystal lattice, but when a sufficient concentration of the higher energy state has been reached, the system becomes unstable and changes to a new crystalline form."

[22] F. Simon and C. v. Simson, Zeits. f. Physik **21**, 168 (1924).

It is predicted that the dielectric constants of solid HCl, HBr, and HI at temperatures just below the melting points will be very high and dependent on the temperature, the values being given by Debye's theory of the orientation of electric dipole molecules; while the low-temperature forms will have low dielectric constants nearly independent of the temperature.

In general it is to be expected that rotational motion of molecules and complex ions of sufficiently low moment of inertia will set in below the melting point of the crystals. This condition of low moment of inertia is satisfied by complexes containing hydrogen atoms and one heavy atom. Thus the forces orienting the tetrahedral ammonium ion in an ammonium salt are much stronger than those acting on a methane molecule, so that the ion will oscillate until a much higher temperature than 20°K is reached; but this temperature of transition to rotational motion is still considerably below the melting point.

The transitions have been observed. Simon[23] and co-workers found from heat capacity measurements that ammonium chloride, bromide, and iodide show a gradual transition covering about a 10° range in the neighborhoood 240°K, the nature of the phenomenon not depending essentially on the anion.[24] X-ray studies showed the crystal structure to be the same before and after the transition, which is accompanied by a small volume change, less than 1%. These investigators attribute the transition to the ammonium ion, but make no other suggestions as to its nature. The observed phenomena are just those expected to accompany the transition from oscillation to rotation of the ammonium ion, however. The increase in the transition temperature in the series NH_4I (−42.5°C), NH_4Br (−38.0°C), NH_4Cl (−30.4°C) further shows the expected effect of increasing interionic forces accompanying decreasing anion radius.[25]

The rotation of the ammonium ion in salts at ordinary temperatures provides justification for the customary treatment of the ion as spherically symmetrical in the theoretical discussion of the structure of ionic crystals. Further, the rotation of molecules such as NH_3 and H_2O about symmetry axes accounts for the fact that these molecules occupy positions in crystals with symmetry elements not compatible with those of the non-rotating molecule. Thus in $Ni(NH_3)_6Cl_2$ the NH_3 molecules lie on four-fold axes, and in alum the H_2O molecules on three-fold axes. The rotation of the molecules,

[23] F. Simon, Ann. d. Physik **68**, 263 (1922); F. Simon and C. v. Simson, Naturwiss. **38**, 880 (1926); F. Simon, C. v. Simson, and M. Ruhemann, Zeit. f. phys. Chem. **129**, 339 (1927).

[24] A very small hump in the heat capacity curve at −30° was also found for ammonium fluoride; the interpretation of this is uncertain (the structure of this crystal is not the same as that of the other ammonium halides).

[25] Small maxima in the heat capacity curves of organic compounds are probably often due to the transition from oscillational to rotational motion of a part of the molecule. Thus the maxima shown by *o*-xylene, *m*-xylene, and hexamethylbenzene (reported by H. M. Huffman, G. S. Parks and A. C. Daniels, J.A.C.S., **52**, 1547 (1930) would be attributed to the rotation of the methyl groups, which have a low moment of inertia and can rotate about the single bond holding the group to the rest of the molecule. *p*-xylene shows no maximum, indicating that the orienting forces on the methyl group are larger, raising the transition temperature above the melting point.

however, gives them an effective infinite symmetry axis, which is compatible with these positions.

The possibility of rotation introduces considerable uncertainty in the conclusions reached by Hendricks[26] in regard to the nature of the aliphatic carbon chain. From the x-ray study of crystals of the mono-alkyl substituted ammonium halides he found that in a number of these crystals the alkyl ammonium ion lies on a four-fold axis of symmetry, a result which apparently excludes the usual staggered chain of carbon atoms, and which caused him to suggest that the chain really is straight. But the moment of inertia of a staggered chain about an axis along the chain would be very small, and we would expect rotation about this axis at ordinary temperatures, giving the chain an effective infinite symmetry axis, which is compatible with the x-ray data. Accordingly, Hendricks' investigation does not require that the staggered aliphatic chain be given up.[27]

It has been found by Lyons and Rideal that solid unimolecular films on water of long chain hydrocarbons with polar ends exist in two possible forms, one with an area of 20.6A^2 per molecule, and the other, stable at higher temperatures, with an area of 26.2A^2 per molecule.[28] These authors suggest[29] that in the more compact form the staggered chains are interlocked, and fit together more closely than at higher temperatures when interlocking is not effective. This explanation is made somewhat more precise by the application of the considerations discussed in this paper. At low temperatures interlocking does take place, the molecules oscillating about certain equilibrium orientations. With increasing temperature rotation sets in, and the film expands; in this state the molecules would be well represented as circular cylinders with a radius equal to the maximum radius of the staggered chain. The phenomenon is exactly analogous to that giving rise to gradual transitions in crystals.

In molecules C_2X_6, such as ethane, C_2H_6, there exists the possibility of the two ends of the molecule rotating or oscillating relative to each other. In case that X is a large atom, as in C_2I_6, the interaction of the two ends of the molecule will be large, and they will carry out small oscillations about the relative orientation in which the atom groups fit closely together, the six atoms X defining the corners of an octahedron. But in C_2H_6 the interaction of the two ends of the molecule will be small, and they will rotate freely about the single bond connecting the carbon atoms, with a frequency which is simply related to the rotational frequency of the entire molecule about its figure axis. The determination of the energy levels characteristic of this motion for molecules of this type, by means of Raman effect or infrared measurements, would permit the evaluation of the potential energy of the molecule as a function of the relative orientation of its ends.

I acknowledge with gratitude the inspiration and assistance received through conversations with Professor W. F. Giauque of the Chemistry Department of the University of California.

[26] S. B. Hendricks, Zeits. f. Krist. **67**, 465 (1928); **68**, 189 (1928); additional paper in press.

[27] Dr. Hendricks has informed me that he agrees with this conclusion.

[28] I am indebted to Professor J. W. Mc Bain for directing my attention to this work.

[29] C. G. Lyons and E. K. Rideal, Nature **125**, 455 (1930).

DEFLECTION OF ELECTRONS BY A MAGNETIC FIELD ON THE WAVE MECHANICS

By Leigh Page

Sloane Physical Laboratory, Yale University

(Received June 26, 1930)

Abstract

The wave equation for a stream of electrons passing through a uniform magnetic field is solved and the characteristic functions discussed. The motion at right angles to the field is found to be completely quantized.

The current density is investigated, and the mean square and mean fourth power radii of curvature found for each quantum state. The mean square radius of curvature is found to be the same for all quantum states of the same energy and identical with that predicted by the classical theory.

The mean radius of curvature is determined by interpolation and is found to be less than that predicted by the classical theory. Therefore values of e/μ calculated by means of the classical formula from measured values of the mean radius of curvature should be too large. The error is estimated and found to be of the same general magnitude as the discrepancy between the results of deflection experiments and those of spectroscopic measurements.

IN his review of the probable values of the general physical constants, Birge[1] gives for the best values of the ratio of charge to rest-mass of the electron:

$e/\mu = (1.769 \pm 0.002)\ (10)^7$ abs e.m.u. from deflection experiments,
$= (1.761 \pm 0.002)\ (10)^7$ " " " from Zeeman effect,
$= (1.761 \pm 0.001)\ (10)^7$ " " " from H and He spectra.

The discrepancy between the value obtained from deflection experiments on the one hand and those obtained from spectroscopic evidence on the other is four times the probable error of the former, indicating that the difference is real and not merely the result of accidental errors. Now the value of e/μ obtained from deflection experiments is calculated on the classical electrodynamics, whereas the others are based on quantum theory. Therefore it is important to examine the Schrödinger theory of the motion of a stream of electrons in a uniform magnetic field in order to ascertain whether or not it introduces a correction into the classical formula for the radius of curvature r of the circular path of the electrons about the magnetic lines of force. This problem has been investigated by Alexandrow[2] on the basis of Dirac's theory. His second order wave Eq (10) differs from the Schrödinger equation which will be used in this paper only in the value of one of the constant coefficients—a difference which is quite negligible for the large energy values which are to be considered. Alexandrow obtains a solution of the wave equation which is everywhere finite and vanishes at infinity, and concludes that the motion is

[1] R. T. Birge, Phys. Rev. Sup. **I**, 47 (1929).
[2] W. Alexandrow, Zeits. f. Physik **56**, 825 (1929).

not quantized, all values of the energy being allowed. His solution (11) however, contains the factor

$$e^{(k/2)\log(y+iz)} = r^{k/2}\left(\cos\frac{k}{2}\theta + i\sin\frac{k}{2}\theta\right)$$

in plane polar coordinates. Now, one of the requirements of the wave mechanics is that a solution, to be allowed, must be single valued. Therefore it would seem that $k/2$ in Alexandrow's solution must be an integer, and consequently the energy, which is a linear function of k, can assume only discrete values, indicating that the motion is quantized. In fact it will appear that Alexandrow's solution is just one of a multitude of characteristic functions corresponding to a stream of electrons of assigned energy.

Solution of the Wave Equation

The wave equation[3] for electrons moving through a magnetic field is

$$-\frac{h^2}{8\pi^2\mu}\nabla\cdot\nabla\psi - \frac{eh}{2\pi\mu ic}\mathbf{a}\cdot\nabla\psi + \frac{e^2a^2}{2\mu c^2}\psi + \frac{h}{2\pi i}\frac{\partial\psi}{\partial t} = 0, \tag{1}$$

where $\mathbf{a}$ is the vector potential. If the field is uniform and in the X direction

$$\mathbf{a} = -j\tfrac{1}{2}Hz + k\tfrac{1}{2}Hy,$$

and if we introduce cylindrical coordinates r,θ,x the wave Eq. (1) becomes

$$-\frac{h^2}{8\pi^2\mu}\left\{\frac{1}{r}\frac{\partial}{\partial r}\left(r\frac{\partial\psi}{\partial r}\right) + \frac{1}{r^2}\frac{\partial^2\psi}{\partial\theta^2} + \frac{\partial^2\psi}{\partial x^2}\right\} - \frac{ehH}{4\pi\mu ic}\frac{\partial\psi}{\partial\theta} + \frac{e^2H^2}{8\mu c^2}r^2\psi + \frac{h}{2\pi i}\frac{\partial\psi}{\partial t} = 0. \tag{2}$$

Putting

$$\psi \equiv X(x)R(r)e^{-im\theta}e^{-2\pi i(W/h)t},$$

where m must be an integer in order that the solution may be single valued, we are led to the two ordinary differential equations

$$\frac{d^2X}{dx^2} + \frac{8\pi^2\mu}{h^2}W_xX = 0, \tag{3}$$

$$\frac{d^2R}{dr^2} + \frac{1}{r}\frac{dR}{dr} + \left\{\frac{8\pi^2\mu}{h^2}W_{r\theta} - \frac{2\pi eH}{hc}m - \frac{m^2}{r^2} - \frac{1}{4}\left(\frac{2\pi eH}{hc}\right)^2r^2\right\}R = 0, \tag{4}$$

W_x being the energy associated with the motion along the lines of force and $W_{r\theta}$ that with the motion in the plane at right angles to the magnetic field.

Equation (3) admits a continuous manifold of allowable solutions[4] representing a uniform current parallel to the field. Our interest being confined to

[3] Condon and Morse, Quantum Mechanics, p. 28.

[4] Condon and Morse, p. 42.

the motion in the plane at right angles to the field, we may put $W_z=0$, $W_{r,\theta}=W$ without limiting the generality of the solution. Our problem, then, is to find the allowed solutions of (4).

If we put

$$\rho^2 \equiv \frac{2\pi eH}{hc}r^2, \qquad w \equiv \frac{4\pi\mu c}{heH}W,$$

(4) simplifies to

$$\frac{d^2R}{d\rho^2}+\frac{1}{\rho}\frac{dR}{d\rho}+\left\{w-m-\frac{m^2}{\rho^2}-\frac{1}{4}\rho^2\right\}R=0. \tag{5}$$

Making the substitution

$$R \equiv \rho^m e^{-\rho^2/4}V(\rho)$$

in (5), where we are supposing m to be positive, we get

$$\frac{d^2V}{d\rho^2}+\left(\frac{2m+1}{\rho}-\rho\right)\frac{dV}{d\rho}+(w-2m-1)V=0. \tag{6}$$

This equation can be simplified by changing the independent variable from ρ to x where $x\equiv\rho^2$. Then

$$4x\frac{d^2V}{dx^2}+2\{2(m+1)-x\}\frac{dV}{dx}+\{w-2m-1\}V=0. \tag{7}$$

Assuming a series solution of the form

$$V=\sum_p A_p x^p$$

we find on substitution in (7)

$$4p(p+m)A_p=\{2p-w+2m-1\}A_{p-1}.$$

Therefore the two independent solutions of the differential equation are ascending series starting with x^0 and x^{-m}, that is, with ρ^0 and ρ^{-2m}. The second is inadmisssible since it makes R infinite at the origin. Therefore we have to consider only the series which starts with a constant term. The successive coefficients are related by the equation

$$A_p=\frac{2p-w+2m-1}{4p(p+m)}A_{p-1}. \tag{8}$$

If the series fails to terminate, this relation may be written

$$A_p=\frac{1}{2p}A_{p-1}$$

for large values of p. Hence the function V approaches infinity for x infinite in the same way as

$$A_0\left[\cdots\frac{\left(\frac{x}{2}\right)^p}{p!}+\frac{\left(\frac{x}{2}\right)^{p+1}}{p+1!}+\cdots\right]=A_0e^{\rho^2/2},$$

making R become infinite of the order $e^{\rho^2/4}$. Consequently the only allowable solutions are those for which the series terminates. We see from (8), then, that

$$w=2s+1, \tag{9}$$

where s is a positive integer equal to or greater than m. The motion, therefore, is completely quantized, the energy values being

$$W=\left(s+\frac{1}{2}\right)h\left(\frac{eH}{2\pi\mu c}\right), \quad s=0,1,2\cdots. \tag{10}$$

The last factor in (10) is just the frequency of revolution about the lines of force predicted by the classical theory.

Putting (9) into (8)

$$A_p=-\frac{(s-m)-(p-1)}{2p(p+m)}A_{p-1}. \tag{11}$$

It is more convenient to express the wave functions in terms of the quantum numbers s and k where $k\equiv s-m$, in place of s and m. The energy is a function of s alone, and for a given s, k may have any of the values 0, 1, $2\cdots s$. For $k=0$ the polynomial V is a constant, for $k=1$ it consists of two terms, and so on. In terms of s and k (11) becomes

$$A_p=-\frac{k-p+1}{2p(s-k+p)}A_{p-1}$$

giving

$$V_{s,k}=\sum_{p=0}^{k}\frac{(-1)^px^p}{2^pp!(k-p)!(s-k+p)!}, \quad k=0,1,2\cdots s, \tag{12}$$

and

$$R_{s,k}=A_{s,k}X^{(s-k)/2}e^{-x/4}V_{s,k}, \quad k=0,1,2\cdots s. \tag{13}$$

Alexandrow's solution of the wave epation is $R_{s,k}e^{-is\theta}$.

The V Polynomials

Denote differentiation with respect to x by D. Then by differentiating (12) we find

$$V_{s,k}=-2DV_{s,k+1}. \tag{14}$$

Next we easily prove

$$V_{s,k}=\frac{1}{k!s!}x^{-(s-k)}e^{x/2}D^k[x^se^{-x/2}], \tag{15}$$

which we can put in neater form if we write

$$X_s \equiv x^s e^{-x/2}.$$

Then (15) becomes

$$V_{s,k} = \frac{1}{k!s!} x^k X_s^{-1} D^k X_s. \tag{16}$$

From (14) and (15) we get the recursion formula

$$[2(s-k)-x]V_{s,k} = 2(k+1)V_{s,k+1} + xV_{s,k-1}. \tag{17}$$

The first four V polynomials are

$$V_{s,0} = \frac{1}{s!},$$

$$V_{s,1} = -\frac{1}{2s!}\{x - 2s\},$$

$$V_{s,2} = \frac{1}{2^2 2!s!}\{x^2 - 4sx + 4s(s-1)\},$$

$$V_{s,3} = -\frac{1}{2^3 3!s!}\{x^3 - 6sx^2 + 12s(s-1)x - 8s(s-1)(s-2)\}.$$

On account of (15) the zeros of $V_{s,k}$ between 0 and ∞ are the zeros of $D^k[x^s e^{-x/2}]$. The latter function vanishes at 0 and ∞ for all k's less than s. Now $x^s e^{-x/2}$ has one turning point (maximum at $x=2s$). Consequently $D[x^s e^{-x/2}]$ has one zero between 0 and ∞, and as it vanishes at both limits, it has two turning points. This requires $D^2[x^s e^{-x/2}]$ to have two zeros and three turning points and so on. Consequently $V_{s,k}$ has k zeros between 0 and ∞ for any k less than or equal to s. This means that all the roots of the equation $V_{s,k}=0$ are real and positive.

The Radial Function

In terms of the quantum numbers s and m the differential Eq. (5) for R is

$$\frac{d^2R}{d\rho^2} + \frac{1}{\rho}\frac{dR}{d\rho} + \left\{2s - m + 1 - \frac{m^2}{\rho^2} - \frac{1}{4}\rho^2\right\}R = 0. \tag{18}$$

If we put $u \equiv \rho^{1/2} R$ this becomes

$$u'' + \left\{2s - m + 1 + \frac{1-4m^2}{4\rho^2} - \frac{1}{4}\rho^2\right\}u = 0.$$

Denoting solutions for the same value of m but different values of s by u_{s_1} and u_{s_2},

$$2(s_2 - s_1)\int_0^\infty u_{s_1}u_{s_2}d\rho = 0 \tag{19}$$

showing that the u functions are orthogonal.

To normalize these functions we must determine the arbitrary coefficient $A_{s,k}$ in (13) so that

$$\int_0^\infty u_s^2 d\rho = \tfrac{1}{2}\int_0^\infty R_{s,k}^2 dx = 1, \tag{20}$$

where x, as before, stands for ρ^2. Squaring (13) and using (15)

$$R_{s,k}^2 = A_{s,k}^2 x^{s-k} e^{-x/2} V_{s,k}^2 = \frac{A_{s,k}^2}{k!s!} V_{s,k} D^k [x^s e^{-x/2}].$$

Integrating by parts, with the aid of (14),

$$\int_0^\infty R_{s,k}^2 dx = \frac{A_{s,k}^2}{k!s!}\int_0^\infty V_{s,k} D^k [x^s e^{-x/2}] dx = \frac{2^{s-k+1}}{k!s!} A_{s,k}^2.$$

To satisfy (20) it is necessary that

$$A_{s,k} = \frac{1}{2^{(s-k)/2}}(k!s!)^{1/2} \tag{21}$$

and the normalized radial function is

$$R_{s,k} = \frac{(k!s!)^{1/2}}{2^{(s-k)/2}} x^{s-k/2} e^{-x/4} V_{s,k}$$

$$= \frac{1}{2^{(s-k)/2}(k!s!)^{1/2}} x^{-(s-k)/2} e^{x/4} D^k [x^s e^{-x/2}]. \tag{22}$$

Also

$$R_{s,k}^2 = \frac{1}{2^{s-k}} V_{s,k} D^k [x^s e^{-x/2}]. \tag{23}$$

The Current

The quantity actually measured experimentally is the deflection of the current of cathode rays or electrons. The current density[5] is given by

$$j = \frac{eh}{4\pi\mu i}(\bar{\psi}\nabla\psi - \psi\nabla\bar{\psi}) - \frac{e^2}{\mu c} a\psi\bar{\psi}$$

$$= -\frac{e^2 H}{2\mu c}\left\{1 + 2m\left(\frac{hc}{2\pi e H}\right)\frac{1}{r^2}\right\} R^2 r\theta_1$$

where θ_1 is a unit vector at right angles to r in the direction of increasing θ. It is clear from the form of this expression that the current lines are circles about the lines of force for all values of the quantum number m. The current between cylinders of radii r and $r+dr$ is

$$j_{s,k} dr = -\frac{eh}{8\pi\mu}\left\{1 + 2\frac{s-k}{x}\right\} R_{s,k}^2 dx \tag{24}$$

[5] Condon and Morse, p. 30.

in terms of the quantum numbers s, k and $x \equiv \rho^2$.

Since the constant factor appearing in (24) is of no significance for our purposes, let us consider the function

$$J_{s,k} = \frac{1}{2}x^{1/2}\left\{1 + 2\frac{s-k}{x}\right\}R_{s,k}^2$$
$$= \frac{1}{2^{s-k+1}}x^{1/2}\left\{1+2\frac{s-k}{x}\right\}V_{s,k}D^kX_s \tag{25}$$

and

$$J_{s,k}d(x)^{1/2} = \frac{1}{4}\left\{1 + 2\frac{s-k}{x}\right\}R_{s,k}^2dx$$
$$= \frac{1}{2^{s-k+2}}\left\{1 + 2\frac{s-k}{x}\right\}V_{s,k}D^kX_sdx. \tag{26}$$

First we will calculate the total current

$$I_{s,k} = \int_0^\infty J_{s,k}d(x)^{1/2} = \frac{1}{4}\int_0^\infty R_{s,k}^2dx + \frac{s-k}{2^{s-k+1}}\int_0^\infty \frac{1}{x}V_{s,k}D^kX_sdx$$

corresponding to each normalized quantum state. The value of the first term on the right is $1/2$ from (20). To evaluate the second we note that if we integrate by parts with the aid of (14)

$$\int_0^\infty V_{s,k-p}D^kX_sdx = \frac{1}{2^{k-p}s!}\,|\,D^{p-1}X_s\,|_0^\infty = 0 \tag{27}$$

provided p is an integer greater than zero and less than k. Now, from the recursion formula (17),

$$V_{s,k} = \frac{s-k+1}{k}V_{s,k-1} - \frac{x}{2k}(V_{s,k-1} + V_{s,k-2}). \tag{28}$$

Consequently

$$\int_0^\infty \frac{1}{x}V_{s,k}D^kX_sdx = \frac{s-k+1}{k}\int_0^\infty \frac{1}{x}V_{s,k-1}D^kX_sdx$$
$$= \frac{s(s-1)\cdots(s-k+1)}{k!s!}\int_0^\infty \frac{1}{x}D^kX_sdx. \tag{29}$$

But

$$\int_0^\infty \frac{1}{x}D^kX_sdx = \int_0^\infty \frac{1}{x^2}D^{k-1}X_sdx = \cdots = k!\int_0^\infty x^{s-k-1}e^{-x/2}dx$$
$$= k!(s-k-1)!2^{s-k}, \tag{30}$$

and

$$\int_0^\infty \frac{1}{x} V_{s,k} D^k X_s dx = \frac{2^{s-k}}{s-k}. \tag{31}$$

Therefore the total current corresponding to each normalized quantum state is

$$I_{s,k} = \tfrac{1}{2} + \tfrac{1}{2} = 1 \tag{32}$$

independent of the quantum numbers s and k.

We are primarily interested in the radius of curvature r in the magnetic field of a current of electrons of kinetic energy W. From the defining equation for $x \equiv \rho^2$ and (10) we have

$$r^2 = \frac{2\mu c^2 W}{e^2 H^2} \frac{x}{2s+1} \tag{33}$$

which is to be compared with the formula

$$r^2 = \frac{2\mu c^2 W}{e^2 H^2} \tag{34}$$

of classical electrodynamics. In the experiments of Wolf,[6] which Birge considers to be the most accurate for the determination of e/μ by the deflection method, s is of the order of magnitude of $(10)^8$. Hence we are concerned only with states for which s is very large.

$J_{s,0}$ AND $J_{s,1}$.

Let us examine more closely the current densities $J_{s,0}$ and $J_{s,1}$ of the first two states of energy corresponding to the quantum number s. The first of these is

$$J_{s,0} = \frac{1}{2^{s+1} s!} \left(1 + 2\frac{s}{x}\right) x^{s+1/2} e^{-x/2}. \tag{35}$$

Its only zeros are at $x=0$ and $x=\infty$. It has one maximum, at $x=2s$. The radius of curvature of the maximum current density, then, is given by

$$r_m^2 = \frac{2\mu c^2 W}{e^2 H^2} \frac{2s}{2s+1} \tag{36}$$

agreeing almost exactly for large s with the classical value (34). The maximum current density is

$$(J_{s,0})_{\max} = \frac{2^{1/2}}{s!} s^{s+1/2} e^{-s} \tag{37}$$

and in the neighborhood of the maximum we have approximately

$$\frac{J_{s,0}}{(J_{s,0})_{\max}} = e^{-(x-2s)^2/8s} \tag{38}$$

[6] F. Wolf, Ann. d. Physik **83**, 849 (1927).

for large s. Consequently the current density falls to $1/e^{\text{th}}$ of its maximum value at a point $\Delta x = 2(2s)^{1/2}$ to either side of the maximum. For $s=(10)^8$

$$\frac{\Delta x}{x_{\max}} = \left(\frac{2}{s}\right)^{1/2} = 2^{1/2}(10)^{-4}$$

showing that the peak is extremely narrow.

The current density of the next state is

$$J_{s,1} = \frac{1}{2^{s+2}s!}\left\{1 + 2\frac{s-1}{x}\right\}(x-2s)^2 x^{s-1/2}e^{-x/2}. \tag{39}$$

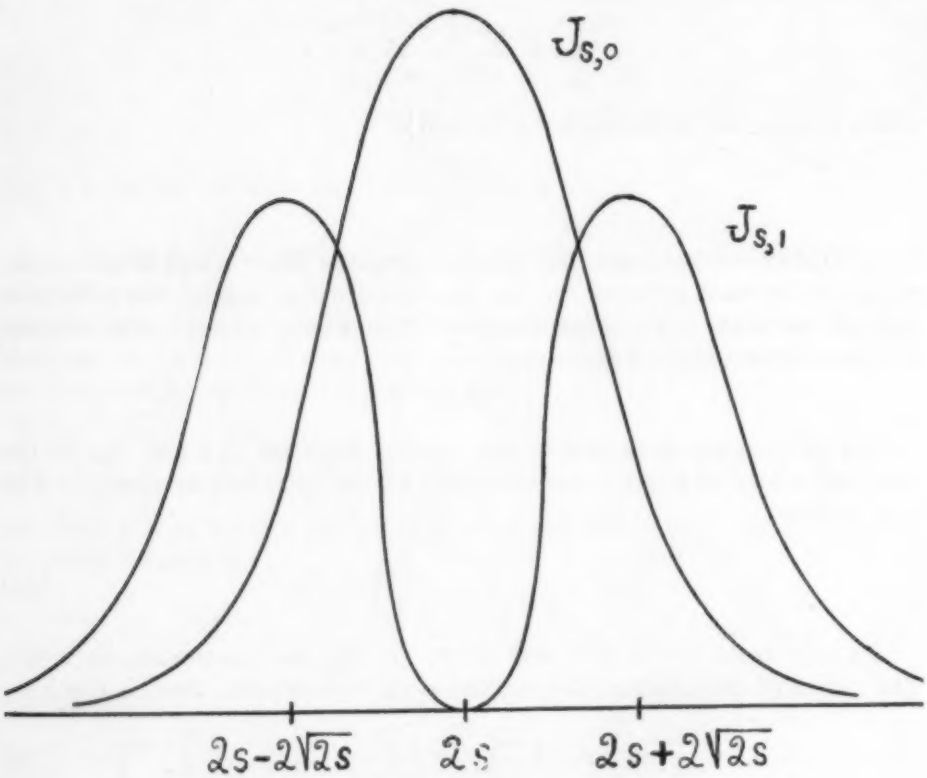

Fig. 1.

Zeros occur at $x=0$, $2s$, and ∞. There are two maxima, at approximately $x=2s\pm 2(2s)^{1/2}+1$. The maximum current densities are approximately the same and equal to

$$(J_{s,1})_{\max} = \frac{2^{3/2}}{s!}s^{s+1/2}e^{-(s+1)}. \tag{40}$$

The graphs of the two functions, $J_{s,0}$ and $J_{s,1}$ are sketched in Fig. 1 for large s, the origin being a great distance to the left of the center of the figure.

Evidently the zeros of $J_{s,k}$ between 0 and ∞ are identical with those of $V_{s,k}$. Thus $J_{s,k}$ has k zeros in this interval.

Mean Radii of Curvature

While the mean radius of curvature of each current cannot be evaluated easily on account of radicals appearing in the integrand, the mean square and the mean fourth power radius of curvature are readily obtained. From (26) and (32)

$$\begin{aligned}\overline{\rho^2} = \bar{x} &= \tfrac{1}{4}\int_0^\infty \{x + 2(s-k)\} R_{s,k}^2 dx \\ &= (s-k) + \frac{1}{2^{s-k+2}}\int_0^\infty x V_{s,k} D^k X_s dx,\end{aligned} \tag{41}$$

and

$$\begin{aligned}\overline{\rho^4} = \overline{x^2} &= \frac{1}{4}\int_0^\infty \{x^2 + 2(s-k)x\} R_{s,k}^2 dx \\ &= \frac{s-k}{2^{s-k+1}}\int_0^\infty x V_{s,k} D^k X_s + \frac{1}{2^{s-k+2}}\int_0^\infty x^2 V_{s,k} D^k X_s dx.\end{aligned} \tag{42}$$

To evaluate the integrals involved, we have, if we integrate by parts with the aid of (14),

$$\begin{aligned}\int_0^\infty x^p V_{s,k} D^k X_s dx &= \frac{1}{2^k}\int_0^\infty x^p V_{s,0} X_s dx - \frac{kp}{2^{k-1}1!}\int_0^\infty x^{p-1} V_{s,1} X_s dx \\ &+ \frac{k(k-1)p(p-1)}{2^{k-2}2!}\int_0^\infty x^{p-2} V_{s,2} X_s dx - \cdots .\end{aligned} \tag{43}$$

For positive integral values of p the series consists of a finite number of terms. Thus for $p=1$,

$$\begin{aligned}\int_0^\infty x V_{s,k} D^k X_s dx &= \frac{1}{2^k}\int_0^\infty \{x V_{s,0} - 2k V_{s,1}\} X_s dx \\ &= \frac{1}{2^k s!}\left[(k+1)\int_0^\infty x^{s+1} e^{-x/2} dx - 2ks\int_0^\infty x^s e^{-x/2} dx\right] \\ &= 2^{s-k+2}[(k+1)(s+1) - ks] = 2^{s-k+2}(s+k+1).\end{aligned} \tag{44}$$

Hence (41) becomes

$$\overline{\rho^2} = \bar{x} = (s-k) + (s+k+1) = 2s+1 \tag{45}$$

independent of the quantum number k. Putting this in (33) we find

$$r^2 = \frac{2\mu c^2 W}{e^2 H^2}, \tag{46}$$

which is identical with the classical formula (34). Hence we conclude that the mean square radius of curvature is the same for all quantum states of the same energy and identical with the square of the radius of curvature given by the classical theory.

Next we shall evaluate (42) for the mean fourth power radius of curvature. In this case we need in addition to (44) the integral (43) for $p=2$. The latter is

$$\begin{aligned}\int_0^\infty x^2 V_{s,k} D^k X_s dx &= \frac{1}{2^k}\int_0^\infty \left\{ x^2 V_{s,0} - 4kxV_{s,1} + 4k(k-1)V_{s,2}\right\} X_s dx \\ &= \frac{1}{2^k s!}\left[\left(1+\frac{3}{2}k+\frac{1}{2}k^2\right)\int_0^\infty x^{s+2}e^{-x/2}dx - 2ks(k+1)\int_0^\infty x^{s+1}e^{-x/2}dx \right. \\ &\qquad \left. + 2ks(k-1)(s-1)\int_0^\infty x^s e^{-x/2}dx\right] \\ &= 2^{s-k+2}[(k+1)(k+2)(s+1)(s+2) - 2k(k+1)s(s+1) + (k-1)k(s-1)s].\end{aligned} \tag{47}$$

Consequently (42) becomes

$$\begin{aligned}\overline{\rho^4} = \overline{x^2} &= 2(s-k)[(k+1)(s+1) - ks] \\ &\quad + [(k+1)(k+2)(s+1)(s+2) - 2k(k+1)s(s+1) + (k-1)k(s-1)s] \\ &= (2s+1)^2 + 2(2k+1)(2s+1) + 1.\end{aligned} \tag{48}$$

The mean fourth power of the radius of curvature, therefore, increases with increasing k and is greater than the square of the mean square radius of curvature for all quantum states of a given energy. If we average over all k's form 0 to s we find

$$\overline{\bar{\rho}^4} = \overline{\bar{x}^2} = 8s^2 + 10s + 4. \tag{49}$$

Discussion of Results

The usual experimental method of measuring the deflection of a stream of electrons by a magnetic field involves the determination of the mean radius of curvature rather than the mean square. On account of the slit or slits used to define the stream, we should expect the greatest number of electrons to be in the states for which k is small, for the increase of spread of J with increase in k would prevent electrons in the higher quantum states from passing through the slit system. In the absence of knowledge of the effect of slit width on the distribution of the electrons, no exact quantitative correction to the classical formula can be given. Certain qualitative conclusions may be drawn, however.

To obtain an estimate of the order of magnitude of the mean radius of curvature of the current for quantum number k we can make use of the known values of $\overline{\rho^0}$, $\overline{\rho^2}$ and $\overline{\rho^4}$. Putting $S \equiv 2s+1$, $K \equiv 2k+1$ we have from (32), (45) and (48)

$$\overline{\rho^0} = 1,$$
$$\overline{\rho^2} = S,$$
$$\overline{\rho^4} = S^2\left[1 + 2\frac{K}{S} + \frac{1}{S^2}\right].$$

If the current distribution were perfectly sharp, we would have

$$\log \overline{\rho^n} = An. \tag{50}$$

If K is small compared to S, the values of $\overline{\rho^0}$, $\overline{\rho^2}$ and $\overline{\rho^4}$ show that the spread of the current is small. Hence we can determine the first order correction to (50) by writing

$$\log \overline{\rho^n} = An + Bn^2$$

and determining the constants A and B to fit the values found for the three means. This gives

$$\overline{\rho^n} = S^{n/2}\left[1 + 2\frac{K}{S} + \frac{1}{S^2}\right]^{n(n-2)/8} \tag{51}$$

Consequently interpolation gives for the mean radius of curvature

$$\bar{\rho} = S^{1/2}\left[1 + 2\frac{K}{S} + \frac{1}{S^2}\right]^{-1/8}$$
$$\doteq S^{1/2}\left[1 - \frac{1}{4}\frac{K}{S}\right].$$

As this is less than $(2s+1)^{1/2}$ the square of the mean radius of curvature is less than the mean of the square. Hence, as e/μ varies inversely with r^2, the calculation of e/μ by means of the classical formula will give too large a value of the specific charge of the electron. Therefore the error indicated by theory is of the right sign to explain the discrepancy between the results of deflection experiments and spectroscopic measurements.

To estimate the magnitude of the error we need the mean value of K for the electrons passing through the slit. The spread of the current is given by

$$\Delta\rho^2 = \int_0^\infty J(\rho - \bar{\rho})^2 d\rho = \overline{\rho^2} - \bar{\rho}^2 = \tfrac{1}{2}K.$$

The quantity $\Delta\rho$ measures the effective distance of the current either side of its mean position. It seems reasonable to infer that half the current passes through the slit when $\Delta\rho/\rho$ is equal to the ratio of the half width of the slit to the radius of curvature. Now the ratio of the half width of the slit to the radius of curvature in Wolf's experiments was 0.04 and s was approximately 1.7(10).[8] So when

$$\frac{\Delta\rho}{\rho} = \frac{1}{2}\left(\frac{K}{S}\right)^{1/2} = 0.04 \quad \text{or} \quad \frac{K}{S} = 0.0032$$

half the current passes through the slit. Putting $S=3.4(10)^8$, $K=10.9(10)^5$ or $k=5.4(10)^5$. Consequently the ratio of the magnitude of each partial current to that of the next of lower index may be taken to be

$$\alpha = (\tfrac{1}{2})^{1/5.4(10)^5}.$$

The mean value of K, then, is

$$\bar{K} = \frac{1+3\alpha+5\alpha^2\cdots+(2s+1)\alpha^s}{1+\alpha+\alpha^2\cdots+\alpha^s} = 1+\frac{2\alpha}{1-\alpha}\,\frac{1-\alpha^s}{1-\alpha^{s+1}} - \frac{2s\alpha^{s+1}}{1-\alpha^{s+1}}$$

$$\doteq \frac{2}{1-\alpha} = 1.56(10)^6.$$

The error in e/μ is that in $1/\beta^2$, that is, $(1/2)\bar{K}/S$. Hence the order of magnitude of the error is

$$\frac{1}{2}\frac{\bar{K}}{S} = 0.0023.$$

As the actual discrepancy between the results of Wolf's deflection experiments and of spectroscopic observations is 0.0045 ± 0.0011, *we conclude that the error indicated by theory is of the correct order of magnitude as well as of the correct sign to account for the observed discrepancy.* In view of the very rough calculation of the mean K, the numerical value obtained above cannot be considered as more than an estimate of the magnitude of the error. The agreement with the observed discrepancy is therefore as good as the method of calculation warrants.

The results of this investigation indicate that in measuring e/μ by the deflection method the classical formula is applicable only if (a) the ratio of slit width to radius of curvature is very small, or (b) the method is one in which the mean square of the radius of curvature is measured. In the latter case it makes no difference in what quantum states the electrons may be, for the mean square of the radius of curvature is the same for all states of the same energy and the value of e/μ is given correctly by the classical formula.

ABSORPTION OF X-RAYS BY LITHIUM

By K. C. Mazumder
London, England

(Received May 26, 1930)

Abstract

The mass scattering coefficient of lithium has been measured between the wave-lengths 0.587−0.100A. The results for the long wave-lengths can be expressed by the equation $\mu/\rho = 0.94\lambda^3 + 0.162$. A very rapid bending of the curve towards the axis λ^3 is noticed below the wave-length 0.2A.

LITHIUM is the lightest element studied in connection with x-ray absorption. Hewlett[1] worked with it twice but did not carry the investigation down to very short wave-lengths. More recently Mertz[2] attacked the problem afresh but he too, did not go beyond the wave-lengths used by Hewlett. The shortest wave-length used by Hewlett was 0.314 and that by Mertz 0.32A. Both of these experimenters were engaged in measuring the scattered rays directly. In the present work, a wider range of wave-lengths, 0.587–0.100A, was used in measuring in the straight-forward way the total absorption coefficient of lithium. The range of wave-lengths was sufficiently long to show that the absorption by even lithium did not follow the simple law $\mu/\rho = K\lambda^3 + \delta/\rho$ for short wave-lengths.

To prevent oxidation of lithium it had to be placed in an air-tight case the wall of which should not absorb any appreciable amount of rays. The scheme adopted in the present work made it unnecessary to measure by separate experiment the amount absorbed by the wall. A somewhat elliptical hole was cut into a steel rod of desired length. The diameter of the rod was equal to the inner diameter of the brass tube through which rays entered the spectrometer. The major axis of the hole was about two-thirds of the diameter of the rod and twice as much as the diameter of the piece of lithium. On either end of the rod was soldered a thick disk of steel with a hole at the center. One of the holes was sufficiently large to allow the lithium rod to be pushed into it. The other hole was so small as to be completely covered by the piece of lithium when it was in the path of the rays. One of the disks had a much larger diameter than the rod so that when the rest of the rod was pushed inside the brass tube the rays had no openings excepting the smaller hole at the center of the disks to enter the spectrometer. Thin pieces of mica were gummed on either end of the rod after the freshly cut lithium was placed inside. This arrangement was completely air-tight and lithium could be kept inside for weeks without any appreciable amount of oxidation taking place. By simply rotating the steel container through 180

[1] Hewlett, Phys. Rev. **17**, 284 (1921); **20**, 688 (1922).
[2] Mertz, Phys. Rev. **28**, 891 (1926).

degrees it was possible to place the lithium in or out of the path of the rays. The same mica windows were in the path in both positions, so the correction for absorption by the walls of the container was not necessary.

The lithium used was obtained from Professor Lyman who procured it for his spectroscopic work. Professor Bridgman has samples of the same lithium analysed in connection with his high pressure work, only traces of aluminum were detected, the amount being 0.7 of 1 percent. The correction for aluminum was made by means of the equation $\mu/\rho = 15.5\lambda^3 + 0.147$, representing its coefficient of absorption. This equation was suggested by Professor Duane and the writer.[3]

The amount of the rays absorbed depending greatly upon the wave-lengths it was necessary to use two pieces of lithium of lengths 5.3 cm and 2.9 cm, the former was used for the hard rays and the latter for the comparatively soft rays. The agreement between the results was very satisfactory.

In order to make measurements of the coefficient of absorption, the crystal and the ionization chamber were set in corresponding positions. The steel container with the lithium was placed in the brass tube. It was first kept in a position such that the lithium was out of the path of the rays. The ionization current was observed. The lithium was then placed in the path of rays by rotating the container through 180 degrees. The ionization current was again observed. Both of these readings were corrected for the natural leakage of the instrument and for stray radiations. From these two readings the corresponding mass absorption coefficient was calculated by means of the equation $\mu/\rho = (2.30/d.t) \log I_o/I$, d being the density and t, the length of the piece of lithium.

TABLE I.

λ in A	λ^3	μ/ρ	λ in A	λ^3	μ/ρ
0.587	0.202	0.330	0.368	0.0498	0.208
.535	.1529	.300	.315	.031	.192
.482	.112	.262	.2625	.018	.179
.429	.079	.237	.209	.009	.169
.368	.0498	.206	.185	.0063	.160
.473	.108	.263	.159	.004	.148
.421	.0745	.232	.144	.003	.134
			.102	.001	.114 (?)

The first five readings were taken with the shorter piece of lithium and the rest with the longer piece. The curve in Fig. 1 has been obtained by plotting the mass absorption coefficient against the tube of the corresponding wave-length. It is seen that the curve is not a straight line. It bends downwards in the region of short wave-lengths, the bending being noticeable in the neighbourhood of the wave-length $\lambda = 0.2$A. If the straight part of the curve is produced it cuts the axis at about 0.1625. This according to the theory is the mass scattering coefficient. The value obtained from J. J. Thomson's expression is 0.175, assuming that all the three electrons in the lithium atom scatter freely.

[3] Duane and Mazumder, Proc. Nat. Acad. Sci. **8**, 45 (1922).

The coefficient of λ^3 is found to be 0.94. The following equation represents approximately the mass coefficient of absorption for comparatively long wave-length

$$\mu/\rho = 0.94\lambda^3 + 0.162$$
$$= 80.5 \times 10^{-3}(N^4/A)\lambda^3 + 0.162$$

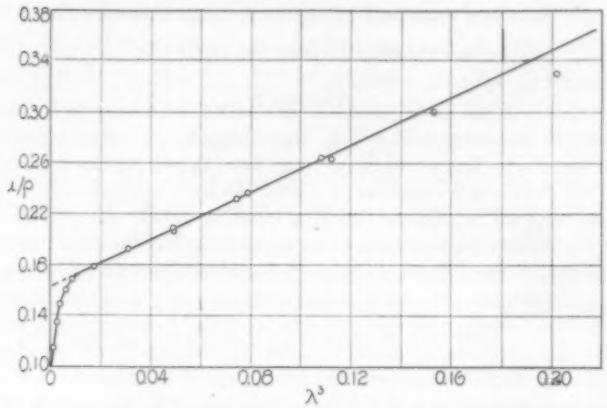

Fig. 1. Mass absorption coefficient plotted against cube of corresponding wave-length.

A and N are the atomic weight and atomic number of lithium respectively.

A slight bending is also noticed in the region of long wave-lengths.

In conclusion the writer wishes to thank Professor Duane for the kind interest he took in the work and for the facilities and suggestions he gave in conducting the experiment. This work was carried out in the Jefferson Physical Laboratory, Harvard University in 1923 but for various reasons it could not be published earlier.

WAVE-LENGTH MEASUREMENTS OF GAMMA-RAYS FROM RADIUM AND ITS PRODUCTS*

By Luville T. Steadman
Sloane Physical Laboratory, Yale University

(Received June 16, 1930)

Abstract

Wave-length measurements.—The wave-lengths of the gamma-rays in the spectrum of Ra, RaB, RaC, and RaD were determined by the method of crystal diffraction. The rays which experienced diffraction on transmission through a crystal of calcite were received in a Geiger counting chamber which was provided with a slit system that could be turned about a pivot situated at the chamber. By turning the crystal a little so that the diffracted rays were not able to enter the chamber, a method was developed for obtaining the background of the intensity curve and the intensities of the γ-rays, and for investigating the intensity of a possible continuous γ-ray spectrum. Practically all the wave-lengths found by other investigators were obtained and good agreement among all the results was noted. In addition, several other short wave-length γ-rays were found, of which the shortest was 0.42 X.U. Four of them were again determined from measurements made with a diamond which also revealed a γ-ray of wave-length 0.17 X.U.

Intensities of the rays.—In general the changes in intensity from one wave-length to another throughout the spectrum corresponded to those given by other workers, but the intensities of the rays were not found to vary as much.

Continuous spectrum.—A determination of the background of the intensity curve showed that no continuous γ-radiation of any appreciable intensity was present. A more precise measurement made at a wave-length of 53.9 X.U. indicated that a continuous spectrum of γ-rays if existing at all raises the background intensity to less than one tenth the height of the least prominent peaks here found. It has already been concluded from indirect reasoning that the continuous γ-ray spectrum is unimportant.

Introduction

THERE are several methods by which a rough estimate of the hardness of the gamma-radiation from radioactive elements has been obtained. The quantity which characterizes the hardness has been termed the effective wave-length, and its magnitude is closely associated with the wave-length of some line or lines of strong intensity in the source of the radiation. Kohlrausch,[1] Compton,[2] and Ahmad,[3] have applied the x-ray absorption formula, $\mu = AZ + B\lambda^3 Z^4$, to their work on the absorption of γ-rays and have given $\lambda_{eff.}$, for the hard γ-rays from RaC to be from 14 to 20 X.U. Similar results were obtained from measurements on the intensity of scattered rays by Owen-Fleming-Fage.[4] The diffraction of γ-rays by a single atom depends

* Part of a dissertation presented for the degree of Doctor of Philosophy at Yale University.

[1] K. W. F. Kohlrausch, Wiener Ber. **126**, IIa, 441, 683, 887 (1917).

[2] A. H. Compton, "X-Rays and Electrons," p. 390.

[3] N. Ahmad, Proc. Roy. Soc. **A109**, 207 (1925).

upon the interference between the rays scattered by the electrons grouped close together in a heavy atom. Compton[2] has found $\lambda_{eff.} = 25$ X. U. by this method. He also obtaned a value for $\lambda_{eff.} = 16$ X. U. by calculating the wave-length of the scattered rays from their absorption coefficient.

A quantitative investigation of the various wave-lengths in the γ-ray spectrum of a radioactive element was first made by Rutherford-Andrade.[5] They used a crystal of rock salt to reflect the rays emitted by the disintegration products of radium contained in an emanation tube. The diffracted rays which emerged from the crystal at definite angles depending on their wave-lengths, were detected by their action on a photographic plate. However, the lines found by them belonged for the most part to the spectra of hard x-rays emitted by the atoms in the source after they had been excited by the nuclear γ-rays of high energy value.

The introduction of the counting method to the study of the high frequency γ-radiation from radium and its products by Kovarik[6] enabled him to find many of the true nuclear γ-rays. The rays, after reflection by a calcite crystal were detected by means of a Geiger counter.

The problem was also taken up by several investigators[7,8,9,10,11,12] who employed the β-ray spectrum method which makes use of the photoelectric effect of the γ-rays. Ellis-Skinner in particular give values for the wave-lengths of some twenty-two γ-rays of nuclear origin in RaB+RaC. In addition, relative intensities have been assigned to the lines. The theory in connection with this has been developed by Ellis-Wooster.[13] They have taken into account the observed intensities of the β-ray groups as indicated by the photographic plate and also the probability of conversion of the γ-rays into β-rays. However, their method for obtaining the wave-lengths and the intensities of the γ-rays is not considered to be as direct and straightforward as that of crystal diffraction.

Recently, Frilley[14] has made some experimental improvements in the method of Rutherford-Andrade and has been able to extend the measurements by means of photographic registration of the γ-rays. He has identified a large number of the wave-lengths obtained by the β-ray spectrum method. Great difficulty has always been experienced when trying to use the photographic plate to find rays of very short wave-length on account of the large quantity of primary radiation coming from the source. A general back-

[4] E. A. Owen, N. Fleming, W. E. Fage, Proc. Phys. Soc. London **36,** 355 (1924).
[5] E. Rutherford and E. N. daC. Andrade, Phil. Mag. [6] **27,** 854 (1914), [6] **28,** 263 (1914).
[6] A. F. Kovarik, Phys. Rev. [2] **19,** 433 (1922).
[7] E. Rutherford, H. Robinson and W. F. Rawlinson, Phil. Mag. [6] **28,** 281 (1914).
[8] C. D. Ellis and H. W. B. Skinner, Proc. Roy. Soc. **A105,** 60 (1924).
[9] C. D. Ellis and W. A. Wooster, Proc. Camb. Phil. Soc. **22,** 849 (1925).
[10] O. Hahn and L. Meitner, Zeits. f. Physik **26,** 161 (1924).
[11] J. Thibaud, C. R. **179,** 1322 (1924), Journal de Physique [6] **6,** 82 (1925).
[12] L. F. Curtiss, Phys. Rev. [2] **27,** 257 (1926).
[13] C. D. Ellis and W. A. Wooster, Proc. Camb. Phil. Soc. **22,** 595 (1925), Phil. Mag. [6] **50,** 521 (1925), Proc. Camb. Phil. Soc. **23,** 717 (1927).
[14] M. Frilley, C. R. **186,** 137 (1928), Ann. de Physique [10] **11,** 483 (1929).

ground of stray and scattered radiation also makes it hard to distinguish very weak lines.

The general consensus of opinion thus far has been that there is no continuous spectrum for the γ-rays. This view has been arrived at on consideration of the results of several experiments including the counting by Kovarik[15] of the number of γ-rays from RaB to RaC per atom disintegrating, the study of the intensities in the β-ray spectra by Gurney,[16] the measurements by Ellis-Wooster[13] on the heating effect of the γ-rays from RaB +RaC, and all the work mentioned above on the γ-ray wave-lengths and their intensities. It was concluded that the energy given off in the heating effect when the rays were absorbed in a suitable material could just about be accounted for by the total energy of all the monochromatic rays observed. There was no necessity for postulating a quantity of energy in the form of a continuous radiation. Because of the indirect method of measurement however it has usually been considered that there has been as yet no real proof either for or against the existence of a continuous spectrum.

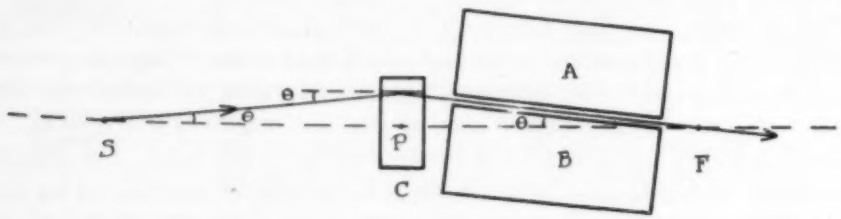

Fig. 1A. Crystal set.

In view of this fact and in particular because the lines determined by the β-ray spectrum method had not been completely checked by any crystal diffraction method, and in addition because some of the lines found by one observer had not been found by others, it was considered advisable to continue the investigation of these problems using the counting method. The experimental method used in the present measurements differed from that devised by Kovarik principally in the fact that diffraction of the rays was accomplished by transmission through a crystal instead of by reflection from the surface planes. The crystal was not rotated. Consequently there was one less experimental quantity to be determined and the range of the instrument in the direction of short wave-lengths was increased. The author was able to check nearly all the wave-lengths found before and to extend the measurements to several new γ-rays of very short wave-length. Additional direct evidence was obtained which supports the view of the non-existence of a continuous spectrum of any appreciable intensity. The intensity values found for the γ-rays are more or less in agreement with the results of other observers.

[15] A. F. Kovarik, Phys. Rev. [2] **23,** 559 (1924).
[16] R. W. Gurney, Proc. Roy. Soc. **A112,** 380 (1926).

Experimental Method

The diffraction of a single γ-ray is represented in Fig. 1A. *S* is a point source of the rays situated on the line *SPF* which may be considered as a line of reference. The crystal *C* is placed so that one set of its (1 0 0) planes is parallel to this line and perpendicular to the page. Then, a γ-ray of wave-length λ, coming from *S* and making an angle θ with the crystal planes, may undergo diffraction during transmission through the crystal, and if so the diffracted ray will pass over the point *F*. It can be shown from simple geometrical considerations that $FP = PS$ where *P* is a point at the center of the crystal. Such a ray must satisfy the Bragg formula for diffraction,

$$n\lambda = 2d \sin\theta$$

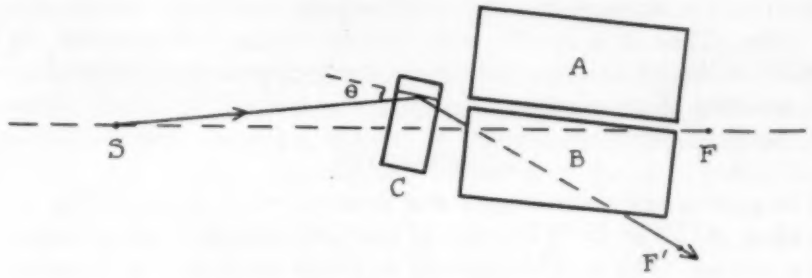

Fig. 1B. Crystal turned.

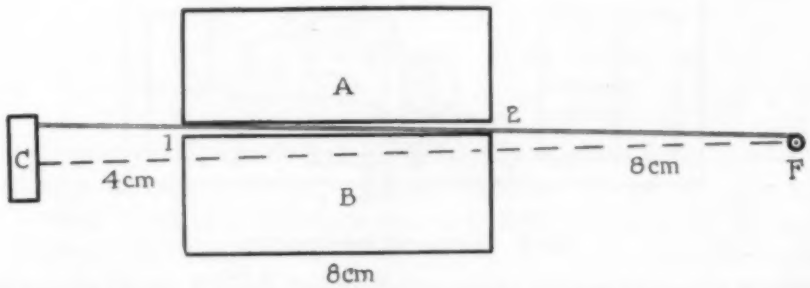

Fig. 1C. Diagram showing that the beam of monochromatic rays which passes into the counting chamber may have a width less than that of the slit.

where *n* is an integer, *d* the grating space, λ and θ the wave-length and angle of diffraction respectively. As the angles of diffraction concerned with here are all very small it is sufficient to use the formula $n\lambda = 2d\theta$. Furthermore, the cylindrical source that is used has a definite length and diameter and emits a great many rays in all directions; diffraction therefore will be possible for rays of all wave-lengths provided they are incident at the proper angle θ, and they will pass through the image of the source at *F*. The lead blocks *A*, *B* are shown in positions to form a deep slit or channel through which the rays may pass.

If a detector of γ-rays such as a Geiger counter is placed at *F*, the impulses which are counted will be due to several types of radiation. A considerable

number of γ-rays may pass right through the lead blocks A, B and come either from the source S or from sources of penetrating radiation in the neighborhood. The rays which pass through the deep slit may be diffracted γ-rays satisfying the above expression, rays which are scattered by the crystal and other parts of the apparatus, and also high speed electrons. At very small angles there will be, in addition, a considerable amount of direct radiation coming through the slit system from the source. If the axis of the slit passes through F and makes the angle θ with FPS the γ-rays diffracted at an angle θ are transmitted without absorption. The slit system is pivoted at F.

In Fig. 1B the crystal is shown turned through an angle of a few degrees about an axis perpendicular to the page. The conditions relating to the absorption and scattering by the crystal remain essentially the same for the two cases. Thus it is readily seen that by taking a γ-ray count for both positions of the crystal, one can obtain the background of the spectrum and the intensities of the γ-rays.

Apparatus

The gamma-ray spectrometer was constructed as shown in Fig. 2. The base plate A, 24 in. by 8 in., was of cast iron and had strengthening ribs on the bottom. The lead blocks used to shield the source at S and to form

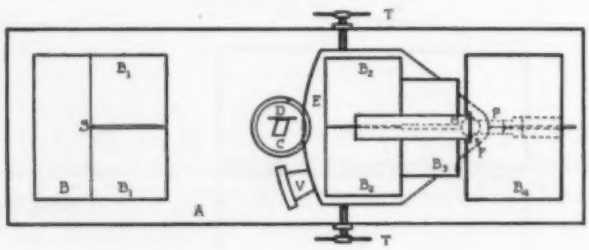

Fig. 2. Gamma-ray spectrometer.

the two slit systems were all 15 cm in height and about 8 cm thick, thickness being measured always in a direction along the axis of the instrument. The two blocks B_1, B_1 placed about 3 mm apart were used to limit the angular width of the incident beam. The spectrometer rested on a stone pier.

The source of γ-radiation was a preparation of radium salt containing 5.002 mg of radium together with its disintegration products. The glass container was 7 mm long and about 1.5 mm inside diameter and, protected by its thin silver casing, was supported so that its long dimension was in the vertical direction. The experiments were concerned mainly with nuclear rays. Since therefore it was desirable to have as few hard x-rays as possible, no other absorbing material was placed between the source and the crystal.

The crystal holder of a Bragg x-ray spectrometer was used to support the crystal and to orientate it in its proper position. The calcite crystal was 7 mm thick, 10 mm wide, and 25 mm high. It was placed with one of its

faces in contact with the plate D. The vertical axis of the crystal holder together with the center of the source and the middle of the pivot determines the axis of the instrument. D was adjusted parallel to this by means of a straight edge. By turning the holder a little so that the horizontal peg in its edge was no longer in contact with the peg in the grooved disk beneath, the position illustrated in Fig. 1B was obtained. The distances between S and C and between C and F were each 20 cm.

A diamond crystal was also used to measure the shortest wave-lengths. Its dimensions were: height 9 mm, width 4 mm, and thickness 2.5 mm. The orientation of the (1 0 0) planes was determined by means of a goniometer. The grating space for the (1 0 0) planes in calcite is given as 3.0288 (10^{-8}) cm. In the case of the diamond the 4th order reflection was the one used as the (1 0 0) planes give no 1st, 2nd, or 3rd order. For diamond 1/4 of d_{100} is 0.885 (10^{-8}) cm.

The steel plate E carrying the slit system could be turned in either direction about the 0.5 inch pivot by means of two small pitch screws. Its zero position with respect to the axis of the spectrometer was determined by the scale and vernier. The angular positions of the slit system, however,

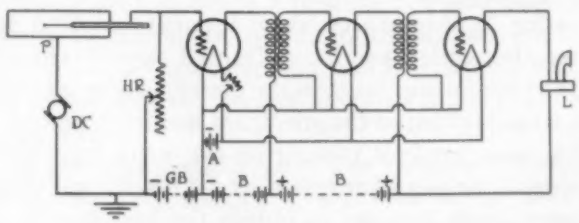

Fig. 3. Geiger counter and amplifier.

were measured by means of a lamp and transparent scale fastened to the wall at a distance of 286.48 cm from a lens and mirror M. The scale was accurately ruled in millimeters and one could estimate to 0.1 mm which corresponds to an angle of 3.600 sec. of arc. Since the angles to be measured were very small, the 0.2 mm distance corresponding to 7.200 sec of arc was taken as the unit of angular measurement. A lead plug 3 mm thick inside the slot cut through B_3 prevented high speed electrons from entering the counting chamber.

The counting chamber consisted of a brass cylinder 13 mm in diameter and 5 cm long with a 3 mm aluminum front, cast in the center of the lead block B_4 which was insulated from the base and to which the positive high potential connection was made. In especially damp weather dry dust free air was introduced into the chamber before counting. The potential necessary for operating the Geiger counter was supplied by a 3000 volt motor-generator set operating on 100 volts from a storage battery. The output was found to be very steady and constant to within 10 volts.

The electrical counting apparatus was essentially the same as that used by Kovarik.[17] Similar arrangements have been used by others for counting

[17] A. F. Kovarik, Phys. Rev. [2] 13, 273 (1919).

purposes. Fig. 3 is a schematic diagram of the electrical circuit. A loud speaker was used in the output circuit and the sharp clicks heard from it, one for each discharge in the chamber, were counted by a hand tally.

Platinum ball points about 0.003 inch in diameter were found to be very satisfactory. A point was made by melting one end of a half-inch piece of 0.001 inch hard drawn platinum wire in a very tiny gas-oxygen flame. As an indication of their practicability it may be said that throughout the experiments only about eight good points were used, and that with them somewhat more than two million γ-rays were counted.

Procedure

The adjustment of the slit system was accomplished by placing one of the blocks B_2 on the carriage before the other and bringing its slit face into line with the axis of the spectrometer by means of a straight edge. The width of the slit formed by the two blocks was changed by moving the second block and inserting various thicknesses of paper between them, after which the paper was removed.

In general, the experimental procedure was to count the number of γ-ray impulses in a period of 20 minutes for each successive angular position of the slit, in order to obtain a curve of intensity plotted against angular measurement for the while beam of diffracted rays. The slit system was always moved in the same direction in the course of a series of measurements. In each series a large portion of the spectrum was investigated.

In the preliminary work of measuring the wave-lengths the slit system was realigned several times and adjustments of the slit width and orientation of the crystal were made in order to obtain the best results. The positions D_1 and $-D_2$ of the peaks on either side of the zero were found for a number of wave-lengths. These positions were correlated in pairs and the mean zero of the spectrum determined from the average of $(D_1-D_2)/2$ for all wave-lengths and used as a basis for further measurements.

The results showed that two diffracted rays could be completely resolved if their angular separation was about 20 sec of arc, corresponding to a difference in their wave-lengths of about 0.6 X.U. Calculation showed however, that for the smallest slit width, 0.126 mm, all the diffracted rays in a beam of at least 5 minutes angular width could pass through the slit and enter the counting chamber. Accordingly, the reasonable assumption was made that the slit must not be in perfect alignment with the image of the source, and in Fig. 1C is shown the manner in which a narrow beam of monochromatic rays from the crystal was assumed to pass through the slit.

Several experiments were performed later which confirmed this view. With the diamond crystal, no peaks could be found when the width of the slit was decreased from 0.126 to 0.063 mm, and also when the width at end 1 was increased to 0.126 again, the width at end 2 remaining 0.063 mm. But when the width at end 2 was made 0.126 and that at end 1 was changed to 0.063 the peaks reappeared. Furthermore, with the calcite crystal and a width of 0.19 mm, the peak at 35 X.U. was found again when the width

at end 1 was reduced to 0.126 mm, but the peak disappeared when end 2 of block *B* was moved the small distance 0.025 mm toward *A*. The position of *A* on the carriage was left unchanged throughout all the experiments. In order to calculate the resolving power, the position of the image of the source with respect to the pivot and the slit system must be known. Assuming their relative positions to be as shown in the figure, the two experiments indicated that two γ-rays could be resolved in the first case if their angular separation was about two minutes of arc and in the second case if the separation was less than one minute.

In the wave-length measurements it was found necessary to use three different slit widths, namely, 0.126, 0.19, and 0.38 mm. For angles of diffraction less than 40 units the first was used in order to have the rate of counting less than 55 per minute. The second was employed to decrease the slope of the background intensity curve for larger angles, and the third was found to be best for angles of diffraction greater than 195 units.

The portion of the background at large angles due to scattered rays was obtained from additional intensity measurements which were made with the slit closed. An intensity curve taken with the crystal removed did not show any peaks proving that they were due to diffracted rays only. A precise determination of the extent to which a possible continuous spectrum raises the background intensity was made by finding the intensities, for the two positions of the crystal, at a particular point on the curve where no peaks were to be expected either for first, second, or third order diffracted rays of any known wave-lengths.

The zero of the transparent scale was compared frequently with the zero of the steel scale and vernier. The deflections on the scale were noted at the beginning and at the end of each 20 minute period. In this way slight variations in the readings which occurred now and then due to the effect of temperature changes in the spectrometer were taken care of.

The operating potential on the Geiger counter was about 1800 volts, the exact value depending on the sensitive point in use. Its magnitude was always adjusted to the potential at which the impulses due to the γ-rays were slightly drawn out. The number of stray counts, or in other words, the number of impulses received when all sources of radiation were removed to a considerable distance, was about two or three per minute. A small test source placed in a definite position with respect to the counting chamber was used in standardizing the action of the points and in testing new ones. One person did the counting in all the experiments.

The expression for the probability of a number of counts n appearing in an interval of time for which x is the true average count was shown by Bateman[18] to be,

$$P = \frac{x^n e^{-x}}{n!}.$$

[18] H. Bateman, Phil. Mag. [6] **20**, 704 (1910).

It has also been shown from this that the average deviation from the mean for a number of particles N counted in some interval of time t is $(nt)^{1/2}$, where n is the rate of emission. The probable deviation may therefore be taken as $0.67\ (x)^{1/2}$.

Since in the counting experiments there was always the possibility of getting a large deviation at some time or another because of the random nature of the counts, it was the practice immediately to repeat a count

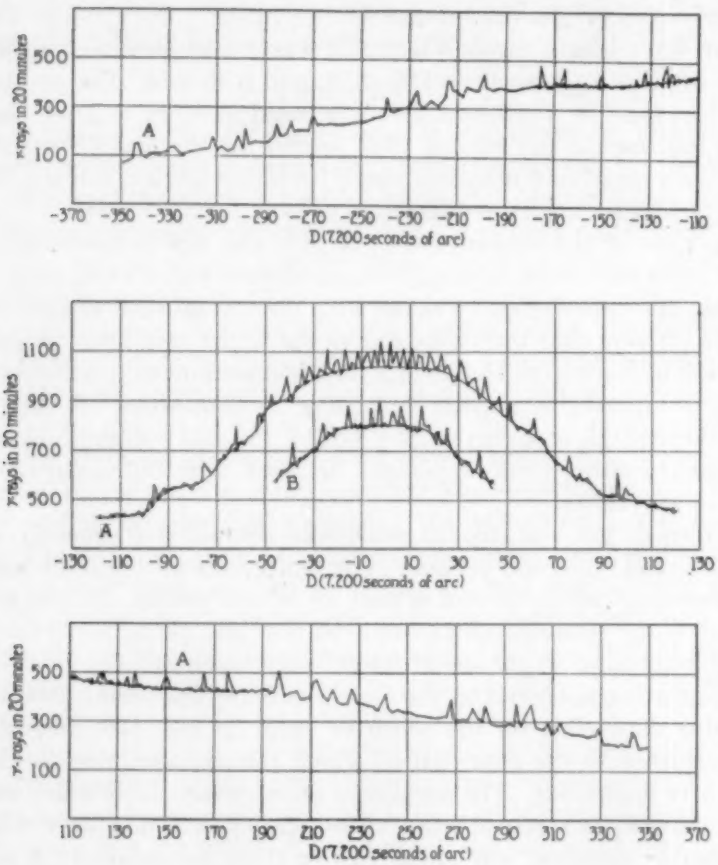

Fig. 4. Gamma-ray spectrum curves. Curve A is for the calcite, B for the diamond crystal.

which showed a large variation and average it with the other. If there was a true γ-ray intensity maximum or minimum for the position of the slit it was then confirmed, if not, the averaging process served to smooth out or reduce the magnitudes of the large deviations.

Results and Discussion

The complete intensity curve is shown in Fig. 4 and is presented in three sections on account of its length. The experimental points have been joined by straight lines. Curve B was taken with the diamond crystal. The small

circles indicate the intensities obtained for the crystal turned and the base line of the spectrum has been drawn through them. The unit of the abscissa D is 7.200 sec. of arc and corresponds to a wave-length of 0.2115 X.U. for curve A and 0.0618 X.U. for curve B.

TABLE I.

D_1	$-D_2$	$(D_1-D_2)/2$	λ X.U.	Intensity	Rutherford-Andrade	Kovarik	Ellis-Skinner	Intensity	Thibaud	Frilley	Intensity	Source of Rays
1260	1260	1260	266.5		262		264			265		RaD
1096	1098	1097	232.0		229		230.3			232		RaB
683	683	683	144.5							144		RaB
547	544	545.5	115.3		115							RaC
343	343	343.0	72.5	6	71	72.2						RaC
329	329	329.0	69.6	3						77[2]	w.	RaB
312	313	312.5	66.1	4		66.1						Ra
308	308	308.0	65.2	2						65	w.	RaB
301	301	301.0	63.7	7								?
298	295	296.5	62.7	8			62.7	2				RaB
285	282	283.5	60.0	6			59.9	1				RaB
279	277	278.0	58.8	4		58.1						RaC
270	268	269.0	56.9	6								?
239	241	240.0	50.8	5			50.7	25				RaB
227	227	227.0	48.0	6		48.4						RaC
214	212	213.0	45.1	8			44.9	4				RaC
213	211	212.0	44.8	7			44.7	3				RaB
199.0	196.5	197.75	41.8	8			41.6	30	42.1	42	v.s.	RaB
175.5	175.5	175.50	37.1	8		37.0	37.1	2				RaC
165.5	165.5	165.50	35.0	7			34.9	40	35.1	35	v.s.	RaB
150.0	150.0	150.00	31.7	5			31.7	6				RaC
135.5	137.0	136.25	28.8	4			28.8	3	29.0			RaC
132.0	134.0	133.00	28.1	5		28.1						RaC
123.0	124.0	123.50	26.1	6			26.2	1	26.5	26	v.w.	RaB
121.0	122.0	121.50	25.7	4			25.6	1				RaB
98.0	99.0	98.50	20.8	4								?
95.5	96.0	95.75	20.2	10			20.2	30	20.2	20	v.s.	RaC
75.0	76.0	75.50	16.0	7					16.0	16	m.	RaC
62.0	61.5	61.75	13.1	9			13.1	7	13.2			RaC
52.0	51.5	51.75	10.95	7			10.92	13	10.94			RaC
47.0	47.0	47.00	9.94	5			9.90	7	9.92			RaC
41.0	41.0	41.00	8.67	10			8.66	16				RaC
34.5	36.0	35.25	7.46	6								?
32.0	32.0	32.00	6.77	6			6.94	8	6.95			RaC
26.5	26.0	26.25	5.55	3			5.56	3	5.57			RaC
24.0	23.0	23.50	4.97	9								?
20.5	18.5	19.50	4.13	6								?
16.5	15.0	15.75	3.33	7								?
13.5	13.5	13.50	2.86	5								?
11.5	11.0	11.25	2.38	7								?
7.5	7.5	7.50	1.59	7								?
4.5	4.5	4.50	0.95	6								?
2.0	2.0	2.00	0.42	10								?
			DIAMOND CRYSTAL									
38.5	38.5	38.50	2.38	10								?
26.0	25.5	25.75	1.59	8								?
15.5	15.0	15.25	0.94	9								?
6.0	6.5	6.25	0.39	7								?
2.5	3.0	2.75	0.17	9								?

The spectrum curve was obtained in five parts, a central portion extending to 45 units and two on either side with overlap. The parts were placed so as to give a continuous curve which was done by changing the ordinates by adding or subtracting a constant quantity. The actual intensity of the background was: 1040 γ-rays in 20 minutes at zero, 420 at 195, and 350 at 340. The intensity of the background for B was 1010 at zero, differing slightly from A because of a readjustment of the slit width. The large increase in intensity for angles less than 70 was due to γ-rays coming directly from the source. About 15 percent of the general background was made up of scattered rays. Because of the method of procedure in counting, previously described, it is estimated that the experimental error in the determination of the intensity of the background, and the intensities at most of the maximum and minimum points on the curve is about ± 15 γ-ray counts.

It is to be noted that the peaks on the curve are sharp and in general are defined by two or more points. No trouble was experienced in repeating the positions of the peaks and in fact many of the peaks were obtained several times. Taking the expected deviation to be $0.67\ (x)^{1/2}$ it is seen that their heights above the background vary from 2 to 7 times the probable deviation depending on the intensity of the background.

The numerical results are given in the Table I. D_1 and $-D_2$ are the positions of corresponding peaks on both sides of the zero of the spectrum. The region of wave-lengths longer than 72.5 X.U. was not completely investigated so that no curves are shown. The values of the γ-ray wave-lengths and their intensities as found by other investigators are also included in the table for the purpose of comparison. The experimental error in the values of λ presented herewith is ± 0.1 X.U. except for wave-lengths longer than 41.8 where it is about ± 0.2 X.U. The four γ-rays of shortest wave-length were also obtained with the diamond crystal. The error in their wave-lengths is ± 0.03 X.U. Ellis-Skinner give an accuracy to their results of one part in 300. Frilley gives an experimental error of ± 0.5 X.U. Consequently there is good agreement among all the results. Many new rays were found and the diamond crystal made it possible to detect the extremely short wave-length of 0.17 X.U. Two additional determinations gave the same value.

The following γ-ray wave-lengths, reported by others for substances certainly present, were not found:

RaB $\lambda = 51.3$ X.U.	Thibaud, $\lambda = 51.5$	Frilley
RaB $\lambda = 47.5$		Ellis-Skinner
RaC $\lambda = 29.5$		Frilley
RaC $\lambda = 23.4$	Thibaud, $\lambda = 24$	Frilley

There is additional information in regard to a few of the wave-lengths, namely:

RaD $\lambda = 265$	Meitner, $\lambda = 264$	Curtiss
RaB $\lambda = 71$	Frilley, possibly 2nd order of $\lambda = 35$	
Ra $\lambda = 66$	Hahn-Meitner	

No particular effort was made to identify higher order diffracted rays and some of those presented in the table may be of that kind.

On account of the complex nature of the radioactive preparation used in the present experiments, it was impossible to tell the exact source of any of the rays. The assignments in the last column, some of which are doubtful, are also from other papers.

The relative intensities of the γ-rays are given in column 5. The height of a peak has been taken as the intensity and a number 10 means that 100 monochromatic rays in addition to the background were counted in 20 minutes. No correction has been made for the fact that three different sizes of slit were used. Some of the peaks were repeated using double the slit width but their heights were found to be increased only about 40 percent. It was therefore considered advisable not to assume any relation between the width of the slit and the intensity of the rays and so attempt to reduce them all to the same basis. On the whole the changes in intensity along the spectrum are in agreement with the results of other observers, but the intensities do not vary as much as in the results of Ellis-Skinner. Although the present method was quite straightforward it is not certain that this disagreement is particularly significant.

It may be seen from Fig. 4 that the base line passes through or a little above the bases of the peaks but not below them as would be the case if there was a continuous spectrum of any appreciable intensity. The more precise measurements made at a wave-length of 53.9 X.U. gave a γ-ray count of 6664 for the crystal set for diffraction through the slit and 6666 in the same length of time for the crystal turned. Since the probable variation in either of these numbers is about ± 0.8 percent, and the smallest peaks on that part of the curve are found to differ from the background by about 9 percent, it would seem that a continuous radiation if existing at all raises the background intensity to less than one-tenth the height of the least prominent peaks here found. Moreover these peaks belong to some of the weakest γ-rays.

It is to be noted that the very short wave-length γ-rays represent a large amount of energy as a wave-length of 1 X.U. corresponds to the energy of an electron after falling through a potential difference of some 12×10^6 volts. The relation between these γ-rays and other high frequency radiations may be inferred from a consideration of the work of Millikan-Cameron[19] and many other investigators. No attempt has been made to correlate the new wave-lengths with the nuclear energy level theories put forward by Ellis[20] and others.

In conclusion the author wishes to express his appreciation to Professor A. F. Kovarik for suggesting and directing the work. He is also greatly indebted to Mr. Donald Cooksey for the loan of the diamond.

[19] R. A. Millikan and G. H. Cameron, Phys. Rev. [2] **32,** 533 (1928).
[20] C. D. Ellis, Proc. Camb. Phil. Soc. **22,** 369 (1924).

THE IONIZATION OF CARBON DIOXIDE BY ELECTRON IMPACT

By H. D. Smyth and E. C. G. Stueckelberg
Palmer Physical Laboratory, Princeton University

(Received June 20, 1930)

Abstract

A new mass spectrograph has been constructed entirely of glass except for the electrodes. Furthermore its design reduces thermal dissociation to a minimum. Using this apparatus the products of ionization in carbon dioxide have been studied. The primary ions are found to be CO_2^+, CO^+, O^+ and C^+ appearing at 14.4, 20.4, 19.6 and 28.3 volts respectively. There is also some O_2^+ produced as a secondary product with an ionization potential of 20.0 volts. Except for CO_2^+ minimum values for all the ionization potentials can be calculated and are found to agree within the limits of error with the observed values.

THE products of ionization in carbon dioxide as analyzed by a mass spectrograph have already been discussed in a brief note by the authors[1] and in a paper by Kallmann and Rosen.[2] The present paper constitutes a final report on the authors' work.

The method used was the familiar modification of Dempster's mass spectrograph first used by one of the authors[3] in 1922 and since then employed by a number of different investigators. It will not be described in detail particularly as this entire field is to be discussed in a forthcoming article in Reviews of Modern Physics. There are, however, a number of minor improvements which should be mentioned.

In the first place the present apparatus is made entirely of glass. The "positive-ray box" which in previous experiments was a rectangular box of brass fitting between the poles of the magnet is now of one inch glass tubing bent in a semicircle and sputtered with platinum to prevent electrostatic charging. One end of this glass "positive-ray box" is sealed to the ionization tube and the other contains the Faraday box which receives the positive ions. This construction eliminates wax joints near the filament and metal parts that cannot be baked out. As a result of it and careful drying of the CO_2, water vapor ions are negligible except at high pressures.

A second change of design is the use of an electron beam parallel to the magnetic field in order to minimize the bad effects of stray field. Such an arrangement has recently been used by Bleakney.[4] A diagram of the central part of the present apparatus is given in Fig. 1.

[1] Smyth and Stueckelberg, Helvetica Physica Acta **2**, 303 (1929).

[2] Kallmann and Rosen, Zeits. f. Physik **58**, 52 (1929) and Zeits. f. Physik **61**, 61 (1930).

[3] For references see Gurney and Morse, Phys. Rev. **33**, 789 (1929) or Kallmann and Rosen, reference 2.

[4] Bleakney, Phys. Rev. **34**, 157 (1929), **35**, 139 (1930).

Finally and most important an attempt has been made to minimize dissociation by the filament. To do this the apparatus is so arranged that the gas first enters the ionization chamber from which it diffuses toward the pumps through the slits S_1 and S_2 and the circular opening O. Thus there is a continuous flow of gas from the ionization chamber through O past the filament. Unfortunately to get sufficient intensity of ionization the filament has to be very close to O so that there is still a certain amount of thermal dissociation. An attempt was made to get some quantitative estimate of this by thermocouple measurements of the temperature in the ionization chamber but the result was indeterminate. The positive-ray results themselves offer the most definite evidence of dissociation, as will appear below.

Experiments and Results

Carbon dioxide was prepared by fractional distillation of commercial carbonic acid gas. After careful drying over phosphorous pentoxide it was

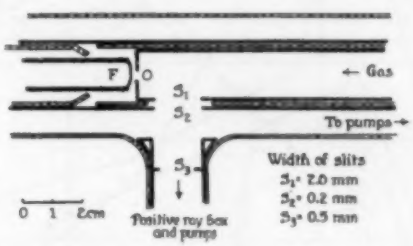

Fig. 1. Diagram of central part of apparatus.

admitted to the apparatus through traps cooled by CO_2 snow and showed no impurities in positive-ray analysis except a trace of water vapor.

First experiments confirmed what we had already found with the old apparatus and what has also been reported by Kallmann and Rosen, namely, that the ions produced are CO_2^+, CO^+, O^+, C^+, and O_2^+. We then proceeded to study these ions in two ways, first by varying the pressure, second by observing critical potentials.

In the pressure runs the field V_1 accelerating the electrons was usually of the order of 40 volts. In both these runs and those on appearance potentials the space OS_1 is, of course, field free, the field V_3 between S_1 and S_2 is of the order of 8 volts and the field V_4, between S_2 and S_4, varies according to the mass of the ion according to the equation $(M/e)\ (V_3+V_4)=K$ where M is the mass of the ion on the $H^+=1$ scale and K for this apparatus and the magnetic field used is about 2600. The pressure used for the most satisfactory of the appearance potential runs was of the order of 0.0008 mm so that the chances of collisions of the second kind or of other secondary effects were small. All the above conditions were varied at one time or another for purposes of control.

Pressure variation. In studying these effects due regard was paid to the recent remarks of Kallmann and Rosen concerning differential absorption

in the magnet space. One of us hopes to discuss this whole problem fully elsewhere, but we may say here that we observed the effect of varying the pressure in the magnet space on the intensities of CO_2^+, CO^+, O^+, and C^+. The effects were small in the range of pressures we were using and the relative intensities were not appreciably changed except in one case. The one ion which behaved differently from the others was C^+ which had an unusually long free path as might be expected from its low ionization potential.

In Fig. 2 the intensities of the different ions are plotted as functions of p_1, the pressure in the ionization tube, for a typical set of observations. Two results are striking, the decrease of CO^+ and the increase of O_2^+ at higher

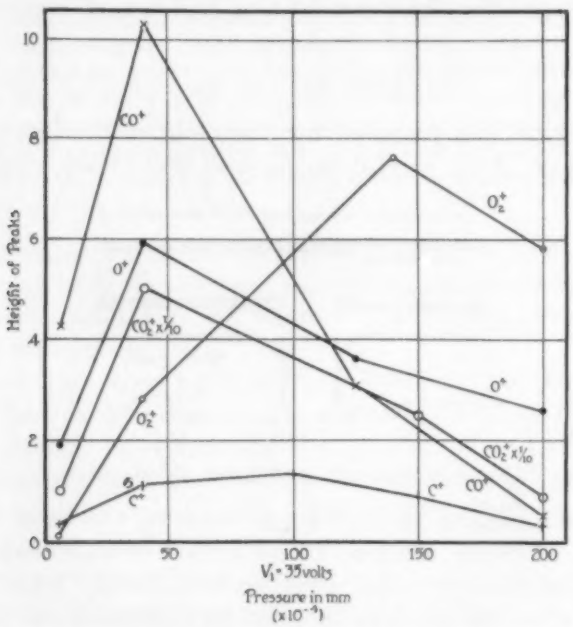

Fig. 2. Intensities of different ions plotted as functions of pressure in ionization tube for a typical set of observations.

pressures. The first is interpreted as the result of collisions of the second kind of the type $CO^+ + CO_2 \rightarrow CO_2^+ + CO$ which should be possible as the ionization potentials are only one or two tenths of a volt apart. At first sight this seems to contradict the statement above concerning the effect of pressure in the magnet chamber. But we may reconcile the results if we remember that the collision $CO_2^+ + CO_2 \rightarrow CO_2 + CO_2^+$ may also occur and would reduce the number of CO_2 ions getting through the magnet chamber but not the number of CO_2^+ ions produced in the ionization chamber. Thus collisions of the second kind in the magnet chamber may have little effect on the relative intensities of CO_2^+ and CO^+ but such collisions in the ionization chamber may greatly favor the CO_2^+. Why the O^+ behaves like the CO_2^+ and CO^+ instead of like the C^+ is not certain. That the C^+ makes few collisions of the second kind is confirmed by its curve in Fig. 2. If that curve

is corrected for the effect of pressure in the magnet space it becomes of the same general type as the CO_2^+ etc. The O_2^+ curve remains as one of entirely different type, a type suggesting strongly a secondary effect. This is supported by the results of Kallmann and Rosen who observed only small traces of O_2^+. Our final conclusion is therefore that all the ions are primary save O_2^+.

Ionization potentials. In determining the ionization potential for different ions argon was used as a standard in the following way. Immediately before and immediately after several of the CO_2 runs argon was run into the apparatus and the electron accelerating voltage observed where A^+ ions were just noticeable. This voltage was the same within the limits of error before and after the CO_2 run and was taken as giving the proper correction to the observed value. That this procedure was justified is supported by the agreement between the ionization potential for CO_2^+ thus obtained and the value observed by Mackay.[5] The ionization potentials for the other ions were then referred to that of CO_2. A typical set of curves at an intermediate pressure is shown in Fig. 3. At lower pressures the O_2^+ usually can not be

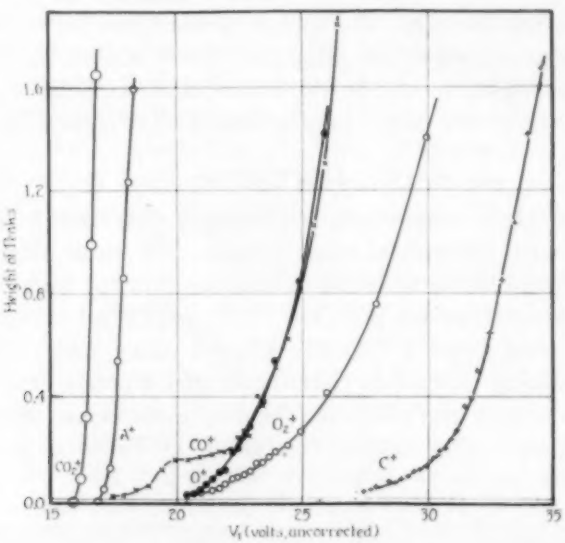

Fig. 3. Typical set of curves at intermediate pressure.

observed but the other curves cut the axis more sharply. The complete weighted results are tabulated below.

From both table and curves we see that CO^+ appears to have two critical potentials. From a comparison of these results with those of an earlier apparatus and from a study of the effect of pressure, filament temperature, etc., we have concluded that the lower potential is due to the presence of CO from thermal dissociation. Whether it may be a true critical potential for CO, to be identified perhaps with Mackay's higher ionization potential at

[5] Mackay, Phys. Rev. **24**, 319 (1924).

TABLE I. *Observed critical potentials with weights.*

Run	P	CO_2^+	A^+	CO^+		O^+	C^+	O_2^+
1	6×10^{-4}	16.0(7)		20.0(6)	24(3)			
2	11.	15.5(5)		20.0(4)				
3	25.	15.5(6)	17.0(6)	19.0(4)	21.5(1)	21.0(4)		22.0(5)
4	100.	15.8(10)		19.0(4)		20.5(7)	28.0(2)	20.0(3)
5*	32.	16.0(10)	17.0(10)	18.0(5)	22.0(7)	21.0(5)	27.8(5)	21.6(5)
6	5.	16.3(8)	17.2(10)	17.0(5)	22.0(3)	22.0(5)	31.0(6)	
7	7.	16.0(9)		18.0(5)	20.8(6)	21.3(10)	31.0(6)	23.0(1)
8	6.	15.9(9)	17.5(10)	18.3(8)	22.7(10)	21.2(10)	30.5(5)	
9	7.	16.0(10)	17.5(10)	17.8(8)	22.0(10)	21.3(10)		
Weighted mean volts above CO_2^+			1.26	2.41	6.00	5.22	13.86	5.6
Value of ionizing potential with estimated error assuming $I_{co_2}=14.4$.			15.66	16.8 ±1.0	20.4 ±.7	19.6 ±.4	28.3 ±1.5	20.0 ±1.0

* Run shown in Fig. 3.

15.6 volts,[5] or whether its position depends entirely on the amount of CO present we are not certain. We incline toward the latter view and would explain our previously reported value and that of Kallmann and Rosen in the same way. The higher break, on the other hand, we believe is a true ionization potential due to the direct production of CO^+ from CO_2.

DISCUSSION

The results given above are particularly interesting because we can compare them with theoretical expectations. We know that carbon dioxide is a straight line molecule with the carbon atom in the middle. It is not surprising therefore that we can get CO_2^+, CO^+ and O^+ all at comparatively low potentials but that to get C^+ we must break away both oxygen atoms and ionize the remaining carbon so that we require considerably higher energy. Let us be more precise and calculate the minimum values where the different ions might appear. The calculations given in Table II are based on the following values.

Heats of Dissociation[6] Process	Volts	Ionizing Potentials[7,8,9,10]	
$CO_2\rightarrow CO+O$	5.7	CO	14.2[7]
$CO\rightarrow C+O$	10.	O	13.5[8]
$O_2\rightarrow O+O$	5.6	C	11.2[9]
		O_2	13.5[10]
		A	15.6[9]

[6] Mecke, Zeits. f. Phys. Chem. **B7**, 108–129 (1930).
[7] Birge, International Critical Tables, Vol. 5.
[8] Frerichs, Phys. Rev. **34**, 1239 (1929).
[9] Russell, Astrophys. J. **70**, 16 (1929).
[10] Stueckelberg, Phys. Rev. **34**, 65 (1929).

The probable errors given for the observed values are estimated and based on the assumption that 14.4 for CO_2^+ is correct. The calculated probable error for $I_o - I_{CO_2^+}$ was only ± 0.074 volts but this is the best determined of the higher ionization potentials.

TABLE II.

Process	Calculated (volts)	Observed (volts) K and R	Observed (volts) This paper
$CO_2 \rightarrow CO_2^+$		14	14.4
$CO_2 \rightarrow CO^+ + O$	19.9	18	20.4 ± 0.7
$CO_2 \rightarrow CO + O^+$	19.2	17	$19.6 \pm .4$
$CO_2 \rightarrow C^+ + O + O$	26.9	29	28.3 ± 1.5
$CO_2 \rightarrow (CO_2^+ + CO_2) \rightarrow 2CO + O_2^+$	19.3		20.0 ± 1.0

The good agreement between our results and the calculated ones is perhaps somewhat fortuitous considering the uncertainty of some of the heats of dissociation involved as well as the errors in our present experiments. It is difficult to make any comparison with the results of Kallmann and Rosen since they give neither experimental data nor estimated error. Their calculated values differ slightly from ours also, presumably due to use of different authorities for heats of dissociation but here again they do not give the data on which they base their estimates so detailed comparison is impossible.

The value calculated for the production of O_2^+ postulates an intermediate process, the formation of an excited CO_2^+ ion. If this is correct it means the CO_2^+ ion has an energy level, perhaps a metastable one, at 5.6 volts above the normal. We are not yet in a position to judge of the reasonableness of this assumption.

Granting the minor uncertainties discussed in the above paragraphs and earlier it still seems clear that we have more complete knowledge of the effect of electron impact on CO_2 than on any other polyatomic molecule. Moreover it is very striking that the observed ionization potentials agree so closely with those calculated from energy considerations alone since such considerations give minimum values. Previous data, both ionization and thermochemical, on other polyatomic molecules are not so definite. Experiments are now being performed on N_2O and NO_2 molecules for which the heats of dissociation and ionizing potentials of the constituent parts are almost as well known as for CO_2.

THE IONIZATION OF NITROUS OXIDE AND NITROGEN DIOXIDE BY ELECTRON IMPACT

By E. C. G. Stueckelberg and H. D. Smyth
Palmer Physical Laboratory, Princeton University

(Received June 20, 1930)

Abstract

The same apparatus used for the study of CO_2 has now been used to study the products of ionization in NO_2 and N_2O. Thermal dissociation is so serious in NO_2 that the results are somewhat unsatisfactory but NO_2^+, N^+ and O_2^+ are found as primary ions and their appearance potentials determined approximately. In N_2O the results were more satisfactory and the appearance potentials 12.9, 16.3, 15.3, 21.4 were found for the primary ions N_2O^+, O^+, NO^+, N^+ respectively. In both gases other primary ions were probably present but obscured by ions from products of thermal dissociation. As in CO_4 the observed potentials agreed within the limits of error with calculated values.

PURSUING the general scheme of investigating the simplest triatomic molecules the authors went on from the experiment on carbon dioxide reported in the preceding paper to study the products of ionization in nitrous oxide and nitrogen dioxide. These substances have almost the same advantages as CO_2 as far as our knowledge of their structure is concerned. Not only are the heats of dissociation of the gases themselves known but also the heats of dissociation and ionization potentials of their constituent parts, N_2, O_2, NO, N and O. Furthermore both N_2O and NO_2 are supposed to be triangular in structure furnishing an interesting contrast with CO_2 which is linear.

Experimentally, however, difficulties of two sorts arose. The first, which was foreseen, was the high degree of thermal dissociation which made any study of pressure variations futile and all results more difficult of interpretation. The second difficulty was a variable error in the voltage scale which made corrections uncertain and the determination of some of the ionization potentials less accurate than in CO_2.

Experiments and Results

The apparatus and procedure were the same as those described in the preceding case except that the electrode in front of the filament was changed from nickel to platinum and two fine wires welded across the hole O to make the field more uniform. (see Fig. 1 in previous paper).

The NO_2 was generated by heating $Pb(NO_3)_2$ and purified by fractional distillation. In the ionization chamber it was dissociated to such an extent that a typical mass spectrum showed NO^+ ions ten times more numerous than NO_2^+ and showed some N_2^+ and O_2^+ ions present. Therefore the possibility must be considered that the NO^+, O^+ and N^+ ions observed came from ionization of NO, N_2 or O_2 rather than directly from NO_2.

The N_2O was generated by heating NH_4NO_3 and was dried over P_2O_5. The dissociation difficulty appeared here also but with certain differences. In this case the N_2O^+ was the strongest ion with O_2^+ and N_2^+ much stronger

and NO^+ relatively weaker than in the NO_2 mass spectrograms. But again care must be taken in interpreting results though in general they are better than in NO_2.

Fortunately the resolution of the apparatus was excellent. Therefore it was possible to observe the appearance potentials of nearly all the stronger ions. The only exceptions were N_2^+ and O_2^+ in NO_2 where the great intensity of NO^+ obscured the appearance potentials of the neighboring ions.

Early in the experiments on NO_2 it was noticed that the appearance potential of NO^+ was not as far below that of argon as might be expected. Therefore it was decided to use the ionization potential of mercury as a second calibration point for correction of observed voltages. As may be seen in the tables below, this gave the surprising result that the observed appearance potential of the Hg^+ ion was only about 3.8 volts below that of the A^+ ion instead of the 5.2 which it should be. This is attributed to some variable charged layer or possibly some geometrical effect. Attempts were made to diagnose it more exactly by measuring the velocity and intensity characteristics of electrons reaching probes inserted just behind the hole O, or just above the slit S_1 (see Fig. 1 in previous paper) but the results were inconclusive. However plotting the observed values for A^+, CO_2^+ and Hg^+ against their true values a correction curve can be drawn and observations of unknown ionization potentials corrected by it. Actually such an interpolation is required in only one case, N_2O^+. Of the other three ions appearing below 14 volts, NO^+ and NO_2^+ both appear at approximately the same place as Hg^+ while the O_2^+ in the N_2O appears by interpolation at 13.5 which is in agreement with the accepted value of the oxygen ionization potential.

A typical ionization potential curve for N_2O is shown in Fig. 1 and the results of a number of runs on NO_2 and N_2O are tabulated below.

TABLE I.

A. NO_2

Run	P	Observed Ionization Potential					
		Hg^+	NO_2^+	NO^+	A^+	O^+	N^+
2	7×10^{-4}		15.0	14.5	18.2		
3	11		17.5	17.2	20.9		
4	10		17.0	16.5	18.9		
5	9 NO gas			17.5	20.0		
6	10		15.0	15.0	18.5	20.5	
7	10	14.5		14.5			
8	12		15.75	15.5	18.5	20.7	23.7

B. N_2O

Run	P	Observed Ionization Potentials (with weights)							
		Hg^+	N_2O^+	NO^+	A^+	O_2^+	N_2^+	O^+	N^+
1	25×10^{-4}		16.5(10)		19.0(10)				
2	18	13.8(10)	15.2(10)		17.3(10)				
3	7	13.6(10)	15.0(10)						
4	12	13.5(10)	15.0(10)		17.5(10)				
5	7		16.1(10)	18.3(10)			18.5(10)	19.7(2)	25.5(2)
6*	12		16.5(10)	18.3(10)		17.0(10)	18.7(10)	19.5(2)	24.5(2)
7	12		16.5(10)	17.8(2)	18.5(2)	17.0(10)	18.5(2)		

* Run shown in Fig. 1.

THE IONIZATION OF NITROUS OXIDE AND NITROGEN DIOXIDE BY ELECTRON IMPACT

By E. C. G. Stueckelberg and H. D. Smyth
Palmer Physical Laboratory, Princeton University

(Received June 20, 1930)

Abstract

The same apparatus used for the study of CO_2 has now been used to study the products of ionization in NO_2 and N_2O. Thermal dissociation is so serious in NO_2 that the results are somewhat unsatisfactory but NO_2^+, N^+ and O_2^+ are found as primary ions and their appearance potentials determined approximately. In N_2O the results were more satisfactory and the appearance potentials 12.9, 16.3, 15.3, 21.4 were found for the primary ions N_2O^+, O^+, NO^+, N^+ respectively. In both gases other primary ions were probably present but obscured by ions from products of thermal dissociation. As in CO_4 the observed potentials agreed within the limits of error with calculated values.

PURSUING the general scheme of investigating the simplest triatomic molecules the authors went on from the experiment on carbon dioxide reported in the preceding paper to study the products of ionization in nitrous oxide and nitrogen dioxide. These substances have almost the same advantages as CO_2 as far as our knowledge of their structure is concerned. Not only are the heats of dissociation of the gases themselves known but also the heats of dissociation and ionization potentials of their constituent parts, N_2, O_2, NO, N and O. Furthermore both N_2O and NO_2 are supposed to be triangular in structure furnishing an interesting contrast with CO_2 which is linear.

Experimentally, however, difficulties of two sorts arose. The first, which was foreseen, was the high degree of thermal dissociation which made any study of pressure variations futile and all results more difficult of interpretation. The second difficulty was a variable error in the voltage scale which made corrections uncertain and the determination of some of the ionization potentials less accurate than in CO_2.

Experiments and Results

The apparatus and procedure were the same as those described in the preceding case except that the electrode in front of the filament was changed from nickel to platinum and two fine wires welded across the hole O to make the field more uniform. (see Fig. 1 in previous paper).

The NO_2 was generated by heating $Pb(NO_3)_2$ and purified by fractional distillation. In the ionization chamber it was dissociated to such an extent that a typical mass spectrum showed NO^+ ions ten times more numerous than NO_2^+ and showed some N_2^+ and O_2^+ ions present. Therefore the possibility must be considered that the NO^+, O^+ and N^+ ions observed came from ionization of NO, N_2 or O_2 rather than directly from NO_2.

The N_2O was generated by heating NH_4NO_3 and was dried over P_2O_5. The dissociation difficulty appeared here also but with certain differences. In this case the N_2O^+ was the strongest ion with O_2^+ and N_2^+ much stronger

and NO^+ relatively weaker than in the NO_2 mass spectrograms. But again care must be taken in interpreting results though in general they are better than in NO_2.

Fortunately the resolution of the apparatus was excellent. Therefore it was possible to observe the appearance potentials of nearly all the stronger ions. The only exceptions were N_2^+ and O_2^+ in NO_2 where the great intensity of NO^+ obscured the appearance potentials of the neighboring ions.

Early in the experiments on NO_2 it was noticed that the appearance potential of NO^+ was not as far below that of argon as might be expected. Therefore it was decided to use the ionization potential of mercury as a second calibration point for correction of observed voltages. As may be seen in the tables below, this gave the surprising result that the observed appearance potential of the Hg^+ ion was only about 3.8 volts below that of the A^+ ion instead of the 5.2 which it should be. This is attributed to some variable charged layer or possibly some geometrical effect. Attempts were made to diagnose it more exactly by measuring the velocity and intensity characteristics of electrons reaching probes inserted just behind the hole O, or just above the slit S_1 (see Fig. 1 in previous paper) but the results were inconclusive. However plotting the observed values for A^+, CO_2^+ and Hg^+ against their true values a correction curve can be drawn and observations of unknown ionization potentials corrected by it. Actually such an interpolation is required in only one case, N_2O^+. Of the other three ions appearing below 14 volts, NO^+ and NO_2^+ both appear at approximately the same place as Hg^+ while the O_2^+ in the N_2O appears by interpolation at 13.5 which is in agreement with the accepted value of the oxygen ionization potential.

A typical ionization potential curve for N_2O is shown in Fig. 1 and the results of a number of runs on NO_2 and N_2O are tabulated below.

TABLE I.

A. NO_2

Run	P	Observed Ionization Potential					
		Hg^+	NO_2^+	NO^+	A^+	O^+	N^+
2	7×10^{-4}		15.0	14.5	18.2		
3	11		17.5	17.2	20.9		
4	10		17.0	16.5	18.9		
5	9 NO gas			17.5	20.0		
6	10		15.0	15.0	18.5	20.5	
7	10	14.5		14.5			
8	12		15.75	15.5	18.5	20.7	23.7

B. N_2O

Run	P	Observed Ionization Potentials (with weights)							
		Hg^+	N_2O^+	NO^+	A^+	O_2^+	N_2^+	O^+	N^+
1	25×10^{-4}		16.5(10)		19.0(10)				
2	18	13.8(10)	15.2(10)		17.3(10)				
3	7	13.6(10)	15.0(10)						
4	12	13.5(10)	15.0(10)		17.5(10)				
5	7		16.1(10)	18.3(10)			18.5(10)	19.7(2)	25.5(2)
6*	12		16.5(10)	18.3(10)		17.0(10)	18.7(10)	19.5(2)	24.5(2)
7	12		16.5(10)	17.8(2)	18.5(2)	17.0(10)	18.5(2)		

* Run shown in Fig. 1.

By using argon and mercury as reference points and using the correction curve discussed above we arrive at the following experimental values where

TABLE II

From	NO_2^+	N_2O^+	NO^+	O_2^+	N_2^+	O^+	N^+
NO_2	11.0?		10.5?			17.7?	20.8?
N_2O		12.9	15.3	13.5	15.5	16.3?	21.4

the question marks indicate that the accuracy is poor, perhaps 10% and we refrain deliberately from giving estimated errors for each separate potential The ones not questioned are probably accurate to about half a volt.

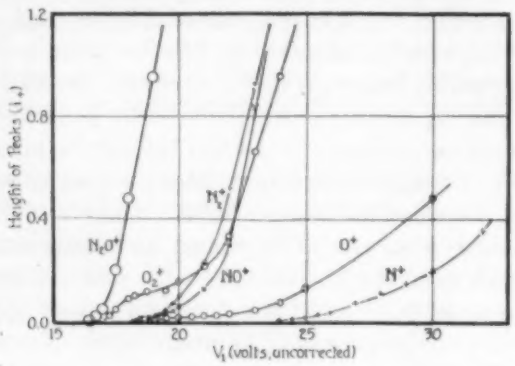

Fig. 1.

DISCUSSION

In comparing these experimental results with theoretical values we must remember that we can safely attribute an ionizing potential to NO_2 or N_2O

TABLE III.

Process	Heats of dissociation Volts	Ionizing potentials	
$NO_2 \rightarrow N+O_2$	4.3	N_2	16.5[2]
$NO_2 \rightarrow NO+O$	3.3	N	14.5[3]
$N_2O \rightarrow N_2+O$	2.0	O_2	13.5[4]
$N_2O \rightarrow NO+N$	4.6	O	13.5[5,3]
$NO \rightarrow N+O$	6.5	NO	9.4[6]
$N_2 \rightarrow N+N$	9.1	A	15.6[3]
$O_2 \rightarrow O+O$	5.6	Hg	10.4[3]

only of the observed value is lower than the theoretical value for production from N_2, O_2, or NO. Even the assurance of the chemists that no NO is to

[1] Mecke, Z its. f. Phys. Chem. **B7,** 108–129 (1930).
[2] Estimated most probable value. Authorities differ.
[3] Russell, Astrophys J. **70.** 16 (1929).
[4] Stueckelberg, Phys. Rev. **34,** 65 (1929).
[5] Frerichs, Phys. Rev. **34,** 1239 (1929).
[6] Birge, International Critical Tables, Vol. 5.

be expected in N_2O must be regarded with skepticism at first though it will be seen later to be verified. With the heats of dissociation given by Mecke[1] and the ionizing potentials from various sources given in Table II the minimum energy can be calculated for fifteen of the seventeen possible processes, which might be expected to occur in NO_2 or N_2O. The two ionization potentials that can not be predicted are, of course, simple ionization of N_2O and NO_2 without any dissociation. Without considering in detail the processes which might lead to each type of ion we may take one as typical. Consider NO^+. In NO_2 it could be produced directly from NO_2 at 12.7 volts but actually it appears very strongly below this point so that presumably it comes from NO present as the result of dissociation and requiring only 9.5 volts for ionization. On the other hand in N_2O, NO^+ first appears at about 15.3 volts whereas it can first be produced directly from N_2O at 14.0. This suggests that it is actually being produced in this way and that there is no appreciable amount of NO itself present. This confirms the views of the chemists on the nature of dissociation in N_2O and allows us to throw out NO as a possible source of N^+ or O^+ in the experiments on N_2O. The results of arguments of this type are embodied in Table IV below.

TABLE IV.

Process	Theor.	Obs.	Remarks
$NO_2 \rightarrow NO_2^+$		11.0	
$\rightarrow NO^+ + O$	12.7		Obscured by $NO \rightarrow NO^+$
$\rightarrow NO + O^+$	16.8	17.7	Definitely occurs
$\rightarrow N + O_2^+$	17.8		O_2^+ present but I.P. obscured by NO^+
$\rightarrow N^+ + O_2$	18.8	20.8	Uncertain, perhaps due to NO
$N_2O \rightarrow N_2O^+$		12.9	
$\rightarrow N_2 + O^+$	15.5	16.3	Definitely occurs
$\rightarrow N_2^+ + O$	18.5		Obscured by $N_2 \rightarrow N_2^+$
$\rightarrow NO^+ + N$	14.0	15.3	Reasonably certain
$\rightarrow NO + N^+$	19.1	21.4	Reasonably certain

It seems that in every case where a definite conclusion can be drawn it is to the effect that the process to be expected does occur and at nearly the minimum possible energy. Perhaps the most interesting processes are $NO_2 \rightarrow N^+ + O_2$ and $N_2O \rightarrow N_2 + O^+$ which evidently do occur although the corresponding process $CO_2 \rightarrow C^+ + O_2$ does not occur. This is in perfect accord with our ideas as to the difference in structure of these molecules.

These results combined with those on CO_2 give a most satisfactory confirmation of predictions of ionization phenomena by the use of thermochemical data, a process that fell into disrepute after its early failure in the case of HCl. Unfortunately there are few other triatomic molecules for which we have sufficient data to make predictions. However the authors hope to continue the work as well as possible.

THE EFFECT OF INTENSE ELECTRIC FIELDS ON THE PHOTOELECTRIC PROPERTIES OF METALS

By Ernest O. Lawrence and Leon B. Linford
University of California

(Received June 20, 1930)

Abstract

The photoelectric effect from thin films of potassium and oxygen on tungsten has been studied as a function of strong accelerating fields. Fields as high as 63,000 volts/cm were used which shifted photoelectric thresholds towards the red, the shifts being approximately proportional to the square root of the applied fields. An applied field of 36,000 volts/cm removed the threshold for a pure potassium layer on tungsten from 5620A to 5880A. A film of potassium on a very thick layer of oxygen on tungsten showed a threshold at 6800A which did not vary with applied accelerating fields. However the magnitude of the emission increased with the field suggesting that thick oxygen layers are rough and applied fields over most of such surfaces are much smaller than calculated from the geometry of the electrodes. A layer of potassium on a thin layer of oxygen on tungsten showed a threshold at 7350A for small applied fields which shifted to 7575A for a field of 18,600 volts/cm. A film of potassium on a thinner layer of oxygen—perhaps less than a monatomic layer—exhibited a threshold in small fields at 5830A which was shifted to 5960A by an applied field of 18,600 volts/cm. From the observations of the variations of the shifts with applied fields calculations of the surface fields were made after the manner of Becker and Mueller. It was found that outside the film of potassium on a thin layer of oxygen on tungsten the field followed closely the Schottky image law in the range 1.5×10^{-6} cm to 10^{-5} cm from the surface. The pure potassium film on tungsten exhibited surface fields which were closely image fields between 8×10^{-7} cm and 1.5×10^{-6} cm from the surface but which departed from the image law at greater distances. These observed departures were about equal to the image fields and were much smaller than the surface fields at like distances outside thoriated tungsten filaments as recorded by the thermionic measurements of several observers. The surface fields in excess of the image fields are ascribable to inhomogeneity of the surfaces, regions of different work functions having linear dimensions of the order of magnitude of 10^{-5} cm.

Shifts of photoelectric thresholds by strong accelerating fields are of particular theoretical interest for they involve changes of the work function of a surface without alterations of the other important characteristics of the metal. It is found that the form of the photoelectric sensitivity versus frequency curve remains unchanged over the range of observations and shifts along with the thresholds in intense fields. Thresholds are not sharp but approach the frequency axis tangentially. These observations are in excellent agreement with the theory of the photoelectric effect based on wave mechanics and the Fermi-Dirac distribution of the electrons in metals worked out by Wentzel and modified by Houston.

THE new quantum mechanics in the hands of Pauli, Sommerfeld, Wentzel, Fowler, Houston, Nordheim and others[1] has been highly successful in dealing with many general properties of metals, and has given a particularly satisfactory account of the emission of electrons from metal surfaces.

[1] An excellent résumé of the subject by L. Nordheim is to be found in Phys. Zeits. **30**, 177 (1929).

The old concept of free electrons in metals has been revived, though to be sure the behavior of these electrons on the present theory differs radically from that of former views. For purposes of discussion of the experimental results herein described it is desirable to emphasize two characteristic features of the new theory.

The first has to do with the work function of a metal surface. The constant b in Richardson's thermionic equation and the photoelectric long wavelength limit have been regarded as measures of the minimum amount of energy given to an electron in the process of its ejection from a metal. On the older theory the free electrons possessed a Maxwellian distribution of velocities and were retained in the metal by a potential difference between outside and inside equal to the work function. The newer theory attributes a Fermi-Dirac distribution of velocities to the electrons and assigns a potential energy barrier at the surface which exceeds the maximum energy of the electrons at the absolute zero of temperature by the amount of the work function. The work function involves more than just the work required to eject an electron from inside to immediately outside a metal, for it includes as well the work required to remove it entirely away from the surface. Outside the metal an electron experiences a force of attraction to the metal produced by its image. In some cases inhomogenous ion layers also produce electrostatic fields near metal surfaces which aid or oppose the removal of electrons.

It is obviously possible to introduce electric fields at metal surfaces which reduce the image and ion fields, and thereby cause reductions of the work function. Such reductions of the work function in strong fields have been observed by workers in the field of thermionics, and indeed variations of the thermionic emission with applied fields have been used to estimate surface electric fields.

The second feature of the new theory is that it yields a definite probability that an electron will pass into a region in which its classically computed potential energy is greater than its total energy before entering the region. The probability of finding an electron in such a region falls off exponentially with the distance into the region. This feature of the theory is one aspect of the wave nature of matter. It is possible to apply such a strong electric field at the surface of a metal that the potential within a few atom diameters of the surface becomes lower than the energy of some of the electrons within the metal. Any electron, which passes into this region of higher potential far enough to reach the point where the applied field has lowered the potential to that corresponding to the energy of the electron in the metal, will be accelerated away from the surface. This effect, which is analogous to the passage of light unaffected from one glass plate into another when the plates are close enough together, satisfactorily explains the observed emission of electrons in strong fields.

These effects of strong accelerating fields on the emission of electrons from metals, also should be clearly displayed by a dependence of photoelectric emission on such fields. The lowering of the work function by fields

should appear as a shift of the photoelectric threshold to the red, as has been pointed out by Becker and Mueller.[2] Similarly the ability of electrons to go through high potential barriers should be evidenced in a like manner. That effects of this sort exist, has been indicated by the observation of Ives[3] who found difficulty in saturating photoelectric currents from thin alkali metal films, while currents from thicker ones were more easily saturated. Suhrmann[4] also noted this lack of saturation, and its variation with the thickness of the film, and noted the further effect that the saturation becomes the more difficult the nearer the frequency of the incident light approaches the threshold value. The reports were only qualitative, and no mention was made of a possible shift in the threshold frequency being associated with the phenomena.[5]

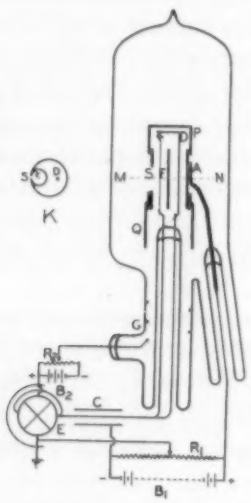

Fig. 1. Diagram of apparatus, showing a section through the photoelectric cell with a schematic diagram of the electrical connections. Also K a cross-section through the anode A along the line MN.

The present work was designed to investigate the matter in a quantitative manner with the primary view of verifying the predictions of the newer theories and also to use the experimental data to elicit information on the surface electrostatic forces near various metal surfaces.

Apparatus and Experimental Methods

Figure 1 shows a section through the photoelectric cell and a schematic diagram of the electrical connections. K is a cross section through the anode A on the line MN. The anode was made from a solid block of nickel in the

[2] J. A. Becker and D. W. Mueller, Phys. Rev. **31**, 431 (1928).

[3] H. E. Ives, Astrophys. J. **60**, 209 (1924).

[4] R. Suhrmann, Naturwissenschaften **16**, 336 (1928).

[5] Nottingham (abstract Feb. meeting Am. Phys. Soc.) has recently observed interesting shifts of photoelectric thresholds produced by very small applied fields.

form of two internally tangent cylinders. In their common wall was a 1 mm slit S, 1 cm long, to allow the light to fall on the tungsten filament F stretched along the axis of the inner cylinder. The filament was held in place by the nickel support D passing through the crescent shaped space between the two cylinders. The screw on cap P and the sliding sleeve Q were so arranged, that when in place they screened all parts of the cathode circuit, inside the tube, from light and external electrical effects. Both filament leads were carried out of the tube so that the filament could be glowed.

The tube was baked out under vacuum for 12 hours at a temperature of 500° C, the metal parts were heated with an induction furnace and the filament glowed at about 2200° C. The potassium was then distilled into the tube after repeated distillations, and the tube was sealed off when the pressure was less than 10^{-6} cm of Hg. To obtain a coating of oxygen on the filament, a little air was allowed into the tube, after baking out and before distilling the potassium, and then pumped out immediately.

Light from a 6 volt, 110 watt ribbon filament lamp, was dispersed by a Van Cittert type double monochromator, which gave light bands about 100 cm^{-1} units wide (corresponding to a width of 32A at 5600A) which were practically free from stray light. Any desired band of the visible spectrum could be selected by moving the middle slit. This made it unnecessary to change the adjustment of the last slit or of the photoelectric cell when measuring the current for various wave-lengths.

The photoelectric current was measured with a quadrant electrometer E using the accumulation of charge method. To prevent leakage of charge from the anode circuit to the electrometer circuit, a guard ring G consisting of several turns of tungsten wire was placed in the stem carrying the filament leads. Metal foil, used as a screen on the outside of the tube, was also connected to the guard ring circuit. A low voltage battery B_2 and potentiometer R_2 were used to balance out the effects of contact potentials.

The accelerating fields were produced by potentials from a 1500 volt bank of storage "B" batteries B_1. These were connected across a resistance R_1 of about 5×10^5 ohms. Only a part of the battery potential was applied between the anode and the electrometer case. The remainder was used to produce a negative potential on the compensating condenser C. The ratio of the potentials on the anode and compensating condenser was so adjusted that the electrometer system was rendered immune to fluctuations in the voltage of the batteries.

The data are shown by plotting the sensitivity curves, that is the photoelectric current per unit light intensity against the frequency of the incident light in sec^{-1} units. The absolute values of the light intensity and of the photoelectric current were not determined. The maximum current was of the order of 10^{-14} amps.

The relative intensities of the light of the various wave-lengths were determined by a vacuum thermopile set in the place of the photoelectric cell.

The accelerating fields were calculated from the applied potentials and

the dimensions of the cylinder and filament. The inside diameter of the nickel cylinder was 0.228″ or 0.579 cm. The field at the surface of the filament in the cell with a filament 0.9 mil (0.0023 cm) in diameter was $E=160V$; and at the surface of the filament 3.0 mil (0.0076 cm) in diameter, $E=60.4\ V$, where V is the applied voltage.

The small diameters of the filaments together with the fact that only about 0.7 cm of the filament was illuminated explain the small values of the photoelectric currents.

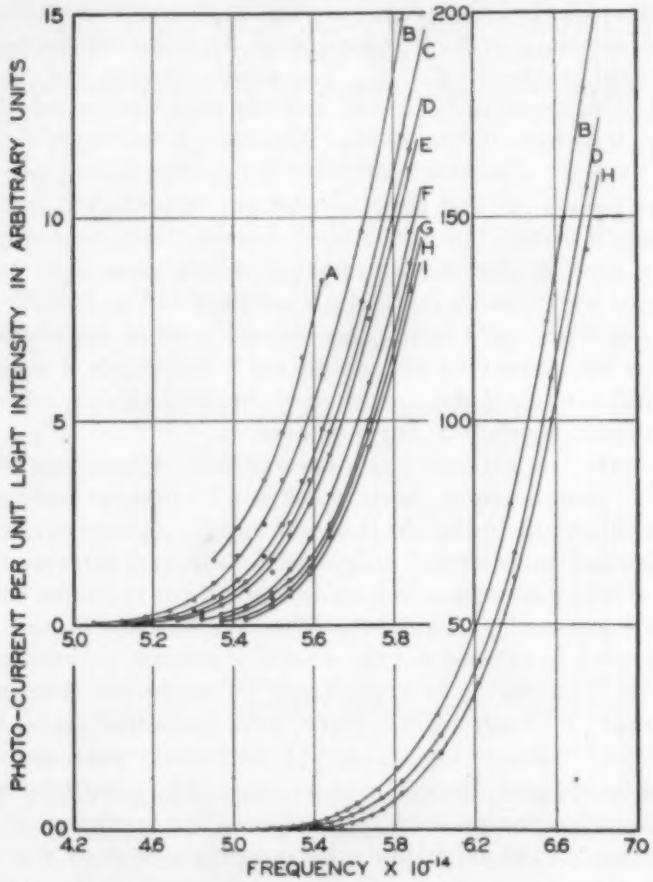

Fig. 2. The photoelectric current as a function of the frequency of the incident light for a potassium film on tungsten for various fields drawing electrons away from the surface. At right, complete curves for three values of the field. At left, similar curves for nine values of the field on an enlarged scale. The fields in volts per centimeter are for the curves A to I: A, 63, 100; B, 36,200; C, 22,100; D, 15,800; E, 9000; F, 3100; G, 1000 H, 260; and I, 0.

Experimental Results

The photoelectric sensitivity curves for a film of potassium on the 0.9 mil tungsten filament, for different voltages are shown in Fig. 2. The three curves to the right are the sensitivity curves over the range of wave-lengths studied. The photoelectric threshold with an accelerating field of 260 volts/

cm, curve *II*, was 5620A (5.35×10^{14} sec^{-1}) and for fields of 36,200 volts/cm, curve *B*, the threshold was shifted to 5880A (5.10×10^{14} sec^{-1}).

At the left, the portions of the curves near the threshold are plotted on an enlarged scale. The scale of frequencies has been doubled and that of the current increased tenfold. The increased scale allows the current taken with

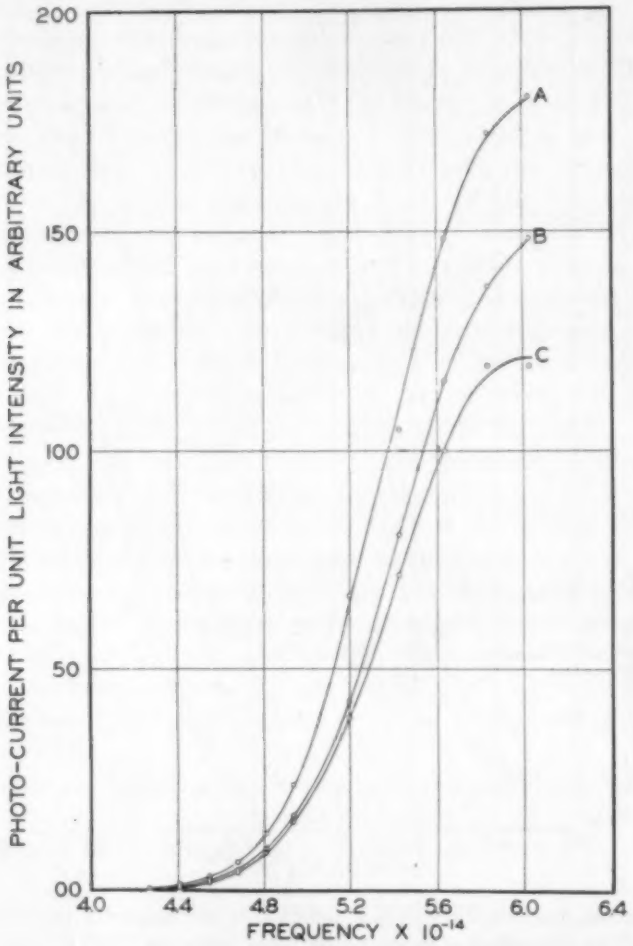

Fig. 3. The photoelectric current as a function of the frequency of the incident light for potassium on a thick layer of oxygen on tungsten. The fields in volts per centimeter for the curves *A* to *C*: *A*, 18,300; *B*, 4570; and *C*, 366.

the nine different accelerating fields to be plotted, while at the right only three representative ones have been selected. The fields for curves *A* to *I* in volts per centimeter are: *A*, 63,100; *B*, 36,200; *C*, 22,100; *D*, 15,800; *E*, 9000; *F*, 3100; *G*, 1000; *H*, 260; and *I*, 0. It was not possible to use higher electric fields, because of the setting in of field currents of the same order of magnitude as the photoelectric currents. *It is evident from the figure that the shift is not proportional to the strength of the field, but as will be shown later,*

is more nearly proportional to the square root of the field. Not only is the threshold shifted, but the entire sensitivity curve is displaced by the field. The curves do not meet the frequency axis at a finite angle, but approach tangentially, as near as can be experimentally determined. The recorded thresholds were arbitrarily chosen as the points where the currents became definitely measurable.

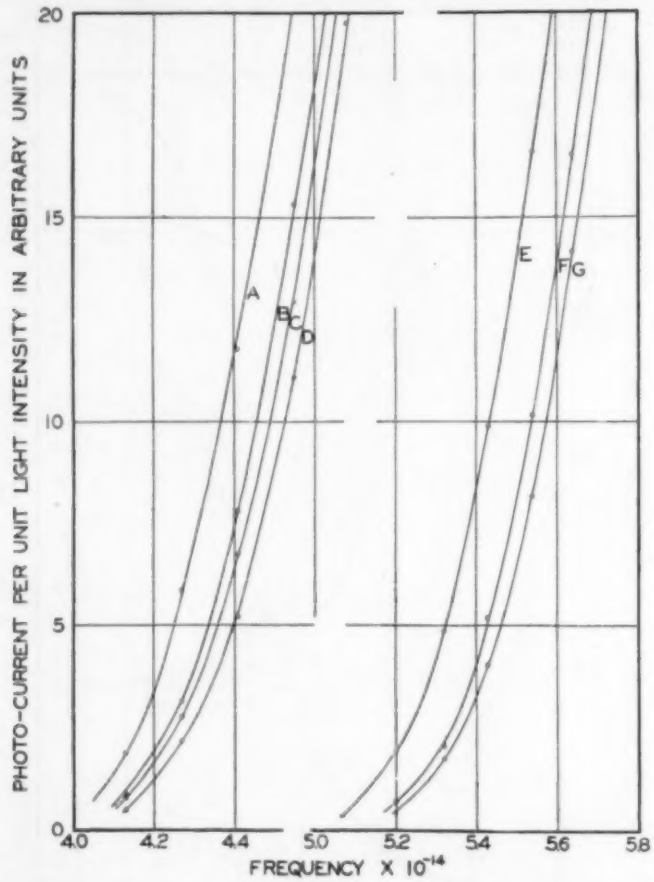

Fig. 4. The photoelectric current as a function of the frequency of the incident light. Curves *A* and *D* for the surface of figure 3 after being heated to 1100° C. The fields in volts per centimeter are: *A*, 18,600; *B*, 4650; *C*, 372; *D*, 0. Curves *E* to *G* show data obtained from the same surface after being heated to 1600° C. The fields are: *E*, 18,600; *F*, 372; and *G*, 0.

To test for the existence of contact potentials between the filament and anode, a photoelectric sensitivity curve was made with a retarding potential of 0.7 volts. The curve cut the frequency axis where the frequency was 1.3×10^{14} greater than for zero potential. This corresponds to a shift of 0.54 volts. Thus the contact difference in potential was less than 0.2 volt in a direction to produce an accelerating field.

A layer of oxygen was allowed on the 3.0 mil filament before the potassium was distilled into the tube. The results shown in Fig. 3 show that the thres-

hold of this surface was not appreciably shifted by fields as large as 18,300 volts/cm. Near the maximum sensitivity, the emission with a field of 18,300 volts/cm was 1.5 times, and at 4570 volts/cm was 1.17 times the emission at 366 volts/cm (curves *A*, *B* and *C* respectively). The oxygen layer shifted the threshold from 5620A for the pure potassium surface to 7100A (4.25×10^{14} sec^{-1}). At the same time the nature of the surface was changed so that the threshold was little affected by the accelerating fields.

The filament was then heat treated at about 600° C for 5 minutes, allowed to cool and observations were made. It was then heat treated at successively higher temperatures up to about 1600° C. Curves *A* to *D*, Fig. 4, show the emission from the filament after being heated to 1100° C and then allowing the potassium to distil back onto the filament with the reduced oxide coating. Heat treating at this temperature produced the first observable difference from the unheated surface. Curves *E* to *G* show the results after the filament had been heated for a few minutes at 1600° C. These curves show only the region near the threshold on the enlarged scale used for the left half of Fig. 2. They are not continued to the frequency axis because when taking the data the region very close to the threshold was not measured in detail. However, single tests made near the threshold showed that for these surfaces these sensitivity curves are tangent to the zero axis.

Of interest is the fact that reducing the thickness of the oxygen film shifted the threshold still farther to the red, that is to 7500A (4.0×10^{14} sec^{-1}), and then the further removal of the film shifted the threshold back to 5880A (5.1×10^{14} sec^{-1}) or nearly back to the value found in the first cell.

The maximum photoelectric emission per unit light intensity of the surface with a thick oxygen layer and that of the same surface after being heated to 1100° C was about one-seventh that of the surface after most of the oxygen had been removed by heating to 1600° C. This latter surface had a photoelectric emissivity about equal to that of the pure potassium film on tungsten.

Throughout the investigation it was noted that after heating the filament, and thereby removing the potassium and some of the oxygen, from 24 to 48 hours elapsed before the characteristics of the surface became constant.

Discussion of Results

Evaluation of surface fields from experimental data.

As previously stated, a considerable portion of the work function of metal surfaces can be accounted for by assuming that the field through which an electron leaves the surface is that due to its own image in the metal. This was considered by Lennard[6] and Debye[7] and discussed in detail by Schottky.[8] If an electron is at a distance x from the surface, its image produces a field E_i of magnitude,

[6] P. Lennard, Ann. d. Physik **8**, 149 (1902).
[7] P. Debye, Ann. d. Physik **33**, 441 (1910).
[8] W. Schottky, Phys. Zeits. **15**, 872 (1914).

$$E_i = -\frac{e}{(2x)^2} = -\frac{e}{4x^2}. \tag{1}$$

The potential of the image field at the distance x from the surface, considering the zero potential to be at $x=\infty$ with no accelerating field, would be:

$$V_i = -\int_{\infty}^{x} E_i dx = -\int_{\infty}^{x} \frac{-e dx}{4x^2} = -\frac{e}{4x}. \tag{2}$$

Now if an external accelerating field E_a be applied, its potential at a distance x from the surface would be:

$$V_a = -E_a x \tag{3}$$

and the potential resulting from the two fields, the sum:

$$V = -\frac{e}{4x} - E_a x. \tag{4}$$

To find the maximum potential, the derivative of Eq. (4) may be equated to zero which is the same as equating the resultant field to zero.

$$-\frac{dV}{dx} = E = -\frac{e}{4x^2} + E_a = 0. \tag{5}$$

Solving for the value of x at the maximum:

$$x_{max} = \frac{1}{2}\left(\frac{e}{E_a}\right)^{1/2}. \tag{6}$$

Substituting this value in (4) gives the value of the maximum potential:

$$V_{max} = -\frac{e}{4}2\left(\frac{E_a}{e}\right)^{1/2} - \frac{E_a}{2}\left(\frac{e}{E_a}\right)^{1/2} = -(eE_a)^{1/2}. \tag{7}$$

Since the potential of the free electron has been chosen as zero, $(eE_a)^{\frac{1}{2}}$ represents the reduction in the maximum of the potential energy curve due to the applied field E_a. If the image forces were the only ones acting on an electron leaving the surface, this reduction in potential would represent the reduction of the work function of the surface.

This simple explanation will not hold for all distances from the surface, since the integral in Eq. (2) becomes infinite for $x=0$, which would represent an infinite work function. However of course for distances of atomic magnitude from the metal, the image forces no longer are of this form. The precise manner in which the field departs from the ideal image law is of no consequence to the present discussion.

Regardless of the assumed law of force near the surface of the emitting metal, an increase in the strength of the accelerating field will reduce the work function of the surface. When an electron is leaving the surface of a metal under the combined action of the surface fields and an accelerating field, it is

retarded until it reaches a distance from the surface x_1 where the applied field equals the surface field. As soon as it passes that point it is free and is accelerated from the surface. If the accelerating field is increased by an amount ΔE_a in es units, the field which the electrons must overcome is reduced by an equal amount, and since the electrons must work against this field for a distance x_1 to escape, the decrease in energy necessary for unit charge to escape would be:

$$-\Delta\chi = x_1 \Delta E_a. \tag{8}$$

Where $\Delta\chi$ is the change in the work function due to the change in the applied field ΔE_a. Dividing Eq. (8) by ΔE_a and considering the limit as ΔE_a approaches zero:

$$\frac{d\chi}{dE_a} = -x_1. \tag{9}$$

Thus observations on changes of the work function in strong fields yield directly the magnitudes of the electric fields near the surfaces. This method of evaluation of surface fields is due to Becker and Mueller.[9]

The above holds for any kind of electron emission, and the photoelectric threshold frequency gives a convenient measure of the work function as given by the Einstein relation:

$$h\nu_0 = e\chi. \tag{10}$$

Differentiating Eq. (10) and solving for $d\chi$ one obtains

$$d\chi = \frac{h d\nu_0}{e}. \tag{11}$$

Substituting the value of $d\chi$ from (11) into (9)

$$\frac{d\nu_0}{dE_a} = \frac{x_1 e}{h}. \tag{12}$$

Or expressing the field E_v in volts per centimeter:

$$\frac{d\nu_0}{dE_v} = -\frac{x_1 e}{300h} \text{ or } x_1 = -\frac{300h}{e}\frac{d\nu_0}{dE_v}. \tag{13}$$

Thus the distance from the surface x_1 where the applied field equals the surface field, is proportional to the slope of the ν_0 *vs.* E_v curve, evaluated at the particular value of the field in question.

This method of determination of the surface fields is independent of an exact measurement of the threshold, and depends only on the measurement of the displacements of the threshold. These displacements were measured a short distance away from the zero current axis, where the slopes of the curves were greater and the accuracy of the current measurements better.

[9] See ref. 2.

This procedure was justified because the electric fields produced a parallel displacement of the curves. The shifts could thus be determined with considerable accuracy.

In Fig. 5 curve *A* shows the Schottky shift as calculated from Eq. (7) making allowance for the change in units. Curve *C* shows the shift of the threshold of the pure potassium surface from the data of Fig. 2. The sur-

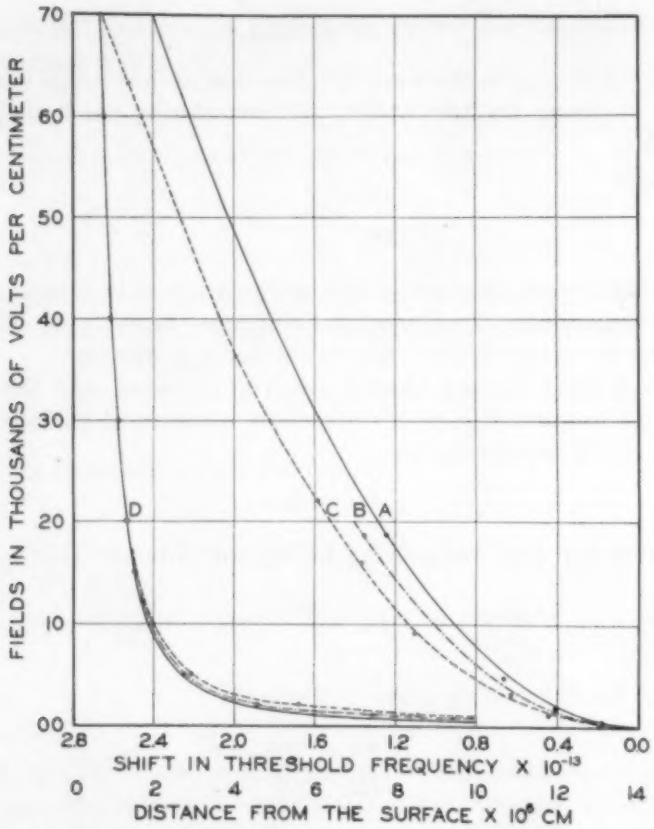

Fig. 5. Curves *A* to *C* show the shift of the threshold as a function of the field. Curve *A* the Schottky shift; *C*, the shift for the pure potassium surface; *B*, the shift for the surface heated to 1600° C, and the black dots the shifts for the surface heated to 1100° C. The curves *D* show the fields near the surface as a function of the distance from the surface. The type of line indicates the curve *A* to *C* from which it was deduced.

face with a thick oxygen layer showed negligible shift and was not plotted. The shifts measured from the curves *A* to *D* Fig. 4 were so nearly the Schottky values that the displacements are shown by the black dots only. This was the surface produced by heat treatment at 1100° C. Curve *B* shows the displacements measured from curves *E* to *G* Fig. 4, and shows the displacements of the threshold of the surface after being heated to 1600° C. From the three curves only two displacements could be measured, but

since both of these fell about midway between the theoretical curve and curve *C*, it was assumed that the complete curve was about as drawn.

The curves marked *D* show the fields calculated from the slope of the experimental curves *B* and *C* as compared with a calculated image field, drawn as a solid line. The single circles above fields of 20,000 volts/cm show the fields calculated from curve *C*. They show that the fields are very closely image fields between 7×10^{-7} and 1.2×10^{-8} cm from the surface. At greater distances, the fields of the two surfaces are greater than image fields. The field near the surface after it was heated to 1100° C is about the image field, and apparently the surface with a thick layer of oxygen under the potassium had only negligible fields which could be overcome by the applied fields.

It is of interest to note how closely the observed surface fields coincide with the image field within 1.2×10^{-6} cm of the surface. The deviation at greater distances is undoubtedly real though small. It is very small compared to the large deviations noted by Becker and Mueller,[10] Reynolds[11] and others for thoriated tungsten surfaces.

The possible sources of fields greater than the Schottky fields at large distances from the surface have been discussed by many investigators.[12] The best explanation seems to be that the potassium film is not uniform over the surface, so that there are areas of different work functions. The areas of lower work function are electropositive with respect to those of higher work function. The electrostatic fields between these areas are in such a direction as to retard electrons leaving the surface through areas of lower work function. Near the threshold frequency, only the areas of lower work function are able to emit, and these electrons emerge with a retarding field equal to that of their image plus that due to the potential differences on the surfaces. The image field falls off as the square of the distance from the surface, while the fields due to these patches fall off much more slowly. Over the center of such a patch the field would be essentially constant to a distance comparable with about one-tenth of the diameter of the patch. Thus the extra field might be negligible compared to the image field near the surface and at greater distances become larger than the image field. It should be emphasized that to account for the deviation from Schottky fields at distances of 5×10^{-6} cm from these surfaces, it is necessary to postulate the existence of patches having a diameter about ten times this magnitude. Irregularities of atomic dimensions such as unequal distributions of ions over the surface as has been proposed by Suhrmann[13] are not capable of accounting for the experimental facts.

Since the film of potassium on the layer of oxygen which removed the

[10] See ref. 2.

[11] N. B. Reynolds, Phys. Rev. **35,** 158 (1930).

[12] O. W. Richardson and A. F. A. Young, Proc. Roy. Soc. **A107,** 377, (1925). See also work of Becker and Mueller, ref. 2, that of Reynolds, ref. 10, and of B. Gudden, Naturwissenschaften **16,** 547 (1928).

[13] R. Suhrmann, Naturwissenschaften **16,** 616 (1928).

threshold farthest to the red exhibited very closely the Schottky field, it follows on this view that such films are homogeneous, and free from patches. In other words, the ions are distributed uniformily over the surface. Moreover it follows that the alkali film surfaces of the present experiments were much more homogeneous than the surfaces of thoriated tungsten studied by Becker and Mueller, Reynolds and others.

It is not evident why the surface with a thick oxygen layer should fail to show a reduction in the work function when the accelerating field is applied. There are two possible explanations. One is that the ions are about 300 atom diameters out from the surface of the tungsten, and the field between the positive potassium layer and the tungsten counteracts the image field in this region. At distances farther out, the image field is small and the counteraction of this by the applied field would not shift the threshold appreciably. The other postulates that the thick oxide layer is extremely rough, and the applied field can lower the work function of only the highest points, and since these constitute only a small part of the area, their emission would not appreciably affect the observed threshold. The principal part of the emission would occur from the hollows where the externally applied fields would be always greatly reduced. The small increase in the field would greatly assist the electrons emitted in the cavities to emerge without striking the walls of the cavity. This latter explanation seems to be more probable since this surface showed much poorer saturation than any of the others.

Comparison with theories of the photoelectric effect.

For the several surfaces and the many surfaces fields, i.e. the many thresholds studied in the present experiments the shape of the photoelectric sensitivity curves remained the same. Thus the form of the curve is practically independent of such superficial factors as the form of potential barriers at metal surfaces and therefore is of interest theoretically as well as experimentally.

From the standpoint of the wave mechanics, Wentzel[14] has calculated the rate at which free electrons in a metal are excited to higher energy states which enable them to escape over the potential wall of a metal surface, when light falls on that surface. He finds that this rate rate Z for light of frequency ν having electric vectors proportional to E_x, E_y, E_z incident on a metal surface with the normal along the x direction is:

$$Z \sim \frac{1}{\nu^{7/2}} \xi^2 \left\{ E_x^2 + \frac{m}{2h\nu} \left[\frac{1}{2} \xi^2 E_x^2 + \eta^2 E_y^2 + \zeta^2 E_z^2 \right] \cdots \right\} \qquad (14)$$

where ξ, η, ζ are the velocity components of the electrons before the excitation by the light. He derived an expression for the total photoelectric emission from a surface by integrating the above expression over the distribution of energies of the electrons in the metal. In order to obtain approximate

[14] G. Wentzel, in Sommerfeld's 60. Geburtstag Festschrift, Probleme der Modernen Physik, edited by P. Debye, p. 79. Leipzig, 1928.

expressions he assumed the distribution of energies to be the Fermi-Dirac distribution at the absolute zero of temperature—a distribution of the form:

$$n(\epsilon)d\epsilon = 4\pi\left(\frac{2m}{h^2}\right)^{3/2}\frac{(\epsilon)^{1/2}d\epsilon}{e^{(\epsilon-\bar{\epsilon})/kT}+1} \tag{15}$$

where $n(\epsilon)d\epsilon$ is the number of electrons having energies between ϵ and $\epsilon+d\epsilon$. It is seen that at absolute zero the number increases as the square root of ϵ to a sharp upper limit for $\epsilon=\bar{\epsilon}$, the maximum energy of the Fermi distribution above which no electrons exist. The expression for the probability of excitation of an electron in the metal by impinging light indicates that the probability varies approximately as the square of the velocity of the electron and as the frequency of the light to the inverse 7/2 power. The Fermi distribution clearly led then to a formula for the total emission as a function of the frequency, having a sharp rise from a threshold value corresponding to the minimum energy necessary for an electron, having the maximum energy $\bar{\epsilon}$ of the Fermi distribution, to escape from the surface. The formula obtained in the case $\nu_0<\nu<\nu_a$ is the following:

$$I \sim [\bar{\nu}^{5/2}-(\nu_a-\nu)^{5/2}]\nu^{-7/2}E_x^2 + \frac{1}{14}[\bar{\nu}^{7/2}-(\nu_a-\nu)^{7/2}]\nu^{-9/2}[3E_x^2+2E_z^2+2E_y^2]+\cdots \tag{16}$$

Where $h\bar{\nu}=\bar{\epsilon}$, the maximum energy of the Fermi distribution at 0°K, $h\nu_a=\epsilon_a$, the energy required by an electron at rest in the metal to escape over the potential barrier, and $\nu_0=\nu_a-\bar{\nu}$ is the threshold frequency. For $\nu<\nu_0$ there is no emission, and for $\nu>\nu_a$, $I\sim\nu^{-7/2}$ The maximum of the photoelectric sensitivity curve is in the interval $\nu_0<\nu<\nu_a$, and this comprises the frequencies used in the present research.

The above expression really gives the rate at which electrons in the metal acquire enough energy to emerge from the metal and of course is equal to the photoelectric emission provided that the excited electrons do not make an appreciable number of inelastic impacts before striking the surface of the metal normally. Houston[15] has pointed out this tacit assumption of electron elastic impacts in Wentzel's derivation and believes a more nearly correct estimate of the photoemission would take account only of the electrons having great enough energies in their velocity components normal to the surface to escape. Integrating then the expression over the distribution of velocities normal to the surface in excess of a minimum value requisite to overcome the potential barrier, Houston has obtained the following expression:

$$I\sim\left(\frac{\bar{\epsilon}}{h\nu}\right)^{1/2}\left\{\frac{E_x^2}{\nu}\left[1+\frac{\bar{\epsilon}}{2h\nu}\right]+\frac{E_y^2+E_z^2}{3\nu}\left[\frac{\nu-\nu_0}{\nu}\right]\right\}\left(\frac{\nu-\nu_0}{\nu}\right)^2 \tag{17}$$

where I is the photoelectric emission at 0°K, $\bar{\epsilon}$ corresponds to the maximum

[15] We wish to thank Professor W. V. Houston for allowing us to read an unpublished manuscript dealing with this point.

energy of the electrons in the degenerate Fermi distribution and ν_0 is the threshold frequency.

Wentzel[16] is in agreement with Houston on the necessity of taking account of the distribution in direction of the velocities of the electrons in the metal in computing the rate of emission and has modified his original expression (16) obtaining

$$I \sim 1/\nu^{7/2}\left\{\tfrac{1}{3}\bar{\nu}\left[\bar{\nu}^{3/2} - (\nu_a - \nu)^{3/2}\right] - \tfrac{1}{5}\left[\bar{\nu}^{5/2} - (\nu_a - \nu)^{5/2}\right]\right\} E_x^2 \qquad (18)$$

+ higher powers in $\bar{\nu}/\nu$ (for $T = 0°\text{K}$) which is essentially the same as Houston's formula in so far as the first term of the expansion in $\bar{\nu}/\nu$ is accurate.

It has been thought by some that photoelectric thresholds are sharp, and thus in accordance with Wentzel's formula[16] and that lack of sharpness is ascribable to experimental errors, such as those introduced by scattered light. Others have observed photoelectric sensitivity curves approaching the frequency axis with zero slope, as is the case in the present experiments.[17] A simple calculation shows that the rounding off introduced by the temperature effects accounts for about half of the observed lack of sharpness of the thresholds in the present experiments, if Wentzel's first method of calculation be assumed. *Houston's calculation* (Eq. (17)) *corrected for temperature effects is adequate to account for nearly the whole tailing off of the here recorded sensitivity curves.* In a later experiment it is hoped to verify the calculated magnitude of the temperature effect by studying the sensitivity as a function of the temperature.

Fowler[18] has discussed the sharpness of photoelectric thresholds in a manner similar to Wentzel's original deduction, and therefore Houston's objections apply equally well to Fowler's conclusions that thresholds are sometimes sharp.

It has been mentioned that electrons can pass through regions of potential greater than that corresponding to their energy. The magnitude of the effect of applied fields at a metal surface is contained in the following formula:[19]

$$D(W) = \frac{4\left[W(W - \epsilon_a)\right]^{1/2}}{\epsilon_a} e^{-4\kappa(\epsilon_a - W)^{3/2}/3E}, \qquad \kappa^2 = \frac{8\pi^2 m}{h^2} \qquad (19)$$

where $D(W)$ is the probability that an electron with an energy W for the component of its velocity normal to the surface, will pass through a potential barrier whose maximum is ϵ_a volts greater than the zero of energy in the metal, when an accelerating field E is applied. For the maximum field, 63,000 volts/cm, used in the present experiments and assuming ϵ_a to be 7 volts, the probability $D(W)$ that an electron whose kinetic energy W is nor-

[16] We wish to thank Professor Wentzel for this information sent to us in a private communication.

[17] For discussion of this see B. Gudden, Lichtelektrische Erscheinungen, p. 37ff. Berlin, 1928.

[18] R. H. Fowler, Proc. Roy. Soc. **A118**, 229 (1928).

[19] See ref. 1.

mal to the surface is 0.1 volt less than ϵ_a, the amount required to go over the potential barrier, is less than 10^{-15}. It is evident therefore that this type of influence of the shape of the photosensitivity curve was inappreciable for the fields used in the present experiments. A more favorable case for the observation of this influence of strong fields on photoelectric emission would be that of a metal having a high work function like pure tungsten where much higher electric fields may be applied before the autoelectronic current becomes appreciable.

The changes of the whole photoelectric sensitivity curves produced by applied accelerating fields observed in the present experiments are of fundamental interest, for the effect of the applied fields is to alter the work function without affecting any other characteristics of a metal concerned in its photoelectric properties. Both Wentzel's and Houston's formulas agree in indicating that over the present range of observation the whole photoelectric sensitivity curve shifts by approximate parallel displacement along the frequency axis with the threshold. Alteration of the nature of the work function (the surface electrostatic fields) does not affect markedly the form of the sensitivity curve. *This prediction of the wave mechanical theory of the photoelectric effect is strikingly confirmed in the present experiments.*

THE MAGNETIC ISOTROPY OF COPPER CRYSTALS*

By Carol G. Montgomery

Sloane Physics Laboratory, Yale University

(Received June 23, 1930)

Abstract

The variation in the magnetic susceptibility with the direction of the applied field was investigated for large single crystals of copper. A modification of Curie's method of measurement was used. A Fourier analysis of the results indicates that there is no variation of susceptibility larger than 1%, a result consistent with the magnetic isotropy of cubic crystals predicted by the theory of W. Thomson.

I. Introduction

SINCE its conception in 1851, the description by means of the familiar ellipsoid of magnetization of the variation of the magnetic susceptibility of a non-ferromagnetic crystal with respect to the direction of the applied magnetic field has been accepted as correct until quite recently. It follows from this theory that for substances which form cubic crystals, there can be no dependence of the magnetic susceptibility upon direction of applied field so that the material must be magnetically isotropic.

In 1926, J. Forrest[1] performed some qualitative experiments on a number of cubic crystals and found that they were not isotropic, but that they showed variations in susceptibility as do single crystals of iron and nickel. McLennan and Cohen[2] investigated the magnetic susceptibility of large single crystals of a number of metals, and found that while bismuth seems to follow a law of variation with the direction of the magnetic field in accord with the accepted theory, antimony deviates noticeably from it. In addition, recent work[3] on the Peltier and Thomson effects, which should obey the same symmetry relations as the magnetic susceptibility, seem also to show a deviation from the theory. Thus the accepted theory may have a more limited range of application than hitherto supposed, and it was deemed advisable to reinvestigate a cubic crystal, and to determine whether or not it is magnetically isotropic.

II. Apparatus and Method of Measurement

In order to measure the susceptibilities of crystals it was decided to use a modification of Curie's method which has been developed to quite an extent by P. Weiss and his collaborators, a description of the final apparatus

* Part of a dissertation presented for the degree of Doctor of Philosophy at Yale University.

[1] J. Forrest, Trans. Roy. Soc. Edinburgh **54**, 601–701 (1926).

[2] J. C. McLennan and E. Cohen, Trans. Roy. Soc. Canada [3] **23** III, 159–168 (1929).

[3] H. D. Fagan and T. R. D. Collins, Phys. Rev. [2] **35**, 421–427 (1930); P. W. Bridgman, Proc. Amer. Acad. **63**, 351–399 (1929).

being given by Foex and Forrer.[4] The apparatus described below differs from theirs in several details.

A beam, 90 centimeters long, composed of three parallel lengths of quarter inch balsa wood, fastened at the ends and in the center at the corners of equilateral triangles, is suspended by five silk threads approximately 50 centimeters in length. These five suspensions are arranged so as to permit translation of the beam only in the direction of its length. They are hung at the top from a heavy iron frame in such a way that their lengths can be separately adjusted. The lower member of the beam is extended at one end and carries a small piece of aluminum with a vertical hole drilled in it about 2 centimeters deep. Into this hole fits the shaft of a crystal holder on which the crystal is placed. The crystal holder consists of a 7 centimeter length of #16 sterling silver wire on which fits a small cylindrical cap of amber, cut away at the top to fit the crystals, and graduated on the side every 10°. These graduations could be observed by means of a reading microscope and the azimuth of the holder thus read off. An electromagnet capable of producing fields up to about 5000 gauss was used. It was equipped with special pole pieces so as to obtain a field which has a high value of the product of the field by its derivative over a large area. Under the crystal holder, a small saddle, constructed out of copper wire and a small piece of paper, was fastened. This could hold either the crystals or the standard on the beam but was out of the field while measurements were being taken.

The other end of the balsa wood beam carried a celluloid cylinder 6 centimeters in diameter and 15 centimeters long, closed at one end, into which fits a piece of wood with a clearance all around of about 4 millimeters. This provides air damping which, combined with the electromagnetic damping of the sample in the field, is quite satisfactory.

At the center of the beam and perpendicular to it, is an aluminum arm extending some 10 centimeters out, to which is firmly waxed a phonograph needle pointing in the direction of the beam. This needle rests against and perpendicular to a microscope cover glass 1 centimeter in diameter. This is attached to the back of a galvanometer mirror suspended at both ends by a tightly stretched vertical quartz fiber of diameter about 50 microns. The plane of the cover glass makes an angle of 135° with the mirror. Light from an illuminated cross hair is reflected by the mirror and falls on a scale some two meters distant. Thus this arrangement acts as an optical lever and gives a total magnification of the motion of the beam of about 1000 times. The whole arrangement was placed in a wooden box having a large glass window on the side in order to stop air currents. The box was put on a stone pier in a sub-basement room to avoid mechanical vibrations.

When current is passed through the magnet coils, a force is exerted on the specimen and the beam will deflect until the force of gravity balances out the magnetic force. Suppose to do this the beam moves a distance x, and let l be the effective length of the suspensions, m the total mass of the suspended system, f the magnetic force, and g the acceleration of gravity.

[4] G. Foex and R. Forrer, Jour. de Physique [6] **7**, 180–187 (1926).

Then

$$x = fl/mg \qquad \text{when } x \ll l.$$

Now if the crystal has a susceptibility* k in the direction of the field, we have

$$f = \int kH_y \frac{\partial H_y}{\partial x} dv$$

where the x-axis is in the direction of the beam, the y-axis in the direction of the field, and the integral is taken over the volume of the crystal. Now if the variation of f with respect to x is small, then

$$x = Ak$$

where A is a constant. Hence, if we have a substance with a known value of the susceptibility, we can measure the susceptibility of any other substance by determining the value of A.

In order to test the validity of the assumption that f does not vary appreciably with the position of the crystal, a series of values of x were measured for various values of the field strength. We see from the above equations that

$$x \sim H_y \frac{\partial H_y}{\partial x} \sim H^2$$

if the assumption is justified, and hence if we plot values of x as a function of H^2 we should get a straight line through the origin. With values of the field strength measured in arbitrary units by a ballistic method, we find that within the limits of accuracy of a reading, we do get such a straight line.

Measurements were made of the variation of susceptibility of single crystals of copper as a function of the azimuth of the field. Gold was used as the standard substance. We see that to compare susceptibilities of two substances by this method we must keep the mass of the beam constant. Hence the following procedure was followed in measurement. The gold standard was placed in the paper saddle, and a copper crystal in the crystal holder. Then a series of deflections of the spot of light was observed for 36 azimuths of the crystal. Then the crystal was removed and placed in the saddle, while the gold was placed in the holder. A series of deflections for four azimuths was then taken. Then both the crystal and the gold were placed in the saddle and the deflections due to the holder alone were observed for the same four azimuths.

The zero shift over the whole period of time required for one such set (about ten hours) was not more than 50 to 75 millimeters.

III. Preparation of Specimens and Determination of their Orientation

The copper crystals used in these experiments were obtained from the Hammond Metallurgical Laboratory, Yale University, through the courtesy

* This is not a true susceptibility, but the difference between the susceptibility of the crystal and the surrounding medium, in this case, air.

of Dr. C. H. Mathewson. They were prepared[5] from the highest purity electrolytic copper by slowly lowering a graphite crucible containing the molten copper out of an induction furnace whose temperature at the center was maintained well above the melting point of copper. The rate of lowering was about 0.6 centimeter per hour. The single crystals so obtained were in the form of rough cylinders approximately a centimeter in diameter and 12 to 15 centimeters long. When these rods were etched in a 50 percent solution of nitric acid for a short time, and then washed, the surface of the rod would shine out brilliantly when held at certain positions with respect to parallel incident light. This is due to the fact that the etching process forms micro-

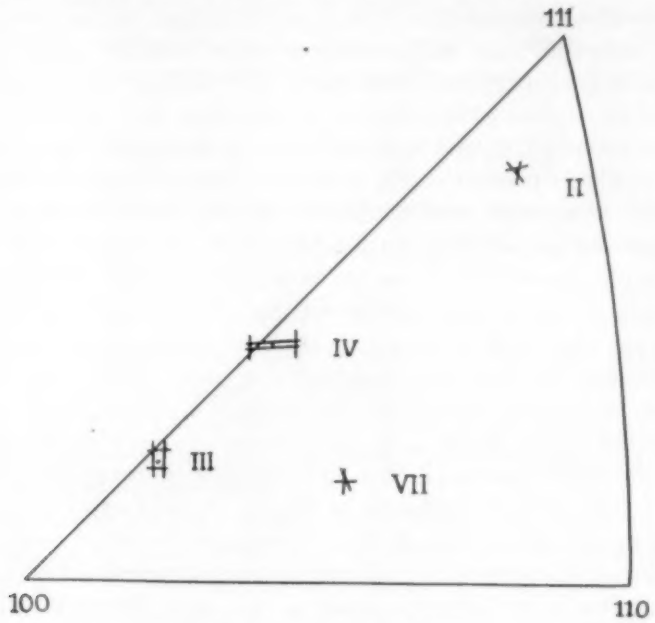

Fig. 1. Stereographic projection of the axes of the crystal rod.

scopic pits in the surface whose sides are definite crystal planes, and it is the light reflected from these pit-faces that gives rise to the selective reflection. It is evident that if the positions of these faces with respect to the rod as a whole could be determined, and the crystallographic form of these faces identified' then the orientation of the crystal lattice with respect to the rod as a whole could be obtained. Bridgman[6] has described one method of accomplishing this, but a more convenient, if not more accurate, arrangement was used here. The lenses were all removed from the telescope tube of a large polarizing spectrometer, and a plane piece of glass was fastened to the end of the telescope so that the normal to its plane was horizontal and made an angle of 45° with the axis of the telescope. The crystal rod was mounted horizontally and attached to a vertical circle carried by the

[5] C. H. Mathewson and K. Van Horn, A. I. M. E. Tech. Pub. No. 301-E-109, Feb., 1930.
[6] P. W. Bridgman, Proc. Amer. Acad. **60**, 305–383 (1925).

collimator tube. The light of a small carbon arc with condensing lenses was thrown on the piece of glass on the telescope and reflected to the crystal. By changing the position of the crystal with respect to the light beam, it could be adjusted so that the light from a reflecting surface could be viewed through the telescope. The spherical coordinates of the normal to the pit-face could then be read off the horizontal and vertical circles. The points corresponding to these coordinates were then drawn on a 15 centimeter marble sphere, and the crystallographic planes corresponding to each reflection maximum could be identified. The position of the rod axis with respect to the crystal lattice was then determined by plotting the observed angles on a stereographic net.

Considerable difficulty was sometimes experienced in getting reflections which could be unambiguously identified. The etching process seems to be a difficult one to control satisfactorily, a condition due to the fact that the reaction is a complicated one and particularly dependent upon the amounts of the end-products present in the etching solution. Various concentrations of nitric acid were tried, and consistent results were obtained more often with a 50 percent by volume solution than with any other. Figure 1 shows the stereographic projection of the rod axes of the crystals used.

The specimens were prepared by cutting off a section from the long rod. In order to cut the single crystal rods without spoiling them by introducing too large strains, the following method was used. Two vises were set up and the jaws accurately aligned on the bench of a milling machine. The rod was well padded with paper and held firmly in one vise between two V-blocks. In the other vise was held a jig consisting of two guide slots attached to a piece of steel at right angles to its length. A hack saw blade, 0.025 inch (0.064 centimeter) thick, with all the set removed from the teeth, fitted into these two slots and could be moved only in the plane defined by them. From 30 to 40 minutes were taken to make a cut, and plenty of oil was used. When a section had been cut off, the burr was removed with a fine file and the surface removed in a 50 percent nitric acid solution until the characteristic shine was restored. Care had to be taken to keep the crystals away from moist air, as they tarnished quite rapidly.

The following table gives the dimensions of the crystals used.

Crystal	Diameter	Length	Mass
II	0.764 cm	0.991 cm	3.921 gram
III	0.767	0.968	3.849
IV	0.770	0.993	4.057
VII	0.772	0.942	3.927
Gold Standard	0.770	0.975	8.752

As a substance of standard susceptibility, a piece of gold was used. It was obtained from Baker and Co. who stated that the purity was over 99.99 percent. A piece was machined out whose size was close to that of the crystal specimens. The value of the susceptibility chosen was that obtained

by Owen,[7] viz., -0.141×10^{-6} cgsm. This same value was obtained by Seeman and Vogt,[8] who have recently investigated copper-gold alloys.

No traces of ferromagnetic impurity could be detected in either the copper crystals or the gold standard.

IV. Reduction of Observations and Results

In order to insure that the copper crystals used were sufficiently representative, average values of the susceptibility were obtained for each. Taking into account small corrections due to the magnetic effect of the crystal holder and of the air, we get the following values of the specific susceptibility of the different crystals:—

Crystal	$\chi_{Cu}\cdot10^{6}$
II	−0.088
III	−0.075
IV	−0.086
VII	−0.091
Mean	−0.085

The spread of values here is just about that to be expected. Owen[7] gives the value

$$\chi_{Cu} = -0.085\cdot10^{-6}.$$

In order to bring out any possible anisotropy in the susceptibility of copper it is sufficient to use relative values of the susceptibility only. The values of the deflections obtained with a crystal in the holder were therefore subjected to a Fourier analysis, obtaining the coefficients of the first four cosine and the first four sine terms.

We obtain the following results in millimeters.

$$\begin{aligned}
x_{\text{cu II}} &= 76.31-1.88\cos\varphi-0.68\cos2\varphi-0.36\cos3\varphi\\
&\quad+0.30\cos4\varphi-0.68\sin\varphi-0.44\sin2\varphi\\
&\quad+0.11\sin3\varphi-0.61\sin4\varphi,\\
x_{\text{cu III}} &= 68.85-2.41\cos\varphi-0.36\cos2\varphi+0.08\cos3\varphi\\
&\quad-0.05\cos4\varphi-0.39\sin\varphi-0.16\sin2\varphi\\
&\quad-0.07\sin3\varphi-0.05\sin4\varphi,\\
x_{\text{cu IV}} &= 75.88-0.95\cos\varphi-0.29\cos2\varphi+0.16\cos3\varphi\\
&\quad-0.03\cos4\varphi-0.45\sin\varphi+0.36\sin2\varphi\\
&\quad+0.15\sin3\varphi+0.03\sin4\varphi,\\
x_{\text{cu VII}} &= 76.30-0.87\cos\varphi-0.26\cos2\varphi+0.38\cos3\varphi\\
&\quad+0.02\cos4\varphi+0.24\sin\varphi+0.41\sin2\varphi\\
&\quad+0.01\sin3\varphi+0.00\sin4\varphi,\\
x_{\text{cu III}'} &= 68.92+1.02\cos\varphi-0.16\cos2\varphi-0.08\cos3\varphi\\
&\quad+0.00\cos4\varphi-1.96\sin\varphi+0.01\sin2\varphi\\
&\quad+0.02\sin3\varphi+0.03\sin4\varphi,
\end{aligned}$$

where φ is the azimuth as read. $x_{Cu\ III'}$ is a set of measurements made on crystal III in a different holder.

[7] M. Owen, Ann. der Physik [4], **37**, 657–699 (1912).

[8] H. J. Seeman and E. Vogt, Ann. der Physik [5], **2**, 976–990 (1929).

Figure 2 gives the observations for crystal III plotted as a function of the azimuth φ. The curve drawn is $A_0+A_1 \cos \varphi+B_1 \sin \varphi$ as determined by the least squares analysis. Due to the fact that it was impossible to secure a holder which was perfectly straight and vertical, the crystal did not rotate exactly about its axis of figure. This gives rise to the large 360° period which the results show. That this is the case is supported by the fact that the 360° periods obtained by the least squares analysis are in close agreement in phase, with the exception of $x_{\text{cu III}}'$ which was made, as has been stated, with a different holder. An additional cause which contributes to this 360° period and may explain a shift in phase is the fact that the crystals were not exactly right circular cylinders. Thus we ascribe the whole of the 360° period to instrumental error. It is impossible to assign a crystallographic basis to the 360° period without attributing hemihedry to copper, for which there is, of course, no shadow of evidence.

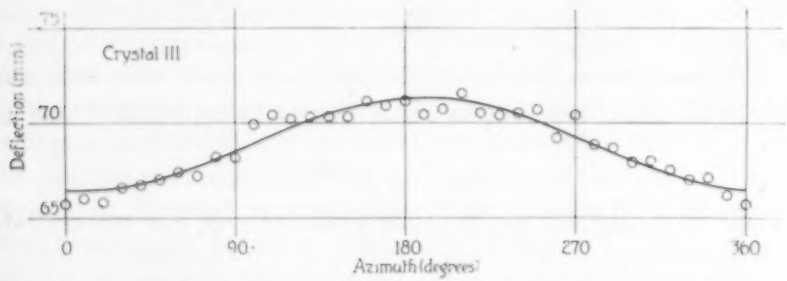

Fig. 2. Values of the deflection of the beam plotted against the azimuth of the crystal.

If there is any anisotropy, it must have four-fold symmetry about a <100> axis, three-fold symmetry about a <111> axis, and two-fold symmetry about a <110> axis. These are all the symmetry properties of a cubic crystal. Now, if without touching the apparatus we repeat a reading, on the average we will find that it cannot be reproduced closer than 0.5 millimeter. This is indicated on Fig. 2 where the diameter of the circles representing the observations gives what we may call the limits of "immediate reproducibility" of an observation. This represents a sort of minimum probable error. The actual probable error is much larger, as other factors such as the variation of temperature and humidity, which affect the length of the fibers, must be considered in assigning a proper value to the probable error. If we take this value of 0.5 millimeter as the minimum probable error, then we can compute from it the probable error in a coefficient of the Fourier series. For a series, representing 36 observations the probable error of a coefficient of a harmonic term is 0.236 times the probable error of a single observation, i.e., in the present case, 0.12 millimeter.

Now the axis of figure of crystal III lies near a <100> axis. Hence, if any anisotropy exists, we should expect a large term in 4φ. We see that the coefficient is actually less than half of the minimum probable error of that coefficient, i.e., it is sensibly zero. By the same reasoning the terms in 3φ are also sensibly zero. There is no physical justification for such terms.

In crystal II, whose axis of figure is close to a <111> axis, we should expect a large term in 3φ. Actually, the 4φ coefficient which has no significance for a three-fold axis, is larger than the 3φ coefficient, and the fact that both coefficients are larger than our minimum probable error should not therefore be taken as significant. We can therefore say that no three-fold symmetry can be detected with any degree of certainty. In a similar way the 3φ and 4φ coefficients of the more unsymmetrical cases of crystals IV and VII may be regarded as negligible.

It is to be noticed that in all cases the terms in 2φ have amplitudes larger than our assigned error. These can all safely be considered as due to the "spread" of the points. That is, we have chosen too small a value to represent our probable error. If we choose an error twice as great, viz., 1.0 millimeter, the probable errors in the 2φ terms become as large as the terms themselves.

We can therefore only ascribe any physical reality to the terms of period 360°, and these, it seems, are wholly due to instrumental defects. To assign a *limit of error* to this work it is only necessary to notice that the coefficients of terms of shorter periods than one revolution are all less than 1 percent of the whole effect, viz., less than about 0.7 millimeter. This represents, of course, not the probable error in a coefficient, but rather a limit of error; the actual probable error is less than this.

It is to be concluded from the experimental work described above that single crystals of copper show no variation of their diamagnetic susceptibility with the direction of the applied magnetic field greater than 1 percent.

The author wishes to express his sincerest appreciation to Dr. L. W. McKeehan for placing the facilities of the Sloane Physics Laboratory at his disposal, and for much helpful guidance and discussion during this work.

TENSION COEFFICIENT OF RESISTANCE OF METALS*

By Harry Rolnick
Sloane Physics Laboratory, Yale University

(Received June 23, 1930)

Abstract

A new method for measuring the change in resistance of a metal under tension has been developed and applied to fifteen metals. A direct current is sent through the wire under test while longitudinal vibrations set up in the wire cause the resistance and consequently the potential drop in the wire to fluctuate. These changes are amplified and measured. In this way it has been found that for bismuth, aluminium, manganin, and constantan the resistance decreases with tension while for all the other metals investigated the resistance increases with tension.

Introduction

THE change in electrical properties of metals under stress was first investigated by William Thomson, later Lord Kelvin, and described by him in a paper entitled "The Electrodynamical Qualities of Metals."[1] Due to the lack of sensitive apparatus, his experiments, which were conducted on copper and iron, gave untrustworthy results. Soon afterwards, H. Tomlinson,[2] at Lord Kelvin's suggestion, undertook to determine the exact change in resistance of wires caused by tension along their length. This remains the most extensive investigation on the subject. Other work has been done by W. E. Williams[3] on bismuth; by Donaldson and Wilson[4] on lead; and by N. F. Smith[5,6] on iron, steel, copper, and brass. The most complete study in recent years has been made by P. W. Bridgman[7,8,9] on many metals which he had at hand in the form of wires because of previous work on their pressure coefficients of resistance.

The method, a static one, used by all other investigators for studying these effects is to put a known load on the wires and then to measure the corresponding change in resistance. From this change is subtracted that produced by alteration in dimensions. The remainder is considered to be the change in resistance due to the stress.

The object of this research was the development of a dynamic method of

* Part of a dissertation presented for the Degree of Doctor of Philosophy in Yale University.

[1] W. Thomson, later Lord Kelvin. Phil. Trans. **146,** 649–672 (1856).
[2] H. Tomlinson, Phil. Trans. **174,** 1–172 (1883).
[3] W. E. Williams, Phil. Mag. [6] **13,** 635–643 (1909).
[4] J. A. Donaldson, and R. Wilson, Proc. Roy. Soc. Edinb. **27,** 16–20 (1907).
[5] N. F. Smith, Phys. Rev. **28,** 107–121 (1909).
[6] N. F. Smith, Phys. Rev. **28,** 429–437 (1909).
[7] P. W. Bridgman, Proc. Am. Acad. **57,** 39–66 (1922).
[8] P. W. Bridgman, Proc. Am. Acad. **59,** 117–137 (1923).
[9] P. W. Bridgman, Proc. Am. Acad. **60,** 423–444 (1925).

measuring the tension coefficient of resistance and its application to metals whose coefficient is not easily obtained by static measurements. In the method finally adopted, the tension applied is alternating, in order to eliminate spurious effects due to thermoelectric forces and other effects of local or variable heating. A direct current is sent through the wire. As a result of the variations in resistance there are corresponding variations in the potential drop across the wire, and these are impressed on the grid of the first tube of calibrated amplifier, by means of which they are magnified and measured. From these data and the value of the direct current through the wire the change in resistivity due to tension is calculated.

Apparatus and Procedure

The wire to be stretched, Fig. I, is fastened at one end to a brass cylinder which is placed in a holder that can be moved by a screw in the direction of the wire axis to control the tension. The other end is wrapped around a hook. A glass rod, welded to the hook, connects it to the moving arm of a moving

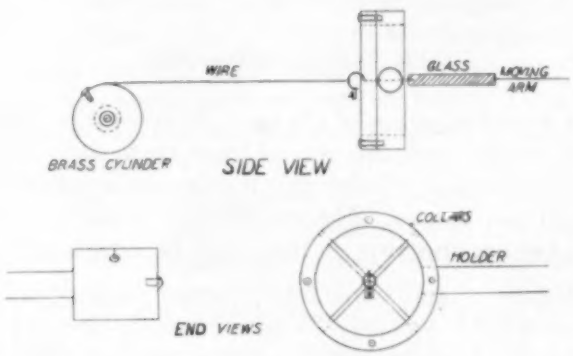

Fig. 1. Diagram of apparatus.

armature loud speaker unit. The hook is held in position by a cross-shaped piece of thin steel cut from an old telephone diaphragm. The ends of this cross are held fast between two brass collars. From them projects a rod which holds the collars securely. This arrangement keeps the motion of the hook axial.

The tension is applied by moving the brass cylinder back by means of the screw, thus stretching the wire. Care must be taken to avoid the production of standing transverse waves which will appear with amplitudes ranging from 1 mm to 5mm if the tension bears the appropriate relation to the length and density of the wire.

The glass rod is put in to insulate the wire from the loud speaker unit. Alternating current of 1025 cycles per second from a tube generator and amplifier is led into the loud speaker coil, and sets the wire into longitudinal vibration with a frequency equal to that of the alternating current. This frequency of current was chosen because it could be conveniently checked by a standard tuning fork making 1024 vibrations per second.

A battery, Fig. 2, sends a direct current through the wire. The change in resistance of the wire changes the potential drop across it, the alternating component is impressed on the grid of a vacuum tube of the amplifier. The choke coil, of 15 henrys inductance, makes the circuit impedance so high that the change in potential drop due to the current change is made negligible.

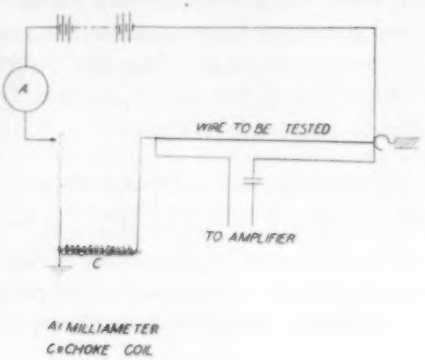

Fig. 2. Battery arrangement.

Fig. 3 is the wiring diagram of the six-tube resistance coupled amplifier. The amplifier is broken into two sets of three each, each part with its own batteries in a sheet tin box. Unless this is done the amplifier maintains continuous electrical oscillations. The connections to the first three tubes are arranged so that either one, two, or three may be used together with the last

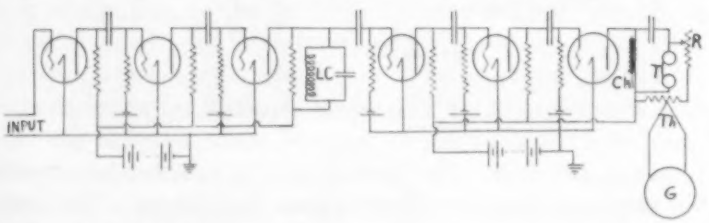

Fig. 3. Wiring diagram of the six tube resistance coupled amplifier.

three. It has been found difficult to get steady amplification without considerable noise with six tubes. Five tubes, with an amplification of about twenty-five thousand, gave very satisfactory performance and this number was used throughout the work. Between the third and fourth stages is fixed a circuit (LC) tuned to 1025 cycles. Its impedance to current of this frequency is five thousand ohms; to all other frequencies its impedance is considerably smaller. Thus it acts as a filter, being a low resistance shunt for all currents of frequencies other than 1025 cycles. Its use makes the amplifier very quiet. The negative side of the B battery and the metal shielding are grounded.

In the last stage is a power tube in the plate circuit of which is a hot-wire vacuum thermocouple (Western Electric No. 232) with an adjustable resist-

ance in series with it. The condenser (*C*) allows only alternating current to go through the thermocouple, which is used in connection with a galvanometer. The phones are used to detect any extraneous disturbance. The amplifier is first calibrated by sending a known e.m.f. into the imput circuit and noting the deflections of the galvanometer in the output circuit.

The amplitude of vibration is measured with an optical lever. The back of a small light mirror about five millimeters in diameter is fastened to a tightly drawn fine wire, and the tip of the mirror rests against a small lip (*A* in Fig. 1) projecting from the hook to which the moving end of the vibrating wire is attached. Light from a slit is condensed on the mirror and focussed on a scale. As the lip moves back and forth the mirror is tipped about the wire holding it. The reflected image of the slit is drawn out into a band, whose width is proportional to the amplitude of vibration of the hook and the end of the wire.

One end of the specimen to be measured is fastened to the hook (Fig. 1) and the other end to the brass cylinder. A slight tension is put on the wire. The mirror is moved into such a position that an image of the slit is thrown on the scale. The oscillator is started and the wire forced into longitudinal vibrations, care being taken to avoid transverse vibrations. The amplifier is then switched on and the galvanometer reading noted. Then a small direct current is sent through the wire and the galvanometer reading again noted. This is repeated for different values of the direct current, which never exceeds a tenth of an ampere. The purpose of the several measurements is to decrease the effect of the errors from irregularities in the operation of the amplifier and those due to outside disturbances. Meanwhile the width of the band of light on the scale is observed from time to time. Galvanometer readings are taken only for equal amplitudes of vibration of the end of the wire, as shown by the width of the band of light. Some wires give considerable trouble in that the amplitude of vibration must be carefully adjusted to avoid breaking the wire in case transverse vibrations are set up.

After enough readings are taken the oscillator is stopped and the length of the wire and distance of the mirror axis from the wire are measured. The resistance of the wire is found with a wheatstone bridge.

Materials Tested and Their Method of Preparation

All the wires were either 0.004″ or 0.005″ in diameter, and all were obtained C.P. from Baker and Co., except molybdenum, tungsten, manganese, constantan, and nichrome. Molybdenum was from the Fansteel Products Co., tungsten from the Lamp Works of the General Electric Co. at Nela Park, manganin (84 Cu 4 Ni 12 Mn), constantan (60 Cu 40 Ni) and nichrome (85 Ni 15 Cr) from the Driver-Harris Co.

Annealing was effected by passing a current through the wire, except in the cases of aluminium and copper. Silver, gold, palladium, and platinum were annealed in air for an hour at a temperature about 300° below their melting points. Aluminium and copper were maintained for two hours at a temperature of 400°C in a steam bath. Molybdenum, tungsten, manganin,

and constantan were annealed in an atmosphere of hydrogen for one hour; manganin and constantan at 700°C, molybdenum at 2000°C, tungsten at 2500°C.

Bismuth, lead, tin and nichrome were not annealed; the first three are self-annealing and nichrome has such a high resistance that a large enough current could not be obtained with the power supply available.

Tin and bismuth were the most difficult to measure both on account of their softness and because the change in potential drop would not remain constant. In the results for these two wires abnormally large errors may be found.

Measurements and Calculations

Length of wire, distance of scale from mirror, width of light band, resistance of wire, direct current through wire, and galvanometer deflections are the only measured quantities. The first three give the fractional change in length of the wire; the last two enter in the calculations of the change of resistance. From the galvanometer deflection the potential difference impressed on the input of the amplifier is obtained and this equals the product of the direct current by the change in resistance. The fractional change in resistivity is calculated from the following relation:

$$\Delta R/R = (1 + 2w - K)\frac{\Delta l}{l} + \frac{\Delta \rho}{\rho}.$$

where w = Poisson's ratio, K = a constant and l = length of wire.

The factor $(1+2w)\Delta l/l$ is the change in resistance due to alteration of dimensions of the wire In most cases the values of Poisson's ratio were taken from tables.[10] For some metals this ratio was computed from the compressibility (k) and Young's Modulus (E) for the material. The formula used in $w = 0.5 - Ek/6$. Table I indicates how close the calculated values of

Table I.

Metal	$E\times10^{-11}$	$k\times10^{11}$	$Ek/6$	w (calculated)	w (observed)
Silver	7.90**	1.02	0.134	0.366	0.38*
Aluminium	7.05**	1.38	.162	.338	.34*
Gold	8.0**	.603	.0805	.42	.42*
Cadmium	5.0	2.27	.203	.297	.30*
Copper	12.3	.756	.155	.345	.35*
Iron	21.3	.606	.215	.285	.28*
Nickel	20.2	.542	.182	.318	.31*
Lead	1.62	2.38	.064	.436	.45*
Palladium	11.3	.536	.101	.40	.40*
Platinum	16.8	.372	.104	.396	.39*
Tin	5.43	2.02	0.183	.317	.33*

* E. Grüneisen, Ann. d. Physik [4] **25**, 825–851 (1908).

** Kaye and Laby's Tables. E = Young's Modulus in c.g.s. units, k = compressibility in c.g.s. units, and w = Poisson's ratio.

the ratio are to observed values. All the values of the constants used were taken from the International Critical Tables unless otherwise noted. Young's

[10] E. Grüneisen, Ann. d. Physik [4] **22**, 801–851 (1907).

Moduli for molybdenum and nichrome were measured for this investigation with an apparatus constructed by Mr. L. R. Jackson of this laboratory.

The term $-K\Delta l/l$ is the change in resistance produced by a change in temperature of the wire as it is stretched and released. When a wire is suddenly stretched there will be a fall in temperature if the metal expands when heated and this temperature change is reversible.[11,12] The change in temperature is given by the formula:

$$\Delta T = -TaP/C_p d$$

The fractional change in resistance due to this change in temperature is

$$\Delta R/R = -K\Delta l/l$$

$$K = abTE/C_p d$$

In these formulae T=absolute temperature; a=thermal coefficient of expansion; P=applied tension; C_p=specific heat; d=density; b=temperature coefficient of resistance; and E=Young's Modulus.

Table II contains the values of w and K used, together with the computed values of $\Delta R/R$, $\Delta\rho/\rho$, and $\Delta\rho/\rho$ divided by $\Delta l/l$.

TABLE II.

Metal	w	K	$\frac{\Delta l}{l}\times 10^4$	$(1+2w-K)\frac{\Delta l}{l}\times 10^4$	$\frac{\Delta R}{R}\times 10^4$	$\frac{\Delta\rho}{\rho}\times 10^4$	$\frac{\Delta\rho}{\rho}\div\frac{\Delta l}{l}$
Silver	0.38	0.68	0.274	0.295	0.86	0.565	2.06
Aluminium	.34	.66	.80	.816	.274	−.542	−.68
Gold	.42	.563	.211	.27	.75	.48	2.27
Bismuth	.34	.40	.229	.294	−.50	−.794	−3.52
Copper	.35	.677	.629	.64	1.64	1.00	1.59
Molybdenum	.33	.402	.408	.514	.963	.449	1.10
Lead	.45	.424	.236	.349	.613	.264	1.12
Palladium	.40	.44	.327	.445	1.33	.885	2.70
Platinum	.39	.45	.395	.525	1.89	1.36	3.44
Tin	.33	.244	.216	.320	1.54	1.22	5.65
Tungsten	.32	.76	.827	.73	1.94	1.21	1.46
Zinc	.30	1.05	.172	.094	.638	.544	3.16
Manganin	.33	.00	.498	.83	.28	−.55	−1.10
Constantan	.33	.00	.517	.86	.735	−.125	−.246
Nichrome	.30	.02	.35	.55	.928	.378	1.08

The probable error in the resistance measurement, in the length of the wire, usually about sixty centimeters, in the distance of the mirror to the scale, and in the direct current is less than one-half of one percent in each case. The width of the light band, from one to four centimeters, was measured with a probable error of from one to three percent, being higher for smaller widths. The resultant error in the fractional change in length is about of the same magnitude. The probable error in measuring the alternating potential difference is dependent on the accuracy with which the amplifier has been calibrated and on the steadiness of the galvanometer deflections.

[11] W. V. Houston, Introduction to Mathematical Physics, p. 192.

[12] P. G. Nutting, Jour. Wash. Acad. of Sci. **19**, 109–115 (1929).

The calibration is accurate to one percent, and the precision of the galvanometer reading is within two percent except in the measurements on bismuth and tin. For these metals, the galvanometer deflections were so unsteady as to cause a probable error of about ten percent in the potential difference measured.

Into the calculations there enter the thermal expansion coefficient, the temperature coefficient of resistance, the specific heat, Young's modulus and the density, all in correction terms, while Poisson's ratio enters directly. The uncertainty in the values of these constants varies considerably from metal to metal. The constants entering indirectly contribute about two percent to the uncertainty while Poisson's ratio can not be relied on within five percent. Thus the final results have errors of about seven percent due to constants used in calculating. Improved values of these constants will permit correspondingly greater accuracy in the final results. The measured quantities contribute about three percent more so that the possible error of the results is about ten percent. In the case of bismuth and tin the possible error is about 20 percent.

TABLE III. *$\Delta\rho/\rho$ for a tension of 1 kg/cm² by different observers.*

Metal	Bridgman	Tomlinson	Rolnick
Aluminium	$+1.8\times10^{-6}$	-0.63×10^{-6}	-0.96×10^{-6}
Silver	+3.4	+2.07	+2.51
Gold	+3.87		+2.86
Bismuth	−36.5		−32.2
Copper	+1.33	+.88	+1.32
Lead		+9.75	+7.0
Palladium	+1.66		+2.44
Platinum	+1.56	+2.25	+2.08
Tin		+5.89	+10.6
Zinc		+2.75	+3.26
Manganin	−.76		−.91

For bismuth, W. E. Williams gives $\Delta R/R = -53.5\times10^{-6}$ while the writer obtains $\Delta R/R = -28.1\times10^{-6}$.

In Table III is a comparison of my results with those of other investigators. These results have all been reduced to fractional changes of resistivity with a tension of 1 kg/cm², using the values of Young's Modulus mentioned above. Considering the wide variation between the results of other workers, the present results tally fairly well with theirs.

The writer is deeply indebted to Professor L. W. McKeehan for his suggestion of the problem and for his advice and encouragement during its progress.

VIBRATIONS OF A NON-PLANAR MEMBRANE

By George R. Stibitz
Cornell University

(Received June 16, 1930)

Abstract

Equations of motion are deduced for a non-planar membrane in small oscillation about any position of equilibrium. Cylindrical and conical membranes are discussed briefly as special cases; with certain types of boundary conditions there is no solution of the problem when stiffness is entirely omitted, and this is particularly true of the cone because of a characteristic singular point in the differential equations.

1. Introduction

NUMEROUS investigators have published studies of the vibrations of the plane membrane, including besides the usual circular drumhead the square, triangular and other shaped drumheads of uniform surface density and also the loaded drum, in which the density of the membrane is not uniform. Two articles in recent years have treated the statics of non-planar membranes, and to these the present writer is much indebted. They are the articles of Max Lagally[1] and of Frank Löbell.[2]

In this paper we will consider the problem of a membrane with very large elastic constants, whose middle surface is analytic and whose mass is uniformly distributed over that surface. We obtain the equations of motion for a general surface of this type as a system of three linear partial second-order differential equations. As a special case, we consider a type of symmetric vibration of a surface of revolution and finally the vibrations of a cone. In each case the vibrations are considered to take place about a strained equilibrium position of the membrane.

Let the middle surface of the membrane be described by a variable vector, r, drawn from any fixed point as origin. We can write r as a function of two parameters. Since the surface is analytic, it can be shown[3] that the parameters, say u_1 and u_2, can be so chosen that the lines described by the vector r when u_1 is constant and when u_2 is constant, respectively, are the orthogonal "lines of principal curvature" of the surface.

Suppose that in such a surface tangential forces act. We define the stress component across any parametric curve u_1 (i.e. a curve along which u_2 is constant) as the vector force per unit length exerted by the "positive" part of the surface on the "negative" part across that curve. By "positive" part of the surface with respect to the curve $u_2=K$, we mean that part defined by the inequality $u_2>K$. The stress component across the u_1 curves we name σ_2, and that across the u_2 curves, σ_1.

[1] Max Lagally, Zeits. f. Angewandte Math. u. Mech. **4**, 377 (1924).
[2] Frank Löbell, Zeits. f. Angewandte Math. u. Mech. **7**, 463 (1927).
[3] Blaschke, Vorlesungen über Differentialgeometrie, p. 62.

Let t_1, t_2 be the unit tangents along the u_1, u_2 curves respectively. If we assume the membrane to be perfectly pliable, then the stresses will lie entirely in the plane of t_1, t_2. Their four scalar components in these directions we define by the vector equations,

$$\sigma_1 = \sigma_{11}t_1 + \sigma_{12}t_2, \quad \sigma_2 = \sigma_{21}t_1 + \sigma_{22}t_2. \tag{1.1}$$

2. The A, B and C Conditions of the Membrane

For convenience in manipulation we define three states or conditions of the membrane. The first of these, state A, is the totally unstrained state. We will also refer to the middle surface of the membrane in this state as the surface A.

Next, let the membrane be stretched in any manner by forces exerted across its boundaries, and let it come to rest. Each element of the surface will then be in equilibrium under the stress forces acting tangentially across its own boundary. Call this state, B.

Finally, let the membrane undergo a small displacement from its equilibrium position B to a third position C. This last will not in general be an equilibrium position, the stress forces exerting a force P per unit area. The elastic constants for the displacement BC may be slightly different from those for AB; call Young's modulus and Poisson's ratio for BC, E and κ respectively.

Let parametric lines u_1, u_2 as described in Sec. 1 be drawn on the surface B, these curves remaining fixed in space when the membrane moves to position C. Let v_1, v_2 be the parametric lines for the actual middle surface of the membrane, these lines moving with the membrane. We will so chose v_1, v_2 that when the membrane is in position B, v_1, v_2 coincide with u_1, u_2.

Since we have assumed the elastic constants of the membrane to be large, the forces arising from displacements of the particles near a point p fixed in the middle surface can be assumed to be only those due to elastic strain of the element as long as the displacements lie in the tangent plane at p. Hence we can neglect the effect of rotation of the element when the axis of this rotation is perpendicular to the surface at p, for this type of displacement produces no strain in the element and the forces due to changes in the directions of the initial stresses will be negligible in comparison with forces due to the strains. On the other hand, displacements perpendicular to the surface do not produce strains in the element to the first order, and the only forces called into existence by such a displacement are those due to the changed directions of the initial stresses. Consequently we cannot neglect the component of rotation of the element which lies in the tangent plane.

3. The Added Stresses

Suppose q is a point on the middle surface near to p, both points moving with the membrane. Let q' and p' be the positions occupied by q and p when the membrane is in state B. Let t be the vector obtained by dividing the vector pq by the constant scalar $p'q'$ and then letting q approach p.

Then

$$t = \frac{\partial r}{\partial s}, \tag{3.1}$$

where s represents arc length in the direction pq. In position C this tangent vector is different in magnitude and direction from the corresponding vector in position B; let the difference vector be δt. Then evidently, if $\bar{r}$ is the vector of the displacement BC, we have

$$\delta t = \frac{\partial \bar{r}}{\partial s}, \quad \delta t_1 = \frac{\partial \bar{r}}{\partial s_1}, \qquad \delta t_2 = \frac{\partial \bar{r}}{\partial s_2}, \tag{3.2}$$

in which the subscripts refer to cases in which pq lies along one of the coordinate lines.

Now in general the element about p undergoes a translation, a pure strain, and a rotation; let g denote the vector rotation and write with the usual notation for the components of strain:

$$\delta t_1 = g \times t_1 + \delta\epsilon_{11} t_1 + \delta\epsilon_{12} t_2, \tag{3.3}$$

$$\delta t_2 = g \times t_2 + \delta\epsilon_{12} t_1 + \delta\epsilon_{22} t_2. \tag{3.4}$$

Taking the scalar products $t_1 \cdot$, $t_2 \cdot$, with 3.3 and 3.4 and combining, we get, using 3.2,

$$\frac{\partial \bar{r}}{\partial s_1} \cdot t_1 = \delta\epsilon_{11}; \qquad \frac{\partial \bar{r}}{\partial s_2} \cdot t_2 = \delta\epsilon_{22}; \tag{3.5}$$

$$\frac{\partial \bar{r}}{\partial s_1} \cdot t_2 + \frac{\partial \bar{r}}{\partial s_2} \cdot t_1 = g \times t_1 \cdot t_2 + g \times t_2 \cdot t_1 + \delta\epsilon_{12} + \delta\epsilon_{21}. \tag{3.6}$$

Noting that $g \times t_1 \cdot t_2 = -g \times t_2 \cdot t_1$ and $\delta\epsilon_{12} = \delta\epsilon_{21}$, we have

$$2\delta\epsilon_{12} = \frac{\partial \bar{r}}{\partial s_1} \cdot t_2 + \frac{\partial \bar{r}}{\partial s_2} \cdot t_1. \tag{3.7}$$

Following the method of Lagally[4] and Love[5] except that we deal with two dimensions instead of three, we obtain the following formulas for the stresses in terms of the strains and the elastic constants:

$$\delta\sigma_{11} = 2\mu\delta\epsilon_{11} + \lambda(\delta\epsilon_{11} + \delta\epsilon_{22}), \tag{3.8}$$

$$\delta\sigma_{12} = \delta\sigma_{21} = 2\mu\delta\epsilon_{12}, \tag{3.9}$$

$$\delta\sigma_{22} = 2\mu\delta\epsilon_{22} + \lambda(\delta\epsilon_{11} + \delta\epsilon_{22}), \tag{3.10}$$

where

$$\lambda = \frac{\kappa E\tau}{1 - \kappa^2}, \qquad \mu = \frac{E\tau}{2(1 + \kappa)}. \tag{3.11}$$

τ being the thickness of the membrane.

[4] Lagalley, Vektorrechnung, p. 260.
[5] Love, Elasticity, p. 98–101.

4. Forces Act ng on the Membrane in Position *C*.

It will be recalled that for the purpose of calculating the changes in stress due to rotation of the tangent plane we need consider only that component of the tangent variation which is normal to the surface; let this component of δt_1 and δt_2 be

$$\delta' t_1 = t_3\left(\frac{\partial \bar{r}}{\partial s_1}\cdot t_3\right), \quad \delta' t_2 = t_3\left(\frac{\partial \bar{r}}{\partial s_2}\cdot t_3\right). \tag{4.1, 4.2}$$

Then the total vector stresses in position *C* are:

across v_2

$$\bar{\sigma}_1 = (\sigma_{11} + \delta\sigma_{11})(t_1 + \delta' t_1) + (\sigma_{12} + \delta\sigma_{12})(t_2 + \delta' t_2), \tag{4.3}$$

across v_1

$$\bar{\sigma}_2 = (\sigma_{21} + \delta\sigma_{21})(t_1 + \delta' t_1) + (\sigma_{22} + \delta\sigma_{22})(t_2 + \delta' t_2), \tag{4.4}$$

or, dropping second order terms, by 1.1,

$$\bar{\sigma}_1 = \sigma_1 + \sigma_{11}\delta' t_1 + t_1\delta\sigma_{11} + \sigma_{12}\delta' t_2 + t_2\delta\sigma_{12}, \tag{4.5}$$

$$\bar{\sigma}_2 = \sigma_2 + \sigma_{21}\delta' t_1 + t_1\delta\sigma_{21} + \sigma_{22}\delta' t_2 + t_2\delta\sigma_{22}. \tag{4.6}$$

The conditions for equilibrium between the stress forces and the surface forces can be obtained by direct consideration in the usual manner of an element bounded by parameter lines, or by the method of Löbell,[2]. The conditions are given by the vector equation,

$$\left(G_1 - \frac{\partial}{\partial s_2}\right)\bar{\sigma}_2 + \left(G_2 - \frac{\partial}{\partial s_1}\right)\bar{\sigma}_1 + P = 0, \tag{5.1}$$

where the *G*'s are the geodesic curvatures as defined below (6.2) and $-P$ is the external surface force per unit area.
Let

$$\delta\sigma_1 = \bar{\sigma}_1 - \sigma, \quad \delta\sigma_2 = \bar{\sigma}_2 - \sigma_2. \tag{5.2}$$

Then, in position *C*,

$$-P = \left(G_1 - \frac{\partial}{\partial s_2}\right)(\sigma_2 + \delta\sigma_2) + \left(G_2 - \frac{\partial}{\partial s_1}\right)(\sigma_1 + \delta\sigma_1). \tag{5.3}$$

But in position *B*, *P* is zero, i.e.

$$\left(G_1 - \frac{\partial}{\partial s_2}\right)\sigma_2 + \left(G_2 - \frac{\partial}{\partial s_1}\right)\sigma_1 = 0. \tag{5.4}$$

Hence in position *C*

$$-P = \left(G_1 - \frac{\partial}{\partial s_2}\right)\delta\sigma_2 + \left(G_2 - \frac{\partial}{\partial s_1}\right)\delta\sigma_1. \tag{5.5}$$

5. Scalar Components of $\delta\sigma_i$ and of P

Assume as basic vectors the unit vectors t_1 and t_2 introduced in Sec. 1, and define $t_3 = t_1 \times t_2$. Define the components of $\bar{r}$, the vector of displacement BC, by

$$\bar{r} = r_1 t_1 + r_2 t_2 + r_3 t_3, \tag{6.1}$$

and the normal and geodesic curvatures of the parametric lines by

$$\begin{aligned} N_1 &= -\frac{\partial t_1}{\partial s_1} \cdot t_3 = \frac{\partial t_3}{\partial s_1} \cdot t_1, \qquad N_2 = -\frac{\partial t_2}{\partial s_2} \cdot t_3 = \frac{\partial t_3}{\partial s_2} \cdot t_2, \\ G_1 &= \frac{\partial t_1}{\partial s_1} \cdot t_2 = -\frac{\partial t_2}{\partial s_1} \cdot t_1, \qquad G_2 = \frac{\partial t_2}{\partial s_2} \cdot t_1 = -\frac{\partial t_1}{\partial s_2} \cdot t_2. \end{aligned} \tag{6.2}$$

The geodesic torsion, $(\delta t_1/\delta s_2) \cdot t_3$, is zero for lines of principal curvature, as are also the scalar product of a unit vector and its derivative. Substituting from 6.1 and 6.2 in 4.1 and 4.2, we see that

$$\delta' t_1 = \left(\frac{\partial r_3}{\partial s_1} - r_1 N_1\right) t_3, \qquad \delta' t_2 = \left(\frac{\partial r_3}{\partial s_2} - r_2 N_2\right) t_3. \tag{6.3}$$

Similarly from 3.8–3.11, 3.5, 3.6, 6.1, 6.2, we have the result:

$$\delta\sigma_{11} = (2\mu + \lambda)\left(\frac{\partial r_1}{\partial s_1} - r_2 G_1 + r_3 N_1\right) + \lambda\left(\frac{\partial r_2}{\partial s_2} - r_2 G_2 + r_3 N_2\right), \tag{6.4}$$

$$\delta\sigma_{22} = (2\mu + \lambda)\left(\frac{\partial r_2}{\partial s_2} - r_2 G_2 + r_3 N_2\right) + \lambda\left(\frac{\partial r_1}{\partial s_1} - r_2 G_1 + r_3 N_1\right), \tag{6.5}$$

$$\delta\sigma_{12} = \mu\left(\frac{\partial r_1}{\partial s_2} + \frac{\partial r_2}{\partial s_1} + r_2 G_1 + r_2 G_2\right). \tag{6.6}$$

Comparing these results with 4.5, 4.6 and 5.2 we obtain finally:

$$\begin{aligned} \delta\sigma_1 = {} & \sigma_{11}\left(\frac{\partial r_3}{\partial s_1} - r_1 N_1\right) t_3 + \left[(2\mu + \lambda)\left(\frac{\partial r_1}{\partial s_1} - r_2 G_1 + r_3 N_1\right)\right. \\ & \left. + \lambda\left(\frac{\partial r_2}{\partial s_4} - r_2 G_2 + r_3 N_2\right)\right] t_1 + \sigma_{12}\left(\frac{\partial r_3}{\partial s_2} - r_2 N_2\right) t_3 \\ & + \mu\left(\frac{\partial r_1}{\partial s_2} + \frac{\partial r_2}{\partial s_1} + r_2 G_1 + r_2 G_2\right) t_2. \end{aligned} \tag{6.7}$$

Interchange of the subscripts 1 and 2 in 6.7 gives us the equation for $\delta\sigma_2$.

Substituting these results in the equation for P, (5.5), and carrying through the necessary algebra, we have P, the force per unit area due to the stresses, expressed in terms of components along the vectors t_i. Define the scalar components of P by

$$P = P_1 t_1 + P_2 t_2 + P_3 t_3. \tag{6.8}$$

Resolving P into its components, we have ultimately:

$$
\begin{aligned}
P_1 = &- r_1\left[2\mu G_1^2 + \lambda\frac{\partial G_2}{\partial s_1} + \sigma_{11}N_1^2 + 2\mu G_2^2 - \mu\frac{\partial G_1}{\partial s_2}\right] \\
&- r_2\left[(2\mu + \lambda)\frac{\partial G_1}{\partial s_1} + \sigma_{12}N_1N_2 - \mu\frac{\partial G_2}{\partial s_2}\right] \\
&+ r_3\left[(2\mu + \lambda)\frac{\partial N_1}{\partial s_1} + \lambda\frac{\partial N_2}{\partial s_1} + 2\mu G_2(N_2 - N_1)\right] \\
&- G_2(2\mu + \lambda)\frac{\partial r_1}{\partial s_1} - \mu G_1\frac{\partial r_1}{\partial s_2} - (4\mu + \lambda)\frac{\partial r_2}{\partial s_1} + 3\mu G_2\frac{\partial r_2}{\partial s_2} \\
&+ [\lambda N_2 + (2\mu + \lambda)N_1]\frac{\partial r_3}{\partial s_1} + N_1\sigma_{12}\frac{\partial r_3}{\partial s_2} + N_1\sigma_{11}\frac{\partial r_3}{\partial s_1} \\
&+ (2\mu + \lambda)\frac{\partial^2 r_1}{\partial s_1^2} + \mu\frac{\partial^2 r_1}{\partial s_2^2} + \mu\frac{\partial^2 r_2}{\partial s_2\partial s_1} + \lambda\frac{\partial^2 r_2}{\partial s_1\partial s_2},
\end{aligned}
\tag{6.9}
$$

from which P_2 is found by interchange of subscripts 1 and 2;

$$
\begin{aligned}
P_3 = &\; r_1\left[N_1G_1\sigma_{12} + N_1G_2(\lambda + \sigma_{11}) + N_2G_2(2\mu + \lambda) - \sigma_{11}\frac{\partial N_1}{\partial s_1} - \sigma_{12}\frac{\partial N_1}{\partial s_2}\right. \\
&\left. - N_1\left(\frac{\partial\sigma_{11}}{\partial s_1} + \frac{\partial\sigma_{12}}{\partial s_2}\right)\right] + r_2\left[N_2G_2\sigma_{12} + N_2G_1(\lambda + \sigma_{22}) + N_1G_1(2\mu + \lambda)\right. \\
&\left. - \sigma_{22}\frac{\partial N_2}{\partial s_2} - \sigma_{12}\frac{\partial N_2}{\partial s_1} - N_2\left(\frac{\partial\sigma_{22}}{\partial s_2} + \frac{\partial\sigma_{12}}{\partial s_1}\right)\right] - r_3[(2\mu + \lambda)(N_1^2 + N_2^2) \\
&+ 2\lambda N_1N_2] - \frac{\partial r_1}{\partial s_1}[N_1(2\mu + \lambda + \sigma_{11}) + N_2\lambda] - N_1\sigma_{12}\frac{\partial r_1}{\partial s_2} \\
&- N_2\sigma_{12}\frac{\partial r_2}{\partial s_1} - \frac{\partial r_2}{\partial s_2}[N_1\lambda + N_2(2\mu + \lambda + \sigma_{22})] + \frac{\partial r_3}{\partial s_1}\left[\frac{\partial\sigma_{11}}{\partial s_1} + \frac{\partial\sigma_{12}}{\partial s_2}\right. \\
&\left. - G_1\sigma_{12} - G_2\sigma_{11}\right] + \frac{\partial r_3}{\partial s_2}\left[\frac{\partial\sigma_{22}}{\partial s_2} + \frac{\partial\sigma_{12}}{\partial s_1} - G_2\sigma_{12} - G_1\sigma_{22}\right] \\
&+ \sigma_{11}\frac{\partial^2 r_3}{\partial s_1^2} + \sigma_{12}\left(\frac{\partial^2 r_3}{\partial s_1\partial s_2} + \frac{\partial^2 r_3}{\partial s_2\partial s_1}\right) + \sigma_{22}\frac{\partial^2 r_3}{\partial s_2^2}.
\end{aligned}
$$

6. Equations of Motion

The equations we have deduced are valid for any small displacement $\bar{r}$. If $\bar{r}$ is a function of time, then P is also a function of time. We may suppose that at each instant each element of the membrane is vibrating under the influence of the tangential stress-forces P and the resistive forces due to the radiation of energy and to internal friction. Then the sum of the real forces acting on the element must be equal to the effective forces. Suppose

the resistive forces to be proportional to the velocity, $\dot{\bar{r}} = \delta\bar{r}/\delta t$. We can then write,

$$P - R\dot{\bar{r}} - m\ddot{\bar{r}} = 0, \quad R = \text{const.} > 0. \tag{7.1}$$

The three scalar equations implied by 7.1 together with the value of P obtained from 6.9 and 6.10 furnish us with the required system of partial differential equations of motion of a general surface.

Let us seek normal vibrations of the form

$$\bar{r} = \rho e^{ipt}. \tag{7.2}$$

Substituting in 7.1,

$$P^* - Rip\rho + mp^2\rho = 0, \tag{7.3}$$

where P^* is the function obtained by replacing each component of $\bar{r}$ in P by the corresponding component of ρ. Equation 7.3 is then the equation for the amplitudes of the normal modes of vibration of the general surface.

7. Applications to Surfaces of Revolution

For the surface of revolution we choose as coordinates, (1) distance measured from the origin along a generator, $u_1 = s_1$, (2) the angle of revolution from a fixed plane, u_2. If we consider only vibrations in which r_2 is zero, and in which r_1 and r_2 are functions of u_1 alone, then the amplitude equations become:

$$\begin{aligned}
&-\rho_1\left[\lambda\frac{\partial G_2}{\partial u_1} + \sigma_{11}N_1^2 + 2\mu G_2^2 + Rip - mp^2\right] \\
&+\rho_3\left[(2\mu+\lambda)\frac{\partial N_1}{\partial u_1} + \frac{\partial N_2}{\partial u_1} + 2\mu(N_2 - N_1)G_2\right] \\
&-\frac{\partial\rho_1}{\partial u_1}G_2(2\mu+\lambda) + \frac{\partial\rho_3}{\partial u_1}[\lambda N_2 + (2\mu+\lambda)N_1] + \sigma_{11}N_1\frac{\partial\rho_3}{\partial u_1} + \frac{\partial^2\rho_1}{\partial u_1^2}(2\mu+\lambda) = 0,
\end{aligned} \tag{8.1}$$

$$\begin{aligned}
&\rho_1\left[N_1G_2(\lambda+\sigma_{11}) + N_2G_2(2\mu+\lambda) - \frac{\partial N_1}{\partial u_1}\sigma_{11} - N_1\frac{\partial\sigma_{11}}{\partial u_1}\right] \\
&-\rho_3[(2\mu+\lambda)(N_1^2+N_2^2) + 2\mu N_1N_2 + Rip - mp^2] \\
&-\frac{\partial\rho_1}{\partial u_1}[N_1(2\mu+\lambda+\sigma_{11}) + N_2\lambda] + \frac{\partial\rho_3}{\partial u_1}\left[\frac{\partial\sigma_{11}}{\partial u_1} - G_2\sigma_{11}\right] + \frac{\partial^2\rho_3}{\partial u_1^2}\sigma_{11} = 0,
\end{aligned} \tag{8.2}$$

and the curvatures are,

$$N_1 = -\frac{y''}{(1-y'^2)^{1/2}}, \quad N_2 = \frac{(1-y'^2)^{1/2}}{y}; \quad G_1 = 0, \quad G_2 = -\frac{y'}{y}; \tag{8.3}$$

where y is the ordinate of the generating curve, expressed as a function of u_1, and the primes mean the ordinary derivative with respect to u_1.

The equations for the cone are still simpler, for $y = u_1 \sin\alpha$, 2α being the

angle of the cone, and one easily sees that for equilibrium $\sigma_{11} = \text{const.}/u_1 = c/u_1$, so that the equations become, if $R=0$:

$$\frac{\partial^2 \rho_1}{\partial u_1^2} + \frac{1}{u_1}\frac{\partial \rho_1}{\partial u_1} + \frac{\kappa a}{u_1}\frac{\partial \rho_3}{\partial u_1} - \frac{a}{u_1^2}\rho_3 + \left(q^2 - \frac{1}{u_1^2}\right)\rho_1 = 0, \qquad 8.4$$

$$\frac{c}{(2\mu+\lambda)u_1}\frac{\partial^2 \rho_3}{\partial u_1^2} - \frac{\kappa a}{u_1}\frac{\partial \rho_1}{\partial u_1} + \left(q^2 - \frac{a^2}{u_1^2}\right)\rho_3 - \frac{a}{u_1^2}\rho_1 = 0, \qquad 8.5$$

where $a = \cot\alpha$, $q^2 = mp^2/(2\mu+2)$, m mass per unit area of the membrane. Let us introduce the new variable z for qu; then, using primes here to denote differentiation with respect to z, we have,

$$\rho_1'' + \frac{1}{z}\rho_1' + \frac{\kappa a}{z}\rho_3' + \left(1 - \frac{1}{z^2}\right)\rho_1 - \frac{a}{z^2}\rho_3 = 0, \qquad 8.4b$$

$$\rho_3'' - \frac{\lambda a}{cq}\rho_1' - \frac{2\mu+\lambda}{cq}\frac{a}{z}\rho_1 + \frac{2\mu+\lambda}{cq}\left(z - \frac{a^2}{z}\right)\rho_3 = 0. \qquad 8.5b$$

If we suppose the initial stress to be different from zero everywhere in the range we are considering, then it is possible, by taking each of the first derivatives as a new dependent variable, to form a system of four simultaneous first-order differential equations, each of which has on the left side a different first derivative and on the right only an algebraic expression in the four unknows; the right hand sides of these equations are all homogeneous and the coefficients of the unknowns are bounded and continuous for u greater than zero. Under these conditions it can be shown that four linearly independent continuous solutions exist throughout the range for which z is greater than zero. As is usual in vibration problems, there exists a discrete set of values of z, and so of p, for which the boundary conditions can be satisfied. In any given numerical case these can be found by numerical integration.

If, however, the initial stress is zero, i.e. $c=0$, then ρ_3'' disappears from 8.5*b* and it is not possible to throw the equations into the form specified above. If we then eliminate ρ_3 from 8.4*b* and 8.5*b* we obtain for ρ_1 a differential equation of the second order only, so that for ρ_1 we have only two index solutions and ρ_3 is given by 8.5*b* in terms of these. There are thus, in general, not enough independent solutions to satisfy the boundary conditions. Furthermore, the coefficients in the equation so obtained for ρ_1, which is rather complicated and will not be written down here, has two pairs of singular points, one at $z^2 = a^2$, and the other at $z^2 = a^2(1-\kappa^2)$. It is necessary to examine the solution for ρ_1 at these points by means of a series; we omit the rather tedious details and outline the result. In the region about $z=a$ we find that the indicial equation has the two roots 0 and 2. These differ by an integer, so that we can be certain of only one analytic solution through the point, but we find by actual calculation of the first three terms of the series that there are in fact two independent solutions, since if we use the zero root the second power of z has an arbitrary coefficient. Hence $z=a$ is

not an irregular singular point. Making the same kind of an examination of the point $z=a(1-\kappa^2)^{\frac{1}{2}}$, however, we find the roots of the indicial equation to be 0 and 0. We can apply the usual method for finding the second solution[6] and find for it

$$\bar{\rho}_1 = \rho_1 \int \frac{(z^2 - a^2)}{(z^2 - a^2 + a^2\kappa^2)} \frac{dz}{z\rho_1^2}. \qquad 8.6$$

This solution obviously has a pole of the first order at the point under consideration. Hence there is one and only one solution that is continuous throughout the range, $u_1 > 0$. Furthermore, although ρ_1 is continuous through the point $z=a$, yet ρ_3 is discontinuous there, for upon solving for ρ_3 in 8.5 we have

$$\rho_3 = a\frac{\rho_1 + \kappa z\rho_1'}{z^2 - a^2}, \qquad 8.7$$

from which it is evident that ρ_3 has a pole of first order at this point.

Although it was thus impossible to obtain an actual solution from the equations for the case of a cone without initial stress, it seemed desirable to obtain a rough idea of what the vibrations may be like. Accordingly, the series for ρ_1 was evaluated near $z=a(1-\kappa^2)^{\frac{1}{2}}$ for the case of a paper cone with a vertical angle of 120 degrees ($a=0.58$) and the solution was then carried to $z=7$ by numerical integration. The shape of the solution thus found suggests comparison with a sine curve. For very great distances out along the cone, 8.4*b* reduces to, $\rho_1'' + \rho_1 = 0$, so that ρ_1 approaches sin z while $\rho_3 \to 0$, which is simply the solution for a plane membrane of the same material. With this function as our norm, we find that the numerical solution, after vanishing at $z=0.78$, showed a first node-to-loop distance of about 1.0 times the quarter wave-length for the plane longitudinal vibrations of the same frequency; the next succeeding node-to-loop distances were very roughly 1.2, 1.0 and 1.1 times the normal quarter-wave length. The second loop had an amplitude about two-thirds that of the first. Comparison might also be made with Bessel's function, for the equation differs markedly from

$$\rho_1'' + \frac{1}{z}\rho_1' + \rho_1 = 0$$

only within the first half wave or so and approximates to it very closely indeed beyond the first wave-length. The simplest solution of this equation $J_0(z)$ or Bessel's function of order zero, is very similar to the curve found here; the first two loops have an amplitude ratio of 3/4 as against 2/3 for the curve found for ρ_1 but this difference is in part due to their being displaced half a loop outward.

The singular point, $z=a(1-\kappa^2\alpha)^{\frac{1}{2}}$ occurs for ordinary materials where the distance from the axis along a line drawn perpendicular to the surface of the cone is about a seventh of a wave-length.

[6] Ince, Ordinary Differential Equations, p. 22.

Because of the complexity of the equations of the cone it is difficult to examine the effect of reducing the basic stress. A case which is simple enough to handle mathematically, and which may suggest what happens to the vibrating cone under similar conditions, is the circular cylinder. For this membrane the equations are:

$$\rho_1'' + h\kappa\rho_3' + q^2\rho_1 = 0, \quad k\rho_3'' - h\kappa\rho_1' + (q^2 - h^2)\rho_3 = 0,$$

where k is the tension divided by $2\mu+\lambda$ and $1/h$ is the radius of the cylinder. Since all the coefficients are constants, we can assume a solution of the form,

$$\rho_1 = e^{nu_1}, \ \rho_3 = \zeta e^{nu_1}.$$

We find that

$$\zeta = -\frac{n^2 + q^2}{h\kappa n}$$

and we obtain for n two pairs of solutions, of which one is independent of k to the first order whereas the other becomes infinite as k approaches zero: $n = q\{(q^2-h^2)/[(1-n^2)h^2-q^2]\}^{\frac{1}{2}}$ or $\{[(1-\eta^2)h^2-q^2]/k\}^{\frac{1}{2}}$. As an illustration of the problem with boundary conditions, let the membrane be rigidly fixed at $u=0$ and $u=1$. We now find a variety of different modes of vibration, in fact, the spectrum of characteristic frequencies consists of three different ranges. There is an infinity of modes with frequencies such that $q^2 < h^2(1-\kappa^2)$, which we may call the low-frequency range; and also an infinity of frequencies given by $q^2 > h^2$, called the high-frequency range; solutions corresponding to intermediate frequencies also exist, but whether they could be made to satisfy these boundary conditions was not definitely determined. The low-frequency modes with positive tension and the high-frequency modes with negative tension are found to be of the form, $n = \pm n_1 i$ or $\pm n_2$ and

$$\rho_1 = C\left[\sin(n_1u_1 + \gamma) + \frac{n_1\kappa^2h^2}{n_2(q^2 - h^2)}(e^{-n_2u_1} \pm e^{-n_2(1-u_1)})\right],$$

$$\rho_3 = -\frac{n_1\kappa h}{q^2 - h^2}C[\cos(n_1u_1 + \gamma) - e^{-n_2u_1} \pm e^{-n_2(1-u_1)}].$$

As the basic stresses approach zero and $n_2 \to \infty$, we note that ρ_3 remains finite relative to ρ_1; the effect of the stress as seen in the exponential terms is merely to reduce ρ_3 rapidly to zero at the ends. That is, with vanishing stress the oscillations take on the form obtained from the differential equation for zero stress, while the boundary conditions for ρ_3 are satisfied by means of an added sharp kink at each end.

On the other hand, the high-frequency modes under tension, and the low-frequency modes under compression are of the form, with $n = \pm n_1 i$ or $\pm n_2 i$

$$\rho_1 = C_1 \sin(n_1u_1 + \gamma_1) + C_2 \sin(n_2u_1 + \gamma_2),$$

$$\rho_3 = b_1C_1 \cos(n_1u_1 + \gamma_1) + b_2C_2 \cos(n_2u_1 + \gamma_2).$$

The second pair of terms in this case represent a short-wave "crinkle" superposed upon the main wave-form represented by the first terms. In this case, as the basic stress vanishes, the wave-length of the crinkle approaches zero, but it appears that its amplitude does not vanish relative to the main wave.

The question obviously presents itself as to how the physical cylindrical membrane with fixed ends and without stress actually vibrates. We may suspect that the slight stiffness which such a membrane must actually possess takes the place of the small basic stress used above and that the modes actually found would have either a superposed crinkle throughout the length of the cylinder or a sharp kink at the ends, similar to what we have found by our analysis.

It seems possible that the difficulties which were encountered above in the case of the cone are in practice surmounted in a similar manner.

The writer wishes to acknowledge the assistance given by Professor E. H. Kennard during the preparation of this paper, especially in the latter part of the article, that dealing with the cylindrical membrane.

CAPILLARY RETENTION OF LIQUIDS IN ASSEMBLAGES OF HOMOGENEOUS SPHERES

By W. O. Smith, Paul D. Foote and P. F. Busang
Gulf Research Laboratory, Pittsburgh, Pa.

(Received June 16, 1930)

Abstract

The pore space in an assemblage of uniform spheres was initially filled with liquid. After very slow drainage the amount of liquid retained by the spheres was experimentally measured. The liquid is retained in the form of rings at the contacts of adjacent spheres. The radii of curvature of the ring surfaces are computed in terms of surface tension, grain radius and pressure drop across the liquid-vapor interface, permitting calculation of the volume retained per sphere contact. The number of contacts per unit volume of spheres is obtained from porosity measurements using the theory developed earlier. Computed and observed data on total volume of retained liquid are in agreement.

IF THE pore spaces in an assemblage of spheres be completely filled by a liquid which is then allowed to drain, a portion of the liquid is retained. The retention occurs during the passage of the liquid-gas interface through the grain assemblage. It is current opinion, as expressed in the semi-technical literature, that such liquid remains in the form of a fairly uniform layer which envelops the separate grains. In order to account for the observed retention, the thickness of the layer would have to be several thousand molecular diameters. Molecular forces, however, decrease extremely rapidly with distance, and unless chemical reactions, such as those involving gel formation, take place, layers exceeding three molecular diameters are improbable. Much of the work on retention has been done with comparatively fine sands and the actual mechanism of the phenomenon has escaped notice. Under the microscope, however, one may readily observe that a small ring of liquid is retained at the point of contact of two spheres. This type of retention is easily demonstrated by dipping two small balls or shot in a liquid and observing the retained liquid when the spheres, in contact, are withdrawn. It also follows from thermodynamical considerations that the major retention occurs in this manner. Equilibrium requires a minimum of free energy, and when the spheres are sufficiently small that gravitational effects are negligible, a given amount of retained fluid must be so distributed that the surface energy is a minimum. This occurs when the liquid is collected about the points of contact of the spheres.

The ring volume can be calculated approximately. Consider a capillary ring of liquid as shown in Fig. 1 with the two principal radii of curvature y and R taken as positive numbers. Complete wetting or zero contact angle with the spheres is assumed. Let Δp be the difference in pressure just outside and inside the liquid surface, and let σ be the surface tension. Then

$$\Delta p = \sigma\left(\frac{1}{R} - \frac{1}{y}\right) \tag{1}$$

From geometry it follows, if r is the radius of the spheres, that

$$\frac{1}{R} = \frac{2(r - y)}{y^2} \tag{2}$$

and accordingly,

$$y = \frac{-3 + (9 + 8r\Delta p/\sigma)^{1/2}}{2\Delta p/\sigma}. \tag{3}$$

Putting $y/r = k$ and $R/r = \alpha$, the volume v of the ring of liquid is readily found to be

$$v = 2\pi r^3 \frac{\alpha}{1+\alpha} f(k, \alpha) \tag{4}$$

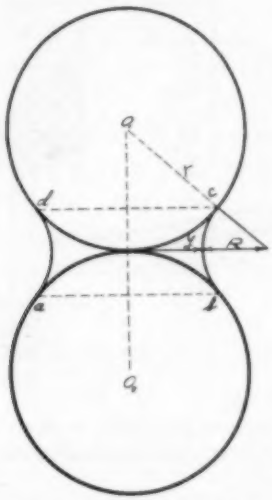

Fig. 1. Capillary ring of liquid between two spheres.

where

$$f(k, \alpha) = (k + \alpha)^2 - \alpha(k + \alpha)\left\{1 - \frac{1}{(1+\alpha)^2}\right\}^{1/2} - \alpha(k + \alpha)(1 + \alpha)\sin^{-1}\frac{1}{1+\alpha} + \alpha^2 - \frac{\alpha}{1+\alpha}.$$

This gives the volume of a single ring formed at a contact of two spheres in terms of parameters involving the quantity Δp which will be given consideration later.

In an earlier paper[1] the writers showed that in the natural piling of uniform spheres to a porosity P, the average number n of contacts per sphere is given by the approximate relation

[1] Smith, Foote and Busang, Phys. Rev. **34**, 1271–1274 (1929).

$$n = 6\frac{1 + 1.828x}{1 + 0.414x} \tag{5}$$

where

$$x = (0.476 - P)/0.217$$

The number N of spheres per unit volume is

$$N = \frac{1 - P}{4\pi r^{3/3}}. \tag{6}$$

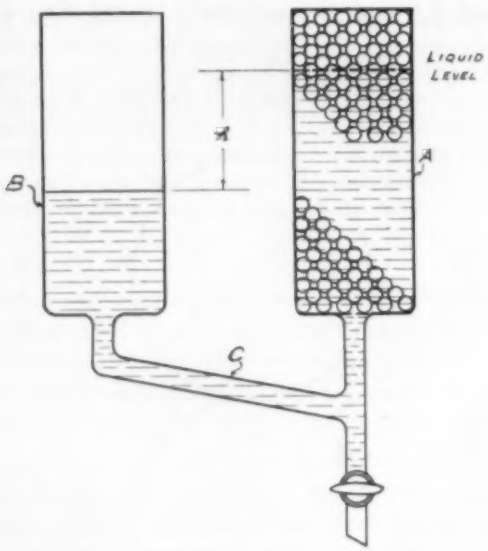

Fig. 2. Schematic diagram of drainage experiments in which the meniscus surface is above the free surface by the distance h equal to the capillary rise.

Since in the complete assemblage, two spheres determine a single contact, the number of contacts per unit volume is $Nn/2$ and the volume V of liquid retained per unit volume of packed space is

$$V = Nnv/2. \tag{7}$$

The value of Δp depends upon the manner in which drainage occurs. In general the flow of fluid through any single pore composed of three adjacent grains is along the axis normal to the plane of the grain centers, as is the case with a meniscus falling in a simple cylindrical tube. The interface always drops in a direction parallel to the axis of the tube provided that it is not too large. Let us consider a single contact and the pores on either side. As the complex meniscus of the whole sand body falls, the portion of it in this restricted region drops through the adjacent pore spaces wrapping itself around the contact point. As the interface falls further the liquid immediately under the contact point is constricted and finally breaks, leaving that around the contact in the form of a ring and separated from the main body

of liquid. The final curvatures of the ring are closely equal to those which it had just prior to breaking and these are determined by the pressure difference Δp prevailing at that instant, subject, of course, to the limitation that the spheres are not too large.

The simplest case is that in which Δp is the meniscus pressure drop prevailing at maximum capillary rise, a condition which can be produced by allowing the free liquid and meniscus to fall simultaneously and very slowly in a U-arrangement such as is shown in Fig. 2. A contains the grains and B provides the liquid receptacle and is connected to A by a small tube C. If now the liquid is allowed to drain from the system by bleeding it from the stop-cock, the meniscus will remain at a height h above the free liquid in B which will not differ greatly from normal capillary rise provided the drainage takes place sufficiently slowly. The pressure drop Δp across the meniscus formed by the liquid surface within the sphere assemblage is accordingly given by the capillary equation

$$\Delta p = \sigma\left(\frac{1}{r_1} + \frac{1}{r_2}\right) = \rho g h \tag{8}$$

where r_1 and r_2 are the principal radii of curvature of an element of the meniscus, ρ the density of the liquid, g the acceleration of gravity, and h the height of capillary rise for the particular element. In a paper on "Capillary Rise of Liquids in Homogeneous Sands," to appear later, the writers show that when h is large the average value of $\rho g h$ over the entire meniscus is given by the approximate relation:

$$\overline{\rho g h} = \frac{2\sigma}{r}\left(\frac{0.651 + 0.256x}{0.349 - 0.256x}\right) \tag{9}$$

From Eqs. (3), (8), and (9), we find

$$k = \frac{y}{r} = \frac{-3 + (9 + 8A)^{1/2}}{2A} \tag{10}$$

where

$$A = 2\left(\frac{0.651 + 0.256x}{0.349 - 0.256x}\right)$$

and from Eqs. (2) and (10)

$$\alpha = k/(Ak + 1) \tag{11}$$

The Eqs. (10) and (11) determine α and k from which v can be calculated by substitution in Eq. (4).

It will be observed that retention of this type is independent of the density, surface tension and viscosity of the particular liquid used. No dependence on viscosity, of course, is to be expected because of the very slow rate of drainage. Also the retention per unit volume of packed space is inde-

pendent of the radius of the spheres used, being a function of the porosity alone as can be seen by substitution of Eqs. (4) and (6) in Eq. (7) from which we obtain

$$V = \frac{3}{4}n(1 - P)\frac{\alpha}{1 + \alpha}f(k, \alpha). \tag{12}$$

Fig. 3 shows the volume V of retained liquid per unit volume of packed space as a function of the porosity and is plotted from Eq. (12). A curve of this type is to be expected. While the number of contacts increases as we decrease the porosity, the height of capillary rise increases as do also the resulting ring curvatures. Hence the volume of a single ring must decrease with decreasing porosity, offsetting the increased number of contacts.

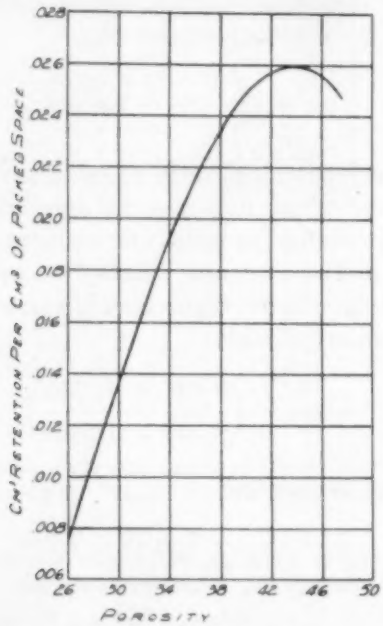

Fig. 3. Volume of retained liquid per unit volume of packed space as a function of porosity.

An experimental investigation was undertaken to test the validity of Eq. (12). The arrangement used is shown in Fig. 4. In principle it is a duplication of that shown in Fig. 2. A, C and D are spherical reservoirs each enclosing a volume of about two liters. A wire gauze was placed at the bottom of A in which the spherical grains were packed. C and D respectively served to fill and collect the liquid whose retention was to be investigated. B, a 3 cm cylindrical glass tube was used as a free liquid container during capillary drainage. a, b and c denote stop cocks for closing off the principal reservoirs. f and g are ground glass stoppers each provided with a small capillary to prevent excessive loss of liquid by evaporation, but permitting atmospheric pressure to prevail.

The procedure was to fill the flask C and weigh it. It was then placed in connection with the free liquid reservoir B by means of a large ground glass stopper d. With stop-cocks a and c open and b closed, the liquid was allowed to slowly fill A to the top of the grains. Valve a was then closed and the surplus liquid in C drained into the flask D, connected to the system $A-B$ by a ground glass stopper e. The valve b was closed so that initially B was completely filled. Valve b was now opened a little and the liquid in the U-system $A-B$ allowed to drop sufficiently slowly to keep capillary equili-

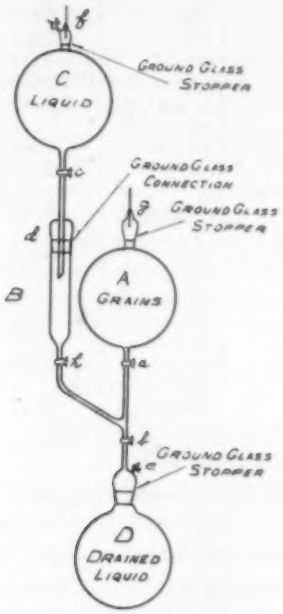

Fig. 4. Arrangement of apparatus in drainage experiments.

brium preserved. The surplus liquid was collected in D and weighed. That which remained in A was calculated from the difference in weights of liquid drained from C and into D.

With the smaller sizes the drainage time was necessarily longer, with a consequent increase in experimental losses. For this reason the retention of glass pearls and sands, was determined by taking small samples of about 100 grams each from the grain reservoir immediately after drainage. These were quickly weighed, dried in an oven at 80°C and reweighed, the difference being the weight of the retained liquid. Lead shot of radii 0.219 cm and 0.165 respectively as well as glass pearls of radii 0.0316 cm and standard Ottawa silica sand of radius 0.0443 cm were used in conjunction with a series of liquids of different surface tension and viscosity, the former varying between 25 and 72.8 dynes/cm and the latter from 0.009 to 1.38 poises. Kerosene was used in the cases of glass pearls and sands owing to the impracticability of the methods when volatile liquids such as CCl_4 are used. Its viscosity is such as to permit drainage in a reasonable time. Table I

summarizes the results. The observed retentions in cm^3 of liquid per cm^3 of packed volume are listed in column 5 of the table. Column 6 gives the corresponding quantities computed from Eq. (12). The agreement in general is good.

TABLE I. *Experimental data on retention.*

Grain Material	Grain Radius cm	Porosity	Liquid	Retention per cm^3		Density of Liquid	Surface Tension dynes/cm
				Obs.	Computed		
Lead Shot	0.219	0.404	CCl_4	0.0235	0.0250	1.587	24.9
			C_6H_6	.0261	.0250	.875	27.7
			$C_6H_5CH_3$	.0258	.0250	.861	26.7
			Turbine Oil	.0201	.0250	.918	34.3
			Zephyr Oil	.0245	.0250	.846	30.9
			Cayuga Oil	.0222	.0250	.883	32.3
			C_2H_5OH	.0246	.0250	.807	25.4
			Water	.0273	.0250	1.000	72.0
			Mean	.0243	.0250		
Lead Shot	0.165	0.396	CCl_4	.0264	.0279	1.587	25.0
			Zephyr Oil	.0285	.0279	.847	30.9
			Cayuga Oil	.0290	.0279	.847	32.3
			Pequod Oil	.0250	.0279	.893	33.7
			C_2H_5OH	.0276	.0279	.807	25.6
			Water	.0283	.0279	1.000	72.8
			Mean	.0275	.0279		
Glass Pearls	0.0316	0.373	Kerosene	.0255	.0235	.811	28.6
20–24 mesh sand	0.0443	0.359	Kerosene	.0292	.0222	.811	28.5

The results indicate that the wetting layer, a few molecules in thickness, is the only film present in assemblages of uniform spheres, and the volume of liquid so held is negligible in comparison with that found in the form of rings at the grain contacts. The quantities retained are obviously too large to be accounted for by the molecular forces involved in the formation of adsorbed films on a uniform surface. The shot and glass beads used had fairly uniform surfaces while the sand did not. Where rough surfaces are involved, small depressions filled with liquid can exist provided only that they are sufficiently deep to permit proper equilibrium curvatures. Such a type of surface film is permissible, and may account for the fact that the experimental values for sands are in excess of those calculated, although the lack of sphericity of the sand grains may be the controlling factor.

A REPRESENTATION OF THE DYNAMIC PROPERTIES OF MOLECULES BY MECHANICAL MODELS

By C. F. Kettering, L. W. Shutts and D. H. Andrews
General Motors Corporation, Research Laboratories,[1] Detroit, Michigan.

(Received June 23, 1930)

Abstract

Mechanical models have been constructed to represent the dynamical systems believed to exist in the molecule. Assuming that the intramolecular forces lie along lines associated with the chemical bonds and that for small vibrations they obey Hooke's law and have the mechanical character of spiral springs, it is possible to get a picture of the forces and masses which can be represented on a large scale by steel balls and spiral springs. Models have been constructed for some of the simpler nonpolar molecules. They are found to have characteristic frequencies which correspond very closely to the frequencies observed in the Raman spectra, and it is possible by this means to identify the Raman lines with definite types of motion of particular atoms in the molecule. This substantiates the view that Raman lines correspond very closely to characteristic fundamental molecular frequencies.

Introduction

THIS paper describes an attempt to make some mechanical models of the dynamical systems of forces and masses which are found in real molecules. The possibility of doing this lies in the fact that according to optical and thermal data the smaller nonpolar molecules are dynamically rather simple.[2,3] This simplicity is brought about in several ways. In the first place the only effective masses in the molecule are the nuclei of the atoms which may be regarded as point masses. The space relations of these masses to each other can be deduced to a large extent from the studies of the crystal lattice by means of x-rays. In the second place the forces in the molecule also appear to be simple in nature, lying for the most part along the lines which join the nuclei and which have been associated with the chemical bonds. In fact, the forces of the bonds are so much greater than any of the other forces acting on the atoms that they alone are of importance dynamically.

The problem is further simplified by the nature of the bond itself which behaves in a manner very analogous to a spiral spring. Thus for the small displacements with which we deal in studying the behavior of the molecule in the lowest vibrational levels we can see that the bond forces will obey

[1] The results reported here were arrived at largely as a development of the concepts of molecular structure originated by the senior author (C.F.K.). The success of the project is due chiefly to the cooperation of the many members of the laboratory staff who assisted in both the mechanical and physical part.

[2] J. W. Ellis, Jour. Franklin Inst. **208**, 517 (1929); E. O. Salant, Proc. Nat. Acad. Sci. **12**, 334, 370 (1926).

[3] D. H. Andrews, Proc. Roy. Acad. Amsterdam **29**, 744 (1926); Chem. Reviews **5**, 533 (1928), Phys. Rev. **34**, 1626 (1929); **36**, 544 (1930).

Hooke's law with regard to the extension or compression of the bond. There is, however another feature of the mechanical nature of the bond which has been largely neglected heretofore. The organic chemist in trying to explain the behavior of ring compounds has suggested that the bonds from a carbon atom will normally bear certain spatial relations to each other. This normal position has been generally accepted as that in which the bonds make the tetrahedral angle with adjoining bonds. In a cyclic compound such as a ring composed of four carbon atoms, it has been assumed that a strain is introduced by the alteration of the angles between the bonds. The concept has thus arisen that, in addition to elasticity of stretching, the bond has also elasticity of bending. This idea has been substantiated by recent data from the Raman spectra which show the force necessary to bend a bond is about one fifth that necessary to stretch it.

Data from the Raman and infrared spectra, as well as from specific heats,[3] have also indicated another regularity in the nature of the bond which simplifies considerably the construction of a mechanical model. It is found that the restoring force due to the stretching of a normal nonpolar bond is always about the same whether the bond be between two hydrogens, a hydrogen and a carbon, two carbons, a carbon and an oxygen, or any other similar position. It thus would appear to be possible to represent all the bonds in a mechanical model by means of the same kind of spiral spring. If the ratio of the stretching force constant to the bending force constant were chosen correctly it should be possible to make a model which would quite closely represent the actual molecule.

Until recently the data have been quite incomplete from which one could find the fundamental mechanical frequency in a molecule. Developments[3,4,5] in the study of the Raman spectra, however, indicate that the frequencies found there do correspond rather closely to real mechanical frequencies in the molecule. It therefore seems probable that if a mechanical model of a molecule were correctly constructed the characteristic frequencies found in it should correspond term by term to the frequencies observed in the Raman spectra. We should be able to get from a Raman frequency to a model frequency and *vice-versa* by multiplying or dividing by the proper constant which depends on the ratio of the mass of the molecule to the mass of the model, and of the force of the chemical bond to the force of the spring which represents it.

The Construction of the Model

The first problem in constructing the model was the determination of the ratio of the stretching to the bending force in the spring which was to be used to represent the chemical bond. In order to simplify the problem it was decided to omit the hydrogen atoms from the first series of models, thus representing only the atoms of atomic weight of twelve or greater. The hydrogens, being so light, have almost no appreciable energy at ordinary tempera-

[4] A. Dadieu and K. W. F. Kohlrausch, Berichte der Deutschen Chemischen Gesellschaft, Jahrg. **63**, 251 (1930).

[5] A. S. Ganesan and S. Venkateswaran, Indian Journal of Physics **4**, 195 (1929).

tures, and contribute very little to the dynamical character of the system. We were thus left with the problem of determining the nature of the bond between two atoms like carbon, oxygen, or chlorine.

We have a direct indication of the strength of the carbon-carbon bond in the Raman spectrum of ethane. There is one line at 990 wave numbers which with very little doubt corresponds to the frequency of vibration of the two carbon atoms. By means of the formula,

$$\nu = \frac{1}{2\pi}\left(\frac{k}{m}\right)^{1/2} \tag{1}$$

where ν is the frequency, m is the reduced mass of the system, and k is the force constant, we can calculate what the stretching force for the carbon-carbon bond will be. It turns out to be about 4×10^5 dynes per cm. Methyl alcohol which is dynamically similar to ethane gives a similar value for the force.

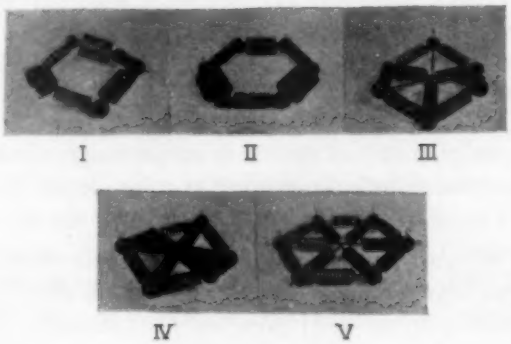

Fig. 1a.

The calculation of the bending force is quite a bit more uncertain as it is only involved when we have at least three atoms in the molecule. From the study of ethyl alcohol and benzene and its derivatives, the value of 0.66×10^5 dynes per cm has been calculated by defining the bending force as a force necessary to displace an atom in a direction perpendicular to the bond joining it to another atom which is held stationary. While this concept of the bending force may seem somewhat arbitrary, it would appear to be the best means of approach available at the time. A better knowledge of just what it is can probably be obtained as our knowledge of molecular dynamics increases.

From a consideration of these values, a helical spring to represent the bond was decided upon. It has the following characteristics:

Mean Diameter of Coil	13/16 in.
Diameter of wire	#11 (0.120)
No. of active turns	10
Free length	2–1/2 in.
Force per inch deflection	53 lbs.

The actual weight of the spring when completed was $1\frac{1}{2}$ ounces. Steel balls $1\frac{1}{8}$ in. diameter weighing 0.2 lbs. each were used to represent the carbon atoms. To obtain the desired value for the bending of the spring, the distance between the centers of the balls was set at $3\frac{3}{4}$ in. Some of the models constructed in these proportions are shown in Fig. 1a.

Method of Study

In order to study the fundamental vibration frequencies of such models, it is necessary to activate them by means of vibrational impulses of various frequencies. This was successfully accomplished by using a rubber band to attach one of the balls to an oscillating arm having $\frac{1}{4}$ in. stroke. This arm was operated by a reciprocating yoke on an eccentric driven by a variable speed motor. The model was suspended on rubber bands in such a manner that the frequency of the natural period of the suspension was much lower than the lowest period in the model.

Since the vibrations of the models covered a range of frequencies from 200 to 3500 cycles per minute, it was necessary to use some special means of observation in order to determine the characteristic motion of the various vibration periods. This was accomplished by illuminating the model with a neon lamp of a specially constructed stroboscope giving a large field of illumination. The circuit breaker of the stroboscope was geared to the activating motor shaft so that the neon lamp flashed at a frequency 2% slower than the exciting frequency applied to the model. Thus when the model was vibrating, a slow motion image, 1/50th of the actual frequency, was obtained. Thus at a frequency of 3000 cycles per minute, the model would appear to move through one cycle per second making it very easy to study the characteristics of the motion.

The tuning was found to be very sharp. When the motor was running at a speed which did not correspond to a characteristic frequency, the model was absolutely quiet. When the motor speed came within about five percent of a characteristic frequency, however, the balls began to move over the paths characteristic of that frequency and with closer tuning would generally vibrate with an amplitude of the order of 1/2 in. This, of course, depends on the type of motion and the point of activation to some extent. The tuning was sharp enough, though, so that the characteristic frequencies could be determined to within two or three percent, and it was easy to see just what type of motion corresponded to that frequency.

There was little complication because of harmonics. One or two of the lowest frequencies would sometimes appear when the speed of the motor was double their fundamental value, but could easily be recognized as harmonic because the balls were vibrating with twice the frequency which they should have had for that motor speed. The amplitude of these harmonics was always small. There seemed to be a little trouble from spurious vibrations, that is, vibrations occurring because the springs actually had mass. These are called spurious because they would not be found in the real molecule where the

only mass is in the nuclei. They were easily recognized by studying the motion of the springs under the neon light.

The method of study consisted in activating the model starting with a frequency of about 100 r.p.m. and raising the motor speed continuously to the maximum of 3600. As the characteristic frequencies were reached, they would be recognized by the appearance of motion of the balls under the neon light and the frequencies of revolution would be tabulated as read from a tachometer connected to the motor shaft. After going through the range of frequencies, a further study would be made by approaching each frequency carefully from above and below and observing as accurately as possible the motions of the balls at that frequency. The same model would be vibrated at several different positions by attaching the activating rubber band in various ways. It was found that while this sometimes altered the amplitude of the various frequencies, their values and number remained the same. In this way we have secured data on the characteristic frequencies of models of a number of the commoner organic compounds. A discussion is given in detail in the following paragraphs.

Results

Models without hydrogen represented

Benzene. Benzene was chosen as one of the compounds for study because of the uncertainty regarding its structure. Five different models of benzene, illustrated in Fig. 1a, were constructed as follows:

I. The Kekulé formula. The six balls representing the carbon atoms are arranged in a hexagon, and joined with alternate single and double bonds so placed that the tetrahedral angle is formed between any two adjoining bonds. The double bonds are made by putting two of the standard springs in parallel. The result is a "puckered" hexagon.

II. The Kekulé formula, plane. This is similar to model I except that the bonds are so arranged that the balls form a hexagon in a plane.

III. Centric formula. In this model the six balls are joined by single bonds into a "puckered" hexagon. There are in addition three cross bonds joining carbon atoms opposite each other in the ring. Each of these cross bonds is formed of a standard spring with a sufficient extension of wire on one end to give it the necessary length. In model IIIa the three cross bonds can slide over each other freely. In model IIIb they are clamped together in the center.

IV. Centric formula. This is the same as the preceding model except that the cross bond is formed by two standard springs joined together in the center. In IVa the bonds slide freely at the center and in IVb they are clamped together.

V. Centric formula. This is similar to the preceding model except that the bonds are so arranged that the six balls lie in a plane.

In order to compare the frequencies found in these models with the Raman spectra, it is necessary to calculate a conversion factor for passing from r.p.m.

to wave numbers. This conversion factor C may be expressed in terms of the masses and elastic constants by means of the equation

$$C = \frac{\nu \text{ r.p.m.}}{\bar{\nu}} = 60c\left(\frac{k_s}{k_m}\cdot\frac{m_m}{m_b}\right)^{1/2} \tag{2}$$

where $\bar{\nu}$ is the frequency in wave nos., ν r.p.m. is the frequency in r.p.m., k_m is the elastic constant for the bond in the real molecule, k_s is the elastic constant of the spiral spring, m_b is the effective mass of the ball, m_m the mass of the nucleus, and c the velocity of light.

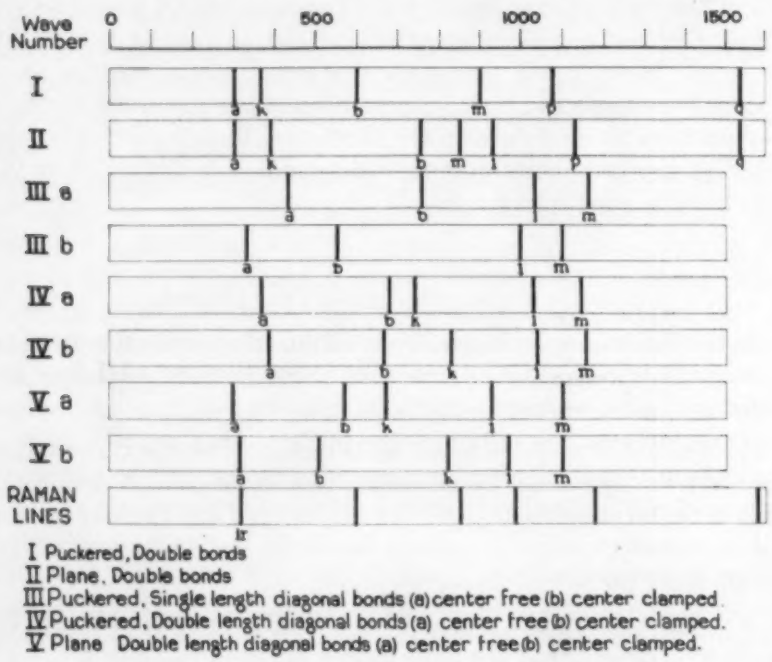

Fig. 1b. Models of benzene.

In the case of the fastest motion in benzene, the effective mass will be approximately that of a ball plus one and one-half springs. Of course this effective mass will be different for different types of vibration, but this seems to be sufficiently close approximation. Using the proper values, we find that C has a value of 3.1, which may be considered equal to three, within our limit of error.

The results of the study of these models are shown in Fig. 1b. The Raman spectrum for benzene is shown in the last line of the figure. The lines at 1500 cm^{-1} and at 3000 cm^{-1} (not shown) are almost surely due to the hydrogen which is not represented in this model. The four lines between 600 and 1200 cm^{-1} have been reported by almost everyone studying benzene and are known quite accurately. There seems to be also considerable evidence for a frequency in the neighborhood of 360. A series of bands observed in the in-

frared[6,7] indicate a fundamental frequency at 360 cm^{-1} and the specific heat[3] of benzene also gives very strong evidence for a frequency in this neighborhood. These five frequencies then seem to be the characteristic frequencies due to the vibration of the carbon atoms in benzene.

As may be seen in Fig. 1b, the centric models are in fairly good agreement with the Raman spectrum. They show five fundamental frequencies of the type indicated in Fig. 2. These types of motion are also in agreement with those which had previously been assigned to benzene[3] on the basis of its specific heat and Raman spectra. The degrees of freedom observed in the different types of motion add to give the correct number for the six carbon atoms, namely, twelve.*

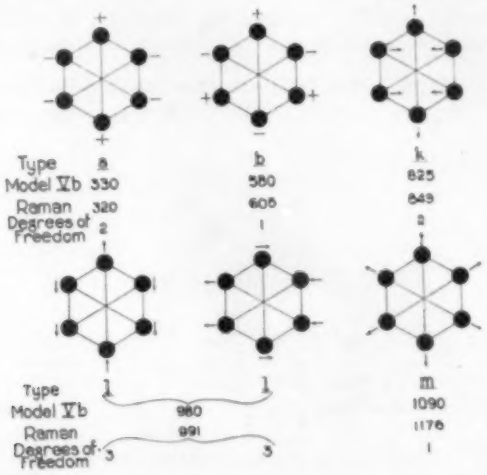

Fig. 2. Types of motion in benzene. + and − indicate motion out from and into plane of paper.

It is a little difficult to say just which model is in best agreement with the Raman spectrum. The evidence is perhaps a little in favor of *Vb*. This would be in accord with other observations which favor a plane hexagon for benzene. The double bond models, Kekulé formula, are distinctly different from the others in the higher frequencies. As may be seen in Table I, there is a frequency (p) which arises from a stretching of the single bonds. We would also expect a frequency (q) arising from a stretching of the double bonds. It was not possible with the present appratus to excite this frequency because of the speed limitation of the motor, but calculation shows it would correspond to about 1540 cm^{-1}. As shown in the last column, there is fair agreement between these frequencies and the Raman frequencies at 1176 and 1592 cm^{-1}. It is true that we had assumed the latter to be close to a lateral motion of the

[6] J. W. Ellis, Phys. Rev. **27**, 298 (1926).

[7] L. Marton, Zeits. f. Phys. Chem. **117**, 97 (1925).

* The six carbon atoms with three degrees of freedom each give eighteen degrees of freedom in all. Substracting six for the translation and rotation of the molecule as a whole, we should have twelve internal degrees of freedom.

TABLE I. *Models without hydrogen represented.* $\bar{\nu} = (r.p.m.)$.

Benzene

Model	I	II	IIIa	IIIb	IVa	IVb	Va	Vb	Raman[8]
a	300	320	435	340	385	400	325	335	360*
b	615	770	755	—	650	665	580	585	605
k	390	400	—	550	735	850	680	815	849
l	950	940	1035	1000	1015	1015	945	955	991
m		865	1160	1150	1150	1150	1090	1080	1176
p	1080	1135	—	—	—	—	—	—	(1176)
q	(1540)	(1540)	—	—	—	—	—	—	(1592)

* Value from infrared spectra, see reference 6.

Toluene

Type	Model	Raman[8]
t_1	205	215 cm^{-1}
t_2	235	
a	400	345
		520*
b	635	622
k_1	750	730
k_2	835	786
l_1	960	1005
l_2	990	1029
m	1150	1162

* Not observed by all investigators.

Models with chlorine $1.8\nu = (r.p.m.)$.

Carbon tetrachloride		Chloroform	
Model	Raman[8]	Model	Raman[8]
220	216 cm^{-1}	235	261 cm^{-1}
305	313	360	367
—	459	—	669
—	762	—	762
1000	791	1195	1218
1540	1535	1750	1441

Models with hydrogen represented. $\bar{\nu} = (r.p.m.)$.

	Ethane			Ethylene			Acetylene	
Model		Raman[9]	Model		Raman[8]	Model		Raman[9]
C-C	1275	990 cm^{-1}	C-C	1725	1623	C-C	2025	1960
H_t	725	1460	H_t	775	1342	H_t	750	
	870			825				
H_l	2800	2890	H_l	3000	2880	H_l	2960	
	3000	2950			3019		2980	
					3240			
					3272			

[8] R. G. Dickinson, R. T. Dillon, and F. Rasetti, Phys. Rev. **34,** 582 (1929).
[9] M. Daure, Compt. Rend. **188,** 1452 (1929).

Methyl alcohol			Ethyl alcohol		
Model		Raman[5]	Model		Raman[5]
C-O	1200	1031 cm^{-1}	C-C-O x	250	450 cm^{-1}
H_i	875	1257	C-C-O y	1125	884
		1360	C-C-O z	1350	1047
H_i CH_3	2900	2834	H_i	750	1461
H_i OH	3000	2939			1165
					1276
			H_i CH_3	2940	2872
			H_i CH_3	2960	2930
			H_i OH	3025	2973

hydrogens, but this is not absolutely certain. We may conclude that there is some evidence in favor of the double bonded structure, but until we are a little more certain of the correct way to represent the double bond, too much weight must not be placed on this evidence.

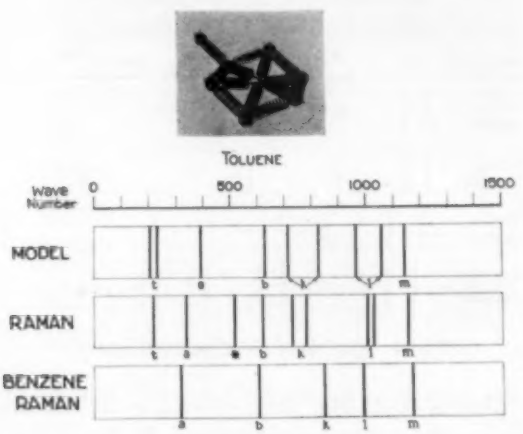

Fig. 3. Models of toluene.

Toluene. The model for toluene is the same as model IV$_b$ of benzene, with a ball and spring added to represent the methyl group. This group is attached so that it lies in the plane of the ring. The results are shown in Fig. 3. The addition of the methyl group causes a splitting of two of the frequencies which involve several degrees of freedom into doublets. Apparently one of the lines represents a motion which has its principal axis through the pair of carbon atoms in the ring which are in line with the methyl group, and the other two correspond to types of motion with the principal axis passing through the other two carbon atoms in the ring. This splitting may be seen by comparing the Raman spectra of benzene and toluene, and the model duplicates it almost exactly. There are also two low frequencies which represent the motion of the methyl group like a tail wagging. This interpretation has been verified by the heat capacity[3] which shows a large value at low temperatures which must be due to the presence of low frequencies.

Carbon tetrachloride. In order to investigate the effect of changing mass in the model, a representation of carbon tetrachloride has been constructed, the chlorine atoms being balls, the weight of which bears the proper ratio to the standard ball which represents the carbon atom. The results are shown in Fig. 4. If we use the same conversion factor of three, there is a discrepancy between the model frequencies and the Raman frequencies. This seems to be due to the fact that the force constant for the carbon-chlorine bond is somewhat smaller than for the carbon-carbon. An arbitrary conversion constant was therefore used which was somewhat smaller than the other one. There is no frequency in the model for the Raman line at 452 cm^{-1}. It seems quite possible that this is a first harmonic of the line at 216 cm^{-1}.

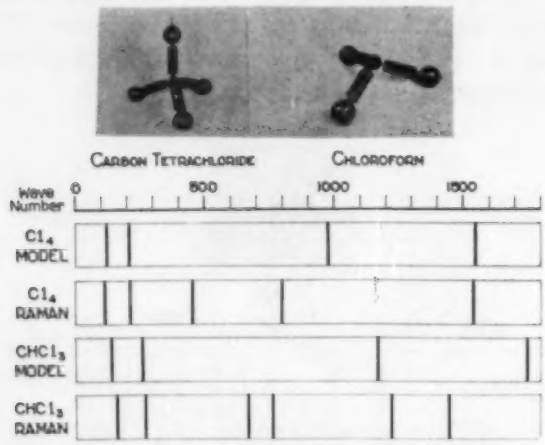

Fig. 4. Models of chlorine compounds.

Chloroform. This is just like the model for carbon tetrachloride except that the one chlorine atom has been omitted. If the value of the conversion constant suitable for the carbon-chlorine bond is used, the lines are in fair agreement with the Raman spectra.

Models with Hydrogen Represented

In order to make a model in which the frequencies of the hydrogens could be represented and could be observable with the means at our disposal, it was necessary to change the scale of the model. For convenience we used, to represent the hydrogen, the ball which had previously represented the carbon, and carbon was now represented by a ball of twelve times the mass of the small ball. A spring of the same wire and same number of turns as before was used to represent the bond. Its length was, however, shortened by a third because in the molecule the distance separating C-H is 1A, while that separating C-C is 1.5A. With this means, models were constructed and vibrated and the results are as follows:

Ethane. In the model of ethane it was found that there was one frequency corresponding to the vibration of the two carbon atoms with respect to each

other, also vibration of the hydrogen atoms at approximately three times the frequency of the carbon atoms. Of course, a new conversion constant must be used now that the mass has been changed. It might be calculated from the one previously adopted, but the difficulty of correcting for the mass of the springs makes this almost impossible. Since we are primarily interested in the ratio of the frequencies, it seemed wiser to adopt an arbitrary constant, and as it happens that in this model r.p.m. corresponds almost exactly to wave numbers, we have taken the conversion constant to be unity for the sake of simplicity.

As may be seen in Fig. 5, the ratio of the carbon frequencies (C-C) to the longitudinal hydrogen frequencies (H_l) is approximately that found in the Raman spectra for longitudinal vibrations. The model, however, shows transverse frequencies for the hydrogen (H_t) around 800 cm^{-1}. The line in the

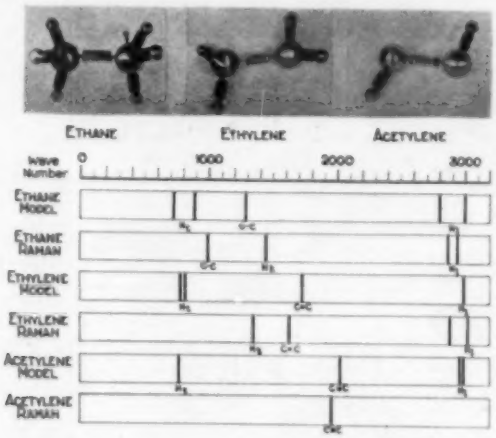

Fig. 5. Models with hydrogen represented.

Raman spectrum which has been identified with this vibration lies at 1420 cm^{-1}. The reason for this discrepency between the model and the spectrum is hard to explain. Apparently the force constant for lateral displacement of the hydrogen is quite a bit larger than the corresponding force in the carbon-carbon bond. We can not hope, of course, for a perfect representation of the real molecule, and it seems that we must be content here with having the number of frequencies correspond while the numerical value of this type of frequency lies considerably lower in the model than it does in the spectrum.

Ethylene. By putting a double bond between the carbon atoms, we shift the carbon-carbon frequency to about 1700 cm^{-1}. This corresponds to the shift observed in the Raman spectrum. The frequencies of the hydrogen are but slightly affected as the spectrum also shows.

Acetylene. Putting a triple bond between the carbon shifts the frequency to a little over 2000 cm^{-1}. This corresponds to the spectrum observed.

Methyl alcohol. Dynamically, this is quite akin to ethane. We find about the same frequency for the vibration of the two heavy atoms and the frequen-

cies in the same region for the vibration of the hydrogens as shown in Fig. 6. Again transverse vibrations of the hydrogens lie considerably lower than the lines ascribed to them in the Raman spectra.

It is very interesting to see the distinction between the two lines around 3000 cm^{-1}. When the model is vibrated at 2900 cm^{-1} the three hydrogens of the methyl group move in toward and out from the carbon while the hydrogen attached to the oxygen stays quiet. At 3000 cm^{-1} the three methyl hydrogens become quiet and the hydroxyl hydrogen vibrates. Since the masses and forces are the same in each case, this difference in frequency must be due to the fact that we have three balls reacting against the central ball in the one case and only one in the other case. It would, therefore, look as if the lines in the Raman spectrum could be positively identified with specific atoms in the molecule.

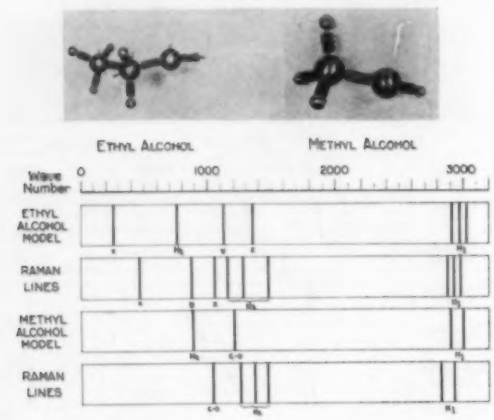

Fig. 6. Models with hydrogen represented.

Ethyl alcohol. This was constructed in the same way as the preceding models. We now have however, the possibility of three types of frequencies nvolving the large balls. The spectrum has the same general character as that of methyl alcohol. We now, however, find three lines around 3000 cm^{-1}. The lowest of these frequencies makes the three hydrogens in the methyl group vibrate while the others stand still. The next makes the two hydrogens in the CH_2 group vibrate, and the highest vibrates the hydrogen of the hydroxyl while the others remain quiet. We thus have a confirmation of the identification of these Raman lines with individual atoms. The transverse vibrations of the hydrogen again are lower than the lines identified with them in the Raman spectrum. The two upper vibrations (y, z) of the heavy atoms agree fairly well with the corresponding Raman lines. The lowest of the three (x) lies somewhat lower than the corresponding Raman line. This is probably due to the fact that in the model the mass is not distributed in space in the same way as in the molecule.

Conclusion

The general agreement which we have found between the characteristic frequencies of the models and the lines in the Raman spectra substantiates the character of the dynamical system in the molecule which we assumed in building the models. It seems reasonable to conclude that the molecular forces are directed along the lines associated with the chemical bonds and that mechanically, they are analogous to spiral springs. It appears also that the great majority of Raman lines have values of the frequency closely corresponding to fundamental mechanical frequencies in the molecule. Some of these frequencies are determined largely by the character of the whole molecule while others correspond to individual atoms or small groups of atoms. The mechanical model should prove very valuable in making these identifications and in ascertaining the structure of the molecule.

THE RELATION BETWEEN THE RAMAN SPECTRA AND THE STRUCTURE OF ORGANIC MOLECULES

By Donald H. Andrews
Chemistry Laboratory, Johns Hopkins University

(Received June 23, 1930)

Abstract

The following procedure is proposed for identifying the type of vibration in the molecule to which an observed frequency in a Raman spectrum corresponds. It is assumed that the only forces acting between the atoms in the molecule are those produced by the chemical bonds, and that there is a restoring force if the bond is stretched or if the angle which the bond makes with the other bonds on an atom is altered from the normal equilibrium value. It is also assumed that all non-polar chemical bonds have the same force constants in organic compounds. The different frequencies observed in the Raman spectra may then be considered as due solely to the variation in mass of the atoms concerned and to their space relation to each other, that is, whether they are in a straight chain, a branching chain, a ring, etc. It is possible to calculate in this way the number of Raman lines which should be observed for any compound, and the frequencies they should have. There is fair agreement with the observed spectra close enough so that the lines can be identified with different types of motion in the molecule.

Introduction

IN SPITE of the great deal of work which has been done on the Raman effect since its discovery two years ago we still lack a theory which is satisfactory for explaining at all completely the relation between the structure of organic molecules and the frequencies in the light which they scatter. The simplest explanation is that the shift in the frequency of the scattered light corresponds to a fundamental mechanical frequency in the vibrating molecule. This hypothesis has been supported by the extensive work of Dadieu and Kohlrausch[1] who have measured the Raman spectra for a large number of compounds, and have pointed out a great many significant relations between Raman lines and molecular structure in their own results and those of others working in this field. For example, certain special groups in a molecule such as hydrogen bound to carbon or two carbons bound by a double bond appear to have lines of definite frequency associated with them. Moreover, the calculation of the binding force between the atoms from the values of the Raman shifts lead to such uniform values among a wide variety of compounds that it seems reasonable to suppose that the frequencies of the Raman shift must correspond very closely to fundamental frequencies in the molecule.

Now, this hypothesis would also lead us to expect a close correspondence

[1] A. Dadieu and K. W. F. Kohlrausch: Phys. Zeits. **30,** 384 (1929); Berichte d. deutschen chem. ges. **63,** II, 251 (1930); Wiener Berichte IIa, **138,** 41, 336, 420, 607, 635, 799 (1929); **139,** 77 (1930).

between the frequencies of the Raman shifts and the frequencies in infrared absorption spectra. This has not been found to be true, particularly where the infrared absorption spectra can be interpreted with some degree of assurance, as in the simplest diatomic and triatomic molecules. However, Langer and Meggers[2] pointed out that in order to have such correspondence there must be a certain amount of freedom in the selection rules such as may not be found in triatomic or smaller molecules, but which may well be present in the case of molecules of more than six atoms, the class into which most organic compounds fall.

Granting that such a correspondence exists, the problem is still larger than merely finding relations between certain lines and certain characteristic groups in the molecule if we are to explain Raman spectra at all completely. Considering the mechanical nature of the vibrating system which we find in the molecule, it becomes evident that the majority of frequencies correspond to types of motion in which the whole molecule takes part rather than individual groups of two atoms. Now the problem of the dependence of frequencies on individual pairs of atoms as contrasted with the molecule as a whole is a moot question. Ellis[3] and Marton[4] have shown that certain band series in the infrared seem to be characteristic of pairs of molecules, and relatively independent of the structure of the molecule in which the pair is located. It appears, however, that this condition occurs only in special cases. For instance it may be due to the difference in mass of the vibrating particles. Thus in the case of hydrogen attached to carbon, we may expect the frequency ν, to be given rather closely by the equation for the harmonic oscillator

$$\nu = \frac{1}{2\pi}\left(\frac{k}{\mu}\right)^{1/2} \tag{1}$$

where k is the elastic constant of the C-H bond, and μ the reduced mass, determined by the equation

$$\frac{1}{\mu} = \frac{1}{m_1} + \frac{1}{m_2}$$

where m_1 is the mass of the hydrogen atom and m_2 the effective mass of the rest of the molecule. Since the ratio of m_2 to m_1 will nearly always be greater than twelve, it may be seen that the effect of the mass or structure of the rest of the molecule on the frequency will be small. Again this effect may be due to a pair of atoms being very tightly bound to each other and loosely bound to the rest of the molecule. An example of this is the $-C=O$ group which will be discussed later. On the other hand the majority of the frequencies will not depend on a pair of atoms, but on the nature of the molecule as a whole. This point is well brought out in Dennison's very complete analysis of the frequencies in me-

[2] Langer and Meggers, Bureau of Standards Journal of Research **4**, 711 (1930).
[3] J. W. Ellis, Phys. Rev. **27**, 298 (1926).
[4] L. Marton, Zeits. f. Phys. Chem. **117**, 97 (1925).

thane.[5] It is therefore, evident that if we are to explain the general nature of Raman spectra, we must formulate some ideas about the nature of the mechanical system in the molecule.

The Nature of the Mechanical System in the Molecule

There appear to be a few simple postulates which give us a basis for a qualitative explanation of Raman spectra. They may be summarized as follows:

(1) The frequencies of the Raman shifts correspond to characteristic fundamental mechanical frequencies in the molecule.

(2) The masses in this vibrating mechanical system are the nuclei arranged in space as indicated by the x-ray studies of crystal structure and by the deductions from organic chemistry.

(3) The forces under which these masses vibrate may to a first approximation be considered as acting along the lines associated with the chemical valence bonds. They can be characterized by two elastic constants, one of which, the stretching constant, gives the restoring force when two atoms are pulled apart unit distance from their equilibrium position in the molecule. The other, the bending constant, gives the restoring force when the angle is altered between the bonds joining a central atom to two other atoms.

(4) The amplitude of vibration will be so small compared with the equilibrium distance between the atoms that the variation of the force with distance will obey Hooke's law.

(5) The elastic constants for any type of bond are independent of the structure of the molecule in which it occurs, if there are no neighboring dipoles.

The reasonableness of the first postulate, at least for the cases we are considering, seems to be granted by those who have carried on the work in this field up to the present time. The second is self-evident. The third will perhaps seem more reasonable to those who have studied molecules from the chemical point of view than to those who are more familiar with their physical aspects. Nearly every chemist feels that the structural formulas of organic chemistry have met with such broad success in correlating chemical facts that the implications behind them must be given great weight. These formulas are based primarily on the assumption of the constancy of valence, one for hydrogen, two for oxygen, three for nitrogen and four for carbon; and on the hypothesis that the structure of a group or radical may remain unchanged throughout a complicated series of chemical reactions involving other parts of the molecule. In explaining the infrared spectra of methane Dennison[6] postulated forces acting between the hydrogens which were stronger than the forces joining the hydrogens to the carbon. It might be possible to reconcile the existence of such forces with the behaviour of atoms in organic molecules, but it is certainly much simpler to think of the invariance of structure during chemical transformations as due to forces which act in the place where we have pictured the bond.

[6] D. M. Dennison, Astrophys. J. **62**, 84 (1925).

If, however, we are to confine the forces which determine the structure of the molecule to the lines associated with chemical bonds we must say something more about the nature of the force than merely calling it attraction or repulsion. For example, there is considerable evidence that a long chain of atoms has a certain tendency to stay straight, and that there is resistance to bending. This idea has been made use of in organic chemistry by postulating that the normal position for the four valences around the carbon atom is at the tetrahedral angle. It is found that when closed rings of less than five carbon atoms are made, where the angle between the valences is less than 109,° there is instability and a tendency for the ring to break. This was pointed out by Baeyer in his "strain theory" of the organic ring compounds. It has also been evident from the observations on the specific heats of organic compounds that there must be thermal vibrations which involve bending of the molecule. This has been pointed out by E. O. Salant[6] and by the author[7] who attempted a calculation of the force constants from specific heat data.[8] Ellis has suggested that the 6.2μ band attributed to the C-H group is due to this type of vibration.[9] In a diatomic molecule this characteristic of the forces would not of course come into play since the motion of the two atoms would have to be merely toward and away from each other in order to preserve the conservation of momentum. However, in a triatomic molecule we can expect a type of motion in which there is a variation of the angle between the lines joining the two outside atoms to the central atom, and in such a case it is possible to define the forces acting in terms of the increased separation of the atoms, stretching, and of the variation of the angle, bending.

The justification of the fourth postulate may be seen in a calculation of the energy of most of these compounds at room temperature. It is found that for nearly all types of motion the molecules are in the zero vibrational level. The transition which causes the Raman shift appears to be from the zero to the first vibrational state in nearly all cases. For vibrations of this amplitude we may expect the forces to obey Hooke's law, and we can therefore expect that the motion will be that of a harmonic oscillator. The frequency will be related to the force and mass by Eq. (1).

The fifth postulate states that the strength of the bond for small amplitudes of vibration depends only on the two atoms which it connects, and is relatively independent of the structure of the rest of the molecule. The strongest support for this lies in the constancy of the characteristic frequencies for such bonds as C−H, C=C, and C=0 throughout extensive series of compounds. This has been clearly demonstrated in the results of a number of authors,[1] particularly Dadieu and Kohlrausch.[1] In fact it had been rec-

[6] E. O. Salant, Proc. Nat. Acad. Sci. **12,** 334 (1926).

[7] D. H. Andrews, Proc. Roy. Acad. Amsterdam **29,** 744 (1926). Comm. Phys. Lab., Leiden, Suppl. **56,** 16 (1926).

[8] D. H. Andrews, Chem. Reviews **5,** 533 (1928). See also Phys. Rev. **34,** 1626 (1929), where a brief outline was given of the ideas presented in this present paper.

[9] J. W. Ellis, Jour. Franklin Inst. **208,** 517 (1929).

ognized on the basis of infrared spectra and specific heat data that the non-polar bond joining together atoms of H, C, O or N has nearly always the same elastic constant. For the stretching[11] of the bond the value is generally about 4×10^5 dynes per cm. The latest values for the elastic constants of various bonds are tabulated by Dadieu and Kohlrausch[1] where it may be seen how remarkably uniform these values are.

Molecular Structure and Raman Spectra

These five postulates permit us to draw some conclusions as to what we will expect to find in the Raman spectra. In the first place, as has already been pointed out, the frequency of the hydrogen atoms will be relatively independent of the structure of the molecule, and will appear as the fastest of all the frequencies since hydrogen is so much lighter than any of the other elements. On the other hand in compounds of heavy atoms such as chlorine

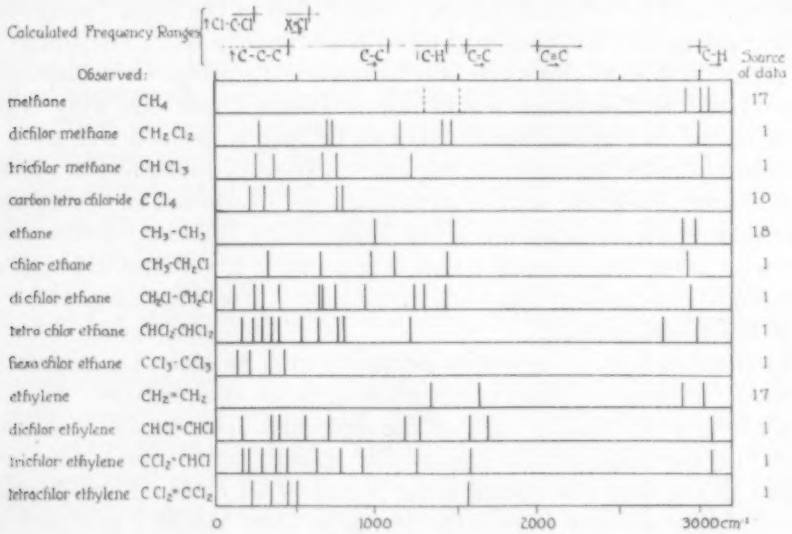

Fig. 1. Frequencies for three series of chlorine derivatives of methane, ethane and ethylene.

or bromine we will expect to find lines corresponding to much lower frequencies. Next with regard to the frequencies depending on the molecule as a whole we may say that the more complex the molecule, the lower the range of frequency, since a complex molecule will in general permit a kind of wave motion which will be of lower frequency than that for any pairs of atoms. By this effect frequencies may be secured which are as low as one tenth the value for a single pair of atoms, since the extension of the molecule into a chain may make possible very long wave length vibrations. On the other hand the frequency cannot be *increased* more than perhaps twenty percent

[10] A. S. Ganesan and S. Venkateswaran, Indian Journal of Physics **4,** 195 (1929). A. Petrikaln and J. Hochberg, Zeits. f. Phys. Chem. **B3,** 217 (1929). P. Pringsheim and B. Rosen, Zeits. f. Physik **50,** 741 (1928).

[11] J. R. Bates and D. H. Andrews, Proc. Nat. Acad. Sci. (U. S. A.) **14,** 124 (1928).

by increasing complexity, since the number of forces acting on any one atom is limited to the number of valence bonds which it can possess. Thus, the only way of increasing the force acting on it is by introducing some strain, such as in ring formation and this effect is very small. With this in mind we may proceed to examine the frequencies which have been experimentally observed.

Lines associated with hydrogen. One of the earliest regularities to be pointed out in the Raman spectra was that of the lines in the neighborhood of 3000 cm^{-1} which appear to be due to the vibration of hydrogen attached to carbon. In Fig. 1 the frequencies have been plotted for three series of chlorine derivatives of methane, ethane and ethylene, respectively. It may be seen that in all compounds where hydrogen is present we have lines in the 3000 cm^{-1} region, but that when hydrogen is no longer present as in carbon tetrachloride, hexachlorethane, and tetrachlor ethylene there are no frequencies in this region.

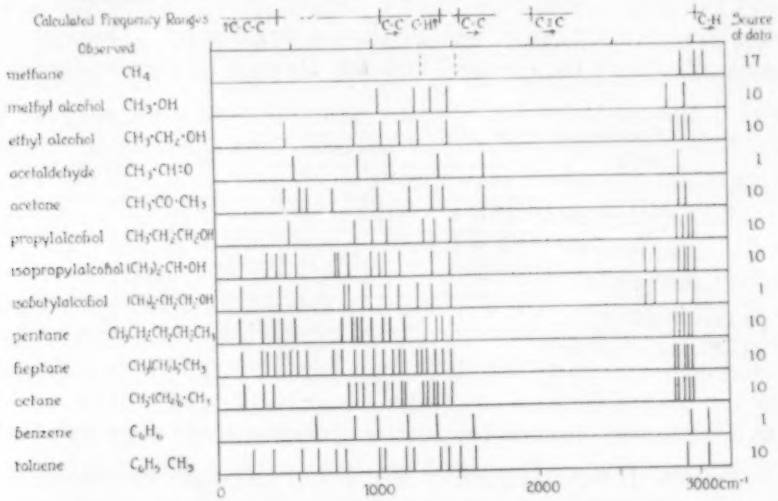

Fig. 2. Frequencies observed in a number of carbon compounds.

Further observation of these data, moreover, indicate that there is a region from about 1100 to 1600 cm^{-1} where this same regularity holds true. Now Dennison[8] in his analysis of methane frequencies concluded that there would be two frequencies in this region, as shown by the dotted lines in Fig. 1, which correspond to motions of hydrogen of the type which we have called bending. It is a little surprising that no Raman frequencies were observed in the 1400 cm^{-1} region but this may be due to the difficulty of working with gases, or to the more rigid selection rules which we may expect to find in smaller molecules. Ellis[9] also has suggested that the 6.2μ band in the infrared may be due to this type of motion. It therefore seems reasonable to say that we have in these two groups of frequencies, 3000 cm^{-1} and 1400 cm^{-1}, the frequencies of the two types of motion which we would expect the hydrogen atoms to have, namely stretching and bending. Granting

this, we may procede to an explanation of the remaining lines outside these regions which may be due to the heavier atoms.

Carbon frequencies. Fig. 2 shows the frequencies observed in a number of carbon compounds. As is to be expected methane shows only frequencies in the region which we have associated with hydrogen. Passing to ethane, however, as is shown in Fig. 1, we have in addition to the lines around 1400 cm^{-1} and 3000 cm^{-1} a line at 1000 cm^{-1} and as has been concluded by others,[1] this appears to be the frequencies of two carbon atoms vibrating with respect to each other. The spectrum of methyl alcohol is very similar to this as we might expect since we have merely replaced a carbon by an oxygen atom.

If the frequencies in ethane at 1000 cm^{-1} are really due to the carbon-carbon vibration, we would expect it to shift when a single bond is replaced by a double bond. This is found to be true in the spectrum of ethylene in which the line at 1000 cm^{-1} disappears and the line at 1600 cm^{-1} appears.

There has always been considerable dispute among chemists as to whether a double bond is stronger or weaker than a single bond. This question has been ably discussed by Fajans[12] and the Raman frequencies substantiate

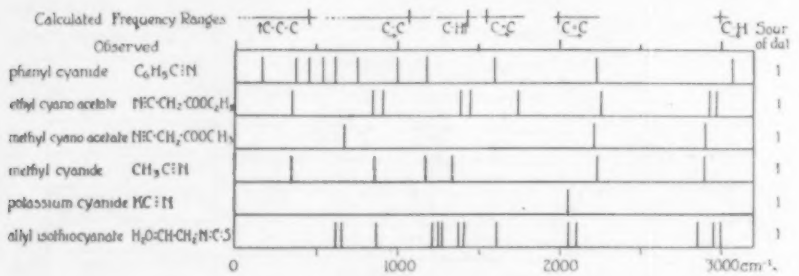

Fig. 3. Frequencies observed for a number of compounds containing triple bonds.

his conclusions. If we make use of Eq. 1 and calculate the elastic constant for these two frequencies, we find that the shift is that which would correspond approximately to the doubling of the elastic constant. This is an additional confirmation that we have identified the line correctly. Moreover if we examine compounds in which there are double bonds such as the C=O bond in acetaldehyde and acetone we find frequencies in this region. Over twenty compounds have been examined by Dadieu and Kohlrausch[1] in which these frequencies due to the double bond appear. If we increase the strength of the binding still further by passing to the triple bond we find higher frequencies just as should be expected. Fig. 3 shows the frequencies observed for a number of compounds containing triple bonds.

This group of frequencies shows very well the way in which a frequency depending principally on the strength of one particular bond, in this case the triple bond, may also be influenced by the structure of the molecule.

[12] K. Fajans, Chem. Ber. **53**, 643 (1920), **55**, 2826 (1922).

If we regard these groups as of the type $X-C\equiv Y$ it may be seen that the frequency will depend on the linkage $X-C$ and on the mass of X as well as on $C\equiv Y$. Thus in acetylene, since the hydrogen, X, is light, the only effective force for this vibration is $C\equiv Y$, giving a frequency of about 1950 cm^{-1}. In compounds of the cyanide type, however, where X is a heavy atom the force $X-C$ also contributes to the vibration and we find the frequencies in the neighborhood of 2200 cm^{-1}. It is particularly interesting to note that in $KC\equiv N$ the frequency is again lower. It seems quite possible that this is due to the fact that the $K-C$ bond is presumably polar and much weaker than the $C-C$ bond.

Another interesting compound in this connection is allyl iso-thiocyanate where we have a carbon atom between two double bonds. Two double bonds so placed are as effective as a triple bond and we find a corresponding frequency.

Effect of increasing molecular complexities. Having identified the above lines which correspond to vibrations of pairs of atoms we may proceed to examine the frequencies which appear to be due to vibrations of the molecule as a whole. The simplest illustration of the effect of increasing the complexity may be seen by comparing methyl and ethyl alcohol. We may regard these as diatomic and triatomic molecules respectively since the hydrogens are so light that they do not affect appreciably the vibration of the heavy atoms. In methyl alcohol we have a single line at 1000 cm^{-1} due to the C-O vibration, as would be expected for a diatomic molecule. In a triatomic molecule, however, we would expect three fundamental frequencies since the total number of degrees of freedom is nine and of these three will be translational, and three rotational for the molecule as a whole, leaving three for vibration. Now according to our postulates the effective forces joining the atoms will be the forces of the two chemical bonds, namely C-C and C-O. For each of these bonds we will expect one restoring force if the bond is stretched and another restoring force if the angle between the two bonds is altered corresponding to a bending of the molecule. It is a little difficult to say off-hand what the relative values of these two forces will be but from the analogy of the stretching and bending frequencies for hydrogen attached to carbon, we may expect the bending force to be only about one-quarter as strong as the stretching force.

This particular case has been carefully investigated by Yates.[13] He has assumed forces of this type and finds that there should result one comparatively low frequency corresponding to the bending of the molecule and two frequencies not far from that for the diatomic molecule. If we ascribe the three frequencies between 1200 and 1400 cm^{-1} in the ethyl alcohol spectrum to hydrogen, the three remaining lines are in good accord with Yates' calculation. The spectrum of acetaldehyde which may similarly be regarded as a triatomic molecule shows a close resemblance to that of ethyl alcohol as

[13] Yates, The character of the elastic forces in the homopolar chemical bond. See succeeding article.

might be expected. If it is true that the line at 450 cm^{-1} corresponds to a bending of the molecule then the fact that this frequency becomes only slightly higher in passing from ethyl alcohol, C-C-O, to acetaldehyde, C-C=O indicates that doubling the bond decreases the ease of bending only slightly. On the other hand the appearance of the line at 1600 cm^{-1} shows that the force involved in stretching has been greatly increased.

Passing to more complicated molecules, we now find low frequencies appearing presumably corresponding to the presence of wave motion involving more than three atoms. Moreover, the number of lines increases, and as we get to heptane we find a fairly even distribution of the lines from the hydrogen region down to the low frequencies. The experimental observation of these more complex compounds is somewhat difficult because of the tendency for fluorescence which gives a continuous background, masking many of the lines. A number of the lines are also of very low intensity so that the agreement between different observers for compounds of the complexity of heptane is rather poor. For that reason, it is dangerous to draw too definite conclusions. However, one or two points seem worth mentioning. Lewis[14] in a study of the possible frequencies in compounds of this type points out that the frequencies should be fairly evenly distributed from the lowest, corresponding to the longest wave-length possible in the chain, up to the highest, corresponding to the vibration of a pair of atoms. Pentane and heptane have spectra in accord with this view. It also seems worth noticing that the number of lines below the hydrogen region, which we may take as ending at about 1100 $cm,^{-1}$ corresponds roughly to the number of degrees of freedom for internal vibration of the heavy atoms which would be calculated from the number of atoms present in the molecule. Thus for heptane we should have $(3\times7)-6=15$. In the region below 1100 cm^{-1} where these frequencies should appear we find fifteen lines for heptane and twelve for pentane, but for octane there are only ten, so that the argument is hardly conclusive.

Conclusions

The way in which the above postulates accounts for the great majority of Raman lines may be seen from the following calculation. We take 5×10^5 and 0.6×10^5 dynes per cm for the stretching and bending constants respectively of the single non-polar bond. These are the best average values from the latest data and the actual values for the various bonds do not appear to deviate from these by more than ten per cent. We can then calculate the ranges in which frequencies should appear in the different compounds, from the atomic weights and number of bonds involved. The variation in frequencies between different compounds is thus considered to be due only to the variation in the masses of the atoms and in the number and position of the bonds. The stretching constant for a double bond is taken as twice that for a single bond, and for a triple bond, thrice.

[14] A. B. Lewis, Coupled vibrations with applications to the specific heat and infrared spectra of crystals. P. 568, this issue.

The values of the frequency which would be expected for the vibration of pairs of atoms can be calculated quite simply with the help of Eq. (1). The results of these calculations have been summarized in Table I. The values for C-H, C-O, and C-N are in good agreement with the observed lines which have been attributed to these bonds.

The case of C_6H_5-Cl is not so clear. It has been difficult to say just which Raman line is due to the vibration of the Cl. However, a series has been observed in the infra-red by Ellis[15] which appears to be due to this type of motion and its fundamental frequency agrees very well with that calculated here.

The C=C bond in ethylene has a frequency which is well accounted for if we take the elastic constant as twice that for the single bond. With the C=O bond, however, we find the frequency to be quite a bit higher. Here the carbon is also joined to two other carbon atoms and since these bonds probably make an angle of about 109°with the double bond we may say as

TABLE I.

Bond	Compound	μ	k	Frequency Calc.	Obs.
		Stretching			
C−H	H_3C-CH_3	1.0	5×10^5 dynes/cm	2920 cm^{-1}	2950[18]
C−C	H_3C-CH_3	7.5	5	1070	990[18]
C−O	H_3C-OH	8.0	5	1030	1031[10]
C−Cl	C_6H_5-Cl	23.6	5	600	596[15]
C=C	$H_2C=CH_2$	7.0	10	1560	1600[17]
C=O	$(CH_3)_2-C=O$	8.0	15	1790	1704[10]
C≡C	$HC\equiv CH$	6.5	15	1990	1950[18]
C≡N	$C_6H_5-C\equiv N$	7.0	20	2210	2227[1]
		Bending			
H−C−H	CH_4	0.5	0.6	1430	1520[5]
C−C−O	CH_3-CH_2-OH		0.6	480	450[10]
Cl−C−Cl	CCl_4	17.5	0.6	240	216[10]

[17] R. G. Dickinson, R. T. Dillon, and F. Rasetti, Phys. Rev. **34**, 582 (1929).
[18] M. Daure, Compt. Rend. **188**, 1492 (1929).

a first approximation that the effective force acting on that side of the carbon atom will be about equal to a single bond. An approximate calculation then gives the frequency as 1790 cm^{-1} which accounts at least qualitatively for the increase in frequency over the value for ethylene.

In the same way we find that C≡C in acetylene has a frequency accounted for by thrice the value for the single bond while the $C_6H_5-C\equiv N$ frequency lies higher by about the amount we should expect from the addition of the extra bond to the carbon atom.

The calculation of the bending frequencies may be made most simply in the case of molecules like methane or carbontetrachloride. One of the types of motion with the slow frequency will be that where the central atom stands still and the outer atoms vibrate toward and away from each other in pairs without stretching the bonds. In other words, we have a pure type

[15] Ellis, Phys. Rev. **28**, 25 (1926).

of bending motion. As a first approximation we can treat this by means of Eq. (1) since the motion of a pair of atoms will be the same as if they were directly joined by an elastic force. Giving the value of 0.6 dynes per cm to this effective force which we believe is brought about by the bending of the bonds, we find values as shown in the second part of Table I. The first agrees fairly well with the value ascribed by Dennison[5] to this type of motion in methane. The second agrees with the slowest observed Raman frequency, and there is evidence that this frequency is the one associated with this type of motion in a study of molecular models to which reference will be made later.

The case of ethyl alcohol which is more complex has been treated by Yates.[13] With these values in his equation we find 480 cm^{-1} for the frequency due to bending, in good agreement with the slowest observed Raman line.

The calculated frequencies are indicated in Fig. 1 by the vertical lines in the crosses at the top of the figure. The horizontal lines indicate roughly what we should expect from the modification of the frequency by additional bonds or chain formation. Thus, as we have seen in the case of C=O the frequency is raised about five per cent by the addition of the two bonds on the left of the carbon. On the other hand by lengthening out the carbon chain as in pentane the original C-C frequency can in a sense be modified to perhaps a third of its value or less.

It may be seen that for the compounds, for which the Raman shift frequencies have been plotted in the figures, we find frequencies just in those ranges which we would expect according to the structure. This seems to be the best evidence we have that the postulates regarding the nature of the mechanical system in the molecule are reasonable and that the Raman frequency shifts do correspond to fundamental mechanical frequencies.

Considerable light has also been thrown on this problem by a study of mechanical models of molecules[16] which was based on the ideas developed by C. F. Kettering on the nature of elasticity in molecules. The problem has also been discussed from several other points of view by Yates[13] and Lewis[14] to whose papers reference has already been made. The conclusions drawn from these different lines of approach to the problem seem to be in substantial agreement.

[16] C. F. Kettering, L. W. Shutts and D. H. Andrews, p. 531, this issue.

THE ELASTIC CHARACTER OF THE HOMOPOLAR CHEMICAL BOND

By Robert C. Yates
Mathematics Department, Johns Hopkins University

(Received June 23, 1930)

Abstract

An attempt is made to obtain frequencies of internal vibrations of some organic molecules by the consideration of certain mechanical systems.

The system of three particles is studied assuming the forces of restitution elastic. Certain proportionality constants are determined, using a representative compound, which characterize the single valence bond. Calculated wave-numbers for CO_2, CS_2, CH_2Cl_2, C_2H_5OH are compared with observed data from Raman spectra.

I. Introduction

THERE has been a recent impulse on the part of the physical chemist to determine precisely the character of the chemical bond that retains the atoms in mutual attraction in molecular structures of organic compounds. An attempt in this direction has been made[1] under the assumption that the valence bond is of spring-like nature and the forces set up by a displacement are elastic. Mechanical models of representative molecules have been constructed accordingly and experiments run to observe the fundamental modes of vibration.[2] The correlation between such observed frequencies and those obtained from the Raman spectra was found to be surprisingly good. This prompted the desire to look more closely into several types of systems and to set up the dynamical equations of motion yielding frequencies that might be compared with experiment.

II. Statement of the Problem

We shall thus be concerned with the small vibrations of a system of particles about a position of stable equilibrium under certain definite assumptions, these assumptions to be supported by the closeness of agreement in the end.

The intramolecular forces that arise are set up by the mutual attraction and repulsion of the atoms, suggesting not only an elastic force between any two but also a force of restoration dependent on the angular divergence of neighboring bonds.

Definitely, it is assumed that the force tending to restore a particle after a displacement is the sum of two types of forces: the first acting along the

[1] D. H. Andrews, The Relation Between the Raman Spectra and the Molecular Structure of Organic Compounds, p. 544, this issue.

[2] F. Kettering. L. W. Shutts, D. H. Andrews, A Representation of the Dynamic Properties of Molecules by Mechanical Models, p. 531, this issue.

line of connection with another particle and proportional to the linear displacement (Hooke's law); the second acting at right angles to the first and proportional to the change in the angle between two adjoining bonds. This last may be restated as being proportional to the arc displacement.

We consider here only small displacements and higher order infinitesimals, in the presence of those of lower order, are neglected throughout. The motion of the particles is assumed to be in a given plane.

III. Determination of the Force Constant k_1

Consider two particles of masses m_1 and m_2 constrained to linear motion. Assuming the force acting between them proportional to the diisplacement we find as is well known the frequency of vibration given by

$$\nu = (1/2\pi)(k_1/M)^{1/2} \tag{1}$$

where M denotes the relative mass $1/m_1+1/m_2$ and k_1 a factor of proportionality. If $m_1=m_2\equiv m$, we have

$$k_1 = 2\pi^2\nu^2 m. \tag{2}$$

In order to evaluate k_1 we take the carbon-carbon combination of the diatomic molecule and assign the wave number of 1000 to motion along the line of connection.[1] This gives approximately $k_1=4\times10_5$ dynes per cm.

Before we may find a corresponding value for the remaining constant k_2, that controls the restoring force arising from a change in the angle between neighboring bonds, we must look first at the system of three particles.

IV. The System of Three Particles

Consider the system of three particles of masses m_1, m_2, m_3, connected by two bonds as shown. We place the particles at the vertices of an isosceles triangle and select a reference frame with horizontal axis parallel to its base. These give the relations

$$\left.\begin{aligned} 2f/m_3 &= b/m_1 - c/m_2 \\ m_1 d &= m_2 a \end{aligned}\right\} \tag{3}$$

If the origin of coordinates be taken at the center of mass, we have

$$\left.\begin{aligned} f &= c - b \\ g &= a + d \end{aligned}\right\} \tag{4}$$

We introduce the notation:

$$\left.\begin{aligned} A &\equiv g/m_3 + a/m_1 \\ B &= c/m_2 + f/m_3 = b/m_1 - f/m_3 \end{aligned}\right\} \tag{5}$$

so that $\tan\theta_2=A/B$

Let the system be displaced to a position shown and let the components of displacement of the particles be $(1/m_i)\cdot(x_i,y_i)$.

The kinetic energy of the system is:

$$T = (\tfrac{1}{2})[(\dot{x}_1^2 + \dot{y}_1^2)/m_1 + (\dot{x}_2^2 + \dot{y}_2^2)/m_2 + (\dot{x}_3^2 + \dot{y}_3^2)/m_3]. \tag{6}$$

The potential energy—dependent on the configuration—is composed of a potential V_1 due to linear displacement and V_2 due to rotation:

$$V_1 = (k_1/2)(\Delta d_1^2 + \Delta d_2^2) \tag{7}$$
$$V_2 = (k_2/2)\cdot\Delta S^2 = (k_2 d_1^2/2)\cdot\Delta\phi^2.$$

In order to find the explicit expressions for the quantities in (7) we obtain from the figure:

$$\left.\begin{aligned} d_1\cdot\Delta d_1 &= -A(y_1/m_1 - y_3/m_3) + B(x_1/m_1 - x_3/m_3) \text{ etc.} \\ d_1^2\cdot\Delta\phi &= d_1^2(\Delta\theta_1 - \Delta\theta_2) = A(x_1/m_1 - x_2/m_2) + B(y_1/m_1 + y_2/m_2 - 2y_3/m_3) \end{aligned}\right\} \tag{8}$$

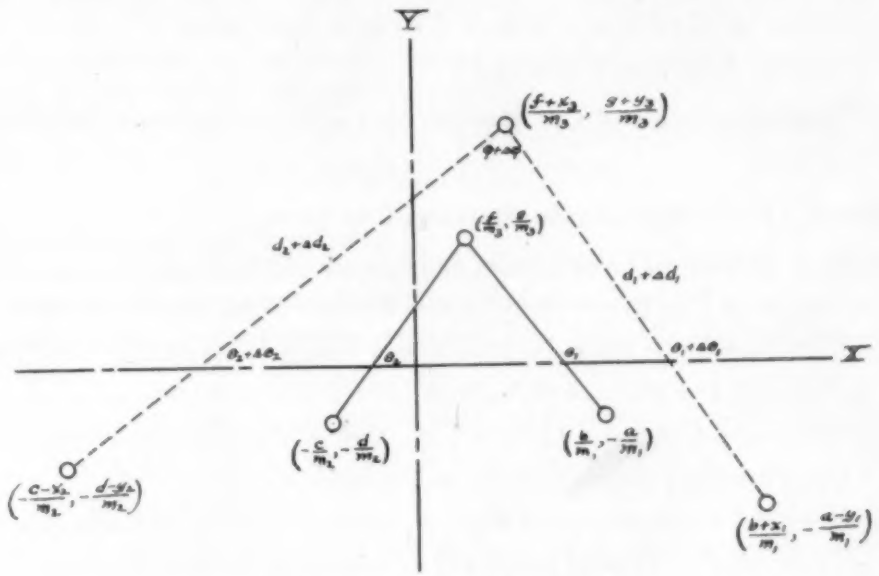

Fig. 1. System of three particles.

Since the resultant of the forces on the system is zero the center of mass will remain at rest in an inertial system. We may, therefore, write

$$\left.\begin{aligned} x_1 + x_2 + x_3 &= 0 \\ y_1 + y_2 + y_3 &= 0 \end{aligned}\right\} \tag{9}$$

Furthermore the moment of the various forces about the origin is zero so that the angular momentum of the system about the origin is constant. Assuming that this angular momentum is zero, we have:

$$m_1\begin{vmatrix} (b+x_1)/m_1 & -(a-y_1)/m_1 \\ \dot{x}_1/m_1 & \dot{y}_1/m_1 \end{vmatrix} + m_2\begin{vmatrix} -(c-x_2)/m_2 & -(d-y_2)/m_2 \\ \dot{x}_2/m_2 & \dot{y}_2/m_2 \end{vmatrix} + m_3\begin{vmatrix} (f+x_3)/m_3 & (g+y_3)/m_3 \\ \dot{x}_3/m_3 & \dot{y}_3/m_3 \end{vmatrix} = 0 \tag{10}$$

which becomes on integrating:

$$By_2 = A(x_1 + x_2) + By_1. \tag{11}$$

The two energy functions may now be rewritten, because of the relations Eq. (9) and Eq. (11):

$$\begin{aligned} T = {} & (\tfrac{1}{2}B^2)\{[B^2/m_1 + A^2/m_2 + (A^2 + B^2)/m_3]\dot{x}_1^2 + (A^2 + B^2)(1/m_2 + 1/m_3)\dot{x}_2^2 \\ & + B^2(1/m_1 + 1/m_2 + 4/m_3)\dot{y}_1^2 + 2[A^2/m_2 + (A^2 + B^2)/m_3]\dot{x}_1\dot{x}_2 \\ & + 2AB(1/m_2 + 2/m_3)(\dot{x}_1 + \dot{x}_2)\dot{y}_1\} \end{aligned} \tag{12}$$

$$\begin{aligned} V = {} & (k_1/2d_1^2)\{[(A^2 - B^2)/m_3 - B^2/m_1]x_1 + [(A^2 - B^2)/m_3]x_2 + AB(2/m_3 \\ & + 1/m_1)y_1\}^2 + (k_1/2d_1^2)\{[(A^2 + B^2)/m_3 + A^2/m_2]x_1 \\ & + (A^2 + B^2)(1/m_2 + 1/m_3)x_2 + AB(2/m_3 + 1/m_2)y_1\}^2 \\ & + (k_2/2d_1^2)\{AB(1/m_1 + 1/m_2 + 2/m_3)x_1 + (2AB/m_3)x_2 \\ & + B^2(1/m_1 + 1/m_2 + 4/m_3)y_1\}^2. \end{aligned} \tag{13}*$$

These functions T and V must satisfy the Lagrangian equations of motion:

$$(d/dt)(\partial L/\partial \dot{x}_i) - (\partial L/\partial x_i) = 0 \tag{14}$$

where $L = T - V$. Inserting the expression L we have:

$$\begin{aligned} & [B^2/m_1 + A^2/m_2 + (A^2 + B^2)/m_3]\ddot{x}_1 + [A^2/m_2 + (A^2 + B^2)/m_3]\ddot{x}_2 \\ & + AB[2/m_3 + 1/m_2]\ddot{y}_1 = -(k_1/d_1^2)[(A^2 - B^2)/m_3 - B^2/m_1]\{[(A^2 - B^2)/m_3 \\ & - B^2/m_1]x_1 + [(A^2 - B^2)/m_3]x_2 + AB[2/m_3 + 1/m_2]y_1\} - (k_1/d_1^2)[(A^2 + B^2)/m_3 \\ & + A^2/m_2]\{[(A^2 + B^2)/m_3 + A^2/m_2]x_1 + [A^2 + B^2][1/m_3 + 1/m_2]x_2 \\ & + AB[2/m_3 + 1/m_2]y_1\} - (B^2k_2/d_1^2) \cdot A \cdot [1/m_1 + 1/m_2 + 2/m_3]\{A[1/m_1 \\ & + 1/m_2 + 2/m_3]x_1 + [2A/m_3]x_2 + B[1/m_1 + 1/m_2 + 4/m_3]y_1\} \end{aligned} \tag{15}$$

$$\begin{aligned} & [A^2/m_2 + (A^2 + B^2)/m_3]\ddot{x}_1 + (A^2 + B^2)[1/m_1 + 1/m_3]\ddot{x}_2 + AB[2/m_3 + 1/m_2]\ddot{y}_1 \\ & = -(k_1/d_1^2)[(A^2 - B^2)/m_3]\{[(A^2 - B^2)/m_3 - B^2/m_1]x_1 + [(A^2 - B^2)/m_3]x_2 \\ & + AB[2/m_3 + 1/m_1]y_1\} - (k_1/d_1^2)[A^2 + B^2][1/m_2 + 1/m_3]\{[(A^2 + B^2)/m_3 \\ & + A^2/m_2]x_1 + (A^2 + B^2)[1/m_2 + 1/m_3]x_2 + AB[2/m_3 + 1/m_2]y_1\} \\ & - (B^2k_2/d_1^2)(2A/m_3)\{A[1/m_1 + 1/m_2 + 2/m_3]x_1 + [2A/m_3]x_2 + B[1/m_1 \\ & + 1/m_2 + 4/m_3]y_1\} \end{aligned} \tag{16}$$

$$\begin{aligned} & A[1/m_2 + 2/m_3][\ddot{x}_1 + \ddot{x}_2] + B[1/m_1 + 1/m_2 + 4/m_3]\ddot{y}_1 = -(Ak_1/d_1^2)(2/m_3 \\ & + 1/m_1)\{[(A^2 - B^2)/m_3 - B^2/m_1]x_1 + [(A^2 - B^2)/m_3]x_2 + AB[2/m_3 + 1/m_1]y_1\} \\ & - (Ak_1/d_1^2)(2/m_3 + 1/m_2)\{[(A^2 + B^2)/m_3 + A^2/m_2]x_1 + [A^2 + B^2][1/m_2 \\ & + 1/m_3]x_2 + AB[2/m_3 + 1/m_2]y_1\} - (B^2k_2/d_1^2)(1/m_1 + 1/m_2 + 4/m_3)\{A[1/m_1 \\ & + 1/m_2 + 2/m_3]x_1 + [2A/m_3]x_2 + B[1/m_1 + 1/m_2 + 4/m_3]y_1\}. \end{aligned} \tag{17}$$

These three Eqs. (15, 16, 17) define the motion of the system and are sufficient to determine the independent quantities x_1, x_2, y_1.

* That the potential function as here written gives the correct forces is seen by calculating straight forwardly the forces acting on the separate particles. For example, the horizontal component of force acting on the first particle is $-(\delta V/\delta \cdot x_i/m_i)$.

On combining these we find:

$$\begin{aligned}
&[B^2/m_1+A^2/m_2+2B^2/m_3]\ddot{x}_1+[(A^2+B^2)/m_2+2B^2/m_3]\ddot{x}_2+AB[1/m_2-1/m_1]\ddot{y}_1 \\
&\quad=(k_1/d_1^2)\,[(A^2+B^2)/m_1+2B^2/m_3]\{[(A^2-B^2)/m_3-B^2/m_1]x_1 \\
&\quad+[(A^2-B^2)/m_3]x_2+AB[2/m_3+1/m_1]y_1\}-(k_1/d_1^2)[(A^2+B^2)/m_2 \\
&\quad+2B^2/m_3]\{[A^2/m_2+(A^2+B^2)/m_3]x_1+[A^2+B^2][1/m_2+1/m_3]x_2 \\
&\quad+AB[2/m_3+1/m_2]y_1\}
\end{aligned} \tag{18}$$

which defines the particular type of motion that is unaffected by any bending of the bonds.

IV (B)

We now make the restriction that the two end particles be of the same mass, say $m_1=m_2\equiv m$. Eq. (18) becomes:

$$\begin{aligned}
\ddot{x}_1+\ddot{x}_2&=-(k_1/d_1^2)[(A^2+B^2)/m+2B^2/m_3](x_1+x_2) \\
&=-k_1(1/m+2\cos^2\theta/m_3)(x_1+x_2)
\end{aligned} \tag{19}$$

where θ is a base angle (see table).

Thus the combined horizontal motion of the two end particles is simply harmonic. The third particle oscillates complementary to this.

Under this first restriction we solve Eqs. (15, 16, 17) explicitly for $\ddot{x}_1$, $\ddot{x}_2$, $\ddot{y}_1$:

$$\begin{aligned}
\ddot{x}_1&=(k_1/d_1^2)\{[(A^2-B^2)/m_3-B^2/m]x_1+[(A^2-B^2)/m_3]x_2+AB[2/m_3 \\
&\quad+1/m]y_1\}-(2Ak_2/d_1^2)\{A[1/m+1/m_3]x_1+[A/m_3]x_2 \\
&\quad+B[2/m_3+1/m]y_1\} \\
\ddot{x}_2&=-(k_1/d_1^2)\{[A^2/m+(A^2+B^2)/m_3]x_1+[A^2+B^2][1/m+1/m_3]x_2 \\
&\quad+AB[2/m_3+1/m]y_1\}+(2Ak_2/d_1^2)\{A[1/m+1/m_3]x_1+[A/m_3]x_2 \\
&\quad+B[2/m_3+1/m]y_1\} \\
\ddot{y}_1&=-(Ak_1/d_1^2B)\{[(A^2-B^2)/m_3-B^2/m]x_1+[(A^2-B^2)/m_3]x_2 \\
&\quad+AB[2/m_3+1/m]y_1\}-(2Bk_2/d_1^2)\{A[1/m+1/m_3]x_1+[A/m_3]x_2 \\
&\quad+B[2/m_3+1/m]y_1\}.
\end{aligned} \tag{20}$$

If we are to find solutions of the type $x_i=C_ie^{\alpha t}$ for the differential equations (Eq. 20) we must require the vanishing of the determinant of coefficients:

$$\begin{vmatrix}
\alpha^2+a_{11} & a_{21} & a_{31} \\
a_{12} & \alpha^2+a_{22} & a_{32} \\
a_{13} & a_{23} & \alpha^2+a_{33}
\end{vmatrix}=0 \tag{21}$$

which is the characteristic equation—a cubic in α^2—where the quantities a_{ij} are the constant coefficients that occur in the differential Eq. (20).

The determinant is readily reduced to:

$$\begin{vmatrix} \alpha^2 + b_{11} & 0 & 0 \\ a_{12} & \alpha^2 + b_{22} & a_{32} \\ a_{13} & b_{23} & \alpha^2 + a_{33} \end{vmatrix} = 0 \tag{22}$$

where

$$b_{11} = (k_1/d_1^2)[(A^2 + B^2)/m + 2B^2/m_3]$$
$$b_{22} = k_1B^2/d_1^2 \cdot m + 2A^2k_2/d_1^2m$$
$$b_{23} = ABk_1/d_1^2m - 2ABk_2/d_1^2m$$

Solving Eq. (22) we get the two factors:

$$\alpha^2 + k_1(1/m + 2\cos^2\theta/m_3) = 0 \tag{23}$$

$$\alpha^4 + [(k_1+2k_2)/m + 2(k_1\sin^2\theta + 2k_2\cos^2\theta)/m_3]\alpha^2 + 2k_1k_2(2/m_3 + 1/m)/m = 0 \tag{24}$$

whose three roots α_1, α_2, α_3, are pure imaginaries and we therefore write $\alpha_i^2 = -\mu_i^2$ from which we may obtain the normal fundamental frequencies of the system.

IV (c)

If all three particles were of the same mass, m, the foregoing expressions would simplify considerably. Under this restriction we rewrite Eq. (23):

$$\left.\begin{aligned} m\mu^2 - k_1(1 + 2\cos^2\theta) &= 0 \\ m^2\mu^4 - [(k_1 + 2k_2) + 2(k_1\sin^2\theta + 2k_2\cos^2\theta)]m\mu^2 + 6k_1k_2 &= 0 \end{aligned}\right\} \tag{25}$$

The normal frequencies of this system are $\nu_i = (1/2\pi)\mu_i$ and the wave-numbers $\bar{\nu}$ are given by

$$\bar{\nu}_i = (\tfrac{1}{3})\nu_i \times 10^{-10} = \left(\frac{1}{6\pi}\right)\mu_i \times 10^{-10}\ \text{cm}^{-1}. \tag{26}$$

V. Determination of the Force Constant k_2

Referring to section III we proceed to calculate k_2 and for that purpose we select as most suitable a molecule of ethyl alcohol, the atoms arranged in groups as shown in the accompanying table.

We assume here that the bonds form the tetrahedral (approximately 109°) angle with each other in the position of rest. As an approximation, the atomic mass of the CH_2 group is taken as fourteen while the other two groups are assigned the average mass of sixteen. The mass of each group is supposed to be concentrated at the nucleus of each heavy atom. It is to be emphasized that there is no bond acting directly between the two end groups. We may thus apply Eqs. (25) of the preceding paragraph.

We find, on using the value of k_2 found in section III: $\bar{\nu}_1 = 1035$ as compared with the observed wave-number 1047.

TABLE I.

	Structure	Force Constants	Calculated			Observed		
			ν_1	ν_2	ν_3	ν_1	ν_2	ν_3
C_2H_5OH	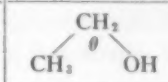	$k_1=4$ $k_2=6$	1035	930	451	1047	884	450[4]
CO_2	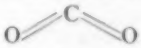	$k_1=8$ $k_2=1.2$	1535	1320	703	3650	2350	683[5]
		$k_1=8$ $k_2=1.2$	1800	970	920			
		$k_1=32$ $k_2=4.8$	3600	1960	1820			
		$k_1=32$ $k_2=0.6$	3600	2817	978			
CS_2	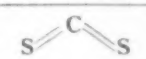	$k_1=8$ $k_2=1.2$	1303	no value	no value	800	655	655[4]
	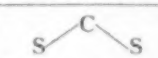	$k_1=4$ $k_2=6$	920	730	570			
CH_2Cl_2	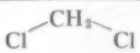	$k_1=4$ $k_2=0.6$	917	1010	728	1151	715	283[4]
	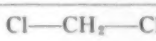	$k_1=4$ $k_2=0.6$	1083	698	487			

[4] A. S. Ganesan and S. Venkatesvaren, Indian Jour. Phys. **4**, 195 (1929).
[5] R. H. Fowler, Statistical Mechanics, p. 64, Cambridge, 1929.

On using the other two fundamental wave-numbers 884 and 450 in the quadratic form (Eq. 23) we solve for k_2, obtaining $k_2=0\cdot6\times10^5$ dynes/cm as an average value. These values for the force constants had already been obtained in a very approximate manner from specific heats and Raman spectra.[3]

VI. SOME APPLICATIONS

We apply the results of the foregoing paragraphs to a few organic molecules, arranging the calculations in the accompaning table.

Carbon dioxide is definitely a double bonded structure and it was therefore supposed that the force constant k_1 would, in this case, be double its value for the single bond. It is found, however, that the values $k_1=32$; $k_2=0.6$ (or 1.2) dynes per cm gives results that best agree with experiment. The atomic arrangement is shown in table 2 under the heading "Structure," first with the bonds forming the tetrahedral angle and second with the atoms lying collinear. This last stable position seems to be most probable. The molecule of carbon disulphide gives best results if taken with the single bond. Dichlor methane not only seems to have a single bond structure but apparently has the straight line arrangement of its groups. Because of the agree-

[3] D. H. Andrews Phys. Rev. **34**, 1626 (1929).

ment between calculated and observed data in most of the cases considered it is fairly conclusive that the force constants as determined are quite valid. The percent of error is in itself not sufficient as an objection if it is considered that the frequencies might lie in the range of 100 to 10000 wave-numbers.

The writer is greatly indebted to Professor D. H. Andrews for suggesting the problem and to Professor F. D. Murnaghan for continued advice in the preparation of the paper.

STUDY OF THE SMALL VIBRATIONS OF SIX PARTICLES IN A SYSTEM ANALOGOUS TO THE BENZENE RING

By Robert C. Yates
Mathematics Department, Johns Hopkins University

(Received June 23, 1930)

Abstract

The system of six particles is allowed to vibrate under certain restrictions, assuming an elastic nature for the restoring forces. Frequencies of vibration are obtained and compared with Raman data lending some support to the Claus construction of the benzene molecule.

Introduction

In A previous paper[1] we have considered the small vibrations about a position of stable equilibrium of a system of three particles under the assumption that the forces set up by a displacement are elastic in character. It was definitely assumed that the restoring force was the sum of two types of forces; the first acting along the line of connection with another particle and proportional to the linear displacement; the second acting at right angles to the first and proportional to the change in the angle between two adjoining bonds. The results obtained for a few organic compounds pointed very strongly to the conclusion that two force constants $k_1=4\times10^5$ and $k_2=0.6\times10^5$ dynes per cm could be assigned as definite properties of the single valence bond which were independent of the particular molecule.

Theory

In this paper we consider the system of six particles, (under the same assumptions as were taken for three particles), all of the same mass m lying in stable position at the vertices of a regular hexagon, whose side is of length a. Each particle has three connecting bonds as shown. If the angular momentum is zero and the center of gravity remains fixed, the system will have nine degrees of freedom. We, however, place certain restrictions on the motion of the system that will reduce considerably the order of the resulting characteristic determinant. The motion of the particles is assumed to be in a given plane and higher order infinitesimals, in the presence of those of lower order, are neglected throughout.

First we allow only motion along the 60 degree lines passing through the center of the hexagon. Let: (a) the displacement of the i^{th} particle from its position of rest be x_i; (b) the change in the corresponding angles formed by the bonds be θ_i, and ϕ_i; (c) the change in the length of the outside bonds be Δ_i. We have:

[1] R. C. Yates, The Elastic Character of the Homopolar Chemical Bond, p. 555, this issue.

$$\Delta_i = (x_i + x_{i+1})/2 \qquad (i = 1, \cdots, 6)$$

The energy functions are set up at once, following the procedure of the first paper:

$$\left.\begin{aligned} T &= (m/2)\cdot \sum_1^6 \dot{x}_i^2 \\ V &= (k_1/2)\cdot \sum_1^6 (\Delta_i^2 + x_i^2/2) + (a^2 k_2/2)\cdot \sum_1^6 (\theta_i^2 + 2\phi_i^2) \end{aligned}\right\} \tag{1}$$

If the center of mass is to remain fixed: $x_1 = x_4$, $x_2 = x_5$, $x_3 = x_6$, leaving three independent coordinates to fix the system.

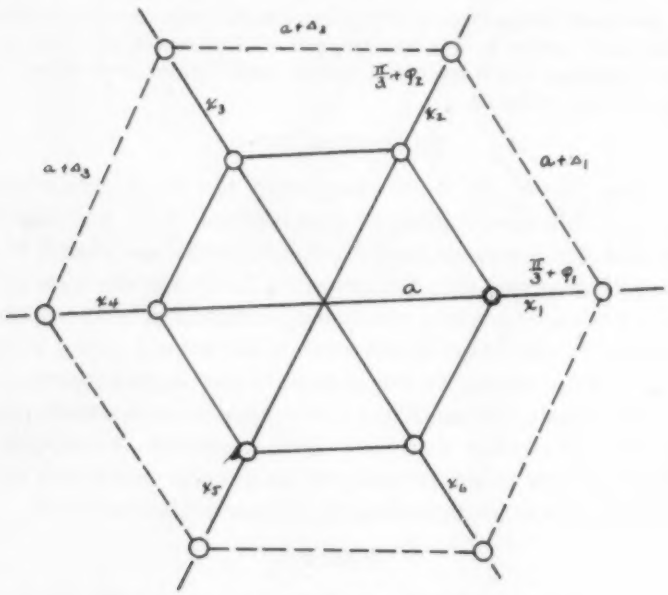

Fig. 1. Vibration along radial lines.

From the figure $\phi_1 = (3^{\frac{1}{2}}/a)x_2$, $\phi_2 = (3^{\frac{1}{2}}/a)x_3$, etc. and since $\theta_1 = \phi_1 - \phi_6$ etc., we may write Eqs. (1) in the final form:

$$\left.\begin{aligned} T &= m\cdot \sum_1^3 \dot{x}_i^2 \\ V &= (k_1/2)(2\sum_1^3 x_i^2 + x_1x_2 + x_1x_3 + x_2x_3) \\ &\quad + 6k_2\left(2\sum_1^3 x_i^2 - x_1x_2 - x_1x_3 - x_2x_3\right) \end{aligned}\right\} \tag{2}$$

The equations of motion are accordingly:

$$\left.\begin{aligned} 2m\ddot{x}_1 &= -(k_1/2)(4x_1 + x_2 + x_3) - 6k_2(4x_1 - x_2 - x_3) \\ 2m\ddot{x}_2 &= -(k_1/2)(x_1 + 4x_2 + x_3) - 6k_2(-x_1 + 4x_2 - x_3) \\ 2m\ddot{x}_3 &= -(k_1/2)(x_1 + x_2 + 4x_3) - 6k_2(-x_1 - x_2 + 4x_3) \end{aligned}\right\} \tag{3}$$

On combining the Eqs. (3), we find the set of normal coordinates

$$z_1 = x_1 + x_2 + x_3 \qquad z_2 = x_1 - x_2 \qquad z_3 = x_2 - x_3$$

with resulting frequencies:

$$\left.\begin{aligned} \nu_1 &= \left(\frac{1}{2\pi}\right)[(3k_1 + 12k_2)/m]^{1/2} \\ \nu_2 = \nu_3 &= \left(\frac{1}{4\pi}\right)[(3k_1 + 60k_2)/m]^{1/2} \end{aligned}\right\} \tag{4}$$

Secondly, we restrict the system to motion on a circle of arbitrary radius $(a+b)$. We select a polar system of reference with pole at the mass center and initial line passing through a vertex of the hexagon.

Let: (a) the angular displacement of the particles be θ_i; (b) the change in the angles between adjoining bonds be α_i, β_i, ϕ_i, where $\phi_i = \alpha_i + \beta_i$; (c the change in the bond length be Δ_i.

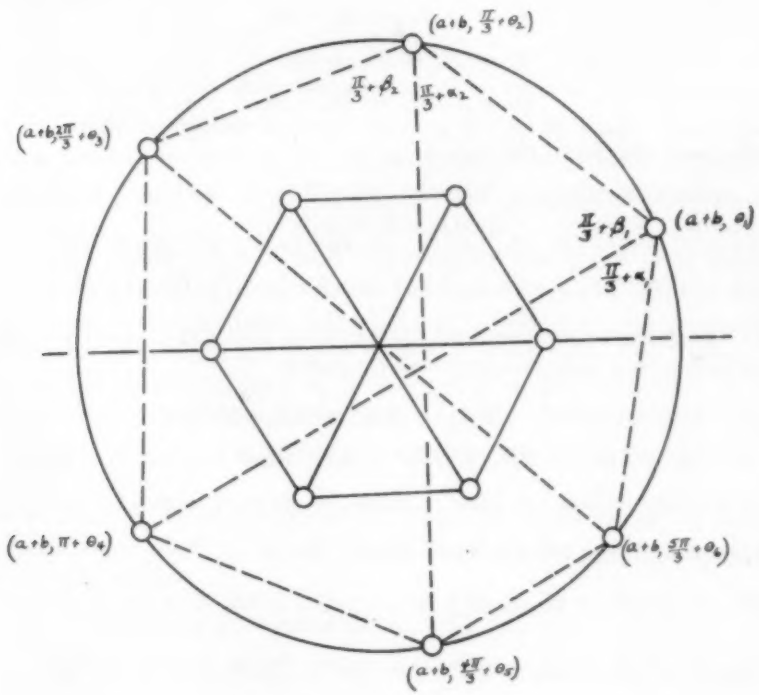

Fig. 2. Vibration on a circle.

The energy functions are:

$$\left.\begin{aligned} T &= (m/2)(a+b)^2 \sum_1^6 \dot{\theta}_i^2 \\ V &= (k_1/2)\left[\sum_1^6 \Delta_i^2 + 3b^2\right] + (a^2 k_2/2) \sum_1^6 (\alpha_i^2 + \beta_i^2 + \phi_i^2) \end{aligned}\right\} \tag{5}$$

From an inspection of the figure we find

$$\left.\begin{aligned} \alpha_1 &= (2\theta_6 - \theta_1 - \theta_4)/2 \qquad \beta_1 = -(2\theta_2 - \theta_1 - \theta_4)/2 \\ \alpha_2 &= (2\theta_1 - \theta_2 - \theta_5)/2 \qquad \beta_2 = -(2\theta_3 - \theta_2 - \theta_5)/2 \end{aligned}\right\} \tag{6}$$

etc. which give expressions for ϕ:

$$\phi_i = \phi_{i-1} - \phi_{i+1}. \tag{7}$$

In order to fix the center of gravity at the pole we must have

$$\left.\begin{aligned} \theta_5 &= \theta_1 + \theta_2 - \theta_4 \\ \theta_6 &= -\theta_1 + \theta_3 + \theta_4 \end{aligned}\right\} \tag{8}$$

If we now put angular momentum about the center of mass equal to zero we obtain the further relation $\sum_1^6 \theta_i = 0$. We thus eliminate θ_4, θ_5, and θ_6 by means of the equations:

$$\left.\begin{aligned} \theta_4 &= -\theta_1 - 2\theta_2 - 2\theta_3 \\ \theta_5 &= 2\theta_1 + 3\theta_2 + 2\theta_3 \\ \theta_6 &= -2\theta_1 - 2\theta_2 - \theta_3 \end{aligned}\right\} \tag{9}$$

We obtain now also from the figure

$$\left.\begin{aligned} \Delta_1 &= b + [a(3)^{1/2}/2](\theta_2 - \theta_1) & \Delta_4 &= b + [a(3)^{1/2}/2](3\theta_1 + 5\theta_2 + 4\theta_3) \\ \Delta_2 &= b + [a(3)^{1/2}/2](\theta_3 - \theta_2) & \Delta_5 &= b - [a(3)^{1/2}/2](4\theta_1 + 5\theta_2 + 3\theta_3) \\ \Delta_3 &= b - [a(3)^{1/2}/2](\theta_1 + 2\theta_2 + 3\theta_3) & \Delta_6 &= b + [a(3)^{1/2}/2](3\theta_1 + 2\theta_2 + \theta_3) \end{aligned}\right\} \tag{10}$$

With the foregoing expressions we may rewrite Eqs. (5) explicitly in terms of the three remaining independent coordinates θ:

$$\left.\begin{aligned} T &= m(a+b)^2[5\dot\theta_1^2 + 9\dot\theta_2^2 + 5\dot\theta_3^2 + 12\dot\theta_1\dot\theta_2 + 8\dot\theta_1\dot\theta_3 + 12\dot\theta_2\dot\theta_3] \\ V &= (k_1/2)[9b^2 + (3a^2/2)(36\theta_1^2 + 60\theta_2^2 + 36\theta_3^2 + 84\theta_1\theta_2 + 60\theta_1\theta_3 + 84\theta_2\theta_3)] \\ &\quad + a^2k_2[24\theta_1^2 + 60\theta_2^2 + 24\theta_3^2 + 66\theta_1\theta_2 + 30\theta_1\theta_3 + 66\theta_2\theta_3] \end{aligned}\right\} \tag{11}$$

The corresponding equations of motion are:

$$\left.\begin{aligned} m(a+b)^2(5\ddot\theta_1 + 6\ddot\theta_2 + 4\ddot\theta_3) &= -(9a^2k_1/2)(6\theta_1 + 7\theta_2 + 6\theta_3) \\ &\quad - 3a^2k_2(8\theta_1 + 11\theta_2 + 5\theta_3) \\ m(a+b)^2(2\ddot\theta_1 + 3\ddot\theta_2 + 2\ddot\theta_3) &= -(3a^2k_1/2)(7\theta_1 + 10\theta_2 + 7\theta_3) \\ &\quad - a^2k_2(11\theta_1 + 20\theta_2 + 11\theta_3) \\ m(a+b)^2(4\ddot\theta_1 + 6\ddot\theta_2 + 5\ddot\theta_3) &= -(9a^2k_1/2)(5\theta_1 + 7\theta_2 + 6\theta_3) \\ &\quad - 3a^2k_2(5\theta_1 + 11\theta_2 + 8\theta_3) \end{aligned}\right\} \tag{12}$$

If here we make the change of variables: $z_1 = 2\theta_1 + 3\theta_2 + \theta_3$, $z_2 = \theta_1 + 3\theta_2 + 2\theta_3$, $z_3 = \theta_1 - \theta_3$, the last set of equations may be replaced by:

$$m(a+b)^2\ddot z_i = -9a^2(k_1/2 + k_2)z_i \quad (i = 1, 2, 3). \tag{13}$$

The characteristic of the differential Eqs. (12) is degenerate and for this particular type of motion there is but one frequency:

$$\nu = [3a/2\pi(a+b)]\left[(k_1+2k_2)/2m\right]^{1/2}.$$

Conclusion

If the hydrogens in the benzene ring are grouped with the carbons and if we assume bonds passing through the center of the hexagon we may apply our results. Using the values for the elastic constants which were secured in the previous paper[2] the values for the three characteristic frequencies are found, as shown in Table I.

Table I.

Force constants	ν Calculated	ν Observed[4]
$k_1=4\times10^5$	—	605
	—	849
$k_2=0.6\times10^5$	—	991
	1145	1176
	1305	
	1750	—

The frequencies in the Raman spectra, believed to be associated with the carbon atoms, are also given. Now it has already been deduced from a study of the relation between Raman spectra[3] that the experimentally observed frequency of 1176 cm^{-1} should correspond to the type of motion where all the carbon atoms move in and out together along the lines through the center of the hexagon. The agreement between this value and the calculated one of 1145 cm^{-1} substantiates this view and indicates that the values chosen for the elastic constants are fairly correct. The other two calculated frequencies fail to agree with any of those experimentally observed. It appears probable that for these the restrictions imposed on the motion were so far removed from the actual state of the molecule that these types of motion do not exist in actuality.

The writer's appreciation is due Professor D. H. Andrews for many valuable suggestions and Professor F. D. Murnaghan for constructive advice in preparing this paper.

[2] R. C. Yates, reference 1.

[3] C. F. Kettering, L. W. Shutts, and D. H. Andrews, Phys. Rev. **36**, 531 (1930). D. H. Andrews, Phys. Rev. **36**, 544 (1930).

[4] A. S. Ganesan and S. Venkateswaran, Indian Jour. Phys. **4**, 195 (1929).

COUPLED VIBRATIONS WITH APPLICATIONS TO THE SPECIFIC HEAT AND INFRARED SPECTRA OF CRYSTALS

By Arthur B. Lewis
The Johns Hopkins University

(Received June 23, 1930)

Abstract

The free periods of certain coupled systems of linear oscillators are considered in this paper. The complete system discussed consists of p identical, coupled, groups; each group containing n identical linear oscillators. The equations of motion of such a system lead to a determinantal equation of the pn^{th} order, of which the well-known determinantal equations of the uniformly loaded string and the finite wave filter are special cases. The solution of this general determinantal equation has been reduced to the solution of certain trigonometric equations. A solution for the free periods of the system is obtained for the case in which the coupling between the groups is small compared to the internal forces of the groups. In case only one or two groups are present the resulting equations can be solved readily to any desired degree of approximation for any values of the forces whatever. Certain special cases are noted in which, for special values of the forces, exact solutions become possible.

Sample calculations have been carried out which illustrate the behavior of the pn free periods of a system of pn particles when various forces act between the particles of the system, and when the pn particles are rearranged in various ways. With the aid of the equations obtained above the specific heats of four of the normal alcohols have been computed at low temperatures and compared with the experimentally determined values. A reasonable agreement is obtained between the observed and computed values, but with the data at hand the agreement cannot be said to be conclusive.

1. Introduction

RECENT investigators in the infrared spectra of organic compounds[1,2] have attained considerable success in organizing their data by assigning certain prominent bands which are common to all organic compounds to certain modes of vibration between the component parts of the molecules under investigation. It is generally agreed that the strong band at about 3.5μ in the spectra of organic compounds is to be identified with the vibration of the hydrogen atom against the carbon atom. Similarly the band at about 28μ is to be identified with the vibration of carbon against carbon. This assumption of the spring-like nature of these chemical bonds is supported by several lines of evidence. The assignment of a characteristic frequency to a given bond permits the calculation of the force constant of the bond. This in turn leads to the calculation of the heat of linkage.[3] There is good agree-

[1] J. W. Ellis, Phys. Rev. **23**, 48 (1924); **27**, 298 (1926), **28**, 25 (1926).
[2] J. W. Sappenfield, Phys. Rev. **33**, 37 (1929).
[3] Grundriss der Phys. Chem., A. Eucken, p. 459ff(1924) (References) J. W. Ellis, Phys. Rev. **33**, 27 (1929).

ment between the observed and computed values. Moreover these characteristic frequencies, when used in Einstein's formula,[4] and Debye's formula,[5] should give the specific heat curve of the compound at low temperatures. There seems to be reasonably good agreement between the computed curves and the observed values.[6]

It has therefore seemed worthwhile to consider a little more closely the free periods of vibration which one would expect from a mechanical model of one of these molecules, or from a group of molecules. To this end we shall consider the molecules under discussion as being represented by a series of massive particles attached at regular intervals to a massless elastic string. We shall first determine the free periods of a single group of massive particles, or of a single molecule, when various restrictions are placed on the ends of the molecule or group. We shall next consider the effect upon these periods of coupling two or more molecules or groups together, and shall thus determine the free periods of a system consisting of a number of identical molecules or groups coupled together. Such a system may be realized in the crystals of organic chain compounds. We shall finally be able to obtain the free periods of a single group of pn particles, and then to determine the effects produced on these frequencies by rearranging the pn component particles into various groupings (such as p groups of n particles each) keeping the total number of particles present always the same.

Mathematically we have here an extension of the problem of the vibration of a loaded string which has been treated by Lagrange,[7] Lord Rayleigh,[8] and others. The second order differential equations which arise from this problem are similar to those which arise in the solutions of the modes of vibration of other systems, particularly in the solution of wave filter problems. The analogous electrical case of the finite wave filter has been treated by Pupin,[9] Campbell,[10] Carson,[11] Wheeler and Murnaghan,[12] and others.

The method of solution consists, as usual, in setting up the differential equations of motion, which can be solved for periodic vibrations if a certain algebraic equation equals zero. This equation is known as the secular or characteristic equation. The roots of this equation give the frequencies of the free vibrations. In what follows we shall limit ourselves to motion in one dimension. In general, under these conditions, a system of N particles will possess N frequencies. If the system is free to move as a whole, or to rotate uniformly, the corresponding frequency is zero.

The system of particles which we shall discuss is obtained by arranging

[4] A. Einstein, Ann. d. Physik **28,** 180 (1907).

[5] P. Debye, Ann. d. Physik **39,** 789 (1912).

[6] D. H. Andrews, Proc. Roy. Acad. Amsterdam **29,** 744 (1926); Chemical Reviews **5,** 533 (1928).

[7] Mecanique Analytique, Lagrange, vol. 1, pp. 382–395 (1811).

[8] Theory of Sound, Lord Rayleigh; vol. 1, p. 120 (1877).

[9] M. Pupin, Proc. A.I.E.E. **16,** 93 (1899).

[10] G. A. Campbell, Bell System Tech. J. p. 1, November 1922.

[11] Electric Circuit Theory and Operational Calculus, Carson, p. 132 ff. (1926).

[12] H. A. Wheeler and F. D. Murnaghan, Phil. Mag. **6,** 146 (1928).

pn equal particles into p groups of n particles each. We now introduce a small quantity, d, which we call the "coupling coefficient" and which measures the ratio of the force acting between the groups to the force inside of the group. An inspection of Fig. 1 will indicate that when $d=1$ the forces acting between the groups are the same as the forces acting within the groups, there is not longer any distinction between "groups," and we have the elementary case of the uniformly loaded string. The situation existing when $d=0$ must be examined with a little more care since d is defined as the ratio of two quantities. If d vanishes due to the fact that the internal forces present in each group are infinite we must say that we no longer have any vibrating group structure present. Our system will therefore vibrate as a uniformly loaded string of p particles, each of mass nm, the force constant of the string being that of the inter-group force. We have present the p frequencies characteristic of these p groups, while the other $p(n-1)$ internal frequencies

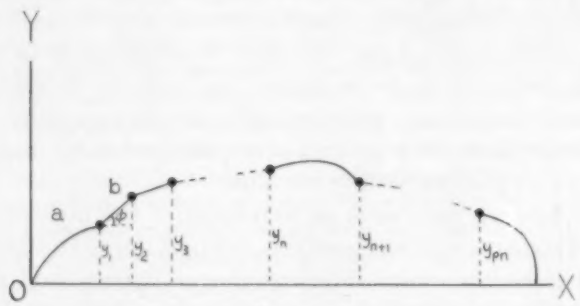

Fig. 1.

have been shifted to infinity. On the other hand if d vanishes due to the fact that the force between the groups has become infinitely small we must say that we have p groups present as before, but each infinitely removed from its neighbors and therefore entirely unaffected by them. We shall therefore expect the pn free periods of such a system to be the n free periods of a single group of n particles with free ends, each free period being repeated p times. These n frequencies characteristic of a single group of n particles with free ends will consist of one frequency, $\nu=0$, which corresponds to the vibration. When d has become small, but both forces remain finite, we can predict in a general way the behavior of the free periods. The p slowest vibrations will be slight modifications of the p vibrations which would be present if each group vibrated as a rigid whole, and on the other hand can be considered as corresponding to the p vibrations of frequency 0 for the p free molecules or groups. Similarly the $p(n-1)$ faster vibrations will be slight modifications of, and will therefore group themselves about, the $(n-1)$ internal vibrations which would be present if each group were entirely separated from its neighbors. While these, however, had been p-fold in the case of the independent molecules or groups, these p coinciding frequencies will be split up now into p separate components by the effect of the coupling.

II. Statement of the Mathematical Problem

Let us consider the motion of a massless, elastic string on which are fastened a number of massive particles of common mass "m". Let these particles be arranged in identical and recurring groups of "n" particles, the common distance between particles of the same group being b. Let the distance between the n^{th} particle of any one group and the 1^{st} particle of the next group be a, there being p groups in all, see Fig. 1. Let the initial, uniform, tension in the string be T. Let us confine ourselves for the moment to small lateral displacements, all in the same plane, these displacements being so small that we may replace the sines of the angles by the angles themselves. This means that we can say, Fig. 1,

$$\sin\phi = \tan\phi = (y_r - y_{r-1})/a \text{ or } (y_r - y_{r-1})/b$$

We will so choose our axes that $y_0 = y_{pn+1} = 0$.

It is to be noted here that the introduction of the concept of an elastic spring under tension is a matter of convenience and not of necessity. In the same way we have restricted ourselves to small vertical displacements from convenience and not from necessity, We might have started equally well with a system of identical groups of particles in equilibrium under the influence of quasielastic restoring forces of any origin whatever. We have in this case to define a force constant which will be the restoring force per unit displacement acting on the r^{th} particle due to its displacement with respect to the $(r+1)^{st}$ or $(r-1)^{st}$ particle. This force constant we may call τ when the neighboring particle under consideration belongs to the same group as the r^{th} particle, and τ' when the neighboring particle under consideration does not belong to the same group as the r^{th} particle. The equations which will be obtained as Eqs. (1) will be found to follow immediately with the replacing of T/a and T/b by τ' and τ respectively. It will be noted in the following equations that the tension T always occurs in the expression T/a or T/b, which has the dimensions $F.L^{-1}$ as it should. It is apparent from what has been said that our coordinates y_r may be looked upon as generalized coordinates, the quantities which will occur in Eqs. (1) as $m\ddot{y}$ may be looked upon as generalized inertial forces, and the corresponding expressions such as $T/b(-y_{r-1}+2y_r-y_{r+1})$ may be looked upon as generalized forces of restitution. The equations which will be obtained as Eqs. (1) are then equally capable of representing motions along the axis of X, perpendicular to the axis of X, rotations about this axis, or oscillations in properly coupled electrical circuits. The quantity defined as "d", Eq. (3) will be given, in the light of the definitions of this paragraph as τ'/τ.

We can now write down the expressions for the kinetic and potential energy of the system,[13] and set up the equations of motion by Lagrange's equations,

$$T - V = L$$

[13] Partial Differential Equations of Mathematical Physics, Webster, p. 91, (1927).

$$\frac{d}{dt}\left(\frac{\partial L}{\partial \dot{y}_r}\right) - \frac{\partial L}{\partial y_r} = 0.$$

More simply we may resolve the forces parallel to the direction of y and obtain, after a little rearrangement,

$$\begin{aligned}
&m\ddot{y}_1 + (T/a)y_1 + T/b(y_1 - y_2) = 0\\
&m\ddot{y}_2 + T/b(-y_1 + 2y_2 - y_3) = 0\\
&\cdots\cdots\cdots\cdots\cdots\cdots\cdots\cdots\\
&\cdots\cdots\cdots\cdots\cdots\cdots\cdots\cdots\\
&m\ddot{y}_n + T/b(y_n - y_{n-1}) + T/a(y_n - y_{n+1}) = 0\\
&m\ddot{y}_{n+1} + T/a(y_{n+1} - y_n) + T/b(y_{n+1} - y_{n+2}) = 0\\
&\cdots\cdots\cdots\cdots\cdots\cdots\cdots\cdots\\
&\cdots\cdots\cdots\cdots\cdots\cdots\cdots\cdots
\end{aligned} \tag{1}$$

We now make the usual substitution

$$y_r = C_r \exp(-\lambda^{1/2}t). \tag{2}$$

Divide the equations by the common factor $\exp((-\lambda)^{1/2}t)$, and multiply by the common factor b/T. The following definitions become obvious,

$$\begin{aligned}
(-mb\lambda)/T + 2 &= A\\
(-mb\lambda)/T + 1 + b/a &= B\\
b/a &= d
\end{aligned} \tag{3}$$

Manifestly

$$A + d - 1 = B.$$

Making the substitutions indicated in Eq. (3) and rearranging terms we obtain from Eq. (1),

$$\begin{aligned}
BC_1 - C_2 &= 0\\
-C_1 + AC_2 - C_3 &= 0\\
-C_2 + AC_3 - C_4 &= 0\\
&\cdots\cdots\cdots\cdots\\
&\cdots\cdots\cdots\cdots\\
-C_{n-2} + BC_{n-1} - dC_n &= 0\\
-dC_{n-1} + BC_n - C_{n+1} &= 0\\
&\cdots\cdots\cdots\cdots\\
&\cdots\cdots\cdots\cdots\\
-C_{pn-1} + BC_{pn} &= 0.
\end{aligned} \tag{4}$$

The condition for a solution giving values for the C's other than zero is that the determinant of the coefficients shall vanish. This gives a determinant of the pn^{th} order which we shall designate as F_p. It is to be understood by this notation that F_p represents the determinant of the pn^{th} order obtained from Eqs. (4) written for p identical groups of n particles each. We shall not be interested in this particular determinant when there are not exactly n particles in each group. The determinantal equation is

$$
F_p = \begin{vmatrix}
B & -1 & 0 & 0 & 0 & 0 & 0 & 0 & 0 & \cdots & & & & \cdots & 0 & 0 \\
-1 & A & -1 & 0 & 0 & 0 & 0 & 0 & 0 & \cdots & & & & \cdots & 0 & 0 \\
0 & -1 & A & -1 & 0 & 0 & 0 & 0 & 0 & \cdots & & & & \cdots & 0 & 0 \\
0 & 0 & -1 & B & -d & 0 & 0 & 0 & 0 & \cdots & & & & \cdots & 0 & 0 \\
0 & 0 & 0 & -d & B & -1 & 0 & 0 & 0 & \cdots & & & & \cdots & 0 & 0 \\
0 & 0 & 0 & 0 & -1 & A & -1 & 0 & 0 & \cdots & & & & \cdots & 0 & 0 \\
0 & 0 & 0 & 0 & 0 & -1 & A & -1 & 0 & \cdots & & & & \cdots & 0 & 0 \\
0 & 0 & 0 & 0 & 0 & 0 & -1 & B & -d & \cdots & & & & \cdots & 0 & 0 \\
0 & 0 & 0 & 0 & 0 & 0 & 0 & -d & B & \cdots & & & & \cdots & 0 & 0 \\
\cdots & \cdots & \cdots & \cdots & \cdots & \cdots & \cdots & \cdots & \cdots & \cdots & \cdots & \cdots & \cdots & \cdots & \cdots & \cdots \\
\cdots & \cdots & \cdots & \cdots & \cdots & \cdots & \cdots & \cdots & \cdots & \cdots & \cdots & \cdots & \cdots & \cdots & \cdots & \cdots \\
0 & 0 & \cdots & & & & & & & \cdots & 0 & -1 & A & -1 & 0 & 0 \\
0 & 0 & \cdots & & & & & & & \cdots & 0 & 0 & -1 & A & -1 & 0 \\
0 & 0 & \cdots & & & & & & & \cdots & 0 & 0 & 0 & -1 & B & -d \\
0 & 0 & \cdots & & & & & & & \cdots & 0 & 0 & 0 & -d & B & -1 \\
0 & 0 & \cdots & & & & & & & \cdots & 0 & 0 & 0 & 0 & -1 & A \\
0 & 0 & \cdots & & & & & & & \cdots & 0 & 0 & 0 & 0 & 0 & -1
\end{vmatrix}
\begin{matrix} \\ \\ \\ \\ \\ \\ \\ \\ \\ \\ \\ \\ \\ \\ \\ \\ \end{matrix}
\begin{matrix} = 0 \quad (5) \\ \\ \\ \\ \\ \\ \\ \\ \\ \\ \\ \\ \\ \\ \\ \\ \end{matrix}
\begin{matrix} \\ \\ \\ \\ \\ \\ \\ \\ \\ \\ \\ \\ \\ \\ \\ pn^{th} \text{ order} \end{matrix}
$$

For convenience the groups have been represented as having a limited number of terms, $n = 4$.

This determinant is a function of the unknown $\lambda (= 2\pi\nu^2$ where ν is the frequency) which is the variable entering through the quantities A and B. The solution of the problem will consist in finding those values of λ which will reduce the determinant to zero. A direct expansion of Eq. (5) will lead to an algebraic equation of the pn^{th} degree in λ. If it were possible to solve this algebraic equation, the resulting pn roots of λ would lead to the pn desired free periods of the system. This is the number of free periods which we expect from the number of degrees of freedom possessed by the system. Such a direct method of solution is not feasible in general. We must therefore look for transformations which will reduce Eq. (5) to a more tractable form. The general method of attack has been pointed out by Wheeler and Murnaghan.[12] The method consists essentially in reducing the expansion of Eq. (5) to a trigonometric equation in which the unknown, θ, is defined as a function of λ. The resulting trigonometric equation is well adapted to the processes of approximation.

An inspection of the determinant F_p will disclose that it is made up of certain simpler and recurring groups. As will be seen later the expansion of the complete determinant is obtained in terms of these sub-groups. We shall therefore define the following determinants:

$$D_n(d,d) = \begin{vmatrix} B & -1 & 0 & 0 & 0 \cdots & & & \cdots 0 \\ -1 & A & -1 & 0 & 0 \cdots & & & \cdots 0 \\ 0 & -1 & A & -1 & 0 \cdots & & & \cdots 0 \\ \cdots & \cdots & \cdots & \cdots & \cdots & \cdots & \cdots & \cdots \\ \cdots & \cdots & \cdots & \cdots & \cdots & \cdots & \cdots & \cdots \\ 0 & 0 \cdots & & & \cdots 0 & -1 & A & -1 & 0 \\ 0 & 0 \cdots & & & \cdots 0 & 0 & -1 & A & -1 \\ 0 & 0 \cdots & & & \cdots 0 & 0 & 0 & -1 & B \end{vmatrix} \quad n^{\text{th}} \text{ order} \qquad (6)$$

$$D_n(1,d) = \begin{vmatrix} A & -1 & 0 & 0 \cdots & & & \cdots 0 \\ -1 & A & -1 & 0 \cdots & & & \cdots 0 \\ 0 & -1 & A & -1 \cdots & & & \cdots 0 \\ \cdots & \cdots & \cdots & \cdots & \cdots & \cdots & \cdots \\ \cdots & \cdots & \cdots & \cdots & \cdots & \cdots & \cdots \\ 0 & 0 \cdots & & & \cdots 0 & -1 & A & -1 & 0 \\ 0 & 0 \cdots & & & \cdots 0 & 0 & -1 & A & -1 \\ 0 & 0 \cdots & & & \cdots 0 & 0 & 0 & -1 & B \end{vmatrix} \quad n^{\text{th}} \text{ order.} \qquad (7)$$

$$D_n(1,1) = \begin{vmatrix} A & -1 & 0 & 0 \cdots & & & \cdots 0 \\ -1 & A & -1 & 0 \cdots & & & \cdots 0 \\ 0 & -1 & A & -1 \cdots & & & \cdots 0 \\ \cdots & \cdots & \cdots & \cdots & \cdots & \cdots & \cdots \\ \cdots & \cdots & \cdots & \cdots & \cdots & \cdots & \cdots \\ 0 & 0 \cdots & & & \cdots 0 & -1 & A & -1 \\ 0 & 0 \cdots & & & \cdots 0 & 0 & -1 & A \end{vmatrix} \quad n^{\text{th}} \text{ order} \qquad (8)$$

The determinant $D_n(1,1)$ is the determinant of the uniformly loaded string,[13] and of the elementary wave filter.[12] The present notation has been adopted since the determinant $D_{pn}(1,1)$, see Eq. (8), can be obtained from the general determinant F_p, Eq. (5), by putting the quantity d everywhere equal to unity. The d's then disappear from the determinant itself, and the quantity B becomes equal to the quantity A, see Eq. (3). Similarly the determinant $D_n(1,d)$ is obtained from the determinant $D_n(1,1)$ by replacing one of the A's which constitute the terminal elements of the principal diagonal by the quantity B which is $A+d-1$. In the same way the determinant $D_n(d,d)$ is obtained from the elemental determinant $D_n(1,1)$ by replacing both of the A's which constitute the terminal elements of the principal diagonal by the quantity B.

Let us now make the following definitions:*

* The author is indebted to Prof. F. D. Murnaghan for these substitutions.

$$H_p = F_p\mu^{-p} \tag{9}$$

$$\mu = +\, d(D_{n-1}^2(1, d) - D_n(d, d)D_{n-2}(1, 1))^{1/2} \tag{10}$$

$$\xi = \frac{D_n(d, d) - d^2D_{n-2}(1, 1)}{\mu}. \tag{11}$$

It can then be readily shown that the expansion of Eq. (5) is equivalent to

$$H_p = \xi H_{p-1} - H_{p-2}. \tag{12}$$

The condition that $F_1 = D_n(d,d)$ leads to the following definitions

$$H_0 = 1 \tag{13}$$

$$H_1 = \frac{D_n(d, d)}{\mu}. \tag{14}$$

We see from an inspection of Eq. (12) and Eq. (11) that the general solution for H_p will depend upon the values assumed by the determinants which we have defined in Eqs. (6), (7) and (8). These determinants are special cases of the determinant F_p as should be evident from Eq. (5). Since a knowledge of these special cases is necessary for a complete solution, we shall digress here to consider the form assumed by F_p when we have only one group present, $p = 1$.

III. Solution of Certain Limiting Cases

(A) The uniformly loaded string (Lagrange's problem).

The solution for the free periods of the uniformly loaded string, which is given by

$$D_n(1, 1) = 0$$

where

$$p = 1$$

$$d = 1 \text{ in } Eq.\ (5)$$

is so well known [12,13] that we shall merely state the result here, since it will be used constantly in what follows. The determinant may be expanded yielding

$$D_n(1, 1) = AD_{n-1}(1, 1) - D_{n-2}(1, 1).$$

This gives

$$D_n(1, 1) = \frac{\sin\,(n + 1)\theta}{\sin\,\theta} \tag{15}$$

if we make the substitution

$$A = (-\,mb\lambda)/T + 2 = 2\cos\theta \tag{16}$$

The solution

$$D_n(1, 1) = 0$$

is given by

$$\theta = K\pi/(n + 1), \quad K = 1, 2, \cdots, n \tag{17}$$

The values of θ given by Eq. (17) together with Eq. (16) connecting $A(\lambda)$ and θ give us the free periods of the system. There are n possible frequencies, as is necessary for n particles.

(B) The single group of n particles with $d \neq 1$ at its terminal elements.

This case may be represented physically by a molecule, as of an organic chain compound, which is restrained at its ends by quasielastic restoring forces which differ from the restoring forces acting within the molecule itself.

Let us consider the case

$$F_1 = 0.$$

The solution in this case is exactly analogous to that of the finite wave filter,[12] and will be obtained in the same way. Let us generalize and assume that the coupling coefficient d is not the same at the two ends. The determinantal equation then becomes

$$D_n(d, d') = \begin{vmatrix} B & -1 & 0 & 0 \cdots & & \cdots 0 \\ -1 & A & -1 & 0 \cdots & & \cdots 0 \\ 0 & -1 & A & -1 \cdots & & \cdots 0 \\ \cdots & \cdots & \cdots & \cdots & \cdots & \cdots \\ \cdots & \cdots & \cdots & \cdots & \cdots & \cdots \\ 0 & 0 \cdots & & \cdots 0 & -1 & A \quad -1 \\ 0 & 0 \cdots & & \cdots 0 & 0 & -1 \quad B' \end{vmatrix} \quad n^{\text{th}} \text{ order.} \tag{18}$$

where

$$B = A + d - 1$$
$$B' = A + d' - 1$$

and all the other quantities have the same meanings as before. Direct expansion shows that

$$D_n(d, d') = D_n(1, 1) + (d + d' - 2)D_{n-1}(1, 1) + (d - 1)(d' - 1)D_{n-2}(1, 1).$$

With the aid of Eq. (15) this becomes, when $D_n(d,d') = 0$

$$D_n(d, d') = \frac{\sin(n+1)\theta + (d + d' - 2)\sin n\theta + (d - 1)(d' - 1)\sin(n - 1)\theta}{\sin\theta} = 0 \tag{19}$$

It is apparent that Eq. (19) may be adjusted to any given values of the coupling coefficients d and d'. That is, we may now write the explicit expressions in terms of θ for $D_n(d,d)$, $D_n(1,d)$, $D_n(1,0)$, and $D_n(0,0)$ from Eq. (19). The solutions of the resulting trigonometric equations can be carried to as

high a degree of approximation as is necessary. Two cases, in which an exact solution becomes possible, are of interest.

The solution for a uniformly loaded string free at one end, $D_n(1,0)$, a case which was discussed but not carried to completion by Lagrange,[7] is obtained by putting $d=1$ and $d'=0$ in Eq. (19). The equation for θ then readily reduces to

$$\frac{\cos(n+\frac{1}{2})\theta}{\cos n\theta \sin \theta/2} = 0$$

Whence

$$\theta = \frac{2k+1}{2n+1}\pi, \quad k = 0, 1, 2, \cdots, n. \tag{20}$$

The solution corresponding to $k=0$ corresponds to a rotation and expansion of the entire system about its point of support, all the particles lying on a straight line. Besides, there are $(n-1)$ oscillatory motions.

The solution for a uniformly loaded string free at both ends, $D_n(0,0)$ is obtained by putting both d and d' equal to zero in Eq. (19). The trigonometric equation then becomes

$$\tan n\theta = 0$$

Whence

$$\theta = \frac{k}{n}\pi, \quad k = 0, 1, 2, \cdots, (n-1). \tag{21}$$

The solution corresponding to $k=0$, which gives $\theta=0$ and consequently $\nu=0$, corresponds to a motion of the entire system as a rigid whole. If $k=n$, which gives $\theta=\pi$, we do not have a solution since in this case both numerator and denominator of Eq. (19) vanish and their ratio is not zero.

IV. Solution of the General Determinantal Equation for p Groups, $H_p=0$

(A) Formal solution in terms of θ and Γ.

We can now proceed with the formal solution of the general determinant H_p.

$$H_p = \xi H_{p-1} - H_{p-2} \tag{12}$$

Eq. (12) is in the standard form[12] and if we make the substitution

$$\xi = 2\cos\Gamma \tag{22}$$

the equation can be thrown into the form

$$H_p = \frac{\sin(p+1)\Gamma + d\sin(n-1)\theta/\sin\theta \times \sin p\Gamma}{\sin\Gamma} = 0. \tag{23}$$

The solution of our problem therefore consists in the solution of Eq. (23) together with our two equations of definition, Eqs. (16) and (22), which may be put in the form

$$\xi = \frac{2(1-\cos\theta)(d-1)\sin n\theta + 2d\sin\theta\cos n\theta}{d\sin\theta} = 2\cos\Gamma \tag{24}$$

$$A = (-mb\lambda)/T + 2 = 2\cos\theta \tag{16}$$

(B) Approximate solution of $H_p=0$.

An exact solution of these equations is not, in general, possible. An approximate solution can be obtained, however, when the coupling coefficient d, is small. We have already found, Eq. (21), that when $d=0$ the values of θ are given by $(k/n)\pi$. Moreover, when $d=1$ the values of θ are given by $k\pi/(n+1)$, Eq. (17). We can therefore say, when d is small,

$$\theta_k = \frac{k\pi}{n} + \Delta\theta_k, \quad k = 0, 1, 2, \cdots, (n-1) \tag{25}$$

where $\Delta\theta_k$ is a small quantity of order d or less. We shall now inquire as to the values assumed by the expression occurring in Eq. (23), $d\sin(n-1)\theta/\sin\theta$, when θ has the value given by Eq. (25). Direct substitution shows that

$$\frac{d\sin(n-1)\theta}{\sin\theta} \cong d(n-1).$$

If we will restrict ourselves to cases in which $d(n-1)$ is small in comparison with unity Eq. (23) becomes $\sin(p+1)\Gamma+$(a small quantity of order dn) $\sin p\Gamma=0$. An approximate solution for Γ will obviously lie near $(s\pi/p+1)$ and we therefore write for the solution of Γ

$$\Gamma_s = \frac{s\pi}{p+1} + \Delta\Gamma_s, \quad s = 1, 2, \cdots, p \tag{26}$$

$\Delta\Gamma_s$ is a small quantity whose value is to be determined by successive approximations. In making this approximation we assume that $(p+1)\Delta\Gamma_s$ is so small that we can replace the sines of the angles by the angles themselves.

The substitution of Eqs. (25) and (26) in Eqs. (23) and (24) and the evaluation of $\Delta\Gamma_s$ and $\Delta\theta_k$ is tedious but straightforward, yielding finally for the pn desired values of θ,

$$\left.\begin{aligned}
&\theta_{0s} = 2\left(\frac{d+d^2}{n}\right)^{1/2}\sin\frac{s\pi}{2(p+1)} \\
&s = 1, 2, \cdots, p \\
&(k=0) \\
&\theta_{ks} = \frac{k\pi}{n} + (-1)^k\frac{d}{n}\cot\frac{k\pi}{2n}\left[(-1)^k\left(1+d-\frac{d}{2n}-\frac{d}{p+1}\right)\right. \\
&\qquad \left.-\left(1+d-\frac{d}{n}\right)\cos\frac{s\pi}{p+1} - (-1)^k\left(\frac{d}{2n}-\frac{d}{p+1}\right)\cos^2\frac{s\pi}{p+1}\right] \\
&s = 1, 2, \cdots, p \\
&k = 1, 2, \cdots, (n-1).
\end{aligned}\right\} \tag{27}$$

The frequencies of the free periods are obtained through the definition

$$A = (-mb\lambda)/T + 2 = 2\cos\theta. \tag{16}$$

From this equation we readily obtain

$$\nu_{ks} = \frac{\lambda_{ks}}{2\pi} = \frac{1}{\pi}\sqrt{\frac{T}{mb}}\sin\frac{\theta_{ks}}{2}. \tag{28}$$

V. Solution for Two Groups Coupled Together

The solution for the free periods of a system consisting of only two groups coupled together is of some interest, since the solutions can be obtained quite as directly as in the case of a single group, and can as readily be carried to any desired degree of accuracy. We shall therefore consider two cases in which there are only two groups present.

(A) Two groups coupled together and to fixed supports.

In this case in which we have two groups coupled together and to fixed supports we obtain from Eq. (5)

$$F_2 = D_n^2(d, d) - d^2 D_{n-1}^2(1, d). \tag{29}$$

The condition for a solution is, as usual,

$$F_2 = 0.$$

Using Eq. (19), $(d = d')$, and Eq. (15), this expression becomes

$$\left[\frac{\sin(n+1)\theta + 2(d-1)\sin n\theta + (d-1)^2\sin(n-1)\theta}{\sin\theta}\right]^2 - d^2\left[\frac{\sin n\theta + (d-1)\sin(n-1)\theta}{\sin\theta}\right]^2 = 0. \tag{30}$$

On transposing, extracting the square root, and using first the + and then the − sign, we obtain the two following equations

$$\frac{\sin(n+1)\theta + (d-2)\sin n\theta - (d-1)\sin(n-1)\theta}{\sin\theta} = 0 \tag{31}$$

$$\frac{\sin(n+1)\theta + (3d-2)\sin n\theta + (2d^2-3d+1)\sin(n-1)\theta}{\sin\theta} = 0 \tag{32}$$

The solution of these equations can be carried to as high a degree of approximation as is necessary, for any values of the coupling coefficient, d, whatever.

(B) Two groups coupled together, but with free ends.

We may also readily obtain the free periods of a system consisting of two groups of n particles each coupled together but with free ends. This means that $d = 0$ at the 1^{st} and $2n^{th}$ particles. The determinantal equation is

obtained from Eq. (5) written for only two groups when the terminal elements B of the principal diagonal are replaced by B' where

$$B' = A - 1.$$

Let us call this determinant F_2'. With the aid of these definitions we obtain by expansion as before, see Eqs. (6), (7) and (9),

$$F_2' = D_n^2(d, 0) + d^2 D_{n-1}^2(1, 0).$$

The condition for a solution is, as usual,

$$F_2' = 0.$$

With the aid of Eq. (19) this becomes

$$\frac{\sin (n+1)\theta + (d-2)\sin n\theta - (d-1)\sin (n-1)\theta}{\sin \theta} = \pm d \frac{\sin n\theta - \sin (n-1)\theta}{\sin \theta} \tag{33}$$

On expanding the multiple angles and collecting we have

$$\frac{2 \sin n\theta(\cos \theta - 1)}{\sin \theta} = 0 \tag{34}$$

and

$$\tan n\theta = \frac{d}{1-d} \cot \frac{\theta}{2}. \tag{35}$$

From Eq. (34) we have

$$\theta = \frac{k\pi}{n}, \quad k = 0, 1, 2 \cdots (n-1) \tag{36}$$

The n roots of Eq. (35) must be approximated.

It is interesting to note that if $d = \frac{1}{2}$, Eq. (35) also becomes capable of exact solution, the roots being given by

$$\theta = \frac{2k+1}{2n+1}\pi, \quad k = 0, 1, 2, \cdots, (n-1)\dagger \tag{37}$$

We obtain the free periods by means of our fundamental definition given in Eq. (16), $A(\lambda) = 2 \cos\theta$.

VI. Discussion

A discussion of the results obtained here is most readily undertaken with the aid of a specific example. We have therefore represented in Fig. 2 the free periods which may be obtained from a group of 9 particles under the various arrangements discussed in this paper. For convenience the factor $(1/\pi)(T/mb)^{1/2}$ has been taken equal to unity. When we have the 9 particles

† Here again the value $k = n$, giving $\theta = \pi$, must be rejected due to the vanishing of the denominator in Eq. (33).

arranged in a uniform group and coupled to a supporting wall with a coupling coefficient $d=1$, we have the frequencies given by the well known formula. Eq. (17), as is shown in case (a). When the coupling coefficient between the group and the support is reduced to $d=0.1$, each of the previous frequencies is decreased, the slower ones more than the faster ones, as is illustrated in case (b). This slowing up of the frequencies with decreasing d is continued until, when $d=0$, the slowest frequency has become zero itself, see case (c). Now let the 9 particles be rearranged into 3 groups of 3 particles each, with a coupling coefficient $d=0.1$ between each group and between the end groups and the supporting walls. The 9 frequencies present rearrange themselves into three sharply defined groups of three frequencies each, see case (d). The number of groups of frequencies present is determined by the number of particles present in each group, that is by the internal structure of the

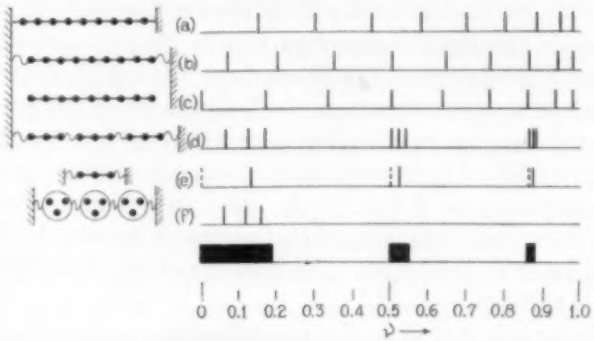

Fig. 2. The free periods obtained from various arrangements of a system consisting of 9 massive particles; $1/\pi \cdot T/mb^{1/2}=1$

groups under consideration. On the other hand the number of separate frequencies present in each group of frequencies is determined by the total number of groups present in the system. In case (e) we have plotted the frequencies due to three particles arranged in a single group with coupling coefficient $d=0.1$. The dotted lines in case (e) represent the frequencies which would be present if $d=0$. Similarly in case (f) we have plotted the frequencies which would present if each group of case (d) vibrated as a rigid whole. We may speak of these frequencies as the "unmodified group vibrations" of such a system as that shown in case (d). Similarly the two higher frequencies of case (e) may be spoken of as the "unmodified internal vibrations." We may therefore say that the effect of rearranging a single group of pn particles into p groups of n particles each is to rearrange the pn free periods of the original group into n distinct groups of p frequencies each. Or, the effect of coupling together p originally independent groups of n particles each is to slightly modify the p slow group vibrations which would be present if each group vibrated as a rigid whole, and to split each of the $(n-1)$ internal vibrations into p separate components.

When the number of groups present has become infinite, as will be true for all practical purposes in any physical crystal, the number of frequencies

present in any one group becomes infinite and we have bands instead of groups, see case (g). The lower limit of each band is determined solely by the corresponding "unmodified" frequency of a single group with coupling coefficient $d=0$. See the dotted lines in case (e), Fig. 2. The upper limit, for any given band, is determined solely by the values of d and n, if $p=\infty$. The first and slowest band corresponds to the well-known Debye spectrum of group vibrations, but with a slightly modified upper limit.

Let us now inquire as to the distribution of the individual frequencies within these groups when p has become large but not infinite. To do this we form $(\partial\nu_{ks}/\partial s)$. From Eq. (28) we get

$$\frac{\partial\nu_{ks}}{\partial s}=\frac{1}{2\pi}\left(\frac{T}{mb}\right)^{1/2}\cos\frac{\theta_{ks}}{2}\frac{\partial\theta_{ks}}{\partial s}.$$

It is evident that the frequencies will be closest together, that is to say the density of lines in the elastic spectrum will be greatest, when $(\partial\nu_{ks}/\partial s)$ is a minimum. An investigation of the above expression with the aid of Eqs. (27) shows that, to a first approximation, the frequencies of the group, or Debye, vibrations crowd together or converge toward the high frequency limit of the group. The grouping of the frequencies is exactly analogous to that holding in cases (a), (b), and (c) of Fig. 2. In the case of the internal vibrations, to a first approximation, the frequencies converge toward both the high and low frequency limits of the group. The lines here have their minimum density at the center of the group.

It is not to be inferred from the preceding discussion of frequencies and bands that each of the frequencies predicted by Eqs. (27) can be expected to appear in the optical spectrum of the corresponding compound. The question of the optical activity of a given frequency is essentially a question concerning the electric moment of the molecule. It is hoped that an investigation of this question can be made at a later date.

VII. Application to the Specific Heats of Organic Compounds

Although it is not the purpose of this paper to discuss in detail the applications of the equations just derived, an obvious example will be given. If we have, by any means, an approximate value for the forces of restitution acting upon an atom in a crystal of an organic chain compound, we have here the means for computing its free periods. By applying the proper Debye or Einstein functions we can then compute its specific heat as a function of temperature. The frequencies arising from the terms containing θ_{0s}, being molecular vibrations, will give rise to a Debye term. It is necessary then to know only the upper limit of the terms defined by θ_{0s}, that is θ_{0p}. When p becomes large this term becomes $\theta_{0p}=2(d+d^2/n)^{1/2}$ For the internal vibrations it will in general suffice to neglect the correction terms in Eqs. (27) and write $\theta_{ks}=k\pi/n$. In case the frequency band is unusually wide, as will be the case with the "internal" bands of hexyl alcohol, we may

use the average frequency of the band in the specific heat formula. Even in this case the correction is practically negligible.

For the force of restitution due to a displacement along the length of the molecular chain we will take 4×10^5 dynes/cm. This force will give a band in the neighborhood of 28μ for all our compounds. For the force of restitution due to a displacement perpendicular to the length of the chain we will take 0.12×10^5 dynes/cm. This value has been chosen more or less arbitrarily to fit the data. It is, however, of the same order of magnitude as the corresponding constants proposed by Andrews[7,14] which range from 0.32 to 0.66×10^5 dynes/cm. It is to be noted that these constants are not forces of restitution due to a displacement along or perpendicular to the length of the valence bond itself, but are precisely as stated forces due to a displacement along or perpendicular to the length of the entire chain. The vibration of hydrogen against carbon has been neglected since others have shown that its effect is negligible.[6]

There seem s to be no reliable method for computing the forces acting between the molecules in organic crystals. The Lindemann formula[15] is strictly applicable to monatomic crystals, and Andrew's modification of it[6] is of doubtful service here because of the high lack of symmetry of the chain molecules. The intermolecular forces have, therefore, been chosen arbitrarily. At low temperatures, 20°K, the internal vibrations have for the most part ceased to contribute to the specific heat. A Debye function has therefore been chosen to fit the data at this point. From the value of ν_0 so chosen it is possible to compute the corresponding force constant and the coupling coefficient d. This has been done.

The Debye function has been computed for three degrees of freedom, which assumes an isotropic crystal. The Einstein functions arising from the internal vibrations have been taken as having two degrees of freedom when the motion is perpendicular to the length of the chain, and one degree of freedom when along the length of the chain. The heat absorbed due to the expansion of the crystal has been computed according to Andrew's modification of Nernst's formula[6]

$$C_p - C_v = (C_v^2)_{\text{molecule}} \times \frac{T}{T_m} \times 0.0214$$

where $(C_v)_{\text{molecules}}$ is the specific heat at constant volume arising from the Debye terms alone, T is the temperature at which computations are being made and T_m is the melting point of the crystal under investigation.

Specific heat data are available for four of the normal alcohols. The computations have therefore been carried through for these substances. The frequencies found, neglecting the correction terms, as well as the total band width to be expected, expressed as percent of the corresponding uncorrected frequency, are summarized in Table I. In this table ν_0 represents the upper

[14] J. R. Bates and D. H. Andrews, Proc. Nat. Acad. Sci. (U.S.A.), **14**, No. 2, 124 (1928), D. H. Andrews, Phys. Rev. **34**, 1626 (1929).

[15] F. A. Lindemann, Phys. Zeits. **11**, 609 (1910).

limit of the Debye terms, chosen arbitrarily to fit the data as stated above. The other frequencies, ν_1, ν_2, etc., represent the internal vibrations. The frequency bands, of width given by $\Delta\nu$, will always extend towards higher frequencies from the uncorrected frequency given in the table.

TABLE I.

	$10^{-11}\times$	ν_0	ν_1	ν_2	ν_3	ν_4	ν_5	ν_6
Methyl Alcohol	(Trans)	29	48					
	(Long)		277					
$\Delta\nu$ in %			0.6					
Ethyl Alcohol	(Trans)	25	35	60				
	(Long)		200	347				
$\Delta\nu$ in %			1.2	0.7				
Butyl Alcohol	(Trans)	48	22	41	57	67		
	(Long)		126	239	329	387		
$\Delta\nu$ in %			16	2.8	0.8	0.1		
Hexy Alcohol	(Trans)	48	16	32	44	55	64	69
	(Long)		91	177	255	320	370	400
$\Delta\nu$ in %			36	6.4	2.3	1.0	0.4	0.1

Using these frequencies the calculations for ethyl alcohol give the following results, where $3D(\ )$ represents a Debye function with 3 degrees of freedom, $1E(\ )$ represents an Einstein function with 1 degree of freedom. etc.

TABLE II. *Ethyl alcohol*, $n=3$.

T°K	30	60	90	150
$3D(120/T)$	3.0	4.9	5.5	5.8
$1E(959/T)$	—	—	—	0.1
$1E(1660/T)$	—	—	—	—
$2E(166/T)$	0.5	2.2	3.0	3.6
$2E(288/T)$	—	0.8	1.8	2.9
C_v corr.	—	0.2	0.4	0.7
Total C_p, Cal/Mol	3.5	8.0	10.6	13.1

The computations for the other alcohols have been carried through and are plotted in Fig. 3, in which the solid lines represent the curves computed in the manner just indicated and the plotted points the observed values given by the authors indicated.

From the Debye functions chosen to fit the data at low temperatures we get values of ν_0 which give us values for the constant d for each substance in the manner indicated above. The results are as follows:

TABLE III.

Substance	No. groups	d
Methyl Alcohol	2	0.011
Ethyl Alcohol	3	0.012
Butyl Alcohol	5	0.070
Hexyl Alcohol	7	0.096

With the exception of ethyl alcohol the coupling coefficient varies approximately as the number of groups in the molecule. The low value of the coupling coefficient in the case of ethyl alcohol may have significance when considered in connection with the ease with which this substance forms glasses at low temperatures.

The agreement of the computed values with the observed values is as close as is to be expected, considering the very approximate nature of the calculations. There are, to be sure, no reasons for believing that these organic crystals are actually isotropic as has been assumed. Neither can we be particularly certain about the correction applied according to Nernst's formula for the conversion of C_v into C_p. The value of the constant 0.0214 was chosen originally to fit the data obtained in the case of certain metals and halogen salts,[16] and we have no *apriori* reason for applying it directly

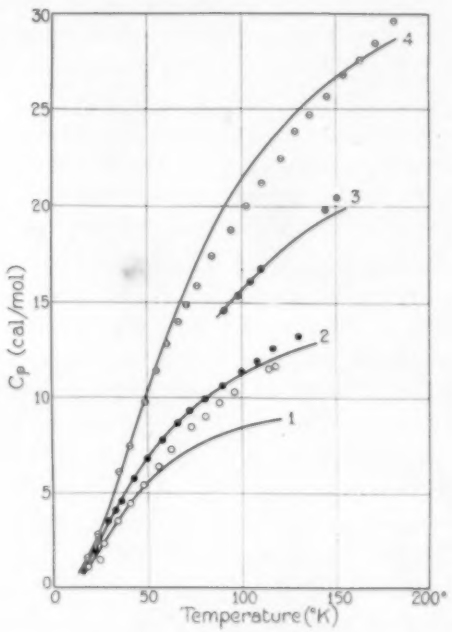

Fig. 3. C_p in cal/mol for the normal alcohols. (1) Methyl Alcohol K. K. Kelley, J. Amer. Chem. Soc. **51,** 180 (1929), (2) Ethyl Alcohol K. K. Kelley, J. Amer. Chem. Soc. **51,** 779 (1929), (3) Butyl Alcohol G. S. Parks, J. Amer. Chem. Soc. **47,** 338 (1925). (4) Hexyl Alcohol K. K. Kelley, J. Amer. Chem. Soc. **51,** 779 (1929).

to the case of organic crystals. Moreover these compounds have been treated as though each molecule was a uniformly loaded string which is actually not the case. The mass of the OH group is actually 17 as against 14 for the CH_2 group and 15 for the CH_3 group.

An additional remark should be made concerning the frequencies given in Table I. The values given under ν_0, the upper limit of the Debye frequencies, have been chosen, as stated, to fit the data at 20°K and, so far as the comput-

[16] W. Nernst and F. A. Lindemann, Zeit. f. Elektrochemie **17,** 818 (1911).

ations are concerned, may be looked upon as arbitrary constants. From these values of ν_0 values have been obtained for d which justify the original assumption that d is a small quantity. In the same way the absolute values of the frequencies of the internal vibrations are arbitrary, since the constant T/b was chosen more or less arbitrarily. These internal frequencies can therefore be considered significant only when taken in the ratio $\nu_1:\nu_2:\nu_3$ etc., or ν_1 (Methyl) : ν_1 (Ethyl) etc. The results of applying Eqs. (27) to the computation of the specific heats of organic crystals are thus largely not characteristic of this paper. That is to say, for reasonable values of d, and within the limits of experimental error, Eqs. (27) indicate that the correction terms in the expressions for ν_{ks} are negligible, and the computation of the internal frequencies reverts to the well-known case of the uniformly loaded string with free ends.

No explanation is offered for the unusually high value of the specific heat of methyl alcohol as compared with the theoretical curve. On the other hand the manner in which the other experimental points have been reproduced by the theoretical curves is taken as evidence of the essential soundness of the underlying assumptions and calculations. If the data were available it would be highly desirable to carry through the corresponding calculations for the higher members of this or some similar series of compounds.

In conclusion the author wishes to acknowledge his indebtedness to Professor D. H. Andrews who originally suggested the problem and who has been most kind in discussing its details. The author is also indebted to Professor F. D. Murnaghan for valuable suggestions in connection with the mathematical treatment. Finally it is a pleasure to acknowledge the continual assistence of Professor K. F. Herzfeld under whose direction this paper was written.

STUDIES IN CONTACT RECTIFICATION. II. THE CUPRIC SULFIDE-MAGNESIUM JUNCTION*

By Milton Bergstein, J. F. Rinke, and C. M. Gutheil
Research Laboratory, P. R. Mallory and Co., Inc., Indianapolis, Ind.

(Received June 19, 1930)

Abstract

The commercial cupric sulfide magnesium junction consists of a disk of heat-treated, compressed cupric sulfide powder contacted under pressure with the suitably oxidized face of a magnesium disk. This rectifier is of the non-integral class and of the sulfide group. Oscillographic evidence indicates the formation of a film which possesses relatively high resistance to current flow from the magnesium to the cupric disk, slow partial destruction of the film on continued current flow in the opposite (low resistance) direction and "reformation" of the film within 0.004 sec when sufficient voltage is applied to send a current in the high resistance direction. Similar evidence indicates that there is no battery or thermoelectric effect within the junction of sufficient magnitude to account for rectification and that film "formation" and "destruction" are consequently electrothermic rather than electrolytic in origin. The phenomenon of "reverse rectification" is described. It is related to the a.c. voltage across the junction. Preliminary results for the relationship between efficiency and operating temperature of a bridge-type unit are in qualitative agreement with the theories which require film formation.

Introduction

A CONTACT rectifier is a device composed of dry dissimilar solids in good electrical contact through which current flows readily in one direction but not in the other. Contact detectors are of this class. They are merely small-current rectifiers. Rectifiers of the cupric sulfide-magnesium type and of the copper oxide-copper type are in commercial use for the rectification of large current at low voltages (usually below 120 volts). A cupric sulfide-magnesium rectifier unit of the bridge type may be made to output anywhere from 1 to 10 amperes d.c. using junctions of 0.515 sq. in. available area none of which are operated in parallel. The number of junctions used depends on the output voltage desired. The current density is higher in this type unit than in any other known commercial contact rectifier.

In a previous paper one of the authors[1] has divided rectifying junctions into general divisions according to mechanical structure and chemical constitution of the electro-negative member and has indicated what phenomena any accepted theory of contact rectification must at least qualitatively explain. Various fundamental mathematical theories[2] as well as

* Paper presented at the Washington meeting of the A. P. S., April 25, 1930.

[1] M. Bergstein, Trans. Am. Electrochem. Soc. **57**, Reprint 19 (1930)

[2] W. Schottky, Zeits. f. Physik **14**, 63 (1923), I. Stransky, Zeits. Phys. Chem. **113**, 131 (1925); R. Audubert and M. Quintin, Compt. rend. **188**, 52 (1929).

symbols of a more mechanical nature[3] have been used to explain contact rectification. These latter depend on an analogy between contact rectifiers and electron tubes. The first theories proposed were based on a supposed thermoelectric or battery effect at the rectifying junction. These have been subjected to some criticism.[4] Flowers[5] favored a theory that a blocking film was alternately formed and destroyed on each half cycle and Goddard's[6] experiments led him to the conclusion, in anticipation of the theories of Ruben and of Slepian,[3] that film formation of some kind is a necessary corollary of contact rectification.

In work on the cupric sulfide-magnesium rectifier it became necessary to establish whether film formation within the junction between the members actually did take place, under what conditions, and in what time. The results of this investigation, and other previously unstudied phenomena of this rectifier junction also, are reported herein.

According to the classification already referred to,[1] the cupric sulfide-magnesium rectifier is of the non-integral class and the sulfide group.

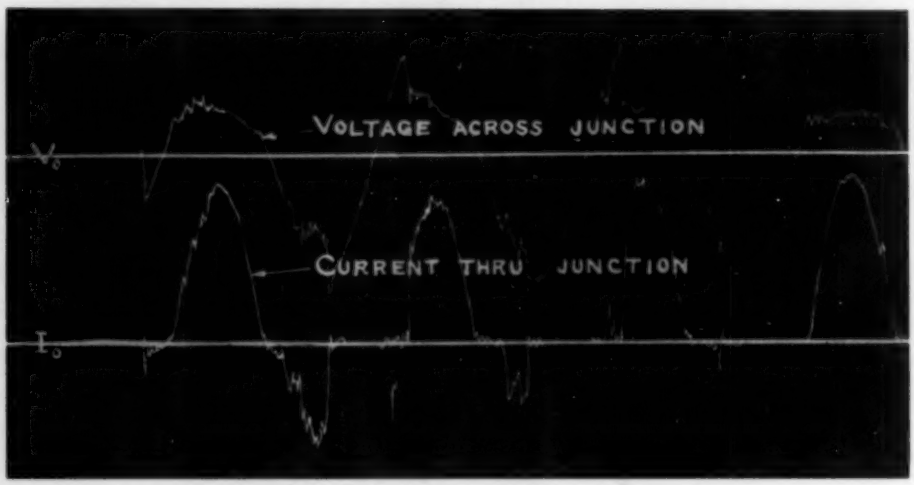

Fig. 1. Initiation of rectification.

EXPERIMENTAL

Nature of the rectifying junction. *Cupric sulfide disk.* The cupric sulfide disk (approximately 0.515 sq. in. in area) is prepared from compressed cupric sulfide powder which is subsequently heat treated to give a hard glassy mass and finally surface-ground to obtain a smooth finish.

[3] S. Ruben, U. S. Pat. 1,751,361 (1930) (filed 1925), L. O. Grondahl, Science **64,** 306 (1926), J. Am. Inst. Elec. Eng. **46,** 215 (1927); J. Slepian, Trans. Am. Electrochem. Soc. **54,** 201 (1928).

[4] F. Braun, Pogg. Ann. **153,** 566 (1874), Wied. Ann. **1,** 95 (1877); **4,** 476 (1878); G. W. Pierce, Phys. Rev. **29,** 478 (1909); Electrician **64,** 425 (1910).

[5] A. E. Flowers, Phys. Rev. **29,** 445 (1909).

[6] R. H. Goddard, Phys. Rev. **34,** 423 (1912).

Particular care is taken in the heat treatment process to keep well below the dissociation temperature of cupric sulfide.

Magnesium disk. Pure magnesium strip of commerce is cleaned and mildly oxidized on the surface by one of a number of suitable processes either chemical or electrolytic. The nature of the oxidizing process is immaterial to this paper provided that a complete coat not so thick as to be too highly resistant be put on. The magnesium strip is subsequently cleaned on one face and punched into disks.

The junction. The oxidized surface of the magnesium disk is then contacted with one surface of the cupric sulfide disk and the two disks locked

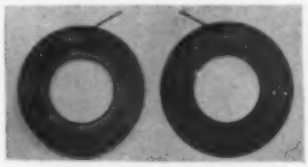

CuS Mg

Fig. 2. Spots of adhesion.

together in a small vise under a pressure of several thousand pounds. The force required depends on the thickness of the oxide coat. When about 4 volts a.c. is applied to such a junction it attains rectifying properties in about the first four cycles as shown in the oscillogram of Fig. 1.

The direction of free passage of current is from cupric sulfide to magnesium. If the junction should now be removed from the vise, it is found

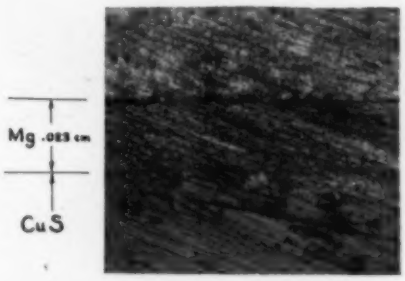

Fig. 3. Cross section of contact spot.

that the two disks are adherent and that the junction now has rectifying properties in spite of the removal of the pressure. If the two disks are pried apart, it is found that adhesion has occurred usually over a very small area. This is illustrated in Fig. 2 in which the points of adhesion on magnesium and cupric sulfide disks from the same junction are shown. If two such disks are again contacted with each other without the application of pressure, it is found that the junction is highly resistant and does not rectify. However, if pressure and voltage be applied as before, reformation takes place usually

at some others pot. In the adhesion between the two disks actual fusion takes place. As indicated in Fig. 3 the structures of both the magnesium and the cupric sulfide are considerably changed at the contact spot. We have shown that this spot is the only place where current flow actually takes place. The simple expedient employed was to cover all of the oxidized magnesium surface except one tiny spot with a coating of insulating varnish. A very small piece of lead was placed on the magnesium behind the clear

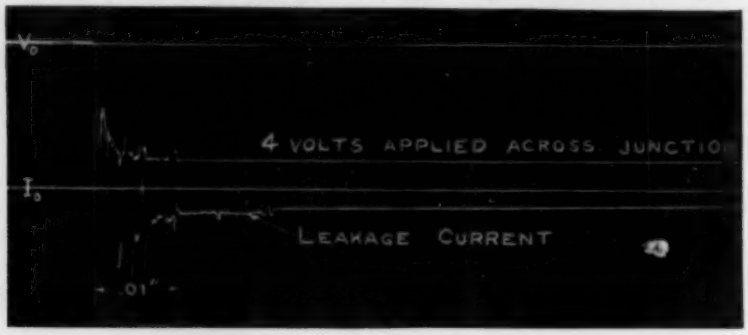

Fig. 4. d.c. formation of junction.

spot and the whole placed in a vise and assembled with a cupric sulfide disk as indicated above. The purpose of the lead was merely to deform the disk at the desired contact point and thus to effect contact with the cupric sulfide disk, which would have otherwise been separated from the magnesium disk by the thickness of the layer of varnish. It was found that a

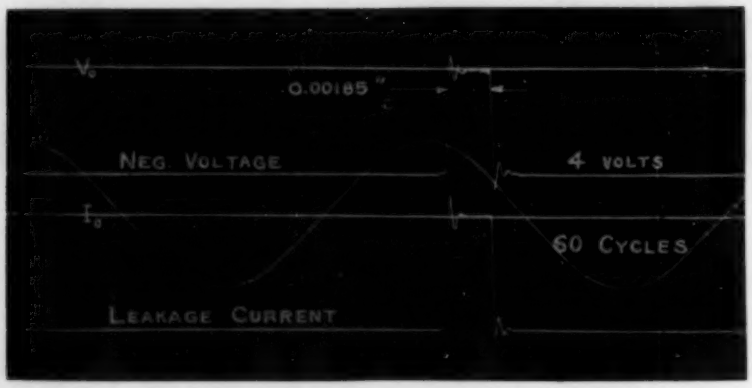

Fig. 5. Interruption in high resistance direction.

junction prepared in this way possessed substantially the same electrical characteristics as one prepared according to the standard practice thus establishing the fact that all the rectification and current flow takes place in the region of integral contact.

The film. Ruben[3] has pointed out that the energy required for this "fusion" probably results from the I^2R loss in the oxide coating and that the

reaction results in the formation of a film to whose properties the behavior of the rectifier can be ascribed. Without examining any of the theoretical concepts involved we will here review the evidence we have accumulated indicating film formation.

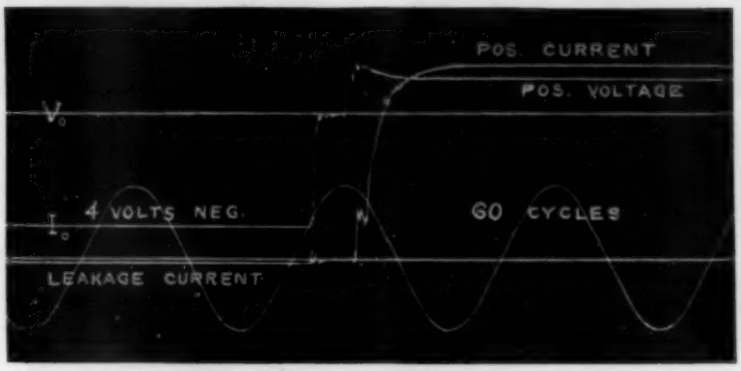

Fig. 6. Interruption in high resistance direction and reversal.

If, instead of applying a.c. to the unformed junction, approximately 4 volts d.c. is applied in the direction magnesium to cupric sulfide, the junction immediately becomes highly resistant in this direction and behaves as

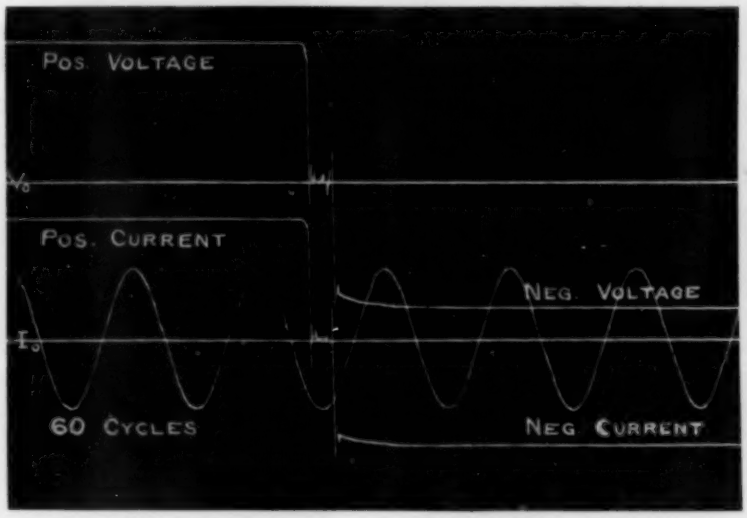

Fig. 7. Interruption in high resistance direction and reversal for cupric sulfide disk alone.

a normal rectifier when subsequently placed on a.c. The oscillogram of the development of this high resistance is shown in Fig. 4. Here we can observe that the resistance is initially extremely low but that in a period of approximately 0.02 sec. it increases to a value of the order of the final resistance in that direction.

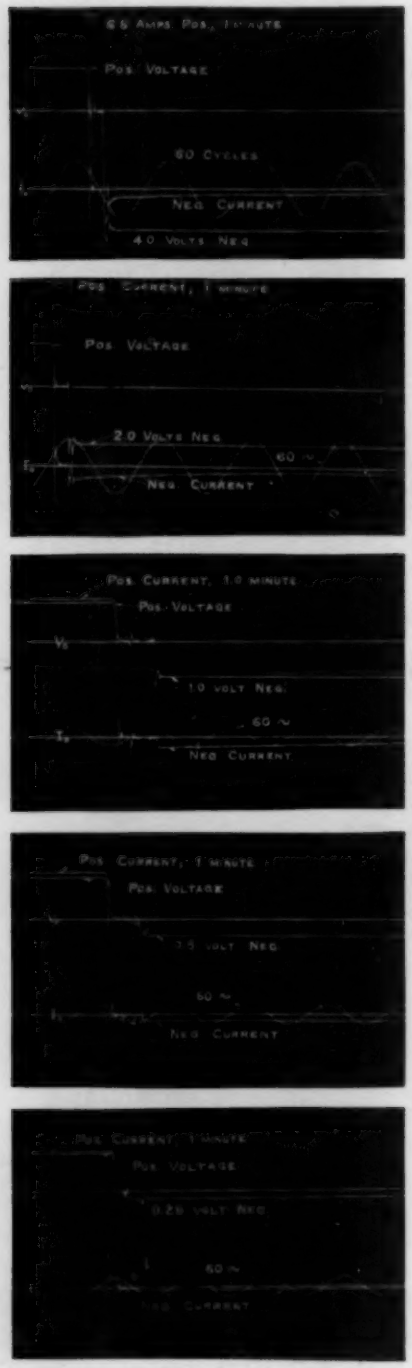

Fig. 8. Oscillograms of interruption and reversal after various periods of current flow in the low resistance direction.

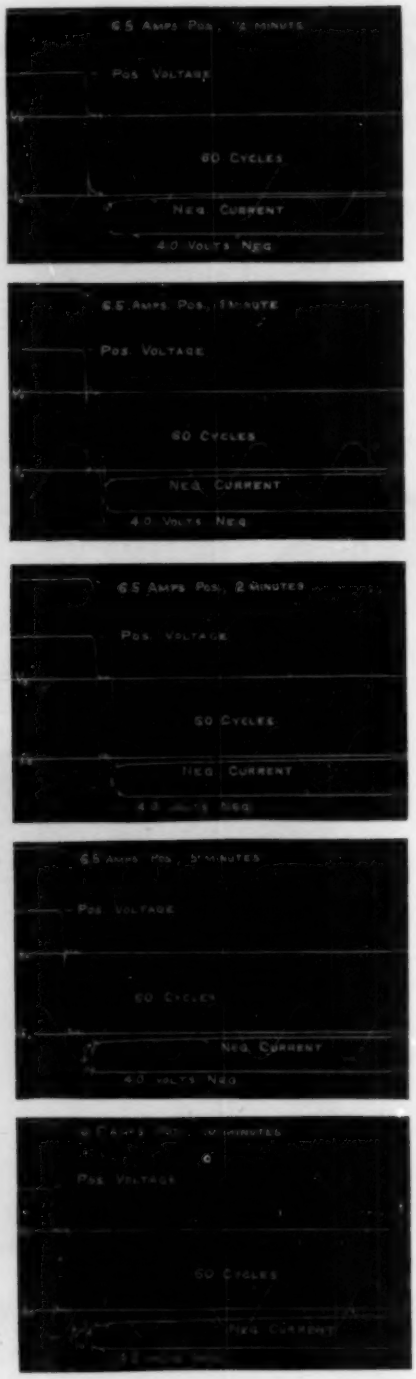

Fig. 9. Oscillograms of interrupuion and reversal after identical periods of current flow in low resistance direction to varying direction.

This characteristic need not be ascribed to a film. It *must* be ascribed to the building up of a resistance and a film appears to be the only source of such resistance. In Fig. 5 we show an oscillogram of current flow in the high resistance direction momentarily interrupted. In this case there is no condition of building up of resistance. The current flow returns immediately to its former value on reclosing of the circuit indicating that whatever is responsible for the high resistance persists in its existence throughout the interval.

In Fig. 6 we show an oscillogram of current flow in the high resistance direction interrupted and reversed. The current does not rise to its maximum value at once on the reversal. About 0.005 sec. is required. However, as shown in Fig. 7, exactly the same phenomenon is observed for the cupric

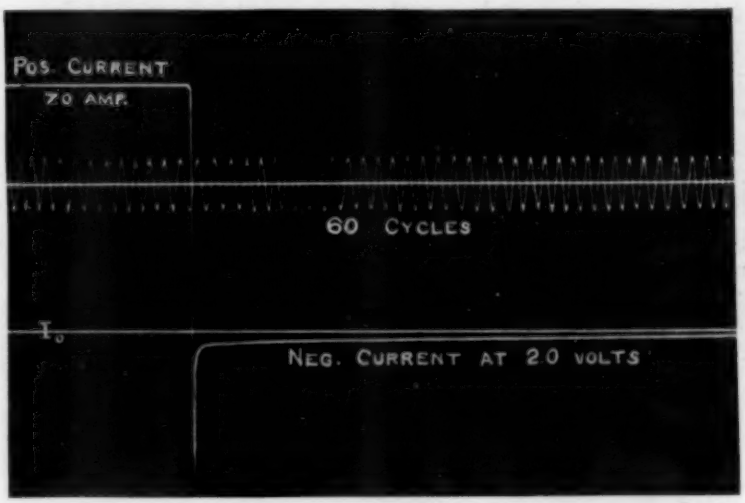

Fig. 10. Growth of resistance after reversal.

sulfide disk by itself between copper contacts. We would consequently be justified in saying that this oscillogram does not necessarily indicate destruction of the film lasting through that period of time. Indeed, the results obtained indicate that there is a gradual destruction of the film in a much longer time interval.

The method used in detecting this film destruction was: first, to form the junction by the regular method by applying an alternating current; second, to permit current to flow in the low resistance direction for varying periods of time; and third, to take an oscillogram at the moment of interruption and current reversal. In Fig. 8 is given a number of oscillograms taken after various periods of current flow in the low resistance direction. It is particularly notable as indicated by the increased time required to attain high resistance, that the apparent time of reformation of the film increases with the time that current has flown in the low resistance direction. Attention is pointed to the case of the unformed junction of Fig. 4 in which film for-

mation was even slower. In this case the complete interpretation of the succeeding figure in the next paragraph should be in point.

In Fig. 9 oscillograms are given for current reversals from low resistance to high resistance after identical periods of current flow but with varying voltage in the high resistance direction. The lower the voltage the longer is the time required for the high resistance to develop. This is exactly what would be expected if a definite amount of work be required to form a highly resistant intermediate layer. The oscillograms at 0.25 and 0.50 volts are, however, more difficult to explain. In these cases we do not have reformation of the film at all.

One possible interpretation of this phenomenon is that on current flow for any long time in the low resistance direction and destruction of the film small, complete, low resistance contacts are made between the cupric sulfide and the magnesium and that these contacts behave like fuses and can be "burned out" only at sufficiently high voltages. Only after "burning out" has occurred does film formation ensue. Indeed, all we may be observing in the apparent reformation of film may be "burning out" of the contacts. In Fig. 10 there is an oscillogram of a similar current reversal in which the recording film was revolved at lower speed. It can be seen that although the resistant film develops almost immediately it continues to "grow" through approximately 0.25 sec. Fig. 11 is a typical oscillogram indicating the opera-

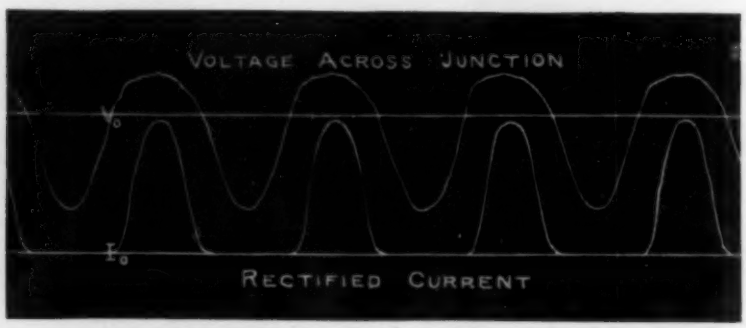

Fig. 11. Operation of a completely formed junction as a half-wave rectifier.

tion of a completely formed junction as a half-wave rectifier. In this illustration there is no sign of any destruction or reformation of a film in the time of a half-wave, but there is evidence that a certain critical voltage must be attained before current flow starts.

Battery and thermoelectric effects. The earliest explanations presented to explain contact rectification involved the propositions that rectification resulted because of a battery or thermoelectric effect within the junction. The first evidence contrary to this theory was presented by Braun,[4] the discoverer of contact rectification. However, this theory is repeatedly reinvoked for each new case of contact rectification and it is consequently necessary to examine the evidence in point that we have collected.

In Fig. 12 is illustrated in diagrammatic form the oscillograph circuit used for this study. V and A represent the voltage and amperage galvanometer vibrators in the oscillograph respectively. J represents the junction.

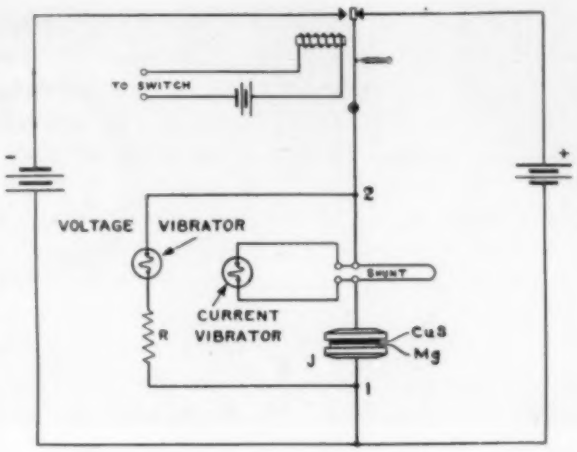

Fig. 12. Oscillograph circuit.

When current is flowing in the direction 1→2, the oscillograph can be adjusted so that the mirror displacements for V and A are in the same direction. If for any reason the circuit should be interrupted and there be a battery effect or thermoelectric effect opposed to the direction of the current, there should occur a reversal of the reading on A and a persistence of a deflection at V in the same direction as prior to the interruption. In other words, a reverse battery or thermoelectric effect will, on interruption of the

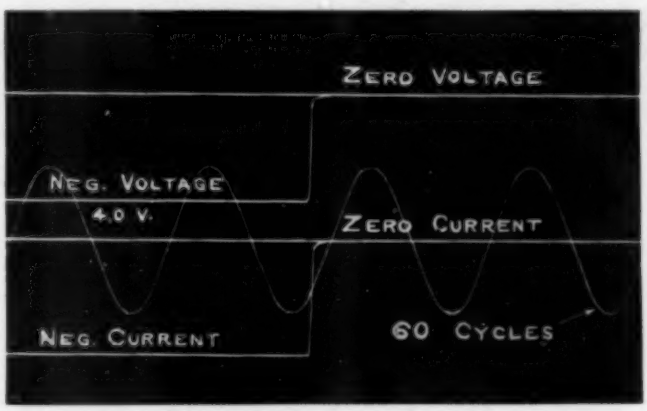

Fig. 13. Breaking circuit in high resistance direction.

circuit, give at least a momentary persistence of deflection of V. A failure to obtain this deflection, after interruption of the current in either direction, is indicated in Figs. 13 and 14. Particularly in the case of Fig. 13, where cur-

rent flow in the high resistance direction is interrupted, would this persistence of the voltage deflection be expected. The purpose of the oscillogram at *A* is merely to give an accurate indication of the time of interruption of

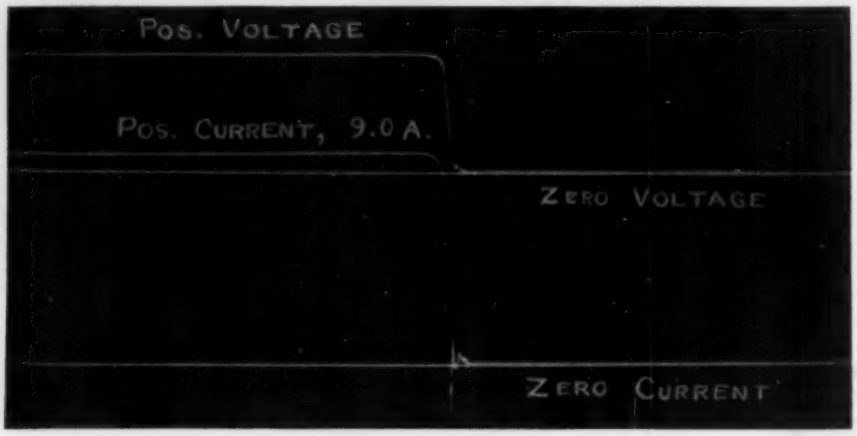

Fig. 14. Breaking circuit in low resistance direction.

the circuit. It is altogether possible that there may be a battery or thermoelectric effect of insufficient intensity to give an opposed deflection at *A*.

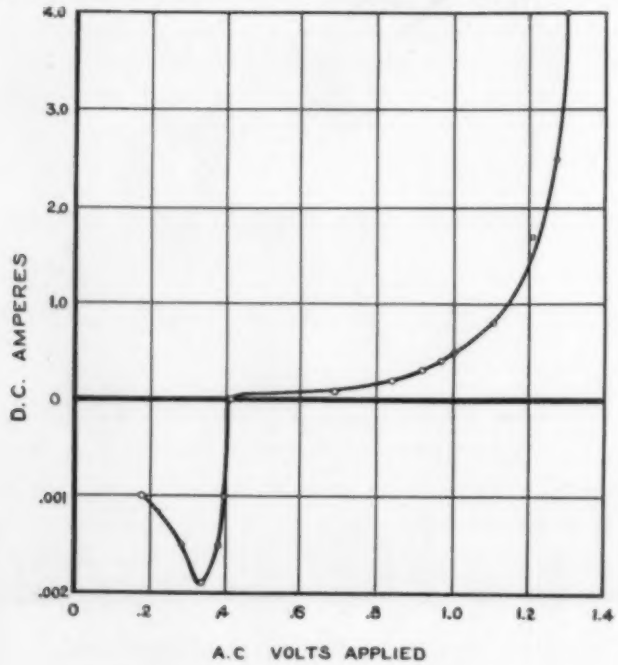

Fig. 15. Relation between d.c. amperes and impressed a.c. voltage.

The momentary opposed deflection on the current oscillograms of some figures at the moment of interruption is attributable to the inertial oscilla-

tion of the vibrator for it is similar in magnitude, direction, and period to the deflection on the voltmeter vibrator.

We may, therefore, conclude that there is no battery or thermoelectric effect in the cupric sulfide-magnesium junction of sufficient magnitude to account for its contact rectifying properties.

"Reverse rectification." The current efficiency of a rectifying junction has a theoretical maximum value for half-wave of 63.6 percent. It has been

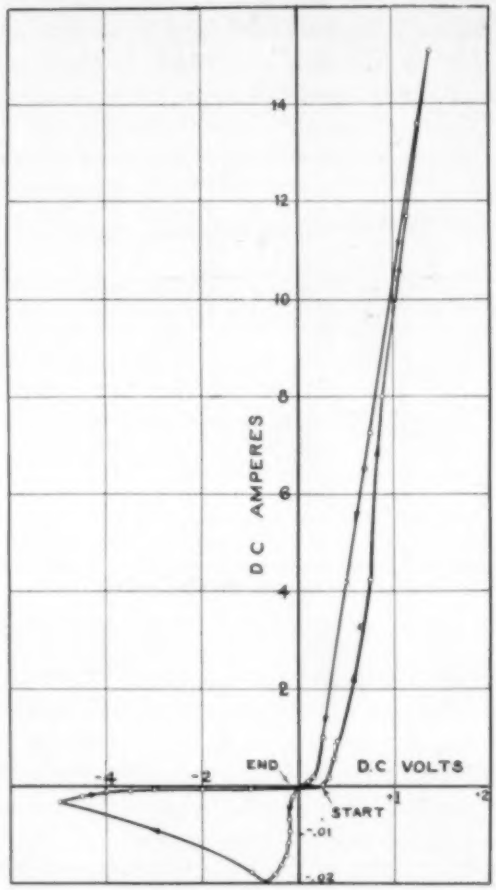

Fig. 16. Relation between d.c. amperes and impressed d.c. voltage.

known for some time that the current efficiency is a function of the applied a.c. voltage. For example, it is evident without any intimate knowledge of the properties of a rectifying junction that above some impressed voltage it will break down and cease to rectify. At that value it is obvious that the rectification efficiency is zero. It is not so well known that for some rectifiers the rectification efficiency decreases to zero at a small a.c. voltage. Goddard,[6] among others has pointed out that the direction of rectified current is sometimes opposed to the direction predicted by experience for the junction studied. For example, if for the cupric sulfide-magnesium junction the

rectified current would flow in the direction magnesium to cupric sulfide, we would be observing the phenomenon of "reverse rectification." Tests that we have conducted indicate that the direction of rectification is related to the impressed voltage. The results are indicated in Fig. 15 in which we have illustrated a sharp reversal of current at approximately 0.4 volts a.c. A number of tests have indicated that the reversal always takes place in this region of voltage. It would be expected from this that the resistance of the junction would be lower at low negative voltages (i.e. from Mg to CuS) than at low positive voltages. This is verified by Fig. 16 in which the direction of taking current readings is indicated by arrows. In this figure also we may be impressed by the fact that there is an apparent destruction of a film which

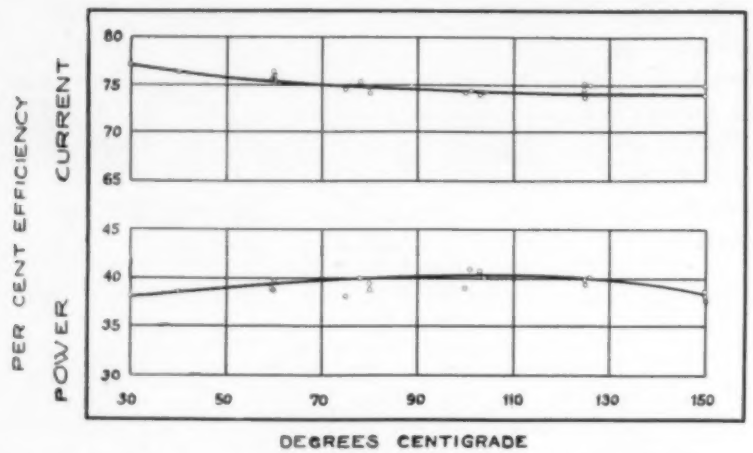

Fig. 17. Relation between efficiency of 4-junction bridge and temperature.

does not begin to reform until between -0.5 and -1.0 volts d.c. when reformation and negative increase of voltage are so rapid that no further readings are possible. This entire phenomenon is not made altogether clear in the light of the 0.25 and 0.50 volt oscillograms of Fig. 9 and the interpretation put on them. The conductive contacts, apparently, are of lower resistance than the film but we would expect them to carry current in both directions (if they do not "burn out") thus resulting in no rectification rather than in reverse rectification. The phenomenon will be subjected to further study.

Relationship between temperature and efficiency. The relationship between temperature and efficiency, for both power and current, is of great importance in the determination of the existence of a hypothetical film. Superficially, without too rigid analysis of the theories requiring the existence of a film in contact rectification, we may say that increase of temperature should be accompanied by lower current efficiency and, within limits, by higher power efficiency. A more detailed analysis of this aspect of the problem over a wide range of temperatures is reserved for a later paper. Fig. 17 indicates that this situation is true for a four junction bridge type rectifier.

The values graphed for power efficiency are arbitrary inasmuch as no correction has been applied for circuit conditions.

Conclusions

1. Oscillographic studies of the cupric sulfide-magnesium junction indicate film formation.

2. An explanation of the results obtained may be based on the hypothesis that "formation" of a film takes place on current flow in the high resistance direction and "destruction" on current flow in the low resistance direction for long intervals of times.

3. "Reverse rectification" is not easily explainable on any hypothesis so far presented. This problem is to be further studied.

4. The variation of efficiency of a bridge-type unit with temperature is in qualitative agreement with the requirements of theories that require film formation. This subject is to be discussed in greater detail in subsequent papers.

5. No battery or thermoelectric effect sufficient to account for the rectifying properties of the cupric sulfide-magnesium junction has been noted. It is consequently suggested that film formation and destruction are electrothermic rather than electrolytic in origin.

LETTERS TO THE EDITOR

Prompt publication of brief reports of important discoveries in physics may be secured by addressing them to this department. Closing dates for this department are, for the first issue of the month, the twenty-eighth of the preceding month; for the second issue, the thirteenth of the month. The Board of Editors does not hold itself responsible for the opinions expressed by the correspondents.

The Presence of Neutral Oxygen in the Gaseous Nebulae

The most stable configuration, s^2p^4, of neutral oxygen gives rise to three terms, ^3P, ^1D and ^1S. McLennan[1] has shown that the green auroral line corresponds to the $^1D-^1S$ transition. Recently Frerichs[2] by a very exhaustive analysis of the oxygen spectrum has been able to predict the positions of the $^3P_2-^1D$ and $^3P_1-^1D$ transitions at 6299 $\pm$5A and 6363$\pm$5A respectively while a private communication to Dr. Frerichs from Professor Paschen states that he has found these lines in the laboratory at 6300.00A and 6363.86A.

Wright's[3] list of nebular lines shows weak unidentified lines at 6302A and 6364A. In agreement with the corresponding transitions in O_{III} the $^3P_2-^1D$ line is two or three times as intense as the $^3P_1-^1D$ line. The general behavior of the lines in various nebulae is in agreement with this identification.

The question at once arises as to why the $^1D-^1S$ line alone occurs under auroral conditions while the $^3P-^1D$ lines alone appear in the nebulae. The theory of the transition probability[4] due to quadrupole radiation (as these lines are "forbidden" by the ordinary selection rules no dipole radiation exists)[5] shows that the mean life of the ^1D state before transition to the ^3P level is much longer, since it is an intercombination line, than that of the ^1S state before transition to the ^1D state. On the other hand the number of atoms reaching the ^1S state is much less than that reaching the ^1D state. This follows from the fact that nearly all of the atoms reaching the ^1S state make the $^1D-^1S$ transition and thus arrive at the ^1D state in addition to those that reach there directly. Since the ^1D state has lower energy than the ^1S state the number reaching it directly is also greater than that reaching the ^1S directly.

Under nebular conditions the mean time between impacts with other atoms is large compared with even the longest of these mean lives and consequently the intensity of the lines is determined largely by the number of atoms reaching the respective upper states. Consequently we should expect the $^1D-^1S$ transition to be much weaker than the $^3P-^1D$ transition. This is verified by the observation that in O_{III} and N_{II}, which have the same set of low terms, the $^1D-^1S$ line is 1/20 to 1/50 as intense as the $^3P-^1D$ lines. A corresponding ratio in O_I would give the $^1D-^1S$ line at 5577A an intensity much below the limit that could have been observed, as the $^3P-^1D$ lines are fairly weak.

On the other hand under auroral condition the collisions between atoms are so frequent that the atom in the ^1D is almost always taken out by a collision of the second kind before it can radiate the $^3P-^1D$ lines. The $^1D-^1S$ transition, however, has a high enough probability so that even under auroral conditions it can take place before a collision of the second kind removes the atom from the ^1S state.

I. S. BOWEN

California Institute,
Pasadena,
July 19, 1930.

[1] McLennan, Proc. Roy. Soc. **A120**, 327 (1928).

[2] Frerichs, Phys. Rev. in press.

[3] Wright, Studies of the Nebulae, Lick Observatory, p. 242.

[4] Huff and Houstoun, Phys. Rev. in press.

[5] Frerichs and Campbell, Phys. Rev. **36**, 151 (1930).

Photoelectric Outgassing

While attempting to study the photoelectric emission from the two sides of an unbacked film of gold, 2×10^{-6} cm thick, it was found that the emission did not hold constant but increased with exposure to ultraviolet. With 360 hours of exposure of the film to ultraviolet the photo-current from the side where the light was incident increased 136 fold and at the same time the long wave limit shifted from 2000A to 2537A.

The emission from the unexposed face increased, in the first 50 hours, about one tenth as much as from the exposed face. It was found that the film was transmitting down to a wave-length of 2259A but only about 10 percent of the energy in the lines below 2537A was being transmitted. On exposure of the second face to the direct radiation of the arc its emission increased as in the case of the first face.

It was found that with the film charged positively, so that the electrons returned to the film after being ejected, the increase in emission was more rapid and the long wave limit shift was greater than when the film was charged negatively. In either case, when the film was exposed through a filter which absorbed all wave-lengths below 2800A but transmitted 55 percent of the total energy of the arc, there was no increase in emission.

A plate of solid gold was treated in like fashion and showed a similar increase in photo-current, which took place much more slowly, accompanied by a shift in long wave limit from about 2000A to 2482A.

At intervals during the exposure of the specimen to ultraviolet fatigue curves, taken by leaving the specimen in a vacuum of 10^{-7} mm of Hg unexposed, showed during the first stages a rapid decrease in photo-current with time of standing, but, after 360 hours of exposure for the film and 160 hours for the solid gold, the photo-current from the former held constant for 3 hours, and from the latter 1½ hours. This seemed to indicate that a fairly stable equilibrium had been reached, and the subsequent fatigue was consistent with the idea that it was due to return of gas to the surface.

The experiment was repeated, using a silver filament approximately 0.025 mm thick, and an increase in emission comparable to that for the gold film was obtained.

The probable explanation is that photo-electrons, both when ejected and returned to the surface by a reverse field, remove adsorbed gas from the surface.

Millikan[1] noted an increase in photoelectric emission on exposure of certain metals to ultraviolet, but did not note the corresponding change in long wave-length limit or that the photoelectrons themselves apparently play an important part in the outgassing.

Work is being carried forward testing this explanation and obtaining more data on photoelectric properties of thin films.

RALPH P. WINCH

Laboratory of Physics,
University of Wisconsin,
Madison, Wisconsin,
July 15, 1930.

[1] Millikan, Phys. Rev. **29**, 85 (1909).

Effect of the Earth's Electric and Magnetic Fields on Ions in the Atmosphere

In a recent letter[1] Hulburt has pointed out that the westward drift of ions in the upper atmosphere predicted in a previous paper of the writer[2] would be prevented by collisions of ions with neutral particles which partake of the earth's rotation. The predicted westward drift was obtained by neglecting the effect of collisions; it remains to consider the modifications of the theory necessitated by taking account of the effect of collisions of ions with neutral particles which rotate with the earth. A little consideration seems to show that the steady-state solution of the problem cannot be anything else than that contained on page 830 of the paper[2] already referred to, where three regions were considered, (1) the interior of the earth, (2) the lower conducting atmosphere, (3) the upper atmosphere. The argument is as follows, references being to the May 1929 paper.[2]

1. Consider first an atmosphere containing no ions. This is the case treated on page 827. As there are no charges in the atmosphere, the potential outside the earth must be a solution of Laplace's equation relative to non-rotating observers, and the components of electric intensity relative to observers on the surface of the earth are given by (14).

It is evident that E_r' is upward (since M is negative) for $r>a$ at all latitudes and E_θ' is directed from the equator toward the poles.

2. Now suppose a few ions to be produced or injected into the earth's atmosphere. They tend to assume a westward drift, but, as Hulburt points out, collisions with neutral molecules interfere with this drift, causing a current in the direction of the electric field. The writer has already investigated the conductivities parallel and at right angles to the field in some detail.[3] This current carries negative ions downward and toward the equator, and positive ions upward and toward the poles, and if the supply of ions is sufficient charges are produced just sufficient to annul the electric field relative to an observer at rest on the surface of the earth. No matter how long the mean free paths and how few the collisions this annulment of the electric field must take place after a sufficient lapse of time.

3. Finally, then, we must have the situation expressed by the equations on page 830, the radius b, however, being that of the outermost limit of the ionized atmosphere. On the surface of the earth we have the negative charge σ_{12} increasing from 0 at the poles to a maximum at the equator. The potential throughout the ionized atmosphere is given by V_2. The atmosphere contains the volume charge ρ_2 which is positive over the poles and negative over the equator. The total charge in a spherical shell of radii r_1 and r_2 is zero, the volume charge being due merely to a *separation* of positive ions which have been urged poleward from negative ions which have been urged equatorward. The volume charge ρ_2 decreases in magnitude as the altitude increases, varying inversely with r^3. Finally at the top of the ionized atmosphere is the surface charge σ_{23}, positive over the poles and zero at the equator. Outside the ionized atmosphere the potential is given by V_3.

4. Now consider ions produced anywhere in the ionized atmosphere ($r<b$). They suffer no drift at all due to the electric field, and rotate with the earth in so far as this effect is concerned. The gravitational drift is all that is left.

5. The case is different with ions reaching the earth from outside. So long as they are outside the ionized atmosphere they suffer the electrical drift (16) with a replaced by b. But when they begin to suffer collisons with air molecules the ions of opposite sign are separated just as in paragraph (2). The negative ones move downward annulling the surface charge σ_{23}, whereas the positive ones move upward and poleward. Effectively, then, the surface charge σ_{23} is raised and b is made larger.

6. Now suppose that ions disappear from the uppermost region of the atmosphere during the night. Then the upper limit of region (2) is depressed, that is, b becomes less. If after sunrise new ions are produced in the upper atmosphere outside the region (2) and in the region (3) which had lost its charge during the night, these new ions start drifting westward but collisions with neutral molecules cause the positives to move polewards and the negatives equatorwards as in paragraph (5). In this way the upper limit of region (2) is raised, b becoming greater.

7. It would seem, then, that ions produced in the portion of the atmosphere which is already ionized should experience no electrical drift relative to the rotating earth. Only those ions which come into the earth's atmosphere from outside or which are produced above the ionized region should suffer the westward drift, and this they should lose in time as a result of collisions.

LEIGH PAGE
Sloane Physics Laboratory,
Yale University,
July 14, 1930.

[1] Hulburt, Phys. Rev. **35**, 1587 (1930).
[2] Phys. Rev. **33**, 823 (1929).
[3] Phys. Rev. **34**, 763 (1929).

Note on Wave-Lengths in the Vacuum Copper Arc

Some months previous to publication, Dr. Kievin Burns sent me for criticism a typed copy of the paper "Wave-Lengths in the Spectra of the Vacuum Copper Arc" by Burns and Walters, publication of the Allegheny Observatory, Vol. VIII, No. 3. I did not fulfill my obligations as a critic properly, for I failed to detect until recently, a rather important error which should have been obvious to me because of my previous work on the copper spark.

Burns and Walters wave-length determinations were made by the usual interferometer method which involves a preliminary wave-

length obtained from some other measurement. The preliminary wave-lengths used for Cu II lines were those given in the tables of spark spectra. Such a choice is perfectly right for low level spark lines, but unfortunately introduces an error of about 2.7 wave numbers into the results for all high level lines, since they appear with approximately that much greater wave number in arc exposures.

The authors of the paper intend to print a corrected list; but, in the meantime, it should be noted that the wave-numbers of all lines involving b^3D and b^1D of Cu II should be increased by approximately 2.7 cm^{-1}. These lines are useful as standards when they are produced in an arc, but not when the source is a spark. In the latter case they are diffuse and displaced to longer wave-length.

The great accuracy of the determination of the sharp lines of Cu II in the ultraviolet will be a boon to spectroscopists because those lines are by far the most useful as standards of measurement in the region λ2400–λ1940.

A. G. SHENSTONE
Palmer Physical Laboratory,
Princeton University,
July 15, 1930.

The Electrolytic Dissociation of Nitric Acid as Revealed by its Infrared Absorption Spectrum

I. R. Rao has recently published an important paper in the Proceedings of the Royal Society (**A127,** 279, 1930) in which he describes a new method of estimating the percent dissociation of electrolytes. He has obtained relative values for the percent dissociation of nitric acid in solutions of varying concentration, which for the first time are independent of assumptions regarding the mobility of the ions. The method, which makes use of intensity studies of a Raman line scattered from water solutions of the acid and attributed to the NO_3 ion, was suggested by the earlier observations of Rao (Nature **124,** 762, 1929), and independently by the observations of one of us (Phys. Rev. **35,** 284, 1930), that large intensity shifts occurred in the Raman scattered lines as the acid was diluted, the presumption being that the lines which grew in intensity upon dilution arose from the NO_3 ion. Although most of this earlier work upon the Raman spectra was done by one of us in the months of April and May, 1929, publication was delayed until Rao's account of nearly identical results, in Nature, stimulated a short report in the February Physical Review. It was of course obvious that studies of the infrared absorption spectrum of the acid solutions should be made. These were begun and are still in progress. Since the work is being interrupted for a brief period, a short account of the results obtained so far seems advisable.

Records of the absorption of the acid solutions of varying concentration and of the fuming acid which contained about 5 percent water were taken on the self-recording quartz spectrograph described by one of us elsewhere some years ago. The unexpected result obtained was that all the water solutions investigated, even the 70 percent commercial concentrated acid, in the region studied (2.4μ–0.78μ), showed only bands which are unquestionably the water bands considerably sharpened and shifted slightly toward shorter wave-lengths, a circumstance which will be discussed in another place. It was only in the fuming acid that new strong maxima appeared which we attribute to the undissociated HNO_3 molecule. Absorption cells varying from less than 1 mm in length up to 10 cm have been employed. It is apparent that the concentration of the entity giving rise to these new maxima, which we believe to be the undissociated HNO_3 molecule, has been enormously reduced in as concentrated a solution as the 70 percent acid, reduced to a point where a column of the 70 percent acid 10 cm long showed no trace of the new maxima.

The bands in the fuming acid have been grouped into three sets, (1) a set of two due to water at 1.42μ and 0.96μ (2) a set of three which fit an anharmonic formula and extrapolate to a fundamental at 2.85μ of wave-lengths 1.47μ, 1.01μ, 0.78μ, and (3) a set of two at 2.12μ and 1.25μ which are interpretated as combinations between a fundamental observed in the Raman effect and bands of the anharmonic series. Others have appeared of whose nature it is yet too early to speak. Records of the acid vapor have been taken also as well as records of the 70 percent acid in which oxides of nitrogen have been dissolved. The vapor records exhibited, among other groups, a group forming an anharmonic

series which we believe to be the same as the series found in the liquid acid, but with every band characteristically shifted toward shorter wave-lengths. This matter is being investigated further. The records of the acid solutions of the nitrogen oxides show no trace of the fuming acid bands, a fact which indicates that these bands are not due to dissolved oxides of nitrogen. In regard to the anharmonic series found in the fuming acid, it is worth noting that the extrapolated fundamental at 2.85μ does not correspond to any fundamental yet observed by means of the Raman effect. Rao reports a band at 3.01μ, but even this has repeatedly failed to appear on plates taken by one of us.

It is hoped that a fuller discussion can be given during the autumn months after experiments, which have been interrupted, are completed.

E. L. KINSEY
J. W. ELLIS

University of California at Los Angeles,
Los Angeles, California.
July 9, 1930.

The Optical Excitation Function of Helium

I have just completed a study of the optical excitation function of helium under conditions which permitted, simultaneously, a study of the electrical conditions in the discharge tube and a determination of the intensities. A new variation of the photographic method has been used for the measurement of the intensities, and the discharge tube has been designed with a view to the elimination of secondary electron emission and of ionization affects. Due to this design, and to a thorough cleaning of the electrodes, the dependance of intensity on either current or pressure is linear indicating that there is no ion current. In earlier work, this linearity has been expected but not obtained.

The results for the singlet system are largely in accord with those obtained by Elenbaas[1] and Hanle.[2] For the triplets, double maxima as reported by Elenbaas, have been found, although the location of these maxima differs somewhat from that previously found. This disagreement is particularly pronounced in the case of the first maxima, which Elenbaas and Hanle both found in the region between 25 and 35 volts. With the present apparatus these maxima occur at approximately 28 volts and it has been possible to correct their position and shape in accordance with the experimentally determined velocity distribution curve of the electrons and the linear relation between current and intensity. This correction shows that the maxima are actually located at the excitation potentials and are of much greater height compared with the background than the experimental curves, without correction, would indicate.

A full report on the apparatus and results will be published in the near future.

WALTER C. MICHELS.
Norman Bridge Laboratory of Physics,
Calif. Institute of Technology,
Pasadena, California.
July 11, 1930.

[1] Elenbaas, Zeits. f. Physik **59**, 289 (1930).
[2] Hanle, Zeits. f. Physik **56**, 94 (1929).

Metastable Atoms and Electrons Produced by Resonance Radiation in Neon

In studies of arcs in pure neon at a few millimeters pressure, we have observed some phenomena which indicate that the resonance radiation from the arc can travel through the un-ionized neon beyond the end of the arc for distances of 20 to 30 centimeters, or more, and the absorption of this radiation produces, by excitation of the gas and by subsequent collisions of the second kind, metastable atoms at the rate of at least 10^{13} cm^{-3} sec^{-1}. In these experiments the neon arc carrying currents of approximately one ampere was passed through a long tube between a hot cathode at one end of the tube and an anode placed near the center. One or more collecting electrodes were placed in the tube beyond the end of the arc, and, in some experiments, movable collectors were used whose distance from the end of the arc could be varied.

The metastable atoms thus produced beyond the end of the arc diffuse into contact with the walls or with metallic electrodes and liberate electrons from the glass or metal surfaces which have velocities of the order of 5 or 10 volts. The walls thus become positively charged and within the space there is a definite concentration of electrons. If a collector is maintained at, say, 70 volts

negative with respect to the anode, the electrons emitted by it serve as a measure of the concentration of the metastable atoms. The concentration of metastable atoms diffusing out of the arc should fall to $1/e^{th}$ of its value every time the distance is increased by an amount equal to 0.4 of the radius of the tube. Within a few centimeters of the end of the arc this theoretical decrement is actually observed, but at greater distances the concentration of metastable atoms decreases far more slowly.

The width of the line corresponding to the resonance radiation in the arc is far greater than that of the absorption line in the unexcited neon, which is determined mainly by the Doppler effect. Assuming this cause of broadening of the absorption line, it can be calculated that between parallel planes the energy absorbed per unit volume in the gas is inversely proportional to the distance from the source and thus, as the end of the arc is approximately a point source of this radiation, the rate of production of metastable atoms should vary approximately inversely as the cube of the distance from the end of the arc. The observed values are in accord with this theory.

The electrons in the tube generated at the walls by the metastable atoms give to the neon a conductivity whose value can be measured, and from the known mobility of the electrons in neon gas, the concentration of electrons can be calculated. For low voltages on the collectors, the currents are determined solely by this mobility of the electrons, and the volt ampere characteristics for small currents are thus linear on both sides of the zero point. For larger negative voltages, the current becomes limited by the number of electrons that can escape from the collector. For sufficient positive voltages, the currents increase more rapidly than corresponds to the linear relationships, this being due to ions produced within the tube by the acceleration of the electrons. The experiments prove that these ions are produced by the ionization of metastable atoms rather than normal atoms, for the rate of production of ions varies approximately with the square of the light intensity. These conclusions are confirmed by experiments with a shutter placed beyond the end of the arc, which can cut off the radiation without interfering with the diffusion of atoms, ions, etc., past the shutter. It is thus proved that the production of metastable atoms is produced by light which travels only in straight lines. The fact that when the collector is positive the electron currents are also proportional to the light intensity proves that the electrons owe their origin not to photoelectric effect from the electrodes, but to the production of metastable atoms or excited atoms. Small disk-shaped collectors have also been used in which one side, which faces the source of resonance radiation, is covered with mica so that the exposed surface cannot receive radiation, and yet the electron current was nearly as great as if the mica were placed on the back side of the collector, proving that the electron currents are generated by metastable atoms which diffuse short distances to the electrode even when the resonance radiation does not reach the electrode itself.

Since the electrons emitted by the collectors possess considerable initial velocities, and since these electrons make elastic collisions with the neon atoms, it is impossible to obtain a saturation current from these electrodes at these gas pressures, for electrons which diffuse back to the electrodes have sufficient energy to be reabsorbed by it. A theoretical investigation shows that in this case the current i_z that flows between any two electrodes is given by the equation,

$$i_z = \frac{16\pi}{3} I_0 \lambda C(V/V_0) \frac{1}{\log(1+V/V_0)}$$

where V is the potential difference between the electrodes, V_0 is the volt equivalent of the velocity with which the electrons are emitted from the cathode, I_0 is the theoretical saturation current density of the electrons emitted from the cathode, λ is the mean free path of electrons, and C is the electrostatic capacitance between the two electrodes (expressed in centimeters). Experiments show that this equation expresses well the volt ampere characteristics of neighboring electrodes in neon exposed to resonance radiation.

IRVING LANGMUIR
CLIFTON G. FOUND

Research Laboratory,
General Electric Company,
Schenectady, New York,
July 9, 1930.

On the Magnetic Deflection of Cosmic Rays

In a recent letter to this section, L. M. Mott-Smith[1] proposed an experiment for deflecting the cosmic rays in a magnetic field which made use of the magnetic induction in the inside of a magnetized iron bar.

This experiment has recently been performed by the writer, using identically the same arrangement and has been shortly described in "Rendicouti della R. Accademia Naxionale dei Lincei", Vol. XI, p. 478, March 1930.

Due to the exceedingly small frequency of coincidences, it was not possible during this first experiment to attain such an accuracy that the expected effect of electrons having a velocity of 10^9 volts lay outside of the average error. A new and more complete experimental set-up is at present under construction and will allow the application of the old method, as well as of a new method (for which Prof. Puccianti is to be thanked). The latter is based on the following principle. Above and below two oppositively magnetized iron bars, which lie close to each other in a horizontal plane, there are placed two counters with their axes parallel to the direction of magnetization. The electrons, passing through the upper counter will be either concentrated upon or deflected away from the lower counter, depending on the direction of magnetization.

Calculation has shown that, for a given size and separation of the counting-tubes, a much larger effect is to be expected from the latter method than from the former.

Moreover, for the explanation of such experiments, there are certain difficulties, which I (as well as L. M. Mott-Smith) did not consider at first. Namely, although the induction represents the average value of the microscopic magnetic field strength, it is probably not allowable *apriori* to assume that this average value is the true value which causes the electron deviation. An exact theoretical treatment of the problem has not been presented.

If the primary cosmic rays are an electron radiation, then (as has already been noted)[2] the earth's magnetic field must also be considered. The effect of the earth's field should be noticeable by an unsymmetric directional distribution of the intensity with respect to the perpendicular. Experiments are being prepared which will test such an effect.

Let us call V the velocity of the electrons in volts, R the earth's radius, M the magnetic moment of the earth, λ the magnetic latitude at the point of observation, θ the angle between the plane of the magnetic meridian and the direction of the path of the electrons (positive toward the east), a a constant, whose value is approximately 3×10^2. Then the theory gives the following results. Electrons may impinge at a definite point of the earth's surface (when $V<aM/R^2$) only if the angle θ satisfies the following inequality:

$$\operatorname{Sin}\theta > \frac{aM}{R^2V}\cos\lambda - \left(\frac{aM}{R^2V}\right)^{1/2}\frac{2}{\cos\lambda}$$

For example at a point where the magnetic latitude is $\lambda=45°$, if $(aM/R^2V)=16$ the above condition shows $\sin\theta>0$. This means that the whole region west of the magnetic meridian is "in shadow". This case comes into consideration for electrons having a velocity of about 4.3×10^9 volt.

If $(aM/R^2V)\cos\lambda-(aM/R^2V)^{1/2}\,2/\cos\lambda>1$ the above inequality has no solution. This means that electrons can never impinge upon the point under consideration.

Here, however, diffusion and loss of velocity in the earth's atmosphere have not been taken into account.

BRUNO ROSSI
Physikalisch-Technische Reichsanstalt,
Charlottenburg, Berlin, Germany.
July 3, 1930.

[1] L. M. Mott-Smith, Phys. Rev. **35**, 1125 (1930).

[2] Bothe u. Kolhörster, Das Wesen der Höhenstrahlung Zeits. f. Physik **56**, 489 (1929).

BOOK REVIEWS

Structure of Line Spectra. PAULING AND GOUDSMIT. Pp. 263, figs. 68. McGraw-Hill Book Company, New York, 1930. Price $3.50.

Goudsmit has often expressed the well-founded opinion that the phenomenally rapid rise of the Bohr theory was due more to the enthusiastic optimism of Sommerfeld than to the brilliancy of Bohr. The exposition of the Bohr-Hund theory that Pauling and he have given recently in their book, "Structure of Line Spectra," shows very markedly their conviction that optimism is also the proper treatment for a theory even when it is as fully developed as the Hund theory now is. I think most physicists will disagree with that idea. A severely critical attitude toward an established theory is much more apt to stimulate the increasingly difficult investigations which are necessary as the theory advances. The book under review will not accomplish that purpose for it leaves one which the impression that here is a practically closed chapter of physics. It seems regrettable that the authors have adopted such an attitude.

It is well known that the wave mechanics gives all the ordinary rules of spectra correctly, but it is also well known that most physicists would find it impossible to grasp the theory of spectra if it were presented solely as a problem in wave mechanics. The authors have wisely chosen to base their discussion on a vector model which can be easily vizualized and which represents reasonably well the phenomena which can only be exactly described in terms of the quantum mechanics. Wherever necessary, the more correct methods and results of the mechanics are introduced, and references are made to the discussions of the same problems in Condon and Morse's "Quantum Mechanics."

The material is excellently arranged and is very lucidly explained. Goudsmit has always used the simplest methods to great advantage in his original papers, and the experimental spectroscopist will be grateful that that simplicity rules in this book. Particularly well-done is the discussion of hyperfine structure, which has recently assumed such importance. Goudsmit has been the leader in that part of the subject, and we can confidently expect him eventually to clear up the rather grave difficulties which, as he points out, still remain.

But, excellent as is this book, I cannot help regretting that the authors have not seen fit to make it a much more complete description of the theory and material of the subject. In many ways it falls behind Hund's "Linienspektren" published in 1927, particularly in the discussion of the relations between complicated spectra. Russell's papers on the energy of removal of electrons from various types of structure are very important for the understanding of spectra, but no discussion of such matters, nor of the limits of series in complicated cases, is given. The latter point should have been considered, if only because Hund's book contains erroneous conclusions.

It is worth drawing attention to the following statements which I believe are inaccurate or misleading. On page 71, Preston's rule for the Zeeman effect of series is stated without any qualification. That rule is true for the special case dealt with but is not generally true. On page 91, it is stated that all the symbols down to Z are needed to account for *observed* spectra. That is yet to be proved. On page 94, it is stated that triplet singlet combinations will "usually" appear not at all or with small intensities. The accuracy of that statement depends upon one's definition of "usually." Considering the authors of this book, the statement on page 98 is strange, "Thus $^3S-{}^3P$ consists of two lines $^3S_1-{}^3P_0$ and $^3S_1-{}^3P_2$." It is noted on page 139 that the intensity ratio for the combination $^3S-{}^3P$ is well varified by experiment on the sodium D-lines, but no mention is made that experiments on other similar pairs of lines disagree radically with the theory. On page 166 there are given rules governing the positions of terms within a configuration. Those rules are in reality fulfilled rather seldom except for the lightest atoms. One of the outstanding difficulties of interpretation is in direct violation i.e. the existence of inverted doublets in alkali spectra. This is not mentioned.

It is unfortunate that the authors did not choose to follow the recently accepted notation in which capital letters are used for the resultant quantum vectors of the atom.

Pauling and Goudsmit have written in this book an excellent account of the explanation of line spectra; but their optimistic attitude has prevented them from making it the complete account that many of us were expecting and that they are quite capable of giving.

A. G. SHENSTONE

The Analytical Expression of the Results of the Theory of Space Groups. RALPH W. G. WYCKOFF. 2nd edit. Pp. 239, figs. 222. Paper covers. Carnegie Institution of Washington 1930.

The first edition has long been out of print and in much demand, so that a simple reprinting would have met a very real need. The second edition, however, does far more than meet this need. The text has been completely rewritten in a more logical manner and, in most instances, with greater lucidity. The only additions here which are of doubtful value are the too greatly abbreviated discussions of the new space-group symbols of Hermann. Mere insertion of these symbols, and reference to the extensive original papers, would have been adequate. An important addition to the tables (132 pp.) of equivalent point coordinates and sub-groups for the 230 space-groups is the series of 200 well-planned and carefully drawn diagrams showing the *special* point-positions for all distinguishable cases. Drawings which show the distribution of symmetry-elements and *general* point-positions are available elsewhere, but these new diagrams with the information on sub-group symmetry contained in their captions, should be of great service in the solution of crystal structures by x-ray methods. The text diagrams are not quite as well drawn as those just mentioned. The original edition was remarkably free from errors. All the serious misprints known to the reviewer have been corrected in the new edition and in the parts newly set (the principal tables were copied photographically) only three trivial mistakes, easily corrected by the casual reader, have been noted in a rather careful survey. The author has always been a stickler for accuracy and has here upheld his principles to the letter.

L. W. MCKEEHAN

Das Ultrarote Spektrum. CL. SCHAEFER AND F. MATOSSI. Struktur der Materie X, Pp. 400, figs. 161, Julius Springer, Berlin, 1930. Price bound, R M 29.80.

Those interested in infrared spectroscopy have been very much pleased that during the past year and a half three excellent books have appeared on the subject. While each of the three has had its particular virtues, the volume by Schaefer and Matossi, the tenth of the Structur der Materie monographs, is perhaps the most comprehensive and will be found to be the most generally useful.

The authors have devoted their first chapter to a careful description of the methods and instruments used in the measurement of infrared spectra. The second chapter deals with the source of infrared radiation, the hot body, and here the laws of black body radiation are given, as well as the measurements of actual hot bodies. The next chapter contains an account of the application of Maxwell theory and the manner in which the electrical and spectroscopic constants of a substance are related. The theory of the grating is also discussed.

The fourth chapter, of over a hundred and twenty pages, deals with the infrared spectra of gases and fluids. Following an exposition of the experimental methods, the authors develop the theory of the diatomic rotator-vibrator both by means of the classical and the wave theory and these results are carefully compared with the experimental data on HCl and other gases. The latter part of the chapter is devoted to a collection of the infrared data on polyatomic molecules together with many of the theories that have been proposed for their explanation. The fifth and last chapter deals with the infrared spectra of solid bodies. Beginning with the Born crystal lattice theory a fine account is given of all the more important experimental and theoretical material which forms the basis for our knowledge of this interesting subject.

It appears that this volume by Schaefer and Matossi may well be one of the important source books for the infrared for some years to come. It is an excellent compilation of all the available experimental material together with a sufficient account of the underlying theory to make the observational results intelligible. The treatment is very clear and the emphasis

which is placed on the theoretical interpretations tends to dispose of the difficulty that a survey of this character must always be somewhat uncritical in nature. The book may be enthusiastically recommended to those who are interested in the subject of the infrared.

D. M. DENNISON

Handbuch der Experimentalphysik. Herausgegaben von W. Wien und F. Harms unter Mitwirking von H. Lenz. Band 24, 2. Teil. Röntgenspektroskopie. AXEL LINDH. Pp. viii+436, figs. 197. Akademische Verlagsgesellschaft. Leipzig 1930. Price bound. R M 42.

When Siegbahn wrote his textbook on the spectroscopy of x-rays, he treated mainly the standard experimental methods and the general regularities in the spectra. The value of Lindh's book, aside from its bringing the bibliography up to 1929, lies chiefly in its shift of emphasis from these general regularities to the exceptions, such as the satellites of x-ray lines and the influence of chemical binding upon an atom's spectrum. The author's contributions in this last field prove him well fitted to discuss it.

After a general discussion of apparatus and gratings, the author considers the different series in detail and gives a general table of levels, revised to 1926. There is a short elementary chapter on the interpretation of the discrete x-ray spectrum. Intensity measurements, the continuous spectrum, and the auxiliary topics of the magnetic spectra of photoelectrons and photoelectric critical potentials, have their own chapters. The Compton effect is not mentioned.

A great part of the volume is given over to the compilation of data, which, when done critically or in connection with still mooted issues, is of course valuable in a handbook of experimental physics. But the inclusive reproduction of tables and figures from old work which can be seen now in some perspective, can hardly be justified. The devotion of a dozen pages to the square roots of all line frequencies (in addition to like data for absorption edges *and* term values), and the reprinting of four figures (122–125) of different ages giving $(\nu/R)^{1/2}$ as a function of Z, instead of one from the author's compiled table, are examples of such practise.

The interpretation of the lines would have been clearer if the author had given the modern spectroscopic L and J values of the levels, and shown in unified tables the two terms associated with each line, as well as the esoteric Greek notation.

J. MACK

Grundlagen der Hydromechanik. L. LICHTENSTEIN. Pp. 506, figs. 54. Julius Springer, Berlin, 1929. Price bound, R M 39.60.

This book by the well-known mathematician of the University of Leipzig constitutes volume 30 of the Springer collection *Die Grundlehren der mathematischen Wissenschaften in Einzeldarstellungen*. As might be expected it is very different from every other treatise on hydrodynamics, for the author, the fundamental problem of hydrodynamics is the integration of certain systems of partial differential equations with assigned boundary conditions and he calls to his aid all the resources of modern mathematics. This makes necessary a large amount of preliminary material; the first chapter is devoted to topology, the second gives a brief but interesting account of vector-analysis, the third treats potential theory, a subject to which the author has made valuable contributions, and so on. It is not until we reach page 290 that the equations of motion are derived. One of the most interesting and important chapters of the book is that devoted to the propagation of discontinuities, a difficult subject, the understanding of which is essential to any comprehension of wave motion. The last chapter is devoted to existence-theory questions.

The book could not profitably be recommended to a beginner, but to one who has studied Lamb and who wishes to understand more fully the mathematical foundations of the subject it should prove very valuable. For practical applications of the theory one must still turn to Lamb and to some such book as Tietjen's account of Prandtl's lectures on hydro- and aeromechanics. The printing has the high degree of excellence we have come to expect in the books of the Springer collection.

FRANCIS D. MURNAGHAN

Einführung in die Theoretische Physik. A. HAAS. Vol. I, Pp. X +396 with 67 figures. Fifth and Sixth Editions. W. de Gruyter and Co., Berlin and Leipzig, 1930. Price bound R M 16.50.

In these last editions the subject matter of Professor Haas' excellent Introduction to Theoretical Physics has been completely worked over, and extensive revisions made both in arrangement and content. Whereas the third and fourth editions of the first volume, from which the English translation was prepared by Verschoyle, contained only two parts—Mechanics, and Theory of the Electromagnetic Field and of Light—, a third part on Thermodynamics has been added to the present editions with a consequent increase in length of some 90 pages.

The subject is developed in the author's customary clear and forceful style and the logical arrangement emphasizes the unity of the subject. Vector methods are used freely throughout the book, the theorems of vector analysis being developed as required. In spite of the fact that some writers in German are beginning to use at least parts of Gibb's significant notation, the author adheres to the clumsy parentheses and brackets, grad's, div's and rot's. A comparison of any vector equation of a little complexity in the parenthesis-bracket notation (such as that on top of page 38) with the same equation in Gibbs' notation, would seem to be all that is necessary to convince anyone of the superiority of the latter.

Pedagogically the text may be criticized in that too frequently abstract theory is developed without any immediate application. Thus the deduction of Hamiltion's canonical equation would appear more important to the student encountering them for the first time if the author had proceded to the Hamilton-Jacobi equation and applied it to the solution of a few problems. Again Euler's equations for the rotation of a rigid body are developed without any considerable application being made.

As usual with Professor Haas' works, a high degree of scientific accuracy is maintained and misprints are nearly non-existent. These last editions will undoubtedly enjoy the high popularity of the earlier editions. The printing is excellent, but in this age of machinery it ought to be unnecessary for the reader to cut every page from preface to index.

LEIGH PAGE

Theoretische Physik. GUSTAV JÄGER. In five volumes. Vol. I Mechanik, Pp. 150; Vol. II Schall und Wärme, Pp. 133; Vol. III Elektrizität und Magnetismus, Pp. 151; Vol. IV Optik, Pp. 148, Vol. V Wärmestrahlung, Elektronik und Atomphysik, Pp. 130. W. de Gruyter and Co., Berlin and Leipzig, 1930.

These tiny volumes ($4\frac{1}{4}'' \times 6\frac{1}{4}''$) can be slipped in the pocket of the student who wishes to prepare for examination during his vacation. While elementary calculus is used freely, the mathematics is of the simplest. The first volume takes up the mechanics of particles including damped simple harmonic motion and Keplerian motion, mechanics of rigid bodies going as far as the symmetrical top under gravity, Lagrange's equations, the special relativity theory, the elements of the theory of elasticity, hydrodynamics of perfect fluids, Poiseuille's formula. The first quarter of Vol. II is devoted to the elements of acoustics, the remainder being concerned with conduction of heat, thermodynamics and kinetic theory of gases. Vol. III deals with electrostatics, magnetostatics, current electricity, electromagnetic induction, alternating currents, going as far as the development of Maxwell's equations. The volume on optics takes up the usual topics of geometrical and physical optics, and some electromagnetic theory of light, ending with a short section on x-rays. The last volume contains the theory of heat radiation, including the Stefan-Boltzmann law, Wien's displacement law and Planck's law, quantum theory of specific heats, the motion of electrons in electric and magnetic fields, metallic conduction, conduction in gases, deflection of alpha-rays, Bohr theory of the hydrogen atom, photoelectric effect, and Compton effect.

The books are clearly printed in type of normal size and strongly bound. The material is well chosen and the subject matter developed clearly and logically although in somewhat concise form. Each volume is provided with table of contents, index, and references for collateral reading.

LEIGH PAGE